



The University of
Nottingham

**Infiltrins as a Novel Regulatory
Principle of Host-Parasite Interactions:
New Targets for Vaccination?**

Abdulaziz Alouffi

Thesis submitted to the University of Nottingham
for the degree of

Doctor of Philosophy

March 2017

Abstract

Infiltrins, or pathogen-secreted host nucleus infiltrating proteins, are potential new targets for the development of more efficient vaccines against helminthic parasites. The archetypal infiltrin is IL-4 inducing principle from *S. mansoni* eggs (IPSE/alpha-1, also known as SmIPSE), a glycoprotein secreted by *Schistosoma mansoni* eggs, and characterised by the simultaneous presence of a classical secretory signal and a nuclear localisation signal. Within minutes following uptake by mammalian host cells, IP SE/alpha-1 translocates to their nucleus and binds to Deoxyribonucleic acid. This suggests that infiltrins, by acting as transcription factors, might play a central role in controlling the host-parasite relationship at the molecular level. Together with their secretory status, this role makes infiltrins interesting targets for vaccination.

In this study, similar properties were demonstrated for nuclear localisation signal of ShIPSE03 (125-SKRRRK~~Y~~-131) located between amino acid position 125 and 131, that plays a necessary and sufficient role in the process of transferring ShIPSE03 and heterologous GFP proteins into the nuclei of host cells. Similarly, a combination of online bioinformatics tools was used to predict the putative nuclear localisation signal motif of Smk5 (256-ELKRR~~VE~~-262) from *S. mansoni* eggs, and FhGST-si (202-LKKRAKT-208) and FhH2A (35-IHRHLKT-41) from *Fasciola hepatica*. To verify the predicted NLSs, putative infiltrins were used to generate a series of truncated constructs fused with *Aequorea coerulea* green fluorescent protein-1 (AcGFP1), which were transfected into mammalian cells. Nuclear localisation of fluorescence confirmed the existence of a single, signal at the C-terminal in ShIPSE03, FhGST-si, and Smk5, and at the N-terminal in FhH2A. The predicted NLS motifs in ShIPSE03 (125-SKRRRK~~Y~~-131), Smk5 (256-ELKRR~~VE~~-262), FhGST-si (202-LKKRAKT-

208) and FhH2A (35-IHRHLKT-41) inserted into Tetra-enhanced green fluorescent protein (EGFP), but not corresponding alanine NLS mutants, redirected the encoded ~100 kDa protein entirely to the nucleus. Use of an IPSE-specific monoclonal antibody or an anti-His antibody showed that wild-type recombinant ShIPSE03, Smk5, FhGST-si and FhH2A added exogenously to HTB-9 or Huh7 cells, fully translocated to the nucleus, whereas the alanine NLS mutant remained in the cytoplasm. Overall, the existence of infiltrins in *S. haematobium* and *F. hepatica* suggests that infiltrins may represent a more general regulatory principle operating within parasitic trematodes.

In terms of the function of IPSE/alpha-1, quantitative real-time polymerase chain reaction data indicated that an increase in Alanine-Transaminase (ALT) activity measured after 72 hours could be a result of increased gene expression after IPSE/alpha-1 nuclear translocation, rather than a true reflection of hepatotoxicity. According to Transepithelial Electrical Resistance (TEER) measurements in electrically tight Caco-2 cells grown in transwell inserts, wild-type IPSE/alpha-1 may play an important role in the down-regulation of intestinal epithelial cell tight junction integrity, might encourage apoptotic mediators and inflammatory responses in intestinal epithelial cells, and impair the intestinal tight junction barrier by causing it to dysfunction. In addition, wild-type IPSE/alpha-1 was able to activate humanised basophil reporter cell lines, such as the RS-ATL8 and NFAT DsRed cell lines.

Acknowledgements

In the name of Allah, the Most Gracious and the Most Merciful. All praises to Allah for the strength He gave me and His blessing in completing this thesis.

First of all, I would like to express my deep and sincere gratitude to my supervisors: Dr Franco H. Falcone, who has supported me throughout my PhD with his wisdom and patience, whilst allowing me the opportunity to explore the work in my own way. One simply could not wish for more than a supervisor who takes on the role of both mentor and friend. My sincere thanks are also due to Dr Cornelia de Moor, for agreeing to co-supervise my project.

I wish to express my sincere thanks to our collaborators: Prof Michael Hsieh from George Washington University and Dr Luke Pennington from Stanford University, School of Medicine, and also Prof Mike Doenhoff, Dr Nigel Mongan from the Faculty of Medicine & Health Science, University of Nottingham, and Dr Robin J Flynn from University of Liverpool.

I am very thankful to those people who helped with materials or opened their laboratory for us: Prof David Heery, Prof Jonas Emsley, Dr Sebastiaan Winkler, Dr Snow Stolnik-Trenkic, Dr Catherine Jopling, Dr Cynthia Bosquillon, Dr Hilary Collins, Dr Richard Argent, Dr Mohammed Ehsan, Dr Osman Adamu Dufailu, Dr Gary Telford, Dr Veeren Chauhan, Dr Daniel Wan, Dr Naim Hage and Dr Szu Wong. Not forgetting all of Franco's group members and Abdullah Alshehri, who helped me from time to time with the lab work.

I wish to express my deepest appreciation to King Abdulaziz City for Science and Technology (KACST) in Saudi Arabia for their financial support. I wish to express

my sincere thanks to people from KACST who have supported me Dr Prince Turki bin Saud Al-Saud (the president of KACST), Prof Nasser Al-Khalifa, Prof Ibrahim Alruqaie and Dr Fahad Abdullah M Alnoeim (cultural attaché in London).

I would like to express my deep and sincere gratitude to my father, Saleh and my mother, Rogyah for allowing me to realise my own potential. All the support they have provided me with over the years is the greatest gift anyone has ever given me. I am very thankful to my brothers and sisters who offered invaluable support and humour over the years. Finally, words fail to express my appreciation for my wife, Asiyah and my daughter, Sarah. Asiyah was always there cheering me up and stood by me throughout the good times and the bad times.

I declare that I am the author of this thesis. This is a true copy of my thesis.

Table of Contents

Abstract	i
Acknowledgements	iii
List of Figures	ix
List of Tables	xii
List of Abbreviations	xiii
Chapter 1 - Introduction	1
1.1 Parasitology and Parasitism	1
1.2 Trematoda or Flukes	1
1.3 Fascioliasis	2
1.3.1 <i>Life Cycle of Fasciola spp.</i>	6
1.3.2 <i>Diagnosis, Prevention and Cure</i>	8
1.3.3 <i>Immune Response to F. hepatica and F. gigantica</i>	10
1.4 Schistosomiasis	12
1.4.1 <i>Life Cycle and Pathogenesis of Human Schistosoma spp.</i>	16
1.4.2 <i>Diagnosis, Prevention and Cure</i>	20
1.4.3 <i>Schistosome Infection and the Immune Response</i>	22
1.4.4 <i>Immune Response to Schistosome Eggs</i>	24
1.5 Infiltrins.....	30
1.6 Aims and Objectives	33
Chapter 2 - General Materials and Methods	37
2.1 Cell Culture	37
2.2 Cell Culture Ware	38
2.3 Cell Toxicity Assay.....	38

2.4 Antibiotics and Transfections	40
2.5 Bacterial Culture	41
2.6 Expression Vectors	41
2.7 pAcGFP1-C3 Vector.....	42
2.8 Tetra-GFP Vector.....	42
2.9 Transepithelial Electrical Resistance	43
Chapter 3 - Bioinformatic and Nuclear Localisation Signal Prediction.....	45
3.1 Introduction.....	45
3.2 Experimental Procedures	48
3.3 Results.....	50
3.4 Discussion	57
Chapter 4 - Recombinant Expression and Purification of Infiltrins.....	60
4.1 Introduction.....	60
4.2 Experimental Procedures	62
4.2.1 Plasmid Preparation.....	62
4.2.2 Expression of Infiltrins.....	65
4.3 Results.....	71
4.3.1 Cloning of IPSE/alpha-1 and Smk5 mature sequence cDNA into the Expression Vectors	71
4.3.2 Expression.....	75
4.4 Discussion	77
Chapter 5 - Infiltrins and Nuclear Transport.....	81
5.1 Introduction.....	81
5.1.1 Classical and non-classical secretory pathways	81
5.1.2 Nuclear Localisation.....	83
5.1.3 Nuclear Localisation of IPSE/alpha-1.....	85
5.2 Experimental Procedures	87
5.2.1 PCR Amplification and Subcloning of Infiltrins into the Vector pAcGFP1- C3.....	87

5.2.2	<i>Subcloning of the Predicted NLS into the Vector pTetra-GFP</i>	91
5.2.3	<i>Cell Culture and Transfection</i>	94
5.2.4	<i>Cell Fixation and Fluorescence Microscopy</i>	94
5.2.5	<i>Cellular Uptake of Infiltrins</i>	95
5.3	Results	96
5.3.1	<i>Uptake of recombinant Putative Infiltrins</i>	96
5.3.2	<i>Analysis of the NLS of Putative Infiltrins</i>	99
5.4	Discussion	107
Chapter 6 - Effects of Sm-IPSE (or IPSE/alpha-1) on Intestinal Epithelium cell Model		115
6.1	Introduction	115
6.1.1	<i>The Transporting Macromolecules Across Mucosal Epithelium</i>	115
6.1.2	<i>Using Calu-3 and Caco-2 cells as intestinal epithelial model in vitro</i>	123
6.1.3	<i>Using Humanised Rat Basophilic Leukaemia Reporter Cell Lines</i>	123
6.1.4	<i>Translocation of Eggs to the Gut Lumen</i>	125
6.1.5	<i>Importance of IPSE/alpha-1 in this Study</i>	128
6.2	Experimental Procedures	130
6.2.1	<i>Activation of the RS-ATL8 reporter system by IgE binding to IPSE/alpha-1</i>	130
6.2.2	<i>Effect of IPSE/alpha-1 on Model Gut Epithelial Membrane Integrity</i>	130
6.2.3	<i>Effect of the NFAT-DsRed on Model Gut Epithelial Membrane Integrity after Activation by IPSE/alpha-1</i>	132
6.3	Results	134
6.4	Discussion	140
Chapter 7 - IPSE/Alpha-1 and Alanine Transaminase (ALT)		147
7.1	Introduction	147
7.1.1	<i>qRT-PCR for assessment of changes in ALT mRNA expression</i>	148
7.2	Experimental Procedures	149
7.2.1	<i>Evaluation of Cytotoxicity</i>	149
7.2.2	<i>Effect of IPSE/alpha-1 on Gene Expression</i>	149

7.3 Results.....	151
7.4 Discussion.....	154
Chapter 8 - General Discussion and Conclusions.....	159
8.1 Infiltrins.....	159
8.2 Egg Translocation and Function of IPSE/Alpha-1	161
8.3 Infiltrins and Future Vaccine development.....	162
8.4 Conclusions and Future Work	164
References.....	166

List of Figures

Figure 1.1: Adult worms and eggs which cause fascioliasis	4
Figure 1.2: Global distribution of human <i>Fasciola</i> spp.	5
Figure 1.3: Life-cycle of <i>Fasciola</i> spp.	7
Figure 1.4: Global distribution of human <i>Schistosoma</i> spp.	15
Figure 1.5: Schistosomes:	16
Figure 1.6: Life cycle of human <i>Schistosoma</i> spp.	19
Figure 1.7: Immune response to Schistosome infection.....	24
Figure 1.8: A mature <i>S. mansoni</i> egg.	25
Figure 1.9: Mechanism of immune regulation by the major components of a schistosome egg.	29
Figure 1.10: Suggested mechanism of infiltrins (working hypothesis).....	31
Figure 1.11: General postulated features of infiltrins as seen in IPSE/alpha-1	32
Figure 1.12: The potential effect of IPSE/alpha-1 on tight junction proteins and gut epithelial membrane integrity	36
Figure 2.1: Schematic of the MTT assay and coloured formazan product.....	39
Figure 2.2: Schematic of the LDH cytotoxicity assay and its mechanism	40
Figure 2.3: Schematic of the resazurin assay and coloured product.....	40
Figure 2.4: Map of the vector pAcGFP1-C3	43
Figure 2.5: Schematic representation of the Epithelial Volt/ohm meter system used to assess the ohmic resistance of a cellular layer.	44
Figure 3.1: Full length cDNA and amino acid sequence of IPSE/alpha-1.	47
Figure 4.1: Amplification of IPSE/alpha-1 and <i>Smk5</i> fragment from <i>S. mansoni</i> egg cDNA.....	72
Figure 4.2: Representative verification of IPSE/alpha-1 insertion into the expression vectors pOPE101 and pCEP4.....	73
Figure 4.3: Representative verification of <i>Smk5</i> insertion into the expression vectors pOPE101, pCEP4 and pTT5	74
Figure 4.4: Analysis of recombinant IPSE/alpha-1 and ShIPSE03	75
Figure 4.5: Analysis of recombinant <i>Smk5</i>	76

Figure 4.6: Analysis of recombinant FhGST-si and FhH2A.....	77
Figure 4.7: Compute tool for Smk5 giving 34 kDa as the theoretical pI/Mw.....	80
Figure 5.1: Ran-GTP nuclear transport cycle.....	85
Figure 5.2: General postulated features of infiltrins as seen in IPSE/alpha-1.....	86
Figure 5.3: Suggested infiltrin mechanism (working hypothesis).....	87
Figure 5.4: Steps involved in the amplification of the infiltrins.....	90
Figure 5.5: Schematic of the tetra-GFP construct and the potential NLS of <i>ShIPSE</i>	92
Figure 5.6: Schematic of the tetra-GFP construct with the NLS of <i>Smk5</i> , <i>FhGST-si</i> and <i>FhH2A</i>	92
Figure 5.7: Cellular uptake of IPSE/alpha-1.....	97
Figure 5.8: Cellular uptake of ShIPSE03.....	97
Figure 5.9: Cellular uptake of Smk5.....	98
Figure 5.10: Cellular uptake of FhGST-si and FhH2A.....	98
Figure 5.11: Diagram representing the different amplified infiltrins.....	100
Figure 5.12: Nuclear translocation of FhGST-si, FhH2A and Smk5 in Huh7 hepatocytes.....	101
Figure 5.13: Localisation of wild-type and mutant Tetra-EGFP-ShIPSE03 NLS.....	103
Figure 5.14: Localisation of wild-type and mutant Tetra-EGFP- Smk5 NLS.....	104
Figure 5.15: Localisation of wild-type and mutants Tetra-EGFP- FhGST-si and FhH2A NLS.....	104
Figure 5.16: Summary of the effects of wild-type and mutants on nuclear localisation of the Tetra-EGFP-ShIPSE03 fusion protein.....	105
Figure 5.17: Summary of the effects of the wild-type and mutants on nuclear localisation of the Tetra-EGFP- <i>Smk5</i> , <i>FhGST-si</i> and <i>FhH2A</i> fusion protein.....	105
Figure 5.18: Cellular uptake of <i>ShIPSE</i> by HTB9 cells.....	106
Figure 5.19: Cellular uptake of IPSE/alpha-1 by Huh7 cells.....	106
Figure 5.20: Summary of the effects of wild-type and mutants on nuclear localisation on the uptake of IPSE/alpha-1 and <i>ShIPSE03</i>	107
Figure 5.21: Binding between a bipartite or monopartite NLS and importin α	111
Figure 6.1 The three potential pathways for crossing the epithelial barriers.....	117
Figure 6.2 The structure of a tight junction between epithelial cells.....	118
Figure 6.3 The interaction of TJ proteins – the ZO protein family.....	119
Figure 6.4 Human and rat receptor (Fc ϵ RI) and mast cells/ basophil activation due to Fc ϵ RI crosslinking.....	124

Figure 6.5 Diagram showing the wall of the large intestine composed of the four typical layers.....	126
Figure 6.6 Diagram showing the sectional view of the small intestine wall and the red circle shows Peyer's patches.	127
Figure 6.7 Culture of Caco-2 cells on Calu-3-derived basement membranes.....	132
Figure 6.8 Activation of basophils and the impact on the integrity of a model gut epithelial membrane.....	133
Figure 6.9 Activation of the RS-ATL8 reporter system by IgE binding to IPSE/alpha-1 expressed in HEK-293 cells	135
Figure 6.10 Effect of IPSE/alpha-1 on the Caco-2 cell layer via TEER.....	136
Figure 6.11 Activation of the NFAT DsRed reporter system by IPSE/alpha-1 and the effect on TEER of the Caco-2 cell layer.	138
Figure 6.12 Activation of the NFAT DsRed reporter system by IgE binding factor IPSE/alpha-1 expressed in HEK293	138
Figure 6.13 DsRed cells as a reporter system 48 hours after stimulation.....	139
Figure 7.1: LDH activity of Huh7 cells cultured in the presence of different concentrations of IPSE/alpha-1 (WT) for 72h. N=3 experiments.	151
Figure 7.2: MTT activity of Huh7 cells cultured with different concentrations of IPSE/alpha-1 (WT) for 72h.	152
Figure 7.3: Resazurin activity of Huh7 cells cultured with different concentrations of IPSE/alpha-1 (WT) for 72h.	153
Figure 7.4: IPSE/alpha-1 has a profound effect on gene expression in human dendritic cells.....	156
Figure 8.1: Full length FhGST-si from <i>F. hepatica</i>	220
Figure 8.2: Full length FhH2A from <i>F. hepatica</i>	221
Figure 8.3: Full length ShIPSE03 from <i>S. haematobium</i> eggs	222
Figure 8.4: Full length Smk5 from <i>S. mansoni</i> eggs	223

List of Tables

Table 1.1: Comparison between the two species causing fascioliasis	5
Table 1.2: Vaccine candidates for <i>Fasciola spp.</i>	10
Table 1.3: Comparison of schistosomes infecting humans	15
Table 1.4: Vaccine candidates for schistosomiasis	21
Table 3.1: Different bioinformatics tools used for prediction of NLS	48
Table 3.2: <i>F. hepatica</i> protein sequences with NLS and CSS motifs commonly identified by four different prediction tools.....	53
Table 3.3: Results of different bioinformatics tools used to assess known NLSs in FhGST-sj, FhH2A, ShIPSE03 and Smk5	55
Table 4.1: Primers and annealing temperature.....	63
Table 4.2: Vector-specific primers.....	65
Table 5.1: Primer sequences	89
Table 5.2: Oligonucleotide NLS primer sequences for Tetra-EGFP (<i>Schistosoma</i>)	93
Table 5.3: Oligonucleotide NLS primer sequences for Tetra-EGFP (<i>Fasciola hepatica</i>).....	93
Table 5.4: Vector-specific primers for pTetra-GFP.....	94
Table 6.1: Functionality of cytokines and their target cells.....	121
Table 7.1: RPL32 primers.....	150
Table 7.2: Average GPT and RPL32 gene expression as assessed via qRT-PCR (see Appendix 7).....	154
Table 7.3: Fold induction of gene of interest (GPT) after normalisation with reference control gene (RPL32).....	154

List of Abbreviations

AAMs	Alternatively Activated Macrophages
ABC	ATP-Binding Cassette
AIC	Air-Interface Culture
ALT	Alanine Transaminase
APCs	Antigen Presenting Cells
ATP	Adenosine Triphosphate
BCA	Bicinchoninic Acid
BM	Basement Membrane
CatL	Cathepsin L
cDNA	Complementary DNA
CEF-6	Cationic Egg Fraction-6
CLR	C-type Lectin Receptor
CLRs	C-type Lectin Receptors
CRM1	Chromosome Region Maintenance 1
CSS	Classical Secretory Signal
DALYs	Disability-Adjusted Life Years
DC-SIGN	Dendritic Cell-Specific Intercellular adhesion molecule-3-Grabbing Non-integrin
DCs	Dendritic Cells
DNA	Deoxyribonucleic acid
DPBS	Dulbecco's Phosphate-Buffered Saline
EBNA	Epstein Barr virus Nuclear Antigen
EBV	Epstein Barr virus
EDTA	Ethylene Diamine Tetracetic Acid
EGF	Epidermal Growth Factor
EGFP	Enhanced Green Fluorescent Protein
ELISA	Enzyme-Linked Immunosorbent Assays
ER	Endoplasmic Reticulum
ES	Excretory/Secretory
ESP	Egg Secretory Proteins
FABP	Fatty Acid Binding Protein

FBS	Foetal Bovine Serum
FGF3	Fibroblast Growth Factor-3
FhGST-si	<i>F. hepatica</i> glutathione S-transferase- sigma
FhH2A	<i>F. hepatica</i> Histone H2A
FhHDM	<i>F. hepatica</i> Helminth Defence Molecule
FhPrx	<i>F. hepatica</i> Peroxiredoxin
GFP	Green Fluorescent Protein
GPT	Glutamate-Pyruvate Transaminase
GST	Glutathione S-Transferase
HEK 293	Human Embryonic Kidney 293
HFV	Human Foamy Viruses
HFV	Human Foamy Viruses
HGNC	HUGO Gene Nomenclature Committee
HIV-1	Human Immunodeficiency Virus type 1
HMM	Hidden Markov Model
HRP	Horseradish Peroxidase
HUGO	Human Genome Organisation
Huh7	Human Hepatoma7
IBB	Importin-Beta-Binding
IEC	Intestinal Epithelial Cells
IFN- γ	Interferon gamma
IgE	Immunoglobulin E
IgG1	Immunoglobulin G1
IgG2	Immunoglobulin G2
IL	Interleukin
IPSE	IL-4 inducing principle from <i>S. mansoni</i> eggs
IPTG	Isopropyl β -D-1-thiogalactopyranoside
JAMs	Junctional Adhesion Molecules
kDa	kilodalton
LB	Luria-Bertani
LB-ATG	Luria Bertani - Ampicillin Tetracycline Glucose
LDH	Lactate Dehydrogenase
LDH	Lactate Dehydrogenase

LeX	Lewis X
MCS	Multiple Cloning Site
MEM	Minimum Essential Medium Eagle
MGL	Macrophage Galactose type Lectin
MIP-2	Macrophage Inflammatory Protein 2
MLC	Myosin Light-Chain
MLCK	Myosin Light Chain Kinase
MMC	Mucosal Mast Cells
Mmcp-1	Mouse Mast cell Protease-1
MMIF	Macrophage Migration Inhibitory Factor
MMP-3	Matrix MetalloProteinase-3
MR	Mannose Receptor
MRs	Mannose Receptors
MTT	Multi-Table Tournament
NES	Nuclear Export Signal
NFAT	Nuclear Factor Activate T cell
NLS	Nuclear Localisation Signal
NPC	Nuclear Pore Complex
NRSB	Non-Reducing Sample Buffer
NSS	Nucleocytoplasmic Shuttling Signal
NTDs	Neglected Tropical Diseases
PAGE	Polyacrylamide Gel electrophoresis
PAMPs	Pathogen Associated Molecular Patterns
PBMC	Peripheral Blood Mononuclear Cell
PCR	Polymerase Chain Reaction
PEI	Polyethyleneimine
pH	potential of Hydrogen
PSI-BLAST	Position-Specific Iterative Basic Local Alignment Search Tool
PTHrP	ParaThyroid Hormone-related Protein
PTHrP	ParaThyroid Hormone-related Protein
qRT-PCR	quantitative Real-Time Polymerase Chain Reaction
RBL	Rat Basophilic Leukaemia
ROCK	RhOassoCiated Kinase

RPM	Revolutions Per Minute
RSB	Reducing Sample Buffer
RT-PCR	The Real-Time Polymerase Chain Reaction
SDS	Sodium Dodecyl Sulphate
SEA	Soluble Egg Antigen
Smk5	Kappa-5 from <i>S. mansoni</i> eggs
SRP	Signal Recognition Particle
SRP	Signal Recognition Particle
Sv40	Simian virus40
TCA	TriChloroacetic Acid
TCBZ	Triclabendazole
TEER	Trans-Epithelial Electrical Resistance
Tf	Transferrin
TfR	Transferrin receptor
TGF- β	Transforming Growth Factor-beta
Th1	Type 1 helper response
Th2	Type 2 helper response
TJ	Tight Junction
TN1	Tryptone N1
TNF- α	Tumor necrosis factor- alpha
Tregs	T Regulatory Cells
VEEV	Venezuelan Equine Encephalitis Virus
WHO	World Health Organization
WT	Wild Type
ZO	Zonula Occludens

Chapter 1 - Introduction

1.1 Parasitology and Parasitism

Parasitism is one member of a symbiotic relationship, whereby a host is utilised as an ecological niche (1). It is advantageous for some species which require a host during a parasitic phase in their life cycles; however, the presence of parasites within hosts for long periods of time usually leads to chronic disease. These parasitic diseases show a virtually worldwide distribution in humans and domestic and wild animals, especially in tropical and poor countries (2) due to the lack of hygiene and the sanitary conditions such as in wetlands and foods (3). Moreover, in some cases hosts are infected with more than one type of parasite (4) (5).

1.2 Trematoda or Flukes

Trematodes or flukes are a form of flatworms of the Phylum platyhelminthes. They are named trematodes because they contain prominent suckers, which help the parasite to adhere to host organs (6). There are estimated to be more than 18,000 species of trematodes, but not all are found in humans (7); however, some species of digenetic trematodes do cause infections in humans (8). Trematoda infect over two billion people worldwide, while the statistics in the livestock sector are unknown (9, 10). Furthermore, schistosomiasis and fascioliasis have been classified as one of the groups of neglected tropical diseases (NTDs) (11). Most flukes have a complex life cycle because they require intermediate hosts, and are also able to live for a long time inside a definitive host (12, 13); for example, the average life of *Schistosoma mansoni* adult worms in the human body

is thought to be 5 years (14). Flukes are classified according to their location in the organs of a host body, such as liver flukes and blood flukes (15). *Fasciola* species and *Schistosoma* species are liver flukes and blood flukes, respectively, and it has been recorded that these flukes infect high numbers of humans and animals worldwide (16-18). Helminths (a taxonomically controversial but very commonly used term for parasitic worms) and their eggs trigger the immune system and elicit a strong Type 2 helper response (Th2).

1.3 Fascioliasis

Fasciola and the common liver fluke are two names used for the same parasite. The infection caused by this parasite is called fascioliasis. *Fasciola hepatica* has been recognised since the pharaonic era and there is evidence of it in mummies; this was the first fluke discovered from the Trematoda class (19). At the end of 19th century, the life cycle of this parasite was elucidated (20). Currently, fascioliasis is classified as a foodborne trematode infection, because the metacercariae of this parasite often infect a host through the consumption of plants or drinking water (21). Fascioliasis has been reported to be a zoonosis (22).

There are two species which cause fascioliasis, *F. hepatica* and *Fasciola gigantica* (Figure 1.1 and Table 1.1), although this chapter will focus on *F. hepatica*. Each species of *Fasciola* requires for its life cycle a specific intermediate host (water snail), a definitive (human or animals) host, appropriate climatic conditions, and fresh water contaminated with cercariae which evolve into the encysted metacercariae on the surface of water plants (23), and this plays an important role in increasing the number of infected humans or

animals (24). In recent years, the number of imported sheep and cattle has increased, especially from countries where fascioliasis is endemic, due to a number of factors including price, and has led to an increase in the number of infected humans and animals (25). Fascioliasis was ignored in the past, and this has led to high levels of pathogenicity, as seen in Bolivia, Peru, Egypt and Vietnam, and this disease has been observed in several clinical situations (26).

F. hepatica infection has been reported to affect around 17 million people, with a further 180 million at risk in more than seventy countries around the world. It has been reported that *F. hepatica* can infect humans via the consumption of aquatic plants, which often grow near water contaminated with *Fasciola* from infected animal's faeces (27, 28). The infection of cattle (approximately 300 million) and sheep (approximately 250 million) results in an annual loss of US\$3 billion in affected countries (29-32), with the most affected being the owners within the animal husbandry industry (33). This has created a serious veterinary issue, and there are enormous losses in the agriculture sector in infected countries (34). The liver fluke is a hermaphroditic trematode and the worms of the fluke are able to attach to the wall of a host organism via an oral or ventral sucker. The worm has the ability to resist bile acid, digestive enzymes and is able to interact with the host immune system through proteases and antioxidant enzymes (35).

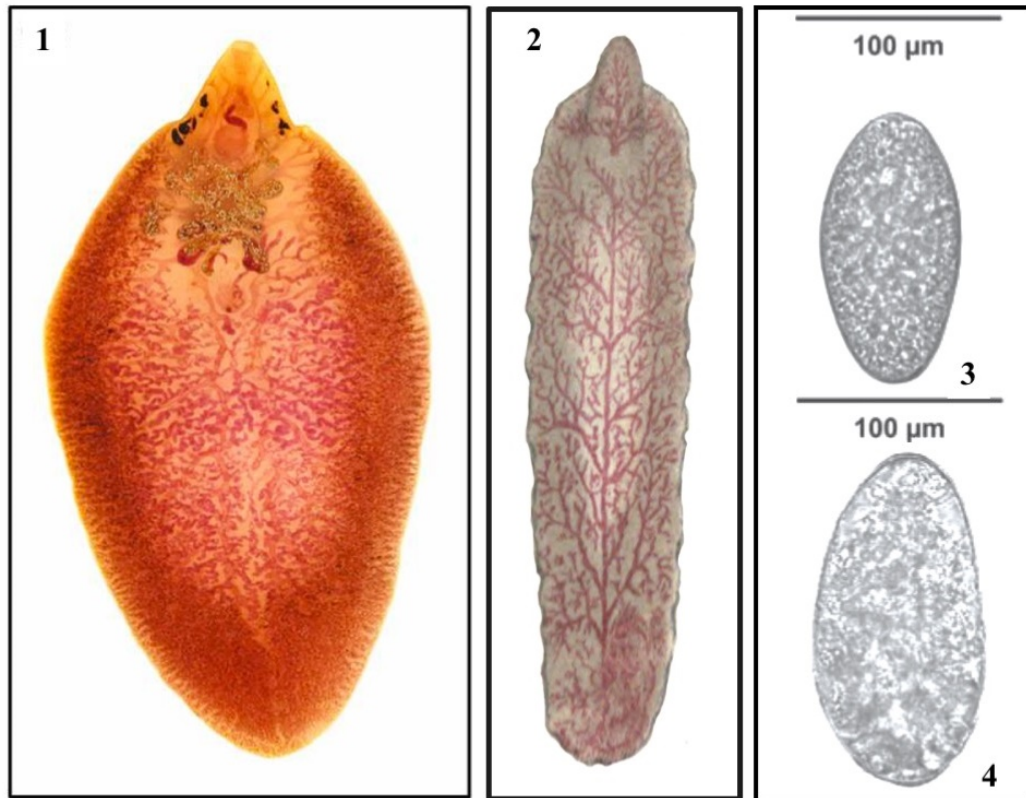


Figure 1.1: Adult worms and eggs which cause fascioliasis

(1 & 3) *F. hepatica*, and (2 & 4) *F. gigantica*. Both eggs are from infected humans: the 3rd image was taken from a Bolivian girl and the 4th image from a Nepalese girl (36). Sources: image 1 (37), image 2 <http://www.bif.org/species/113525060>.

F. hepatica is more prevalent than *F. gigantica*. *F. hepatica* appears in North America, Central America, South America (especially Bolivia, Peru, and Chile), all European countries, most Asian countries (especially Iran) and some African countries (especially in Egypt) (Figure 1.2) (22, 25, 38-40). It has been reported that *F. hepatica* has been found in humans in Iran, Vietnam, Egypt, France, Portugal, Spain, Cuba, Peru and Bolivia (41-44), with Bolivia and Egypt recording the highest number of cases of human infection, more than 360,000 and 830,000 infected humans, respectively (41). *F. gigantica* is found in Asian and Africa countries (45-47), and human infections have been reported in Egypt,

Vietnam and Thailand (34, 44, 48, 49). In the US, farm animals infected with *Fasciola* spp. are reported to range between 5.9% and 68%, depending on the states, whereas in Chile, Nigeria, Thailand, New Zealand, Spain, Switzerland and the UK, the reported rates are 94%, 43%, 47.1%, 8.5%, 29.5%, 18% and 10%, respectively (50-52).

Table 1.1: Comparison between the two species causing fascioliasis

	<i>F. hepatica</i> (53, 54)	<i>F. gigantica</i> (54-56)
	Liver fluke	Liver fluke
Adult worms	Length = 30 mm Width = 13 mm	Length = 30-70 mm Width = 10 mm
Intermediate host (snail)	<i>L. cailliaudi</i>	<i>L. columella</i> or <i>L. truncatula</i>
Egg	80 * 145 µm Ovoid shape, small, indistinct operculum and thin-shelled Yellow to light brown colour 25000 eggs per day in faeces	80 * 140 µm Ovoid shape, small, indistinct operculum and thin-shelled Yellow to brown colour 8000 to 10000 eggs per day in faeces

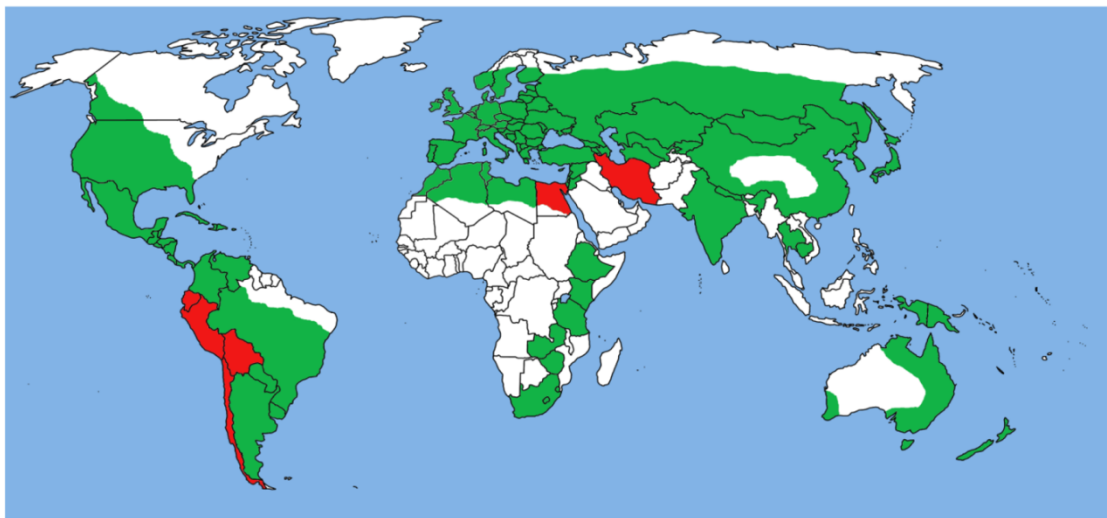


Figure 1.2: Global distribution of human *Fasciola* spp.

F. hepatica is present in North America, Central America, South America (especially Bolivia, Peru, and Chile), all European countries, most Asian countries (especially Iran) and some African countries (especially Egypt), whereas *F. gigantica* is found in Asian and African countries. Source: (57).

1.3.1 Life Cycle of *Fasciola* spp.

The life cycle of *Fasciola* spp. involves two hosts, an intermediate host (water snail) and a definitive (human or animals) host (Figure 1.3). *F. hepatica* and *F. gigantica* have the same life cycle; however, there are some differences in terms of the intermediate (snail) host and their final location in the definitive host (human or animals). The life cycle of *F. hepatica* and *F. gigantica* begins when an infected individual defecates close to fresh water, thereby shedding parasitic eggs into the environment. For example, it has been reported that from one gram of stool more than 5,000 eggs can be present for a human with a heavy *F. hepatica* infection (58, 59). As the eggs come into contact with water they shift from being unembryonated eggs to embryonated eggs, which ultimately hatch and release miracidia; this stage lasts approximately 2-3 weeks (60). The hatched miracidia swim in the water for only 24 hours, where they seek and penetrate specific snail intermediate hosts, *Lymnaea cailliaudi*, *L. columella* or *L. truncatula*, via their mechanical movement and digestive enzymes (22, 61, 62). After 4 to 7 weeks, the miracidium transforms into a sporocyst, and subsequently a high number of rediae, which develop into cercariae. It has been reported that more than 4,000 cercariae are released from each snail after their development (49, 63, 64). The cercariae stick to aquatic plants and then transform into metacercariae, which remain contagious for up to a month, depending upon the environmental conditions (65). The metacercariae of parasites often infect mammals through their consumption of aquatic plants (vegetables) or contaminated water (21), and fascioliasis has been reported to be a zoonosis (22). In a definitive host, following ingestion the metacercariae move to the duodenum, where they then penetrate the intestinal wall and target the liver (64, 66).

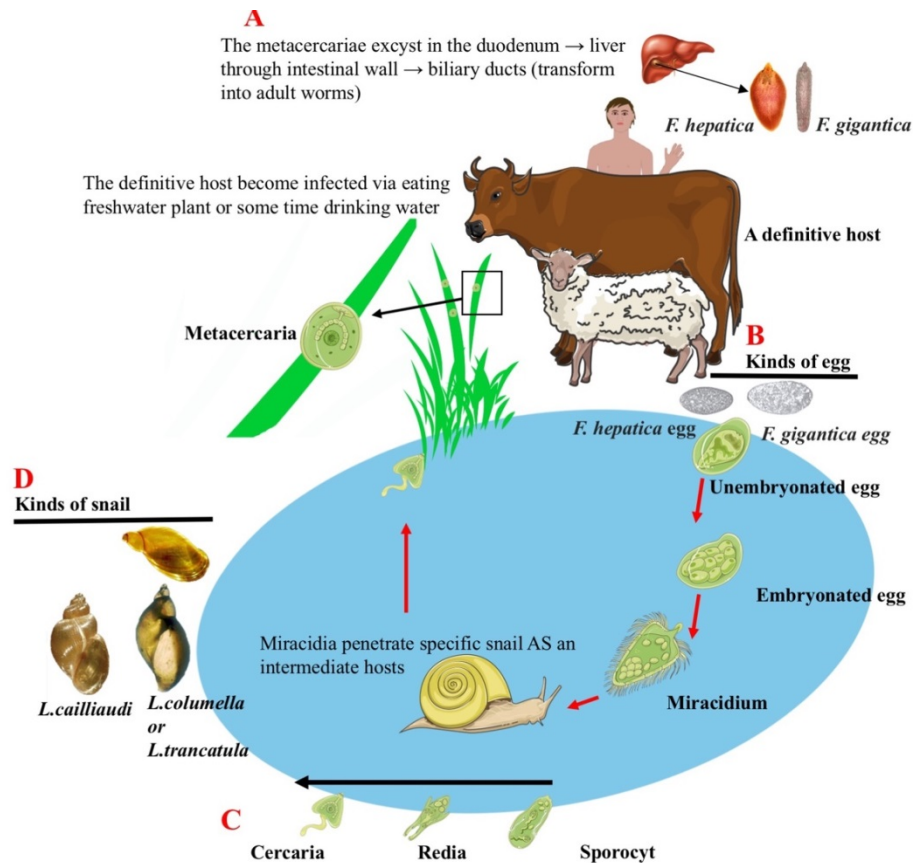


Figure 1.3: Life-cycle of *Fasciola* spp.

(A) Transformation from metacercariae to adult flukes in the definitive host; (B) Types of egg, unembryonated eggs become embryonated eggs hatch and release miracidia; (C) Developmental stages of the parasite inside the snail; and (D) different intermediate hosts (snails).

Subsequently, the metacercariae move from the liver to the biliary ducts, where they undergo further developmental changes to become an adult worm (67). *Fasciola* adult worms have been documented to live 13, 20 and 1-4 years in humans, sheep and cattle, respectively (68, 69). It is estimated that approximately 25,000 *F. hepatica* eggs and 8,000 to 10,000 *F. gigantica* eggs are present in faeces each day (Table 1.1). It has been recorded that the time required for the transformation from metacercariae to adult flukes is approximately 3-4 months in humans and 10-12 weeks in cattle and sheep (54, 70).

1.3.2 Diagnosis, Prevention and Cure

Fascioliasis is difficult to detect and eggs, which are recovered from stools, have to be identified using a light microscope. It takes several months before eggs are present in the faeces of an infected human or animal because the worm in the acute phase has not yet matured (71-73). Eggs can be collected from infected samples via filtration, centrifugation or sedimentation, and it has been reported that differentiation between *F. hepatica* eggs and *F. gigantica* eggs is difficult by microscopy (74), although fascioliasis eggs can be diagnosed using the Kato-Katz technique or FLOTAC method (75, 76). Counting eosinophilia present in a host's blood can assist in the diagnosis of fascioliasis in the early stages, and anaemia and hepatomegaly may also appear during early infections of humans (77-80). Ultrasound can be used to detect *F. hepatica* and *F. gigantica* worms due to hepatobiliary damage, hepatomegaly or their presence within biliary ducts (81, 82). Some modern technologies used in the detection of fascioliasis include antibody assays or serological tests, such as an enzyme-linked immunosorbent assays (ELISA) (83-85). A real-time polymerase chain reaction (RT-PCR) assay and other PCR-based techniques have also been used to detect *Fasciola* spp. DNA in stools or blood samples (86).

Some countries have tried to clean and control the intermediate host (snails) which is a prerequisite for completing the life cycle of the parasite (87-89). However, it is difficult to eradicate snails from the environment.

The drug triclabendazole (TCBZ) is the only safe drug available and is used as the primary agent for the treatment of both human and animal fascioliasis (90, 91). Emetine, dehydroemetine and bithionol are other medications used to treat this infection, but have more serious side effects (23, 26, 39). TCBZ has been successfully used to treat many

millions of people since 1997 in many infected countries (90); however, recent reports have noted a worrying rise in resistance for both human and animal fascioliasis (92, 93).

Consequently, the treatment of this disease may become more difficult in the future, and it is believed that a combined approach of vaccination for control and drugs for treatment will be required for the successful management of fascioliasis. However, current experimental vaccines which target proteins such as the *F. hepatica* helminth defence molecule (FhHDM) and *F. hepatica* peroxiredoxin (FhPrx) do not offer sufficient protection against parasitic infection, with efficacies ranging between 30% and 60% (94-96). The aim of these vaccines is to protect either humans or animals from disease for life (96). Many veterinary vaccines are currently in development, such as those that target the fatty acid binding protein (FABP), cathepsin L (CatL) and glutathione S-transferase (GST) (Table 1.2).

Table 1.2: Vaccine candidates for *Fasciola* spp.

Source: (97)

<i>Fasciola</i> spp.	Host	Vaccine and Major Antigens
<i>F. gigantica</i>	Cattle	FABP from native, GST from rGST <i>S. bovis</i> , GST from native, total CatL from native and peroxiredoxin (Prx) from rPrx, native paramyosin extracted from microfilariae and adults (an invertebrate muscle-associated protein).
	Buffalo	FABP from rFh15, FABP from rFABP, GST from Rgst, leucine aminopeptidase (LAP) from rLAP and FABP + GST from rFABP + rGST.
	Sheep	FABP from native, GST from native, total CatL from native and CatL from FasAc14p peptide.
	Goat	None yet
<i>F. hepatica</i>	Cattle	FABP from native, GST from native, CatL from native CatL1, CatL from rCatL1, cathepsin <i>F. hepatica</i> cysteine protease W (CPFhW) from recombinant inclusion bodies, haemoglobin (Hb) from rHbF2, Hb from native, paramyosin from native, Kunitz type molecule from native, CatL1 or CatL2 + Hb from native and CatL1 + CatL2 from native.
	Buffalo	None yet
	Sheep	FABP from native, FABP from <i>F. hepatica</i> 12 kDa protein (Fh12), FABP from rFh15, FABP from <i>rSchistosoma mansoni</i> (Sm)14, GST from native, total CatL from native, CatL from native CatL1, CatL from native CatL2, CatL from CatL1/ L2 mimotopes, cathepsin CPFhW from recombinant inclusion bodies, LAP from native, LAP from rLAP, paramyosin from native, Kunitz type molecule from native, CatL1 + CatL2 from native and CatL1 + CatL2 + LAP from native.
	Goat	FABP from rSm14 or rSm14 peptide, GST from native, CatL from CatL1, CatL from CatL1 mimotopes and Prx.

1.3.3 Immune Response to *F. hepatica* and *F. gigantica*

The immune system responds to the liver fluke during the early phase of infection and also at different developmental stages, enabling it to survive inside a host body (98). The first interaction occurs 24 hours after metacercariae have entered the host via the consumption of food or water, and by the seventh day *Fasciola* excretory/secretory (ES)

antigens interact with the immune cells of the host, including dendritic cells (DCs), mast cells and macrophages present in the peritoneal cavity and intestinal wall. In the third week, as a result of the interaction between ES antigens and the immune cells of the host, transforming growth factor beta (TGF- β) and interleukin-10 (IL-10) is produced by DCs, while macrophages also produce IL-10. This is associated with a Th2 response, which is triggered following the down-regulation of the type 1 helper (Th1) immune response, which is characterised by the production of cytokines, such as tumour necrosis factor-alpha (TNF- α) and interferon gamma (IFN- γ), and reduced activation of Th17-type immune responses (96, 99-102). There is an increase in the proportion of interleukin-5 (IL-5) and IL-10-producing CD4+ Th2 cells as a response to stimulation by *Fasciola* ES antigens (96). In the chronic stage of this parasitic infection, secretory proteins which can interact with the immune cells of the host are associated with a Th2 response, which is triggered following the down-regulation of an initial Th1-type response (98, 103). The Th2 response stimulates the secretion of immunoglobulin G1 (IgG1) with little or no specific IgG2 (104). This study focuses on two secreted proteins: *F. hepatica* glutathione S-transferase-sigma (FhGST-si) and *F. hepatica* histone H2A (FhH2A) present in *F. hepatica* adult worms.

FhGST-si, which is one of the major *F. hepatica* secreted molecules, is one of three GSTs that have been identified in *F. hepatica*(105). The GST family isolated from *F. hepatica* accounts for approximately 4% of the total soluble protein (106, 107). FhGST-si has been shown to possess prostaglandin-synthase activity and plays a role in detoxification (108). It has been shown that FhGST-si can induce interleukin-12 (IL-12), interleukin-6 (IL-6) and macrophage inflammatory protein 2 (MIP-2) in DCs. Thus, the function and

maturation of DCs may be able to regulate the response of the immune system induced during helminth infection(105). LaCourse *et al.* have shown that the pathology was significantly decreased in infected animals when FhGST-si was utilised as a trial vaccine in a goat (109); however, there was no decrease in the amount of worms. This lack of protection does not necessarily discount the importance of FhGST-si as a potential vaccine candidate, as shown by the strong reduction in pathology, but may indicate that a successful vaccination needs to target more than one individual antigen in the worm in order to be efficient.

The second identified potential infiltrin (or pathogen-secreted host nuclear protein) is FhH2A. Histone proteins are important for chromatin function and organisation in the nucleus, and involves 146 base pairs of DNA wrapped around eight core histone proteins consisting of two copies each of H2A, H2B, H3, and H4. These histones are important for cell division, DNA packaging, the regulation of transcription and DNA repair (110, 111). It has been shown that recombinant histone H2A, from the protozoan parasite *Leishmania*, has an active role in the immune regulation of the T cell response, which leads to stimulated peripheral blood mononuclear cells (PBMCs) and the secretion of IFN- γ (112, 113). The *Leishmania* histone H2A protein has been shown to play a role in protecting and reacting against *Leishmania* (114).

1.4 Schistosomiasis

Schistosomiasis and Bilharzia are two names used for the same parasitic disease that has been recognised since the ancient Egyptian era (115), and our understanding of schistosomiasis has evolved over many years. *Schistosoma haematobium* eggs have been

found in the kidneys of Egyptian mummies and there is evidence that *S. haematobium* was spread between members of the French army during the war against Egypt in 1799–1801 AD (116, 117). In 1851, Theodor Bilharz, a German pathologist, discovered *Distoma haematobium* eggs, later renamed as *S. haematobium*, in an Egyptian cadaver (118). Forty-seven years later, Stiles and Hassel identified a subfamily of *Schistosoma* which they named *S. mansoni*, in tribute to Sir Patrick Manson, the first person to describe the egg stage after identifying a *Schistosoma* egg with a large lateral spine present in the egg shell in the faeces of a soldier from the British Army stationed on an Indian island (119). Da Silva clarified the life cycle of this parasite in 1908 (120). *S. japonicum* was found in the portal venous system of a cat in 1904 (121) and a few years later in 1908, Da Silva clarified the life cycle of this parasite and described its pathology.

There are around 16 *Schistosoma* spp. or blood flukes distributed in several geographic locations (122), with three main species infecting humans: *S. haematobium*, *S. mansoni* and *S. japonicum* (Table 1.3); *S. intercalatum* and *S. mekongi* also infect humans but to a lesser degree (123). Each *Schistosoma* sp. requires for its life cycle a specific intermediate host (water snail), a definitive (human or animals) host, appropriate climatic conditions and fresh water contaminated with *Schistosoma* miracidia (124). Table 1.3 shows some of the differences between *S. haematobium*, *S. mansoni* and *S. japonicum* in terms of the morphology of adult worms and eggs (Figure 1.5). Recently, schistosomiasis has been reported to be a zoonosis and one of the most important (125). *S. mansoni* and *S. haematobium* can be seen as a disease with epidemic proportions, and many challenges. Some individuals are at greater risk of developing the disease, particularly those who live in countries with lower hygiene standards due to the availability of the intermediate host

in water contaminated with urine or faeces from infected individuals (126). This disease is common in swamp water areas, such as lakes and rice fields, and can lead to health crises in these geographic locations. Statistics indicate that 200 thousand people die each year, more than 200 million are infected, and approximately 800 million are at risk of schistosomiasis worldwide (16, 17). For example in Africa, *S. haematobium* and *S. mansoni* threaten more than 106 million people working and living near surface irrigation schemes or dams (126). These numbers are likely to continue to rise (126), (127) (128), unless effective control measures are put in place. In Sub-Saharan Africa, over 250 million people are infected by and schistosomiasis is reported to be the most common NTD. Recently, the disability-adjusted life years (DALYs) estimation for schistosomiasis has been reported as approximately 3.3 million (129, 130).

S. mansoni is perhaps the most prevalent of the three species and can be found in Africa (especially the south, sub-Saharan and Nile River area), South America (especially Brazil, Venezuela and Suriname), the Middle East and the Caribbean. *S. haematobium* is found in Africa (especially sub-Saharan, the south and north) and the Middle East, while *S. japonicum* appears in southeast Asia, Indonesia and some areas of China (131-134). Figure 1.4 shows the countries infected with *Schistosoma* spp. Schistosomiasis was declared eradicated from Japan in 1996, 13 years after the last reported infection.

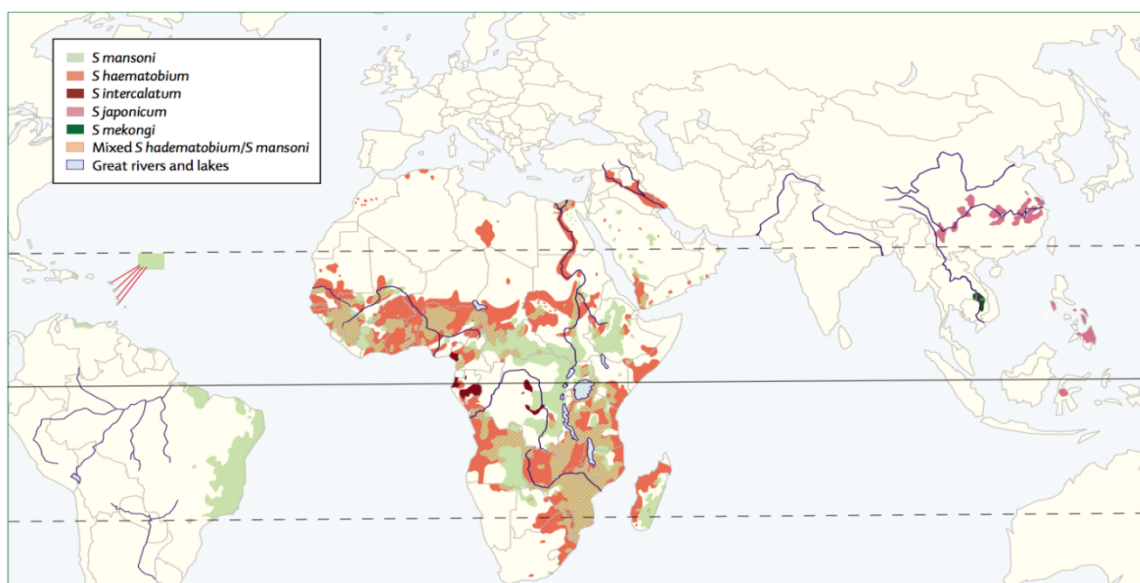


Figure 1.4: Global distribution of human *Schistosoma* spp.

S. mansoni is found in Africa, South America, the Middle East and the Caribbean; *S. haematobium* is found in Africa and the Middle East, whilst *S. japonicum* is present in southeast Asia. Source: (134).

Table 1.3: Comparison of schistosomes infecting humans

Source: (135, 136)

		<i>S. mansoni</i>	<i>S. japonicum</i>	<i>S. haematobium</i>
Adult worm	Location	Mesenteric veins		
	Female size	Length = 10-20 mm Width = 0.16 mm	Length = 20-30 mm Width = 0.16 mm	Length = 10-20 mm Width = 0.16 mm
	Male size	Length = 10-20 mm Width = 0.16 mm	Length = 10-20 mm Width = 0.16 mm	Length = 10-20 mm Width = 0.16 mm
	Life in the human body	The average is between 3 and 10 years, and in rare cases 25 years (14, 129).		
Host	Definitive	Humans, baboons and rats	Humans, bovines, rodents, dogs and pigs	Humans, pigs, dogs baboons and cats
	Intermediate Snail	<i>Biomphalaria glabrata</i>	<i>Oncomelania</i>	<i>Bulinus</i>
Egg	Size	61×140 µm	60×100 µm	62×150 µm
	Shape	Ovoid shape with large lateral spine in the egg shell	Round shape with small lateral spine in the egg shell	Ovoid shape and terminal
	Number of eggs shed per day	200 to 300 eggs in faeces	100 to 300 eggs in faeces	20 to 300 eggs in urine

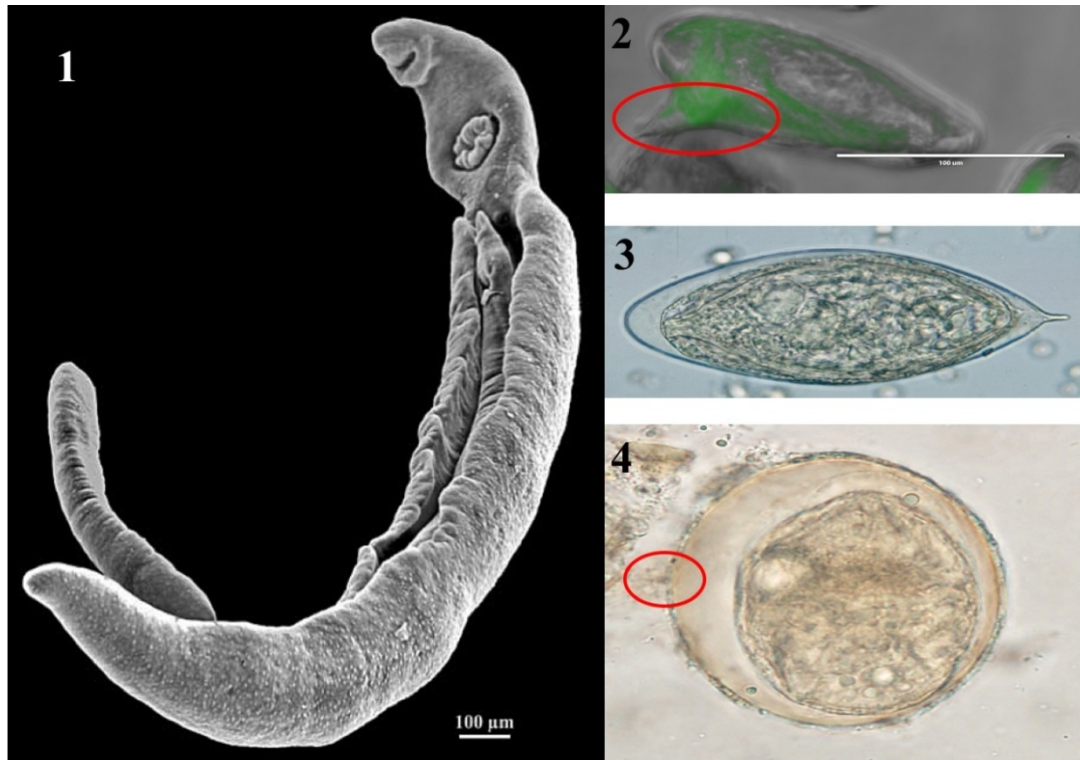


Figure 1.5: Schistosomes:

(1) Schistosome pair; eggs of: (2) *S. mansoni*; (3) *S. haematobium*; and (4) *S. japonicum*. The thin female schistosome is present within the male schistosome gynaecophoral canal (image 1). The red circles indicate the large lateral spine in the egg shell, which is a distinguishing and diagnostic feature of *S. mansoni* eggs (image 3) (137), and also the small spine (Knob) in the egg shell of *S. japonicum* (image 4).

Sources: image 1 (138), image 2 was visualised by fluorescence microscopy (EVOS *fl*, Advanced Microscopy Group, USA), and images 3 & 4 from <https://www.cdc.gov/dpdx/schistosomiasis/gallery.html>.

1.4.1 Life Cycle and Pathogenesis of Human *Schistosoma* spp.

The life cycle of human *Schistosoma* spp. involves two hosts, an intermediate host (water snail) and a definitive (human) host. *S. haematobium*, *S. mansoni* and *S. japonicum* have the same life cycle (Figure 1.6); however, there are some differences in terms of the species of the intermediate (snail) host and their final location in the definitive host (human). The life cycle of *S. haematobium*, *S. mansoni* and *S. japonicum* begins when an infected individual urinates (Sh) or defecates (Sm, Sj) close to fresh water, thereby

shedding parasite eggs into the environment. As the eggs come into contact with the water they hatch and release miracidia. The hatched miracidia swim in the water and seek out and penetrate specific snail intermediate hosts, *Bulinus*, *Biomphalaria glabrata* and *Oncomelania*, respectively, via their mechanical movement and digestive enzymes (139). The miracidium transforms into a primary sporocyst, and following this stage a high number of secondary (daughter) sporocysts grow, which develop into the larval stage, cercariae, and are capable of infecting mammals (140). Each one of these cercariae has a characteristic forked tail, which allows it to emerge from the snail into fresh water and then commence swimming (141). Humans can become infected with *S. mansoni* when standing or swimming in fresh water infested with schistosome-infected snails. Cercariae actively penetrate the human body through the skin, where the tail is shed and they transform into schistosomula after 24-48 hours, before migrating via the venous system to the lungs. After 5 days the schistosomula will have migrated to the heart (left side), before moving into the circulatory system, and then to the liver, where they undergo further developmental changes before travelling to the portal vein of the liver. The developing male and female schistosome pair settle in the mesenteric vein, and mature into adult worms (142, 143). Both sexes of adult worms mate in the portal vein and the female worms of *S. mansoni* and *S. japonicum* lay their eggs in the mesenteric vein and for *S. haematobium* in the venous plexus of the bladder (144, 145). It is estimated that approximately 20 to 300, 200 to 300 or 100 to 300 eggs, respectively, are released daily into human veins by a single female worm and their eggs are deposited in adjacent tissues (146). For *S. mansoni* or *S. japonicum*, the eggs move progressively towards the lumen of the intestine and the majority are shed in the faeces, although a small number may also

appear in the urine (147). However, for *S. haematobium*, the eggs move progressively towards the lumen of the bladder (148), although a substantial proportion of the eggs is carried away by the direction of the blood flow, and remain entrapped in the liver, causing granulomatous inflammation, the main pathology observed (149-151). In chronic infections this can lead to liver fibrosis and portal hypertension (152-154).

There are three stages of pathological response: migratory and acute schistosomiasis, and chronic disease, which is dependent on the eggs rather than the adult worms or larvae. In migratory and acute schistosomiasis, the skin is inflamed, which leads to itchy, maculopapular rashes might develop within hours to a few days (134, 155). From 4 to 10 weeks after the initial ingestion, schistosomulae migrate through the venous system (bloodstream) to the lungs, and then to the liver (143). This is acute schistosomiasis, also called Katayama fever and is the morbid phase which is linked to the beginning of the release of eggs from adult female worms that leads to allergic responses (156). There are several symptoms during this stage, including fever, muscle pain, abdominal aches, fatigue, malaise, gastrointestinal discomfort and lymphadenopathy (157).

The chronic stage occurs after adult worms have laid their eggs and these have accumulated within tissues. Approximately 50% of the eggs laid by female worms remain in the host and this leads to acute and chronic inflammatory responses in the host tissues (158). Eggs from *S. japonicum* and *S. mansoni* accumulate in the portal triad of the liver, which causes Symmers' clay pipestem fibrosis of the liver (159). Eggs also accumulate in the intestinal wall for *S. japonicum* and *S. mansoni* or the bladder wall for *S. haematobium*, leading to inflammation and fibrosis in the surrounding tissues (134, 160, 161). The antigens of *S. japonicum* and *S. mansoni* eggs lead to granulomas,

inflammation, fibrosis and the occlusion of portal veins, which can lead to portal hypertension and venous pressure, ascites and hepatosplenomegaly, or splenomegaly (162-164). It has been reported that some *S. japonicum* or *S. mansoni* eggs might pass through the liver and return to the lungs and nervous system, and this can cause many health problems, such as spinal cord granulomas and occasionally can enter the brain (137). *S. haematobium* can cause bladder fibrosis, increased urinary frequency and haematuria (blood in urine) (165-167). Furthermore, it has been reported that the accumulation of *S. haematobium* eggs can lead to urethral, genital tract and kidney problems, and also carcinomas in the wall of the bladder (168, 169).

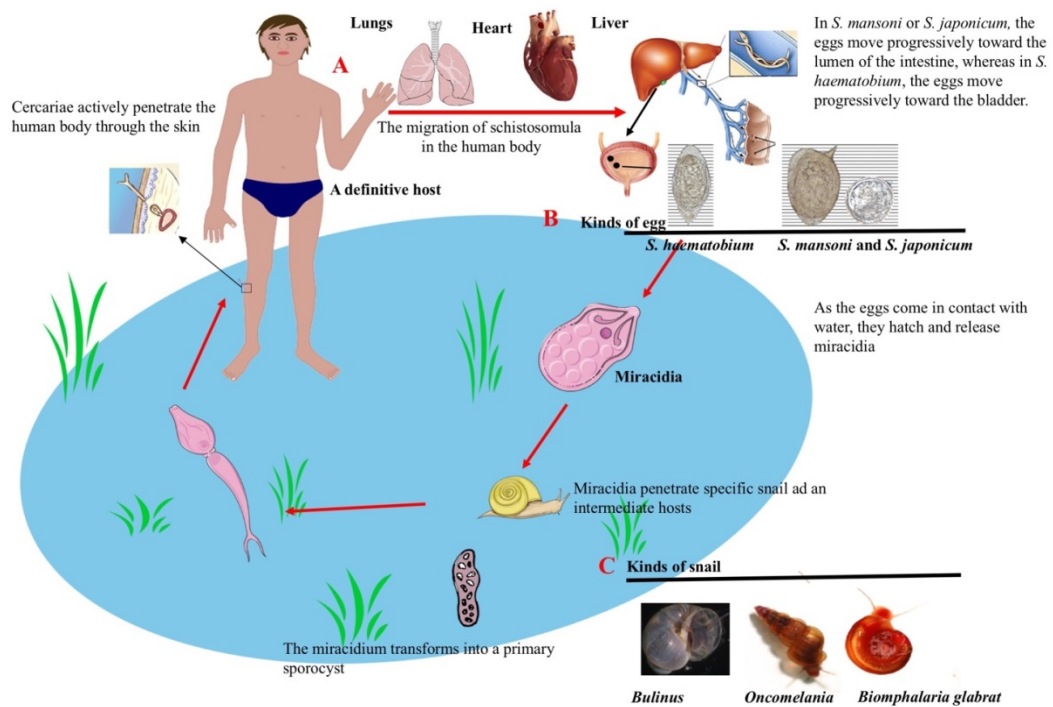


Figure 1.6: Life cycle of human *Schistosoma* spp.

(A) Transformation from cercariae to adult flukes in the definitive host; (B) Human *Schistosoma* egg spp., which hatch and release miracidia; (C) Intermediate hosts (snails).

1.4.2 Diagnosis, Prevention and Cure

Schistosomiasis is easy to detect and eggs recovered from urine or stools are identifiable by microscopy. Eggs are collected from infected samples via filtration, centrifugation or sedimentation and it has been reported that the number of *Schistosoma* eggs isolated from urine and stools is 33-100/10 mL and around 113/gram, respectively (170-174). The lateral spine in the egg shell is a distinguishing and diagnostic feature of *S. mansoni* eggs (137), whereas *S. japonicum* eggs are round in shape with a small lateral spine (knob) present in the egg shall, and *S. haematobium* eggs are oval with a sharp terminal spine (135, 136). The Kato-Katz technique or Kato technique is used to screen schistosomiasis eggs (175). Recently, the mini-FLOTAC method has been developed (176), while ultrasound can also be used to detect schistosomiasis eggs in infected tissues through endoscopic biopsies (177). Some modern technologies are also used in the detection of schistosomiasis, for example antibody assays and serological tests (178-181), together with real time PCR and other PCR-based techniques to detect *Schistosoma* DNA in urine, stool or blood samples (182-185).

In recent years, many affected countries have tried to reduce schistosome infections by providing clean water for drinking and daily use, together with sewage disposal and the draining of swamp water to control for snails (186, 187). Praziquantel is the only drug available for the prevention and treatment of human schistosomiasis (188, 189). This drug has been used successfully over four decades in many infected countries; however, it does not protect against re-infection (190, 191). Praziquantel has been used to treat more than 40 million infected people across the globe, and the World Health Organization (WHO) aims to treat over 100 million infected people per year (16). However, recent reports have

noted increased resistance against this drug (192-194), which will make treatment more difficult in the future. Consequently, similarly to what has already been said regarding fascioliasis above, it is believed that a combined approach of vaccination for control and drugs for treatment will be required for the successful management of schistosomiasis. There have been many attempts to produce vaccines, including Sj23 and SjTPI, Sm14/GLA-SE, Sm-TSP-2; Sm-p80, Bilhvax, Sj97 and SjIR (Table 1.4), but no vaccine has yet been developed for schistosomiasis (195). Many of the current experimental anti-schistosomiasis vaccines targeting proteins are failing to reach the 40% threshold set as a benchmark by the WHO, and even the most promising candidate (Sm Tsp-2) only achieved 57% and 64% in terms of a reduction in adult worm and liver egg burden, respectively (196).

Table 1.4: Vaccine candidates for schistosomiasis

Vaccine and Major antigens	<i>Schistosoma</i>	Status	Developer
Sj23 and SjTPI DNA prime, recombinant protein boost Sj23 (Tetraspanin) and SjTPI (Glycolytic enzyme)	<i>S. mansoni</i> <i>S. haematobium</i> <i>S. japonicum</i>	DNA vaccine trials in water buffaloes and cattle	Univ. of Georgia, Wellcome Trust, NIAID* and NHMRC*
Bilhvax, which is formulated with an alum hydroxide adjuvant. Sh28GST (28-kDa recombinant glutathione-S-transferase) (197, 198)	<i>S. haematobium</i>	Still in Phase III trials in West Africa	INSERM* and Institut Pasteur

Vaccine and Major antigens	<i>Schistosoma</i>	Status	Developer
Sm14/GLA-SE, Sm-14 (14-kDa recombinant fatty acid binding protein) with the adjuvant GLA (199).	<i>S. mansoni</i>	Phase I trials and Phase II trials was planned for 2015 in Africa and Brazil	Oswaldo Cruz Foundation (Fiocruz) tem, WHO
Sm-TSP-2, (9-kDa recombinant tetraspanin) Alhydrogel® with or without GLA (200).		Phase I trials since 2014 at Baylor College of Medicine	Sabin Vaccine Institute and Blavatnik Charitable Foundation Mort Hyman NIAID*
Sm-p80, (a large calpain subunit) with adjuvant. It is a cross-species protection against adult worm (201, 202).		Preclinical process development. it has shown a protection both in mice and baboons.	Texas Tech Medical Center
Sj97 (paramyosin) with adjuvant ISA206 (203).	<i>S. japonicum</i>	Proof-of-concept in animals	Brown University and NIAID*
SjIR, Bivalent [SjIR (insulin receptor), which binds mammalian host insulin, or with SjTPI] recombinant proteins with adjuvant. The glycolytic pathway enzyme triose-phosphate isomerase (TPI) (204).	<i>S. japonicum</i>	Proof-of-concept in animals	Queensland Institute of Medical Research and NHMRC*

*France's Institut national de la santé et de la recherche médicale (INSERM), Australia National Health and Medical Research Council (NHMRC), the National Institute of Allergy and Infectious Diseases (NIAID).

1.4.3 Schistosome Infection and the Immune Response

The immune system responds to this parasite at different developmental stages in different tissues, for example cercariae in the skin, schistosomula in the lung, adult worms in the blood, and eggs in the tissues (Figure 1.7). In the first five weeks, the development of cercariae occurs, and these penetrate the host skin and lead to an IgE-mediated

hypersensitivity reaction in people who have been previously exposed, whereas immunologically naïve individuals, who have never been infected with schistosomes before, will not have any parasite-specific IgE (205), followed by a switch to schistosomula before passing through the lung via the pulmonary artery, leading to the initial immune Th1-type immune response, which is characterised by the production of cytokines including TNF- α and IFN- γ (206-208). The production of IFN- γ and TNF- α has an active role in the regulation of granulomas (209). In murine infection models an increase in the level of IFN- γ leads to a reduced risk of hepatic periportal fibrosis and this has also been observed in infected humans (210, 211), while TNF- α and the cytokines of the Th2-cell response are associated with a progression towards the chronic stage (212). Murine models of schistosomiasis suggest that in weeks seven and eight and after the deposition of eggs, the Th1-like response shifts to Th2-cell response, characterised by the production of cytokines such as IL-4, IL-10, IL-6, IL-9, IL-5 and IL-13 (207, 213), and immunoglobulin isotype switching to IgG1 (in mice; the corresponding human isotype is IgG4) and IgE (214, 215). DCs, with the help of surface molecules such as CD40 and CD154, are instrumental in stimulating a Th2 response (216). In the chronic stage levels of regulatory T cells (Tregs), IL-4, IL-13 and TGF- β all rise. This leads to an increase in the proportion of collagen inside the tissues, which leads to progressive fibrosis and destruction or loss of function of these tissues (217, 218).

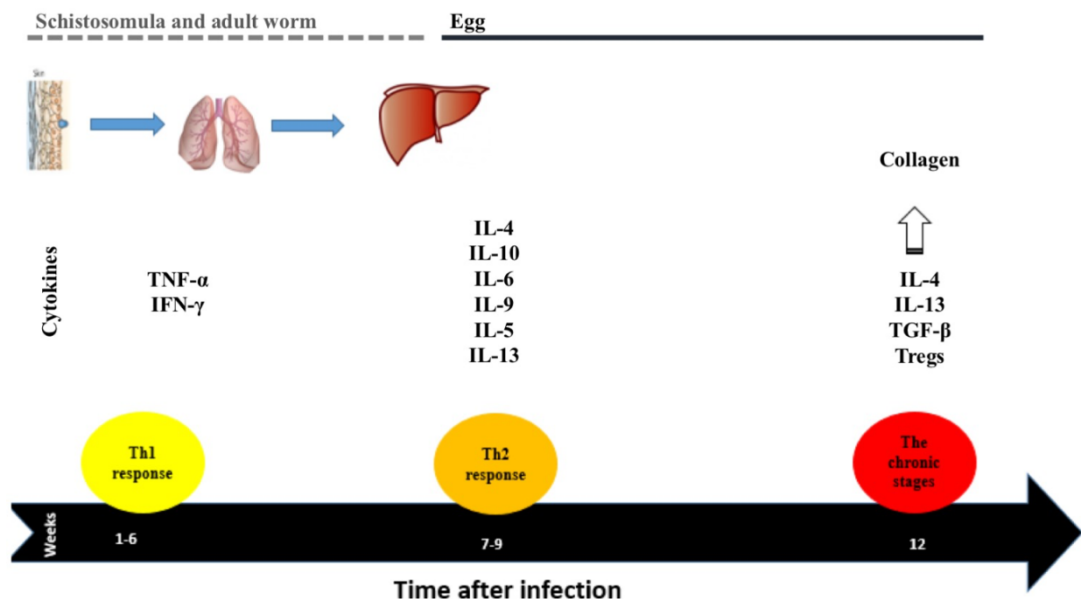


Figure 1.7: Immune response to Schistosome infection

There is a Th1-type immune response characterised by the production of cytokines (TNF- α and IFN γ) during the schistosomula and adult worm stage (weeks 1-7). After deposition of the eggs and egg secretions (weeks 7-9), a Th2-type immune response characterised by the production of cytokines such as IL-4 and IL-10 is initiated. During the chronic stage levels of regulatory T cells (Tregs), IL-4, IL-13 and TGF- β increase the proportion of collagen inside the tissues.

1.4.4 Immune Response to Schistosome Eggs

Interestingly, during their life cycle the eggs of these parasites have an active role, especially in immune interactions. Therefore, this study focuses on different egg secretory proteins (ESP) from *S. mansoni* and *S. haematobium*. Mature eggs consist of an outer shell, three layers around the embryo (miracidium) and the embryo itself. Layer sequences are as follows: Underneath the hard egg shell, the Reynold's layer, followed by von Lichtenberg's envelope, and Lehman's lacuna, which is surrounding the embryo (Figure 1.8) (219-222). These eggs normally require six days after oviposition to develop into a mature miracidium.

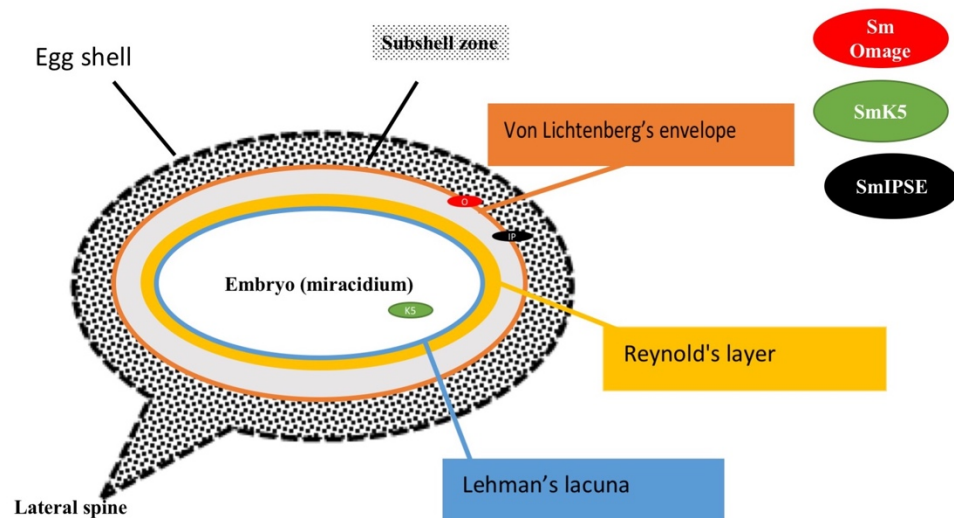


Figure 1.8: A mature *S. mansoni* egg.

There are three layers around the embryo (miracidium): Lehman's lacuna, Reynold's layer and closely adheres to Von Lichtenberg's envelope. IPSE/alpha 1 and omega-1 (black and red circle, respectively) are secreted from the von Lichtenberg's envelope into the subshell zone, while kappa-5 is produced by the miracidium (green circle) in the subshell zone.

Ashton et al. (2001) indicated that only mature eggs are able to release egg secretory proteins (ESPs), especially IPSE/alpha-1 in *S. mansoni*, but not by other stages, such as from adult worms or cercariae (223, 224). Proteins such as IPSE/alpha-1 and Omega-1, which are collectively known as ESPs, are secreted from the von Lichtenberg's envelope into the subshell zone, and gain access to host's tissues through channels present in the egg pore channels present in the shell of the egg (146, 220, 225). Kappa-5 is produced by the miracidium of *S. mansoni* eggs in the subshell zone(226), but has not been described for *S. haematobium* eggs in the literature. Soluble egg antigen (SEA) is a complex water-soluble somatic extract of eggs consisting of various glycoproteins and other components, including large amounts of IPSE/alpha1, omega-1 (223, 224, 227) and kappa-5 (222, 221). These proteins are heavily glycosylated. The role of kappa-5 remains unknown

(146), but it is synthesised in the von Lichtenberg's envelope; however, it does not appear to be secreted by the eggs while in the host tissues (228). Accumulation of eggs and their components leads to inflammation and fibrosis in the surrounding tissues (165, 166). The antigens of schistosome eggs lead to granulomas, inflammation and fibrosis, but while indicating pathology, the granulomas also protect the host from the toxins secreted by these eggs (229).

In terms of the immune response, the egg stage triggers the immune system and elicits a Th2 response (215, 230-232). Proteins from human schistosome eggs have been classified into two types: ESPs and SEA (233, 234), with only mature eggs able to release ESPs such as IPSE/alpha-1, Omega-1 and kappa-5 (Figure 1.8) (222, 226, 235-237) as main components. In 2007, 188 ESPs were identified in *S. mansoni* by proteomic analysis, and 32 of them were novel (238). IPSE/alpha-1 and omega-1 are the most cationic egg fraction-6 (CEF-6) of the SEA in the secretion of *S. mansoni* eggs (239) and these glycoproteins play an important role in host infection for both *S. mansoni* eggs and *S. haematobium* eggs (240).

Omega-1 is a 31 kDa glycoprotein monomer (229). The protein is able to access the cytoplasm of host cells, via various carbohydrate binding receptors. Through the activation of DCs, this glycoprotein is able to drive a Th2 response, and SEA depleted of omega-1 is unable to achieve this (247). *S. mansoni* eggs have been deposited in the livers of mice *in vivo*, and were normally driven via a Th2 granulomatous response, including the cytokines IL-4, IL-5 and IL-13 which will promote switching to Th2 (218, 241). Th2 cells, Tregs and innate cells, for example macrophages, produce IL-10 and increases the production of Th2 cytokines (218, 242). Cooperation between IL-10 and the Th1 response

leads to a reduction in the proportion of collagen inside the tissues (243, 244), which is followed by an increase in the proportion of IL-5 and IL-13-producing CD4⁺ Th2 cells. Chronically, in humans there is a decrease in IL-10 and IFN- γ with periportal fibrosis (245). There are two N-glycosylation sites present within the structure of omega-1, and both sites are fully occupied with core-difucosylated diantennary glycans with one or more LewisX-motifs in the antennae (235). In DCs, omega-1 inhibits protein expression and this leads to a lack of IL-12 and then prevents Th1 polarisation, thereby reducing the response between DC and Th1, and stimulating the production of a Th2 response (171, 246, 247). Pure native omega-1 is hepatotoxic both *in vivo* and *in vitro*, and is a functional T2-type RNase (248, 249). The carbohydrates post-translationally of omega-1 is homologous to the glycosylation of IPSE/alpha-1(236).

IPSE/alpha-1, also known less commonly as SmEP25(228), is secreted as a glycoprotein (250, 251), and is the second most abundant ESP after omega-1 (248, 252, 253). IPSE/alpha-1 is a highly antigenic protein with a homodimeric structure (228, 254). In recent years it has been shown that IPSE/alpha-1 from *S. mansoni* eggs and *S. haematobium* is able to activate basophils via an IgE-dependent, but not antigen specific mechanism, resulting in the production of IL-4 and IL-13 (250, 255). IL-4 release from basophils plays a significant role in developing a polarised Th2 response, whereas IL-13 plays an important role in protective immunity (256), but is also responsible for pathology, due to its pro-fibrotic activities (increased collagen deposition by fibroblasts; see below). The active principle, called IPSE, has been cloned and shown to be identical with a previously described protein called alpha-1, one of the two components of the CEF-6 fraction; and both IPSE and alpha-1 have the same molecular structure and almost the

same N-terminal sequence (223). The homodimeric form of this protein contains four disulphide bridges, three intramolecular and one between two monomers, which are formed by the seven cysteine residues present in the primary sequence (257). IPSE/alpha-1 can interact with immune cells of the host associated with a Th2 response, which is triggered following the down-regulation of an initial Th1-type response. This response by regulatory IL-10, has a central function for alternatively activated macrophages (AAMs), and is stimulated by IL-13, IL-4 (98, 103, 258). During the same stage, Tregs, IL-4, IL-13 and TGF- β levels all rise, leading to an increase in the proportion of collagen inside the tissues, resulting in progressive fibrosis and the destruction or loss of function of these tissues (217, 218). IPSE/alpha-1 has the ability to interact with DCs via binding to C-type lectin receptors (CLRs) such as the mannose receptor (MR) and Dendritic Cell-Specific Intercellular adhesion molecule-3-Grabbing Non-integrin (DC-SIGN) (259).

Kappa-5 is classified as a third *S. mansoni* egg glycoprotein (260), but it may not be secreted(226) through the pores present in the shell of *S. mansoni* eggs due to its size; consequently, and in contrast to IPSE/alpha-1, kappa-5 is not detected in tissue sections surrounding the eggs (261). Kappa-5 (Smk5), which is not found in ESPs, has been identified in both *S. mansoni* eggs and miracidia (226, 262, 263). According to Schramm et al. (2009), kappa-5 is approximately 100 kD, which is identical to a dimeric protein called gp50 from SmEA. IgG and IgE antibodies recognise kappa-5 in Western blots(226). This glycoprotein is a target for antibodies, specifically IgE, in sera from individuals infected with *S. mansoni* (226, 262, 264). Mass spectrometry analysis has shown that the isomer of kappa-5 (50 kDa) includes four positions available for N-glycosylation, and immunogenic GalNc β 1-4GlcNAc (LND) termini(222). For *S. mansoni*

there is binding between kappa-5 and IgG or IgE in sera from infected patients(226).

Figure 1.9 presents the putative roles of IPSE/alpha-1, omega-1 and kappa-5 from human schistosome eggs in the mechanism of immune regulation.

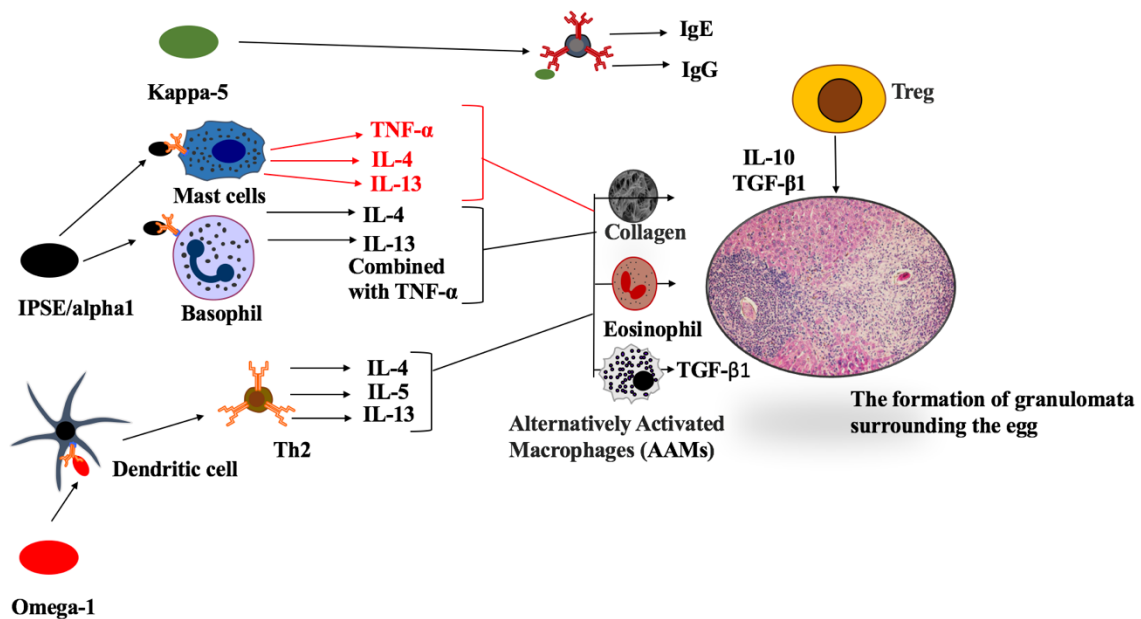


Figure 1.9: Mechanism of immune regulation by the major components of a schistosome egg.

Omega-1 through activation of DCs after binding to the mannose receptor is able to drive a Th2 response and prevents Th1 polarisation. This Th2 response includes the cytokines IL-4, IL-5 and IL-13. IPSE/alpha-1 also has the ability to interact with DCs via binding to C-type lectin receptors (CLRs). This response regulates IL-10, and has a central function for AAMs, and is stimulated by IL-13, IL-4. During the same stage Tregs, IL-4, IL-13 and TGF- β levels rise, leading to an increase in the proportion of collagen inside the tissues, progressive fibrosis and the destruction or loss of function of these tissues. Kappa-5 plays an important role in inducing IgE and IgG secretion from B cells. This is a target for antibodies, specifically IgE, in sera from individuals infected. This figure has been modified from (259).

1.5 Infiltrins

Infiltrins (or pathogen-secreted host nuclear proteins) are a putative new class of proteins. Based on our definition, infiltrins are parasite-secreted proteins with the ability to invade host cells. Infiltrins could be of two types: cytosolic infiltrins (represented e.g. by omega-1) and nuclear infiltrins (represented by IPSE/alpha-1). In both cases, the effects of the pathogen-derived factors would be unfolded inside the cell, in contrast to effects based on signalling through external membrane receptors only. This work focuses entirely on nuclear infiltrins, and we shall henceforth use the term infiltrin, without any adjective. Once inside the nucleus, these proteins can translocate into the nucleus, bind to DNA, and act as transcription factors, potentially creating an environment conducive to parasite survival, transmission and/or immune evasion. For example, in the nuclei of host cells, IPSE/alpha-1 is likely to play an essential role in the modulation of the immune response (265), and this would suggest that infiltrins may be better targets for vaccination because they act as ‘master switches’. This means that by targeting just one protein (the infiltrin vaccine antigen), it is possible to target multiple downstream products which are modulated by the infiltrin’s transcriptional or other yet to be elucidated nuclear activities. In other words, such vaccines could act as multi-target vaccines. This might provide long-lasting protection hence more efficient vaccines against helminthic parasites.

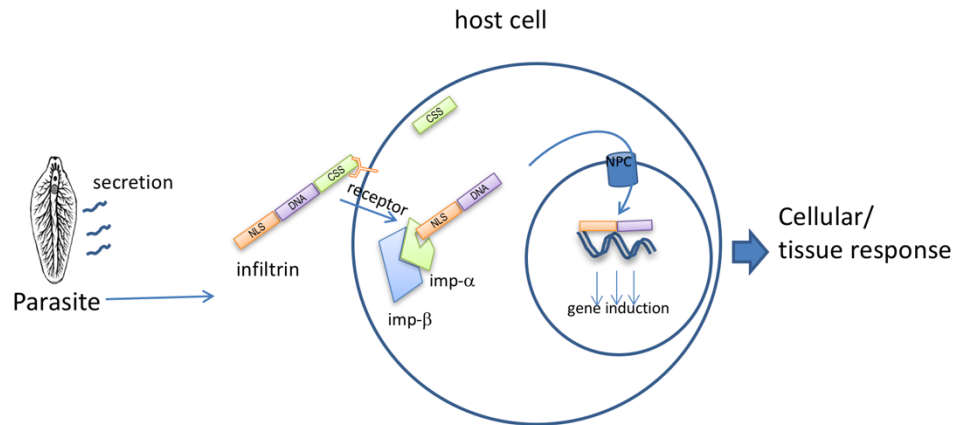


Figure 1.10: Suggested mechanism of infiltrins (working hypothesis)

Infiltrins (or pathogen-secreted host nuclear proteins) are secreted by a parasite and have the ability to enter host cells, either via receptors or via other properties (e.g. cell penetrating peptide-like activities). Once inside, nuclear infiltrins can interact with the host cell nuclear import machinery, e.g. the karyopherins importin α/β (imp- α , imp- β), and translocate to the nucleus through the nuclear pore complex (NPC). Once inside the nucleus, an infiltrin can bind to the DNA and act as a transcription factor, inducing an environment conducive to the parasite's survival and/or transmission.

IPSE/alpha -1 contains a classical secretory signal (CSS) of twenty amino acids at the N-terminus which enables interaction with plasma membrane receptors for successful export through co-translational insertion into the endoplasmic reticulum, and a C-terminal nuclear localisation signal (NLS) consisting of seven amino acids, namely PKRRRTY (223, 265). The signal-recognition particle (SRP) involved in co-translational transport is important in directing the secretory polypeptide chains into the endoplasmic reticulum (ER) lumen by recognising and binding to the CSS, even before the NLS is translated (223, 265, 266). As the targeting to the ER is co-translational, proteins with dual CSS/NLS signals are not able to reach the nucleus of the producing cell even if a C-terminal NLS is present(265). Conversely, the CSS is not usually present in predominantly nuclear proteins, and the CSS motif in IPSE/alpha-1 is cleaved during export(223). IPSE/alpha-1

is largely secreted from the von Lichtenberg's envelope into the subshell zone of mature *S. mansoni* eggs, and reaches into the surrounding host tissues through channels in the egg shell (146). Our group has shown that the C-terminal sequence 125-PKRRRTY-131 is the NLS of mature IPSE/alpha-1, and this plays a necessary and sufficient role in the process of transferring this protein into the nuclei of host cells. This has been observed in the human hepatoma (Huh7) and human osteosarcoma (U-2 OS) cell lines *in vitro* (265). Therefore, IPSE/alpha-1 has both features postulated for infiltrins (Figure 1.11).

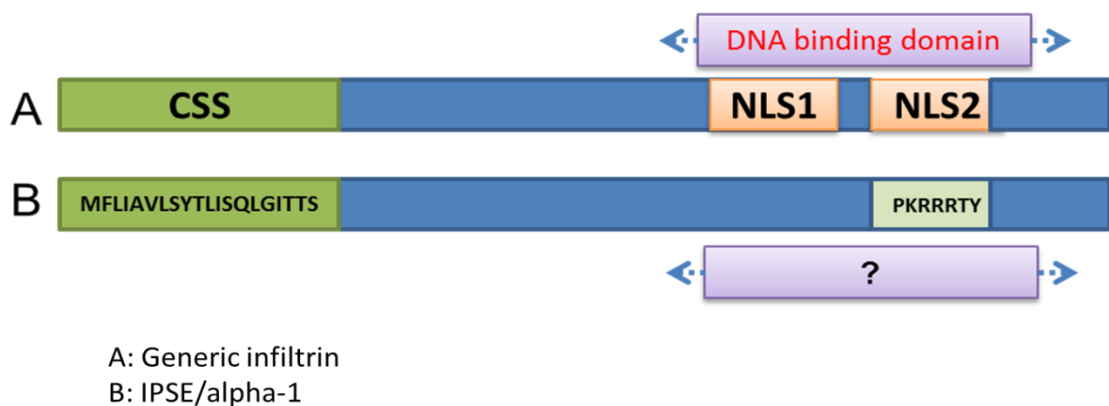


Figure 1.11: General postulated features of infiltrins as seen in IPSE/alpha-1

Infiltrins possess an N-terminal classical hydrophobic secretory signal (CSS) and at least one C-terminal NLS, which can be bipartite or monopartite (A shows a bipartite NLS). Our archetypal infiltrin IPSE/alpha-1 consists of twenty amino acids located at the N-terminus (CSS) and a monopartite PKRRRTY NLS close to the C-terminus. The DNA binding domain has not yet been accurately mapped in IPSE/alpha-1, but is thought to overlap at least in part with the NLS, as IPSE variants with a 10 AA C-terminal truncation do not bind to DNA (267).

1.6 Aims and Objectives

This study seeks to determine whether in addition to IPSE/alpha-1, other parasite-derived secreted factors have the ability to translocate to host cell nuclei. This will be achieved as follows:

- I. Using different bioinformatics tools to assess the existence of candidate infiltrins in *Fasciola hepatica*
 - a. To analyse *Fasciola hepatica* protein sequences predicted in the genome by using default parameters in local installations of NGLoc, NLStradamus and SignalIP and by the Yloc-HTTP client.
 - b. Bioinformatic analysis to predict the existence of a NLS for the IL-4 inducing principle from *S. haematobium* eggs (ShIPSE03), kappa-5 from *S. mansoni* eggs (Smk5), *F. hepatica* glutathione S-transferase- sigma (FhGST-si) and *F. hepatica* histone H2A (FhH2A) .
- II. To recombinantly express and purify candidate infiltrins (ShIPSE03, Smk5, FhGST-si and FhH2A).
- III. To confirm the bioinformatics prediction, by mapping and verifying functionality of the predicted NLS of each candidate infiltrins.
 - a. To assess cellular uptake by treating HTB9 or Huh7 cells with recombinant protein for each candidate infiltrin.
 - b. The ability of the potential infiltrins (ShIPSE03, Smk5 FhGST-si and FhH2A) to translocate into HTB9 or Huh7 cell nuclei will be determined by cloning the genes into the plasmid, pAcGFP1-C3. This will result in

an in-frame fusion with a gene encoding a green fluorescent protein (GFP). Truncated versions fused with GFP will be generated to determine the position of the NLS in the ep[roteins (NLS mapping)

- c. The predicted NLS motif of each infiltrin will be cloned into Tetra-EGFP plasmids (fusion protein of > 100 kDa that is completely excluded from the nucleus in the absence of a functional NLS)

IV. Assessing whether IPSE/alpha-1, has the ability to disrupt the integrity of a model gut epithelial membrane (Caco-2) by measuring the trans-epithelial electrical resistance (TEER). Three possible effects of IPSE/alpha-1 on tight junction (TJ) proteins and gut epithelial membrane integrity will be assessed.

- a. Whether IPSE/alpha-1 targets the intestinal mucosa causing increased intestinal permeability, leading to the induction of a pathologic opening of the intestinal TJ barrier, allowing increased epithelial paracellular transport.
- b. Whether IPSE/alpha-1 with activation of cells from the blood and tissues, such as resident mast cells is able to induce Th2 responses, leading to the opening of TJs between epithelial cells. Here, there are two main points:
 - i. Are effects of IPSE/alpha-1 on epithelium mediated by nuclear activities (e.g. transcription factor-like activities)?
 - ii. Are the effects on epithelium mediated by cytokines induced by IPSE from surrounding cells, e.g. mast cells, releasing TNF-alpha and Th2 cytokines?

- c. Initial investigation of the potential role of resident mast cells as a source of TNF-alpha and Th2 cytokines using basophil reporter cell lines (RS-ATL8 and NFAT DsRed).

V. Assessment of the potential cytotoxicity of IPSE/alpha-1

- a. Toxicity of IPSE/alpha-1 will be measured using different types of *in vitro* viability assays.
- b. The level of mRNA of alanine transaminase will be measured after treating the human hepatoma (Huh7) cell line with wild type and mutant IPSE/alpha-1 by using qRT-PCR.

Overall, the experiments in this section will inform us whether any effects on integrity of epithelial cells (assessed under IV above) are related to cytotoxic effects.

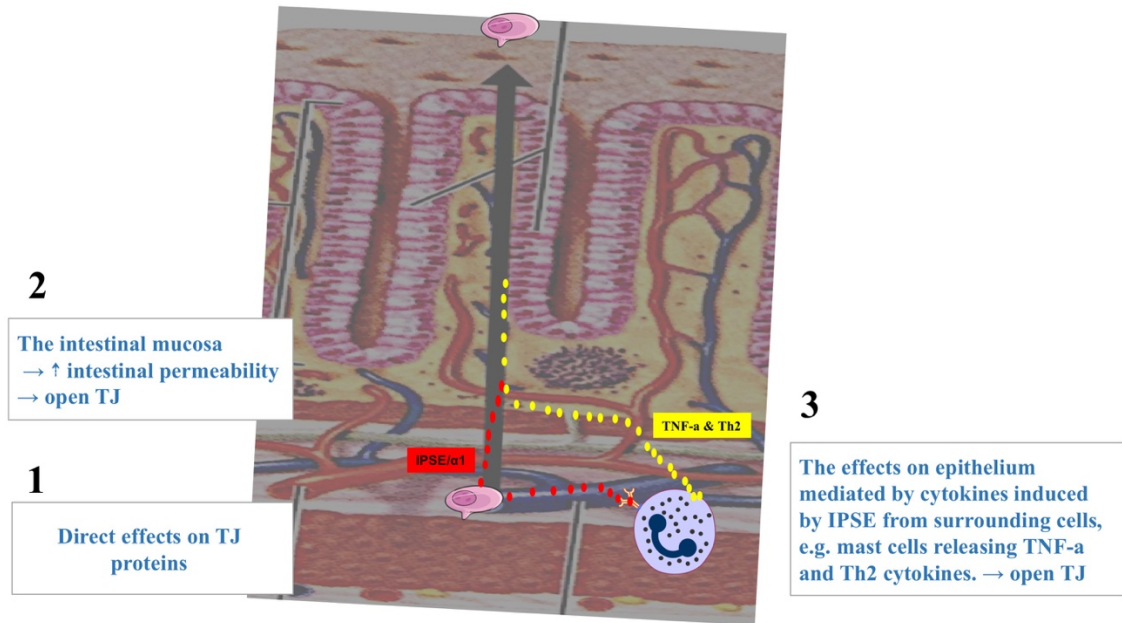


Figure 1.12: The potential effect of IPSE/alpha-1 on tight junction proteins and gut epithelial membrane integrity

There are more than one possibility: 1) Are effects of IPSE/alpha-1 on epithelium mediated by nuclear activities (e.g. transcription factor-like activities). 2) Are effects on epithelium mediated by cytokines induced by IPSE from surrounding cells, e.g. mast cells releasing TNF-alpha and Th2 cytokines. 3) IPSE/alpha-1 may be able to activate cells from the blood.

Chapter 2 - General Materials and Methods

Class II Microbiological Safety Cabinets (MSCs II) are widely used in chemical and biological research and consequently MSCs II (Envair, Lancashire, England) were used for all cell culture work to facilitate aseptic conditions. All experimental procedures complied with health and safety procedures within the workplace. This Chapter describes general methods and materials used throughout the thesis work. Specific techniques are described in the corresponding results chapters.

2.1 Cell Culture

The human bladder cancer cell line (ATCC HTB9) was obtained from Dr. Michael Hsieh (Department of Urology in the George Washington University, USA), and the human hepatoma (Huh7) cell line (Cell Bank number - JCRB0403) was obtained from Dr. Catherine Jopling (School of Pharmacy, University of Nottingham). Calu-3 cells which were obtained from Dr. Cynthia Bosquillon (ATCC number; HTB-55) and used between passages 21-30. Caco-2 cells were obtained from Dr. Snow Stolnik (ECACC number; 86010202) and used between passages 32-38. Humanised rat basophilic leukaemia (RS-ATL8) cells were provided through an MTA by Dr. Ryosuke Nakamura (National Institute of Health Science, Tokyo, Japan) and used between passages 15-22. NFAT DsRed cells were created in our laboratory and used between passages 8-15.

All cells were grown in T75 flasks, at 37°C in a humidified 5% CO₂ incubator, with Minimum Essential Medium Eagle (MEM, Sigma-Aldrich) supplemented with 10% foetal bovine serum (FBS, GIBCO), 2 mM L-glutamine, 100 units/mL penicillin and 100 µg/mL streptomycin (Sigma-Aldrich Co. Ltd., UK). The washing of cells before

dissociation was performed using 10mL of Dulbecco's phosphate-buffered saline (DPBS) without $\text{Ca}^{2+}/\text{Mg}^{2+}$ (Lonza, Switzerland) and detached by trypsinisation for 5-10 min at 37°C using 2 mL trypsin-EDTA (0.05% trypsin and 0.02% EDTA) solution (Sigma-Aldrich); trypsinisation was also used for harvesting and passaging of cells. The fixation reagent was 4% paraformaldehyde (1.6 g paraformaldehyde, Fisher Scientific, UK; heat while stirring to approximately 60 °C in 200 mL 1× PBS, then add a drop of 5 M sodium hydroxide and cool to room temperature).

2.2 Cell Culture Ware

12-well Transwell plates were obtained from Corning Life Sciences (Holland), 2 mm diameter, pore size 0.4 µm with polystyrene membranes; Corning, Life Sciences), cell culture T75 flasks (75 cm², canted neck, vented caps (Sarstedt, Germany) were routinely utilised. Black flat-bottomed, untreated 96-well polystyrene plates (Corning, USA) were used to measure fluorescence, while 96-well white flat-bottomed plates (Nunc, Denmark) were used to measure luminescence. Sterile centrifuge tubes, 15 mL (Corning, USA) and 50 mL (Corning, USA) were employed. Sterile 2 mL cryogenic vials (Nunc) were used to store frozen cells in a freezing container (Nalgene® Mr. Frosty). An improved Neubauer haemocytometer was used for cell counting using 0.4% sterile-filtered Trypan blue for viability assessment (Sigma Aldrich).

2.3 Cell Toxicity Assay

The MTT cell proliferative assay, lactate dehydrogenase (LDH) assay and resazurin assay (also known as the Alamar Blue assay) are widely used for cytotoxicity tests of chemicals (268). The MTT assay is used to measure cell metabolic activity, and is a colorimetric

based assay (269). The viability and proliferation of cells in this assay is assessed by the mitochondrial reductase enzyme, which reduces the yellow tetrazolium salt 3-(4, 5-Dimethylthiazol-2-yl)-2, 5-diphenyltetrazolium bromide (MTT) to a purple formazan dye in living, metabolically active cells. The reaction can be terminated by solubilisation in dimethyl sulfoxide (DMSO) and the optical density (OD) measured at 590 nm with a reference filter of 620 nm (Figure 2.1) (270).

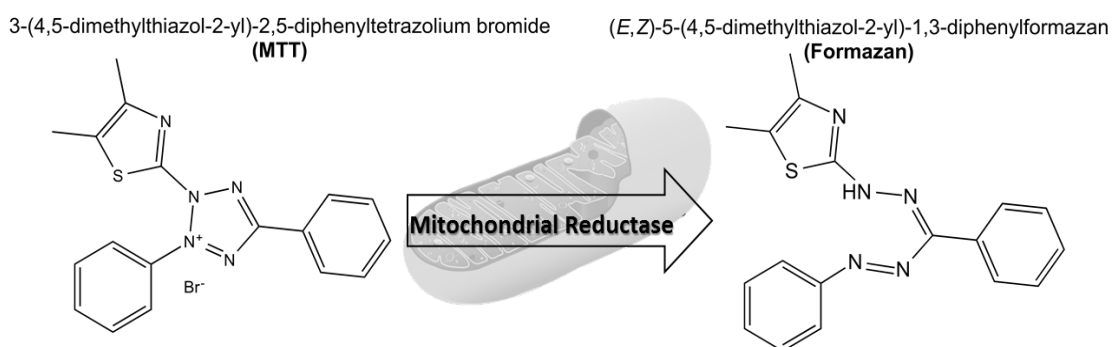


Figure 2.1: Schematic of the MTT assay and coloured formazan product

Source: (1).

The LDH cytotoxicity assay measures LDH enzyme levels that are leaked into the culture medium due to cell membrane damage (271). This assay is therefore used to measure the integrity of the cell membrane. It is based on LDH catalysing the conversion of lactate to pyruvic acid with the parallel reduction of NAD^+ to NADH. The amount of formazan salt which is formed by LDH is measured as the change of absorbance at 490 nm (Figure 2.2) (271, 272).

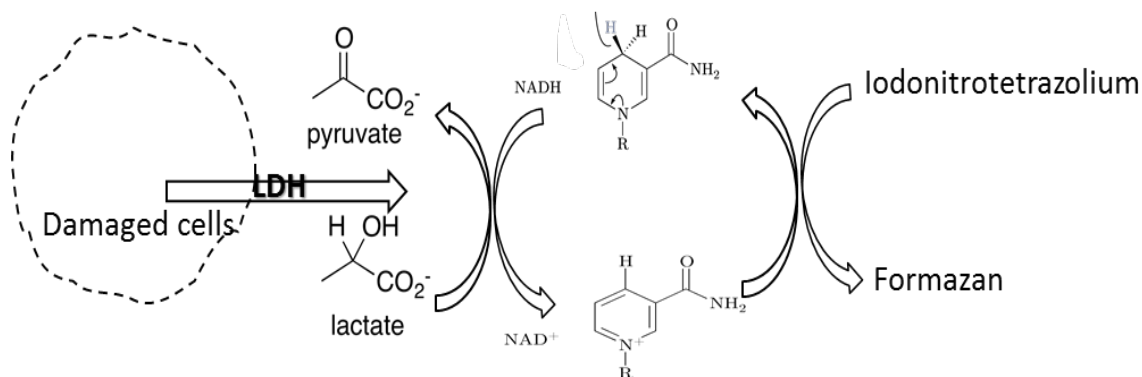


Figure 2.2: Schematic of the LDH cytotoxicity assay and its mechanism

Source: (2).

The resazurin assay uses a blue fluorescent dye to measure cell viability (273). This assay assesses the viability of mitochondrial enzymes through their ability to transfer electrons from NADPH⁺H⁺ to resazurin, which can be assessed via the fluorescence intensity at excitation 540nm and emission 590nm (Figure 2.3) (274).

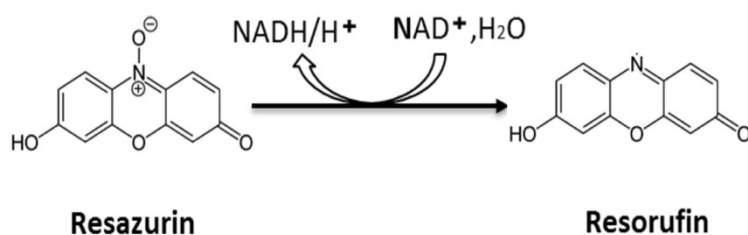


Figure 2.3: Schematic of the resazurin assay and coloured product

2.4 Antibiotics and Transfections

Stock solutions of ampicillin (100µg/mL Sigma-Aldrich,) and kanamycin (100µg/mL Sigma-Aldrich,) were prepared in dH₂O, sterilised by filtration (0.22 µm), aliquoted, and stored at 20 °C and Hygromycin B (300µg/mL Invitrogen, UK) and G418 (250 µg/mL, Fisher, UK) were used as antibiotics for the selection of the selection of plasmids and

stable cell lines, respectively. Transfections were performed using X-tremeGENE9 DNA transfection reagent (Roche Applied Science, Germany) according to the manufacturer's protocol, and transfected at 60-70% confluency.

2.5 Bacterial Culture

Escherichia coli XL10-Gold ultra-competent cells (Stratagene) were used in the expression experiments described. Luria-Bertani (LB) agar and broth (Sigma-Aldrich, UK) were used routinely as the growth medium. This was prepared from 10 g/L tryptone, 5 g/L yeast extract and 5 g/L NaCl in deionized water and autoclaved at 121-124°C for 15-20 min. Both media were supplemented to a final concentration of 100µg/mL of ampicillin or kanamycin to enhance the selection of the desired plasmid. LB broth cultures were incubated at 37°C with shaking at a stirring rate of 450 rpm using a KS 4000 i control Incubator Shaker (IKA, Germany), and LB agar plates were incubated at 37°C (Gallenkamp Ltd., UK).

2.6 Expression Vectors

The first expression vector reported here is pOPE101 (Progen Biotechnik, Heidelberg, Germany). This confers resistance to ampicillin in *E. coli* (XL10 Gold), contains a PelB signal sequence leader for periplasmic localisation at the N-terminal and a strong synthetic IPTG-inducible promoter. There is also a c-myc (EQKLISEEDL) tag for antibody detection and a 6× His-tag for purification at the C-terminus. The second vector, pCEP4 (Invitrogen Ltd., Paisley, UK), confers hygromycin resistance, and contains an Epstein-Barr virus (EBV) origin of replication (OriP) that enables replication of the plasmid DNA, and the functional domains of EBV nuclear antigen (EBNA-1). This vector is suited for

protein expression in HEK293 EBNA (275). EBNA-293 cells and the pCEP4 plasmid were obtained from Dr Szu Wong (School of Pharmacy, University of Nottingham). The third vector utilised in this work is the pTT5 mammalian expression vector, which confers ampicillin resistance to enable for bacterial selection and G418 resistance for selection in the HEK 293-6E cell line. This vector contains a hVEGF signal peptide, 8× His-tag for purification at the N-terminus, followed by the tobacco etch virus (TEV) cleavage site. There is also a β -globin polyadenylation site, Ori and EBV Ori replication fragment. The pTT system is licensed by the Canadian National Research Council (CNRC).

2.7 pAcGFP1-C3 Vector

pAcGFP1-C3 (Clontech, BD Biosciences) has been used for the fusion of infiltrins or truncated versions of each putative infiltrin with in the multiple cloning site (MCS) which contains the recognition site for a range of single-cut restriction enzymes (Figure 2.4)

2.8 Tetra-GFP Vector

The Tetra-EGFP vector contains four EGFP constructs and a MCS inserted between the third and fourth EGFP copy. We used the restriction enzyme *Bgl*II, and the exogenous DNA was inserted using a pair of 5'-phosphorylated double stranded oligonucleotides with corresponding overhangs. This vector was created and kindly donated by Christian Beetz and carries a kanamycin resistance gene (276).

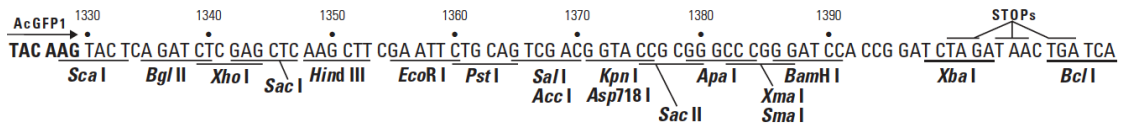
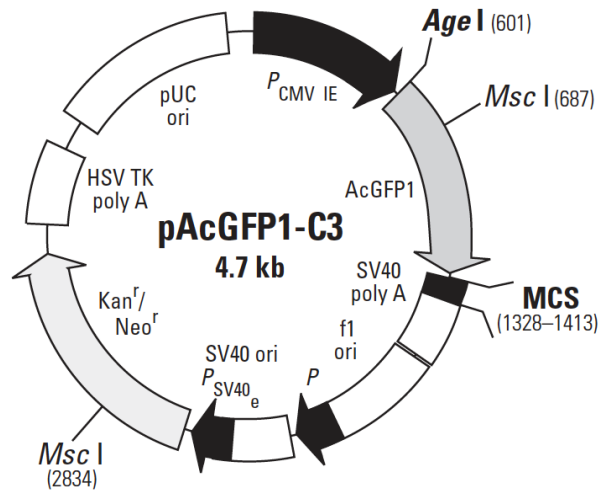


Figure 2.4: Map of the vector pAcGFP1-C3

The AcGFP1 gene is present and the selection gene confers kanamycin or neomycin resistance. This plasmid carries a CMV promoter that is suitable for expression in eukaryotic cells. The multiple cloning site is shown underneath the vector map.

2.9 Transepithelial Electrical Resistance

Transepithelial electrical resistance (TEER) is widely used as it is a non-destructive and reliable method for indicating the opening of TJs in cell culture models of physiological barriers (277, 278). Briefly, the chopstick electrode was sterilised by 70% methylated spirit (IMS) for approximately 25 min. Next, this chopstick was washed with PBS and then placed in the culture medium (long column at the basolateral chamber and short on the apical side). The resulting readings from the screen of the epithelial voltohmmeter were recorded.

TEER was used to measure the effect of IPSE/alpha-1 on model gut epithelial membrane integrity (Caco-2) and the paracellular pathway. Calu-3 and Caco-2 cells were cultured in transwell plates (279).

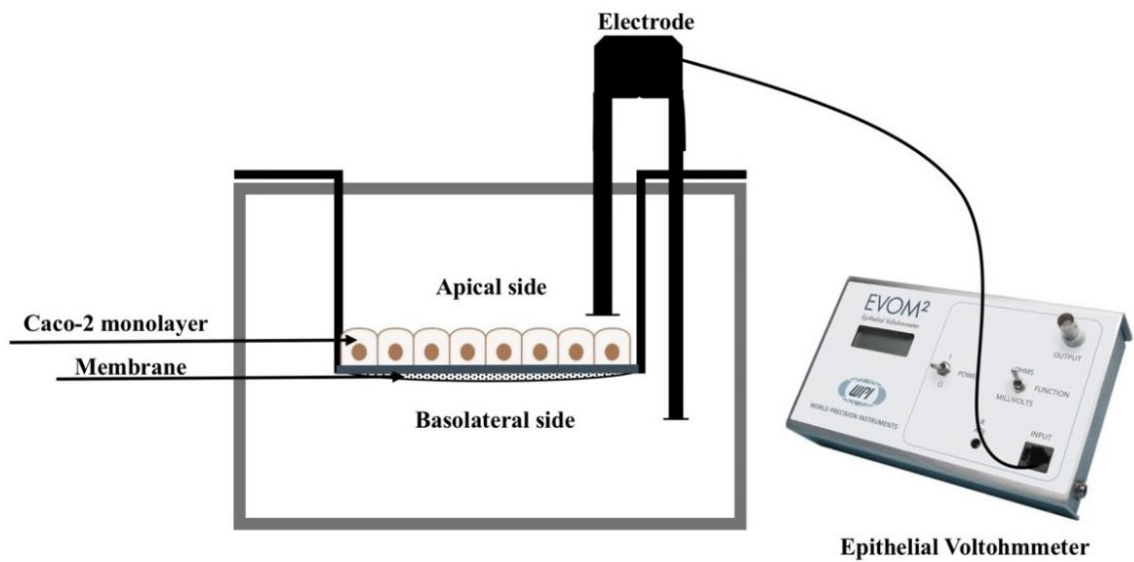


Figure 2.5: Schematic representation of the Epithelial Volt/ohm meter system used to assess the ohmic resistance of a cellular layer.

Chapter 3 - Bioinformatic and Nuclear Localisation Signal Prediction

3.1 Introduction

In this chapter candidate infiltrin proteins are assessed and the results of bioinformatics tools for signal peptide prediction are presented. Nuclear localisation signal (NLS) sequences are involved in the translocation of proteins into the nuclei of mammalian cells and these are essential in mediating nuclear import. The first discovered NLS was described in Sv40 protein from simian virus , with the amino acid sequence PKKKRKV (280, 281). This suggested that NLS are characterised by a sequence of several positively charged amino acids (Lysine or Arginine) .

Different computational approaches to identify putative NLS predictors have been developed using algorithms. NLSs can be identified by using established signal peptide prediction methods, such as NLStradamus(282), NGLoc(283), Yloc-HTTP client(284), PSORT II (285), Nucpred (286), ESLPred (287). For infiltrins, extracellular secretion prediction is possible using e.g. SignalP 3.0 and 4.1 (288, 289), for targeting to the secretory pathway or to mitochondria. Table 2.1 provides a brief summary of the different bioinformatics tools used for the prediction of NLSs; six NLS predictors provide different expectations for the subcellular location of proteins and a NLS, whereas SignalP indicates short signal cleavage site sequences present at the N-terminus of proteins. However, these NLS and secretion predictors are not able to reliably determine these signals and each of these online tools has weaknesses (290). Ultimate verification must be of an experimental nature.

Schramm *et al.* (2003) have shown that the coding sequence of IPSE/alpha-1 is 416 nucleotides or 134 amino acids long. There is a secretory signal of twenty amino acids at the N-terminus; its cleavage during secretion was confirmed by protein sequencing(223). There are two sites for N-glycosylation present within the sequence of IPSE/alpha-1. The homodimeric form of this protein contains four disulphide bridges (three intramolecular and one between two monomers) formed by the seven cysteine residues present in the primary sequence.

The first infiltrin was discovered in 2011 during an *in vitro* study by our group which demonstrated the nuclear import of IPSE/alpha-1 expressed in *E. coli* in human cells, Huh7 and U-2 OS(265). Thus, the archetypal infiltrin is IPSE/alpha-1,. IPSE possesses two conflicting subcellular targeting signals, a classical secretory signal (CSS) and a NLS. PKRRRTY is the predicted NLS sequence putatively involved in the translocation of IPSE/alpha-1 into the nuclei of various mammalian cells, and this matches the experimental data obtained by our group. Therefore, we sought to determine whether potential infiltrins, based on the simultaneous presence of a dual CSS/NLS signal, can also be found in other related trematode parasites. In addition, four potential infiltrins were identified based on their known secretion and prediction of an NLS or their homology; these are: GST-sigma (FhGST-si) and histone H2A (FhH2A) in the liver fluke *Fasciola hepatica*, IL-4 inducing principle from *S. haematobium* egg (ShIPSE03) protein, and kappa-5 from *S. mansoni* egg (Smk5). The case for kappa-5 is more complex and will be discussed at the end of this chapter. The sequence of IPSE/alpha-1 is shown in Figure 3.1.

1	M F L I A V L S Y T L I S Q L G I T T	19
1	ATG TTT CTT ATT GCC GTA TTG TCA TAC ACA TTG ATA AGT CAA TTG GGG ATA ACT ACA	57
20	S D S (C) K Y (C) L Q L Y D E T Y E R G S	38
58	TCG GAT TCA TGC AAA TAT TGT CTA CAA TTG TAC GAT GAA ACG TAT GAG AGG GGT TCA	114
39	Y I E V Y K S V G S L S P P W T P G S	57
115	TAT ATT GAA GTC TAC AAA AGC GTT GGC TCA CTC TCA CCA CCA TGG ACA CCT GGA TCT	171
58	V (C) V P F V N D T K R E R P Y W Y L F	76
172	GTT TGT GTA CCC TTC GTA AAT GAC ACG AAG AGA GAG CGT CCA TAC TGG TAT TTA TTT	228
77	D N V N Y T G R I T G L G H G T (C) I D	95
229	GAC AAC GTC AAT TAC ACA GGT CGG ATT ACT GGT CTC GGA CAT GGT ACC TGC ATT GAT	285
96	D F T K S G F K G I S S I K R (C) I Q T	114
286	GAC TTC ACG AAA TCC GGA TTC AAA GGC ATT TCC TCT ATT AAA CGG TGT ATT CAA ACA	342
115	K D G K V E (C) I N Q P K R R R T Y (C) R	133
343	AAG GAT GGA AAA GTT GAA TGT ATC AAT CAA CCG AAA CGG AGA AGG ACA TAC TGT CGA	399
134	F *	134
400	TTC TAA TCA AGA AAT GTA ATG CGC TTA TAA TTC TTG TGT GCT CTT AAC TAA ATA TAT	456
457	GCA TAT GAA CTG ATG AAA AAA AAA AAA AAA	489

Figure 3.1: Full length cDNA and amino acid sequence of IPSE/alpha-1.

GenBank™ accession number AY028436. The figure highlights the verified classical secretory signal (amino acids 1-20, blue and yellow box, the N-terminal aminoacids in the mature protein verified by sequencing, the 7 Cysteines (circled), the two N-Glycosylation sites (white boxes) and the predicted (later verified) PKRRRTY NLS (azure and red box) (291).

3.2 Experimental Procedures

Fasciola hepatica protein sequences (version PRJEB6687.WBPS5) were accessed from database (http://parasite.wormbase.org/Fasciola_hepatica_prjeb6687) in FASTA format.

The *F. hepatica* protein sequences (33,454 proteins) were analysed using default parameters in local installations of NGLoc, NLStradamus and SignalIP and by the Yloc-HTTP client. This was performed by Dr Nigel Mongan at the Faculty of Medicine & Health Sciences, University of Nottingham. The output was then analysed by myself.

Table 3.1: Different bioinformatics tools used for prediction of NLS

Bioinformatic tool		Ref.
NLStradamus	Based on a probabilistic Hidden Markov Model (HMM) with an architecture. It is a widespread statistical tool for modelling nuclear localisation signal prediction.	(282)
NGloc	An n-gram-based Bayesian classifier. This web server or software is used to estimate subcellular localisation in eukaryotes and some eukaryotic organisms, such as humans and nematodes.	(283)
Yloc	Used for predicting multiple localisation within subcellular proteomes and can be employed for animals, fungi and plants.	(284)
PSORT II	This software, which provides statistical and proteomic analysis, is used for eukaryotic protein sequences or NES Finder programs to identify putative NLS and NES, respectively.	(292)
NucPred	Used for sources of biological information for NLSs through the combined used of algorithms and genetic programming, that is computer programs are the set of genetic information encoded are then evolved using an evolutionary algorithm.	(286, 293)
ESLPred	This software estimates the subcellular proteomes of eukaryotic proteins, whether cytoplasmic, nuclear, mitochondrial or extracellular, using dipeptide composition and the Position-Specific Iterative Basic Local Alignment Search Tool (PSI-BLAST).	(287)

SignalP	Widely used for predicting short signal sequences present at the N-terminal which are between 5 and 30 amino acids long, and found in eukaryotic and prokaryotic proteins. Moreover, SignalP predicts the location of the cleavage site. (294)
----------------	--

First, the outcome of the *F. hepatica* protein sequences using the default parameters was compared using Venn Diagrams (Venny 2.1) at (<http://bioinfogp.cnb.csic.es/tools/venny/>). Then the classical NLSs of FhGST-si, FhH2A, ShIPSE03 and Smk5 were searched using six NLS predictors programs; NLStradamus, NGLoc, Yloc-HTTP client, PSORT II, Nucpred and ESLPred. The sequences of *FhGST-si* (Wormbase database: BN1106_s1081B000242.mRNA-1), *FhH2A* (Wormbase database: BN1106_s45B000421.mRNA-1), *ShIPSE03* (NCBI Reference Sequence: XP_012802396.1) and *Smk5* (clone 4.1.2; GenBankTM accession number AY903301) are shown in Figure 8.1, Figure 8.2, Figure 8.3 and Figure 8.4 in Appendix 9, respectively. The sequences of *FhGST-si*, *FhH2A*, *ShIPSE03* and *Smk5* were 211, 138, 136 and 360 amino acids, respectively.

Using the NucPred tool, it is possible to predict the signal peptide for the overall sequence and also for each amino acid location, which is coloured in terms of its influence on the nuclear localisation classification according to a scale given at the bottom of the figure. For example, in Nuc-Pred software, positive amino acids are shown in red, whereas negative amino acids are shown in blue. The SIM software of the EXPASY server (www.expasy.ch) was used for the comparison of the *ShIPSE03* and IPSE/alpha-1 sequences.

3.3 Results

The *F. hepatica* genome was scanned by our collaborator Nigel Mongan using default parameters for NLS sequences using local installations of NGLoc, NLStradamus, SignalIP and Yloc. In total, 12,852 out of 33,454 *F. hepatica* proteins gave a positive signal peptide prediction using NGLoc, whilst NLStradamus and Yloc detected 1,765 and 2,844, respectively. In contrast, SignalIP4.1 identified only 1,228 proteins as displaying a secretion signal peptide. The predicted protein data from these tools were compared using a Venn diagram and the outcomes were found to agree between all for only 14 proteins (Figure 3.). This would represent the most stringent conditions for prediction of subcellular localisation. These 14 proteins were found to contain both NLS and CSS motifs and also a predicted cleavage site position as identified by SignalIP4.1 (Table 3.2). An additional 348 proteins sequences identified by NGLoc, NLStradamus and Yloc were compared using a Venn diagram (Figure 3.); however, only NGLoc identified *FhGST-si* (Wormbase database: BN1106_s1081B000242.mRNA-1) and *FhH2A* (Wormbase database: BN1106_s45B000421.mRNA-1) as nucleus and plasma membrane targeting proteins, respectively.

In order to determine experimentally whether *FhGST-si* and *FhH2A* from *F. hepatica*, *SHIPSE03* from *S. haematobium* and *Smk5* from *S. mansoni* possess a functional NLS, the full length primary amino acid sequences of these proteins were scanned using a variety of NLS predictors available via the web: PSORT II, ESLPred, NLStradamus, NGLoc, Yloc and NucPred. The subcellular location and presence of a SSC and NLS signal for each of the proteins identified is presented in Table 3.3. The putative NLS of SHIPSE03 was predicted by NLStradamus, PSORT II and NucPred, whilst the putative

NLS of FhGST-si was predicted only by PSORT II, and the putative NLS of FhH2A was predicted only by NLStradamus. There was no NLS prediction for *Smk5*. According to the predicted data from SignalP3.0, FhGST-si, ShIPSE03 and Smk5 possess a CSS at the N-terminal (see Appendix 1), and the Nuc-Pred software (Stockholm Bioinformatics Center) provided possible nuclear localisation scores for FhGST-si, FhH2A, ShIPSE03 and Smk5 of 0.16, 0.05, 0.41 and 0.42, respectively (see Fig. 3.4).

Figure 3.3.4C shows the NucPred outcome for *ShIPSE03*, where positive amino acids are marked in orange (KRRRK at the C-terminal) and the amino acid residues marked by red underlining indicative a putative NLS. Red underlining also indicate potential positive amino acids at the C-terminal of FhGST-si (Figure 3.A), and Smk5 (Figure 3.D), and at the N-terminal of *FhH2A* (Figure 3.B), indicating a putative NLS in each.

A comparison between *ShIPSE03* and IPSE/alpha-1 (Figure 3.) shows 63.4 % identity using the SIM software of the EXPASY server. The mature IPSE/alpha-1 protein sequence was reported by Schramm et al.(2003)(223). ShIPSE03 consists of 134 amino acids encoded by 402 nucleotides and might contains a secretory signal of twenty amino acids at the N-terminus and there is a mature protein sequence which was determined by protein sequencing commences after this secretory signal. Two potential N-glycosylation sites have been identified in ShIPSE03. Furthermore, it can be assumed that the homodimeric form of this protein contains four disulphide bridges (three intramolecular and one between two monomers), which are formed by cross-linking of the seven cysteine residues present in the primary sequence, as in the *S. mansoni* homologue. This IPSE may also possess a C-terminal NLS. However, the secretory signal of twenty amino acids at

the N-terminus and the existence of four disulphide bridges (three intramolecular and one between two monomers) still need to be confirmed experimentally.

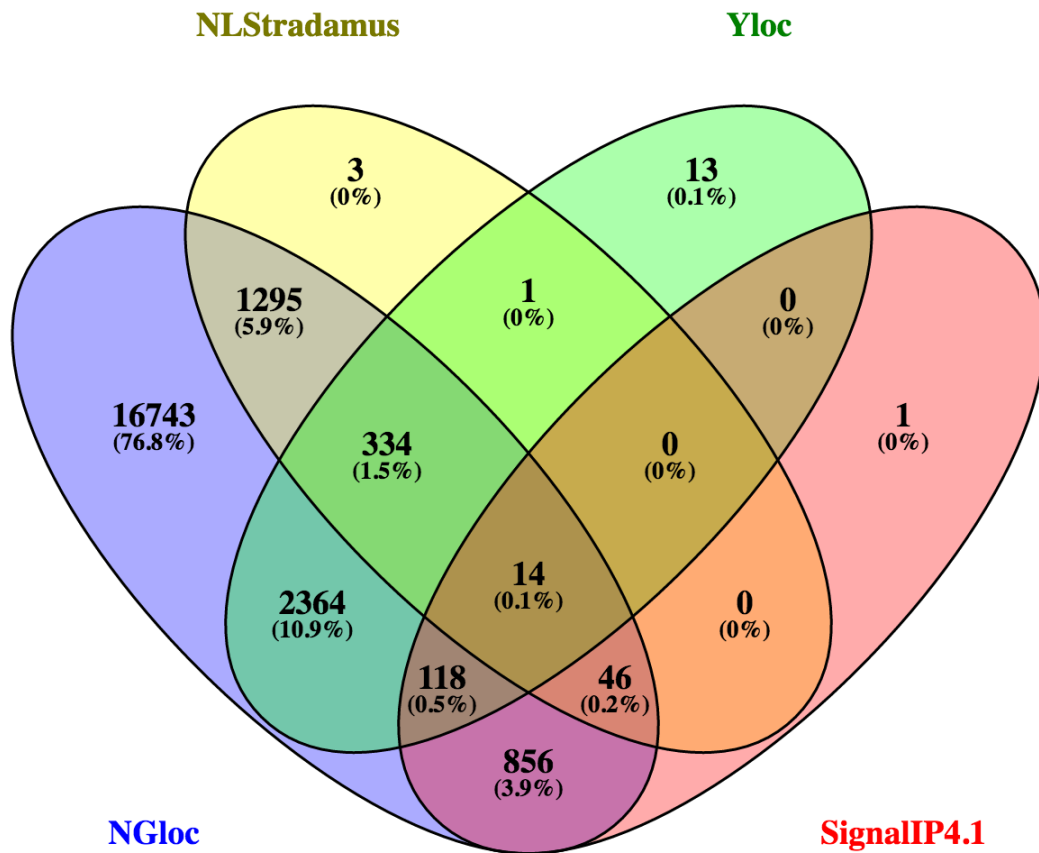


Figure 3.2: A four-circle Venn diagram showing the combined signal peptide prediction and SignalIP4.1 results for *F. hepatica* protein sequences

In total, 14 proteins were identified by all four programs and these are listed in Table 3.2.

Table 3.2: *F. hepatica* protein sequences with NLS and CSS motifs commonly identified by four different prediction tools

Gene ID	Product	Length (amino acid)	Predicted Cleavage Site
BN1106_S1547B000101.MRNA	PC3-like endoprotease variant A	684	SignalP-noTM
BN1106_S174B000284.MRNA	Putative uncharacterised protein	1,450	SignalP-noTM
BN1106_S21B000379.MRNA	Neuropilin and tolloid-like protein 1	1,269	SignalP-noTM
BN1106_S2334B000126.MRNA	Putative uncharacterised protein	897	SignalP-noTM
BN1106_S250B000381.MRNA	Uncharacterised protein	831	SignalP-noTM
BN1106_S3067B000138.MRNA	Uncharacterised	387	SignalP-noTM
BN1106_S4109B000160.MRNA	Uncharacterised	338	SignalP-noTM
BN1106_S620B000156.MRNA	Putative uncharacterised protein	487	SignalP-noTM
BN1106_S707B000541.MRNA	Uncharacterised protein	330	SignalP-noTM
BN1106_S736B000229.MRNA	Uncharacterised	359	SignalP-noTM
BN1106_S8B000452.MRNA	Uncharacterised	219	SignalP-noTM
BN1106_S895B000182.MRNA	Neurogenic locus notch like protein	1,807	SignalP-noTM
BN1106_S2849B000112.MRNA	Uncharacterised	500	SignalP-noTM
BN1106_S623B000237.MRNA	HEAT repeat- containing protein	1,421	SignalP-noTM

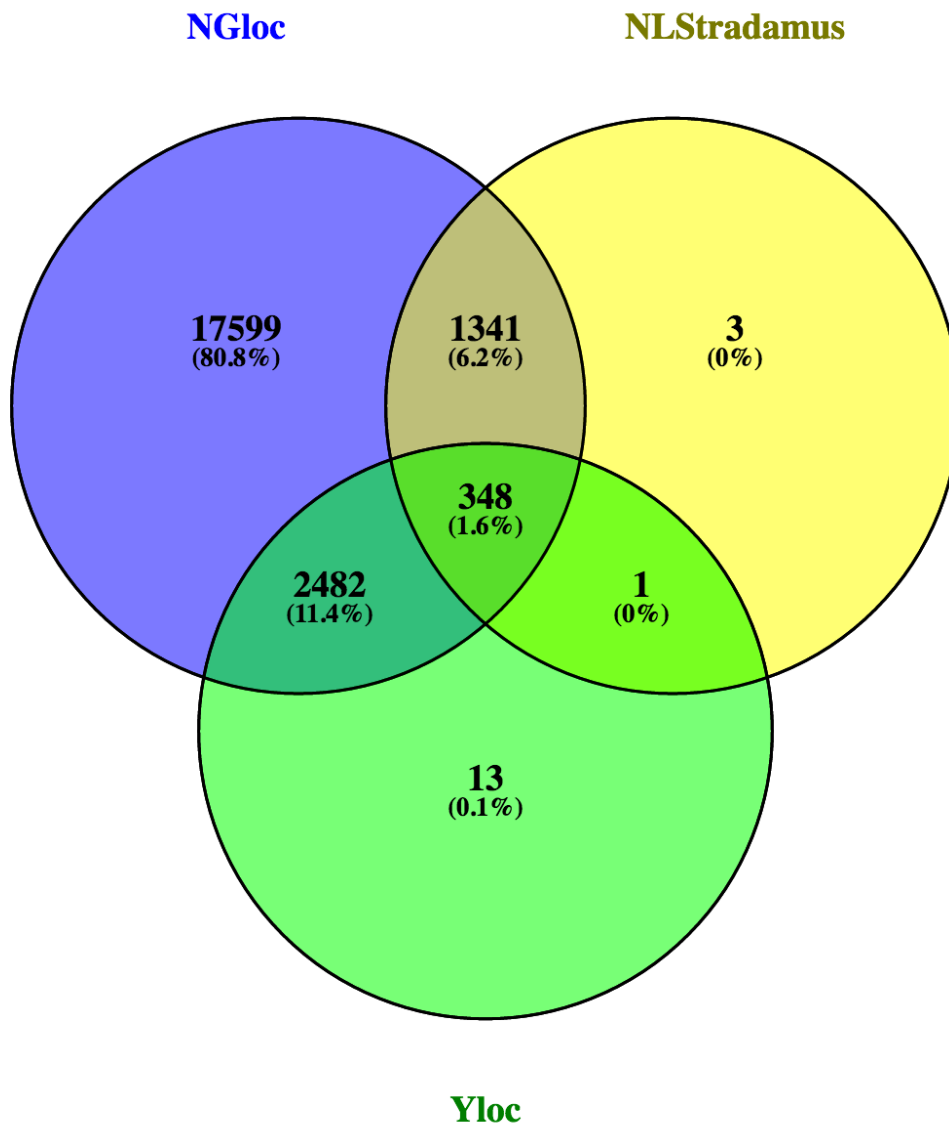


Figure 3.3: A three-circle Venn diagram showing the combined signal peptide prediction and results for *F. hepatica* protein sequences
 In total, 348 genes were predicted to contain NLSs by all three prediction tools.

Table 3.3: Results of different bioinformatics tools used to assess known NLSs in FhGST-si, FhH2A, ShIPSE03 and Smk5

Prediction Tool (website)	Predicted Subcellular Localisation	NLS prediction	Signal peptide prediction	Type	Ref	
SignalP 3.0	<i>FhGST-si</i>		19-20		(289)	
	<i>FhH2A</i>		No Pred			
	<i>ShIPSE03</i>	N.S.	N.S.	20-21		NN/HM
	<i>Smk5</i>			25-26		M
NLStradamus	<i>FhGST-si</i>		No Prediction	N.S	(282, 295)	
	<i>FhH2A</i>		GDKSGKAKAK	9-23		
	<i>ShIPSE03</i>	N.S.	SKRRRKY	N.S.		HMM
	<i>Smk5</i>		No Prediction	N.S		
ESLPred	<i>FhGST-si</i>	C. (94%)			(287)	
	<i>FhH2A</i>	N. (94%)				
	<i>ShIPSE03</i>	C. (53%)	N.S.	N.S.		SVM
	<i>Smk5</i>	C. (94%)				
NucPred	<i>FhGST-si</i>	SP (0.6) & N. (0.16)		N.S.	(286)	
	<i>FhH2A</i>	SP (0.5) & N. (0.05)	Yes	N.S.		
	<i>ShIPSE03</i>	SP (0.40) & N. (0.41)		26-29 (KRRR)		PDB
	<i>Smk5</i>	SP (0.42) & N. (0.42)		N.S.		
PSORT II	<i>FhGST-si</i>	C. (69.6%) & N. (13.0 %)	pat7 123-131 PDGKLRR	GvH 33-34	(285)	
	<i>FhH2A</i>	C. (39.1%) & N. (21.7 %)	None	No Prediction		
	<i>ShIPSE03</i>	C. (4.3 %) & N. (78 %)	RRRK	14-15		
	<i>Smk5</i>	C. (13 %) & N. (43.5 %)	None	12-13		
NGLoc	<i>FhGST-si</i>	N. (16.01%)			(283, 296)	
	<i>FhH2A</i>	N. (66.86%)				
	<i>ShIPSE03</i>	N. (17.38%)	No Prediction	No Prediction		SVM/ other
	<i>Smk5</i>	N. (13.96%)				
Yloc	<i>FhGST-si</i>	C. (98.59%)			(284)	
	<i>FhH2A</i>	N. (99.76%)				
	<i>ShIPSE03</i>	SP (25.4%) and N. (42.5%)	No Prediction	No Prediction		BaCelLo
	<i>Smk5</i>	SP (77.3%) and N. (2.6%)				

Key: C. (cytoplasmic); HMM (Hidden Markov Models); SP (secreted pathway sorting signal); N (nuclear);

N.S. (not suitable); NN (neural networks); SSI (sorting signal information); SVM (support vector machine); k-NN (k-nearest neighbour); PDB (Protein Data Bank). GvH (von Heijne's method of signal sequence recognition which is a weight- matrix method and incorporates the information of consensus pattern around the cleavage sites (the (-3,-1)-rule).

The NucPred score for your sequence is 0.16 (see [score help](#) below)

A) 1 MDKQHF~~KLWYQFR~~GRAEPIRLLLLTCAGVKFEDYQFTMDQWPTIKPTLPG 50
 51 GRVPLLDV~~TGPDG~~KLRRYQESMAIARLLARQFKMMGETDEEYYLIERIIG 100
 101 ECEDLYRE~~VYTI~~FRTPQGEKEAKIKEFKENNGPTLLKLVSESLESSGGKH 150
 151 VAGNRITL~~GDLFL~~FTTLLTHVMETVPGFLEQKFPKLHEFHKSLPTSCSRLS 200
 201 EYLK~~KRAK~~TPF 211

The NucPred score for your sequence is 0.05 (see [score help](#) below)

B) 1 GSMAGGKAGKDSGKAKAKAISRS~~HRAGLQFP~~VGRIHRHLKTRTTSHGRVG 50
 51 ATAAVYSAAILEYLTAEVLELAGNASKDLKVKRITPRHLQLAIRGDEELD 100
 101 TLIKATIAGGGVIPH~~HKSLIG~~KKVPPAKPLGMLE 135

The NucPred score for your sequence is 0.41 (see [score help](#) below)

C) 1 MFLIALLSYTLINQLVITKSDSCKYCLRLYDGKYKSGSYIEVYKSVGSLS 50
 51 PPWIPGSVCVPLIHNSTGPPYWR~~IYEDVNYS~~GKDTAVGHGACIDDFMKS 100
 101 GLRRISSIQKCVYGENMVQCSSES~~KRRRKY~~CRY 134

The NucPred score for your sequence is 0.42 (see [score help](#) below)

D) 1 MLQEYNLLINGVTL~~LISLSGLICEA~~QSPTNDEM~~HATISEYGR~~LYITNIHI 50
 51 HYRLLIMALSPNMKFT~~PGEADN~~ILHKSEEEHQVKWALNYLNAARSTW~~KLE~~ 100
 101 NEDMFKKT~~MSSYV~~GVNKTIVPNFCMTMLQOSSARNWDTNIQKDITYGCEV 150
 151 LKKYSELK~~WGARKK~~LDLMTIRWLNGSDENGQSQ~~HISDKGF~~NYHSKKEYLE 200
 201 CAQSVMKIHR~~TAEVDCR~~STVGEFLKLQ~~QVKDTP~~SSKTQAIQFDKINENF 250
 251 NKSLVEL~~KRRVEN~~LEINRINYLFMNP~~MERVIS~~VIDAMEEEVDH~~KYGV~~YM 300

Positively and negatively influencing subsequences are coloured according to the following scale:

(non-nuclear) negative ||||| positive (nuclear)

Figure 3.4: Protein sequence of FhGST-si (A), FhH2A (B), ShIPSE03 (C) and Smk5 (D) predicted using Nuc-Pred software

The nuclear localisation prediction is shown in different colours according to the scale at the bottom of the figure. The overall sequence score is given above each protein sequence (<http://www.sbc.su.se/~maccallr/nucpred/cgi-bin/single.cgi>).

```

63.4% identity in 134 residues overlap; Score: 491.0; Gap frequency: 0.0%

ShIPSE03      1 MFLIALLSYTLINQLVITKSDSCKYCLRLYDGKYKSGSYIEVYKSVGSLSPWPWIPGSVCV
SmIPSE        1 MFLIAVLSYTLISQLGITTSDSCKYCLQLYDETYERGSYIEVYKSVGSLSPWPWTPGSVCV
          ***** ** ** ***** ** * ***** ***** *****

ShIPSE03      61 PLIHNSTGQPPYWRIYEDVNYSGKDTAVGHGACIDDFMKSGLRRISSIQKCVYGENGMVQ
SmIPSE        61 PFVNDTKRERPYWYLFDNVNYTGRITGLGHGTCIDDFTKSGFKGISSIKRCIQTKDGKVE
          *          ***      ** * * ** * ** * ** * ** * ** * ** *

ShIPSE03      121 CSSESKRRRKRYCRY
SmIPSE        121 CINQPKRRRTYCRF
          *          **** **

```

Figure 3.5: Alignment between ShIPSE03 and IPSE/alpha-1

There is 63.4 % identity at the amino acid level between the two IPSEs using the SIM software of the EXPASY server (www.expasy.ch).

3.4 Discussion

This chapter has sought to determine whether infiltrins, defined as proteins characterised by the simultaneous presence of a dual CSS/NLS signal, could also be found in other related trematode parasites. Alternative bioinformatics tools available via the web were used to predict CSS and NLS motifs for FhGST-si and FhH2A from *F. hepatica*, ShIPSE03 from *S.haematobium* and Smk5 from *S. mansoni*. Adult *F. hepatica* worms secrete numerous proteins which which may be able to reach the nucleus of host cells; however, bioinformatically only 14 proteins within the *F. hepatica* genome were identified as containing both a CSS and NLS sequence, and FhGST-si and FhH2A were not recognised as being amongst these proteins. Nevertheless, many studies have shown that other types of proteins are secreted by *Fasciola* adult worms into the liver, such as FhGST-si and FhH2A proteins (105, 297, 298). This can have several reasons: prediction of subcellular localisation is still inaccurate, and not all secreted proteins are secreted by the classical pathway – there are also non-classical secretory pathways, which cannot be predicted by the available tools (299).

According to the prediction data from SignalIP3.0, FhGST-si, ShIPSE03 and Smk5 contain a CSS at the N-terminal. The putative NLS of SHIPSE03 was predicted by three separate bioinformatics tools and an alignment between ShIPSE03 and IPSE/alpha-1 showed 63.4 % identity using the SIM software of the EXPASY server. IPSE/alpha-1, also called SmIPSE and less commonly SmEP25(228), is secreted as a glycoprotein (250, 251). IPSE/alpha-1 has the same molecular structure and almost the same N-terminal sequence (223). The homodimeric form of this protein contains four disulphide bridges (three intramolecular and one between two monomers) which are formed by the seven cysteine residues present in the primary sequence (257). In 2011 an *in vitro* study by our group demonstrated the nuclear import of IPSE/alpha-1 contains a secretory signal of twenty amino acids at the N-terminus and a C-terminal NLS, namely, 125-PKRRRTY-131, which plays a necessary and sufficient role in the process of transferring IPSE into the nuclei of mammalian cells (223, 265). SHIPSE03 mirrors the same key characteristics of IPSE/alpha-1, as shown in Figure 3..

FhGST-si and FhH2A proteins are secreted by adult *Fasciola* worms in the liver (105, 297, 298). *F. hepatica* protein sequences identified by NGLoc, NLStradamus and Yloc found only 348 proteins in common, and only NGLoc identified FhGST-si (Wormbase database: BN1106_s1081B000242.mRNA-1) and FhH2A (Wormbase database: BN1106_s45B000421. mRNA-1) as being targeted to the nucleus and plasma membrane, respectively. Additionally, Table 3.2 shows that these proteins were predicted by only one tool. General Histone H2A has the ability to be imported into the nucleus via a classical NLS (300). There have been no experimental studies to date on the CSS and NLS motifs

of FhGST-si, and it is important to display experimentally the functional NLS motifs for each protein.

There was NLS prediction for Smk5 in Table 3.2. This protein contains a 25 amino acid of CSS at the N-terminal, four cysteine residues (124, 148, 201, and 217) and three putative N-glycosylation sites (residues 116, 174, and 250)(226). However, it is important that the function of these NLS motifs is verified experimentally for this protein. The NucPred software (Stockholm Bioinformatics Center) showed that FhGST-si, FhH2A, ShIPSE03 and Smk5 each revealed a possible NLS, with NucPred scores of 0.16, 0.05, 0.41 and 0.42, respectively, but again experimental support is required given that the selected proteins possess two conflicting subcellular targeting signals, namely CSS and NLS. From the cell biology perspective, the presence of an N-terminal secretory signal will direct the nascent polypeptide into the lumen of the endoplasmic reticulum, even before the amino acids forming the C-terminal NLS are translated and added to the growing peptide chain. Once inside the ER, the NLS is not a functional signal, as it cannot engage the cytosolic nuclear import machinery (i.e. the karyopherins – see Chapter 5 section 5.1.2). From this, it can be hypothesised that the NLS does not have a function in the parasitic cell from which it originates, but in the surrounding host cells – provided that the molecule is taken up by the cells. This is what we aim to show in Chapter 5. However, we first needed to express the proteins recombinantly in order to perform the planned experiments. The recombinant expression is therefore described next.

Chapter 4 - Recombinant Expression and Purification of Infiltrins

4.1 Introduction

The first objective of this study was to express and purify the recombinant predicted infiltrins IPSE/alpha-1, ShIPSE, Smk5, FhGST-si and FhH2A, in order to generate sufficient amounts for use in downstream experiments. Several papers have reported the successful expression of IPSE/alpha-1 in both *E. coli* and HEK293 cells, and Smk5 in HEK293 cells. IPSE/alpha-1 has been subcloned into the pProEXHTb expression vector to enable its expression as a His-tag fusion protein in *E. coli*, and was subsequently refolded using dialysis in PBS (223). In 2007, recombinant IPSE/alpha-1 was expressed and purified from HEK293 cells transfected with the pMSII expression vector, and released as a His-tagged protein into the culture medium (250). Recombinant Smk5 has also been purified from HEK293 cells, but no information was provided on the type of expression vector utilised (222). To date, no paper has been published on the recombinant expression of the IL-4 inducing principle from *S. haematobium* eggs (ShIPSE). In this study different expression systems were utilised and a brief summary of the functional features of each vector used for the expression of recombinant IPSE/alpha-1 and Smk5 is provided. The expression vectors reported here are the pOPE101 expression vector (see Appendix 2) in *E. coli* (XL10 Gold), and the pCEP4 (see Appendix 3) and pTT5 (see Appendix 4) mammalian expression vectors; further details concerning these vectors were provided in Section 2.6.

Expression and purification of IPSE/alpha-1 and Smk5 has proven to be highly challenging. Recombinant IPSE/alpha-1 and Smk5 were expressed as 6xHis-tag fusion proteins (His-SmPSE and His-Smk5), and expression of recombinant IPSE/alpha-1 and Smk5 was attempted in different expression systems. During the first attempt, each of the genes was successfully cloned into the vector pOPE101 to yield pOPE101-IPSE/alpha-1-WT and pOPE101-Smk5-WT (301). The second expression system tested was to enable the stable high level expression of recombinant secreted protein within mammalian cells. The genes encoding IPSE/alpha-1 and Smk5 were cloned into the vector pCEP4 and the resulting pCEP4-IPSE/alpha-1-WT and pCEP4-Smk5-WT plasmids were transfected into the cell line HEK293-EBNA, a subset of HEK-293 cells, to enable expression via a roller bottle expression system to obtain high yields of IPSE/alpha-1 and Smk5 (302). The third expression system utilised was the vector pTT, as used by our collaborator Luke Pennington in Stanford, who recommended expression vectors for HEK293-6E cells (303), an expression system licensed by the National Research Council of Canada. The human embryonic kidney HEK293-6E cell line is commonly used as a mammalian expression system. HEK293E and 293T, subclones of the HEK293 cell line, express truncated EBVNA1 and the simian virus 40 large-T antigen, respectively. These cells enable suitable folding, are able to grow in a serum-free medium, and accept most types of transfection reagents, such as linear 25 kDa polyethylenimine (PEI) (304-306). PEI is commercially available, cheap, results in reduced toxicity, and gives a transfection efficiency of approximately 80% for plasmid DNA in HEK293 cells (307, 308). The recently developed expression system, pTT, allows for the successful expression of selected infiltrins into HEK293-6E cells using a pTT5 vector and transient transfection

(309). Most importantly, this system allows HEK293-6E cell growth in suspension rather than in monolayers, enabling high cell density, and therefore high yields of recombinant proteins.

4.2 Experimental Procedures

4.2.1 Plasmid Preparation

4.2.1.1 S. mansoni egg First Strand cDNA Synthesis

S. mansoni eggs were obtained from Professor Mike Doenhoff (School of Life Science, University of Nottingham). Approximately 100,000 eggs were extracted from the intestines of mice infected with *S. mansoni* cercariae 42 days earlier (310), and were kept refrigerated in RNAlater until processed. RNeasy® Plus Mini Kit (50, QIAGEN) was used to isolate mRNA from the *S. mansoni* eggs according to the manufacturer's instructions. This involved the addition of RLT plus (lysis buffer), containing β -mercaptoethanol to the eggs, followed by incubation at 37°C for 10 minutes and vigorous vortexing for 10 minutes. mRNA was reverse transcribed to cDNA via RT-PCR) and a GeneAmp® RNA PCR kit (Roche, New Jersey, US). This procedure was completed using oligo(dT) primers and a DNA cycle according to the manufacturer's protocol.

4.2.1.2 PCR Amplification of IPSE/alpha-1 and Smk5

Q5™ high-fidelity DNA polymerase (New England Biolabs, USA) was used to amplify the sequence encoding IPSE/alpha-1 and Smk5 from *S. mansoni* egg cDNA. PCR conditions and thermal cycling were according to the manufacturer's instructions using the primers and annealing temperature shown in Table 4.1. The PCR products were cleaned following agarose gel electrophoresis using Wizard® SV Gel and PCR clean-Up

(Promega) as directed by the manufacturer. The concentration of the DNA was determined using a NanoDrop Spectrophotometer (Thermo Fisher Scientific, UK).

Table 4.1: Primers and annealing temperature

(Some primers have a different name in the database but exactly the same number in it. I altered it to make them easy to follow)

Primer No.	Primer	5'-3' Sequence	Annealing Temp.
1064	SmIPSE-For- pOPE101- <u>PvuII</u>	CGACGAC <u>CAGCTGG</u> ATTTCATGCAAATA TTGTC	58°C
1065	SmIPSE-Rev- pOPE101- <u>NotI</u>	TTAACGG <u>CGGCCGCG</u> GAATCGACAGTA TGTCTTC	
1084	SmIPSE-For-pCEP4 - <u>NheI</u>	CCGCCG <u>GCTAGCAT</u> GTTTCTTATTGC CGTATTG	58°C
1085	SmIPSE-Rev- pCEP4- <u>XhoI</u>	TATATA <u>CTCGAG</u> TTAATGGTGATGAT GGTGGTGGAAATCGACAGTATGTCCTT CT	
1165	Smk5-For- pOPE101- <u>Pvu II</u>	CCGCCG <u>CAGCTGCAGT</u> CTCCTACAAA CGATGAG	58°C
1166	Smk5-Rev- pOPE101- <u>NotI</u>	TTAACGG <u>CGGCCG</u> CCATGTAGACTCC ATACTTGTGA	
1109	Smk5-For-pCEP4 - <u>NheI</u>	CCGCCG <u>GCTAGCAT</u> GCTCAGTCTCCT ACAAACGA	58°C
1110	Smk5-Rev- pCEP4- <u>XhoI</u>	TATATA <u>CTCGAG</u> TTAATGGTGATGAT GGTGGTGCATGTAGACTCCATACTTG TGAT	
1315	Smk5-For-pTT5- <u>PmeI</u>	CGGGCGGTTTAAACATGTTGCAGGAA TACAACCTTCTAATAAACGGA	56°C
1316	Smk5-Rev-pTT5- <u>BamH1</u>	TATTCAGGATCCTCAATGGTGATGGT GGTGATGCATGTAGACTCCATACTT	

4.2.1.3 Cloning

The amplification products were prepared alongside the desired expression vector using restriction endonucleases (New England BioLabs, USA) under the conditions specified by the manufacturer. The amplification products and the expression vectors, pOPE101, pCEP4 and pTT were prepared using six different restriction enzymes, which are indicated within the primer name and the recognition site underlined in the

oligonucleotide sequence (Table 4.1). The amplification products were digested and ligated into the expression vectors using a molar ratio of vector to insert of 1:3 using T4 DNA ligase (Promega UK) according to the manufacturer's instructions. The next step was to transform the plasmids into XL10 gold ultra-competent cells by heat shock: bacteria were defrosted on ice and kept there for 30 minutes, followed by a 45 second heat shock in a water bath at 42°C, then 3 minutes on ice. After the heat shock, cells were grown in 450 µl of SOC medium, allowed to recover and express the antibiotic resistance gene for one hour at 37°C in an incubator with shaking at 120 rpm, followed by recovery for 45 min at 37°C with gentle shaking, and before being plated onto LB agar supplemented with 100 µg/mL ampicillin (pOPE101 and pTT plasmids) or 100 µg/mL hygromycin (pCEP4 plasmid). After 16 hours incubation at 37°C, single colonies were selected using vector-specific primers (Table 4.2) to confirm the presence and identity of the insert. JumpStart REDTaq DNA Polymerase (Sigma) was used for the PCR amplifications, as per the manufacturer's protocol. An annealing temperature of 58°C was used for all the reactions, and the PCR products were screened by standard agarose gel electrophoresis (1% agarose, 0.5×TBE, satined with EtBr). Positive clones were grown in 10 mL of LB broth supplemented with 100 µg/mL ampicillin or hygromycin for 16 hours at 37°C on a shaking incubator at 120 rpm. Plasmid DNA was purified using the Wizard® SV Minipreps DNA Purification System (Promega), as directed by the manufacturer. The concentration of the purified plasmid DNA was measured using a NanoDrop spectrophotometer as directed (Thermo Scientific). The presence of the insert was verified by plasmid DNA sequencing, and verified plasmids were sent to Source BioScience Life Sciences, Nottingham, for sequencing using promoter FOR primers in Table 4.2 (vector

specific primer) The sequencing data was analysed using SnapGene software (GSL Biotech LLC, USA).

Table 4.2: Vector-specific primers

(N.B. Some primers have a different name in our database but exactly the same number in it – these have been altered for simplification)

Primer No.	Construct Backbone	Primer	5'-3' Sequence
1044	pOPE101	pOPE Promoter FOR	TTGACTTGTGAGCGGATAAC
1045	pOPE101	pOPE Terminator REV	ATGTGTCAGAGGTTTTCCACC
	pCEP4	pCEP4 Promoter FOR	AGCAGAGCTCGTTTAGTGAACCG
1100	pCEP4	pCEP4 Terminator REV	TGAACCGTCAGATCTCTAGAAGC
1317	pTT	pTT5 Promoter FOR	GATATTCACCTGGCCCGATCTG
1318	pTT	pTT5 Terminator REV	GGTTCAGTTGGCAAGTTGTACCAA

4.2.2 Expression of Infiltrins

Periplasmic *E. coli* XL10 Gold cell expression and stable high level expression of recombinant secreted protein in HEK293 EBNA cells was used and, in addition, the expression vector pTT5 in HEK293-6E cells was tested. The periplasmic *E. coli* XL10 Gold cell expression and secretory expression within HEK293-EBNA cells following stable transfection will be described first, and then focus will be on the pTT system. HEK293-6E cells, the pTT5 expression vector and 6E protocol was obtained and licensed from the Canadian National Research Council (CNRC), Canada.

4.2.2.1 Periplasmic Extraction from *E. coli* XL10 Gold cells

E. coli XL10 Gold cells were used for expression from IPSE/alpha-1-WT and Smk5-WT plasmids. These were cultured in 10 mL Luria Bertani broth supplemented with Ampicillin tetracycline glucose (LB-ATG) supplemented with ampicillin at a final concentration of 50 µg/mL in order to enhance selection of the desired plasmids, and incubated at 37°C for 16 hours. Next, 2 mL of the overnight culture was aliquoted into

three Erlenmeyer flasks containing 50 mL of LB-ATG, supplemented with 50 μ g/mL final concentration of ampicillin, and incubated at 37°C with shaking at 225 RPM until an OD600 of 0.6 was reached. The three Erlenmeyer flasks of culture were induced with IPTG at 200, 100 and 50 μ M, respectively (final concentration) and the temperature reduced to 24°C for 12 to 16 hours. After 12 and 16 hours, 20 mL from each flask were harvested via centrifugation for 10 minutes at 15,000 g, 4 C, in order to to obtain cell pellets. These cell pellets were resuspended in 2 mL cold Spheroblast solution (20% sucrose dissolved in Tris-HCl pH8.0 supplemented with EDTA to a final concentration of 1mM), placed on ice and shaken at 4°C for 20 minutes, followed by centrifugation at 4°C, 6,200 g for 10 minutes.

The supernatants from the samples were transferred into fresh microfuge tubes and the remaining pellets were used for osmotic shock extraction. In this process the pellets were resuspended in 2 mL of 5 mM cold MgSO₄ and placed on ice and shaken at 4°C for 20 minutes, followed by centrifugation at 4°C, 6,200 g for 10 minutes, and the supernatant was then transferred into fresh microfuge tubes. The remaining pellets were resuspended in 20 mL 1 \times PBS, and 1 mL from each was removed as the soluble fraction while the remainder (insoluble protein) underwent further centrifugation at 10,000 g for 1 minute. The pellets were resuspended in 150 μ L of lysis buffer (50mM Tris-Hcl pH8.0, 500mM NaCl and 5% Glycerol) and 1.50 μ L of lysozyme (Novagen, 1700 KU/mg) and incubated for 30 minutes at room temperature. A sonicator (8 bursts at 10% power) was used for extracting the protein, followed by centrifugation at 14,000 g for 10 minutes.

Both supernatant samples from the periplasmic extraction and osmotic shock extraction were treated with 250 μ L of trichloroacetic acid (TCA) and incubated for 10 minutes at

4°C, followed by centrifugation at 14,000 g for 5 minutes. The pellets were washed twice with 200 µL cold acetone and the centrifugation step repeated. These pellets were resuspended in 100 µL 2×NRSB and 100 µL 1×PBS. Gradient SDS-PAGE (4-15%) was used to separate the samples.

4.2.2.2 Secretory Expression in HEK293-EBNA Cells

HEK293-EBNA cells were grown in a 6-well plate (Sarstedt Inc., US) at 37°C in a humidified 5% CO₂ incubator, with MEM supplemented with 5% heat-inactivated FBS, 2 mM L-glutamine, 100 unit/mL penicillin and 100 µg/mL streptomycin (Sigma-Aldrich Co. Ltd., UK). Transfection was performed using the X-tremeGENE9 DNA transfection reagent according to the manufacturer's protocol. On the following day, the medium was replaced with fresh medium containing 250 µg/mL G418 (Fisher, UK) and 300µg/mL hygromycin B (Invitrogen, UK) for the selection of stable cell lines and plasmids, respectively, until 80-90% confluency was reached. The cells were transferred into T25 flasks and the medium changed to EX-CELL™ 293 Serum-Free Medium for HEK 293 Cells (SAFC) until 80-90% confluency reached. The cells were then transferred to T75 flasks (Sarstedt Inc., US) and finally into a roller bottle (CORNING). The supernatant from HEK-293 cells was filtered through a 0.22µm filter to remove HEK293-EBNA cells and debris, and then the recombinant proteins were purified by nickel affinity chromatography (complete His-Tag Purification from Roche Life Science, Germany). The supernatant was washed with buffer A (20 mM Tris, 300 mM NaCl (pH = 7.4) and subsequently stepwise eluted in buffer A supplemented with 75,125, 250 and 500 mM imidazole.

4.2.2.3 Reagents and Cell Culture

Reagents and cultures were prepared specifically for protein expression in the pTT system and for purification purposes. All pTT constructs were isolated using the Wizard Plus Midiprep DNA purification system (Promega). PEI was prepared at a concentration of 1 mg/mL (Polysciences) in high purity water and sterilised by filtration (0.22 µm). Tryptone N1 (TN1) solution was prepared from 100g of tryptone N1 (Organotechnie, France) in 20mL of 293Freestyle F17 media but without G418, and the solution was stirred for 90 minutes until all the tryptone N1 had dissolved, before finally being sterilised by filtration (0.22 µm).

The HEK293-6E cell line was grown in suspension in HEK293Freestyle F17 medium (GIBCO, Rockville, MD) supplemented with 0.1% w/v Kolliphor P-188, with 4 mM L-glutamine and 25 µg/mL G418 (ThermoFisher, UK) by shaking the cells in 1000 mL flasks (Corning Inc., Corning, NY) at 120 rpm at 37°C in a humidified 5% CO₂ incubator (standard conditions). A Neubauer modified haemocytometer with staining using 0.4% Trypan blue was used for the assessment of cell viability (usually more than 97%) and cell density (around 1.7×10^6 cells/mL) before transfection.

4.2.2.4 Transfection of HEK 293-6E Cells and Protein Purification

A large-scale recombinant protein expression workflow for transient transfection was developed using 1000 mL vented shaking flasks. A 500 mL culture required 12.5 mL of media for the resuspension of DNA and another 12.5 mL of media for the resuspension of PEI. The final DNA concentration of each pTT construct was 0.5 mg, and this was mixed with 1.5 mg of PEI (3:1 PEI: DNA ratio) before being incubated for 3 minutes at room temperature; the resulting complex was then added to the cells and 2.5mL (final

concentration 0.5%) TN1 of the feeding medium was used 24 h after transfection. Our collaborator Luke Pennington (Stanford University) has found that by doubling the culture volume 24 hours post transfection with HEK293 Freestyle F17 media, the protein yields can be increased; however, the standard 6E protocol (from CNRC) does not call for this. This is costly because it uses more expensive media, but 1.5–2 times the protein yield is obtained. The recombinant infiltrins were secreted into the HEK293-6E medium, and harvested after 7 days. The supernatant was subjected to centrifugation at 2,800 g for 10 minutes (4°C), followed by 0.22 µm filtration to remove cell debris and large aggregates, and then purified using TALON[®] Superflow cobalt affinity resin (GE Healthcare, Freiburg, Germany), according to the manufacturer's protocol using three different buffers: binding buffer (50 mM sodium phosphate, 300 mM NaCl 1, pH 7.4), wash buffer (50 mM sodium phosphate, 300 mM NaCl 1, 5 mM imidazole 2, pH 7.4) and elution buffer (50 mM sodium phosphate, 300 mM NaCl 1, 150 mM imidazole 2, pH 7.4). The purification fractions were analysed by both Coomassie blue-stained SDS-PAGE and Western blotting.

4.2.2.5 Analysis of the Purification Fractions

Coomassie blue staining and Western blotting were used to analyse the purification fractions.

SDS-PAGE:

Purified protein from the fraction samples (15 µL) was assessed using Bio-Rad Mini-Protean ready gels (4–20% gradient TGX gel) in a Mini-Protean electrophoresis cell and a Mini-Trans-Blot cell (Bio-Rad, USA), according to the manufacturer's protocol.

Coomassie blue staining and silver staining:

After SDS-PAGE the gradient TGX gels were incubated for half an hour in Instant Blue (Expedeon, Harston, UK) for Coomassie staining, followed by washing in water. Gels were silver stained using a ProteoSilver Plus silver stain kit (Sigma), according to the manufacturer's protocol, although the company recommends the use of double staining (both Coomassie and silver staining).

Western blotting:

Following SDS-PAGE the gradient TGX gels were transferred onto 0.2 µm nitrocellulose membranes using a Trans-Blot® Turbo™ Transfer System (Bio-Rad), as per the manufacturer's protocol (Bio-Rad, USA). The membranes were blocked with blocking buffer (5% (w/v) dried skimmed milk, in 0.01% (v/v) Tween 20, Sigma, UK and Tris-buffered saline, TBS, 150 mM NaCl, Fisher Scientific UK, 50 mM Tris, Sigma, UK, and the pH adjusted with HCl to pH 7.6), followed by shaking for 1 hour at room temperature. Next, membranes were incubated at 4°C overnight with mouse anti-His antibody (GE Healthcare, 27-4710-01) as the primary antibody, which was diluted 1:5000, followed by three 10 minute washes in TBS containing 1% Tween. The membranes were covered with: anti-mouse IgG (whole molecule) diluted 1:5000, and goat HRP-conjugated antibody- (Sigma) diluted 1:400 as the secondary antibody for one hour at room temperature, followed by washing in the manner described above. Images of the membranes were obtained using a Fuji LAS 4000 imager (Fujifilm, Japan) under the high binning mode with chemiluminescence-luminol reagent (3 µL of 30% H₂O₂(BDH, UK), Tris/HCl 0.1 mM, pH, 8; 2.5 mM luminol (Sigma, UK) and 400 µM coumaric acid (Sigma, UK)).

4.3 Results

4.3.1 Cloning of IPSE/alpha-1 and *Smk5* mature sequence cDNA into the Expression Vectors

The expression vectors pOPE101, pCEP4 and pTT were used for the expression of recombinant proteins in *E. coli* (XL10 Gold), and the cell lines EBNA-HEK293 and HEK293-6E, respectively. The first step in cloning IPSE/alpha-1 and *Smk5* was a PCR to amplify a fragment of the IPSE/alpha-1 and *Smk5* genes from *S. mansoni* egg cDNA. The outcome of each amplification was confirmed via an agarose gel to be the expected size of 371 bp for IPSE/alpha-1 (Figure 4.1A) and 900 bp for *Smk5* (Fig. 4.1-B). Purified IPSE/alpha-1 and *Smk5* fragments and recipient vectors were then restriction-digested according to the desired location of IPSE/alpha-1 and *Smk5* in the pOPE101, pCEP4 and pTT expression vectors. For the pTT constructs, wild-type and mutant pTT5-SmIPSE and pTT5-ShIPSE03 plasmids were obtained from our colleagues in the schistosomiasis research group led by Michael Hsieh (Department of Urology in the George Washington University, USA) and Luke Pennington (School of Medicine in Stanford University School of Medicine, USA), whereas the pTT5-Smk5-WT plasmid was created in our laboratory. After ligation and transformation into XL10 Gold ultra-competent cells for plasmid propagation, colony PCR was used to determine whether the transformants hosted plasmids holding IPSE/alpha-1 or *Smk5* using vector primers (Promoter FOR and Terminator REV shown in Table 4.2). Thus, amplicon sizes revealed whether the colonies were positive or negative for IPSE/alpha-1 (Figure 4.2) or *Smk5* insertion (Figure 4.3). Through this process, IPSE/alpha-1 and *Smk5* fragments were successfully cloned into the pOPE101 vector designed for protein expression in *E. coli* (Figure 4.4A), and also into

the pCEP4 vector designed for protein expression in the EBNA-HEK293 cell line (Figure 4.4B). Furthermore, the *Smk5* fragment was cloned into the expression vector pTT5 for protein expression in the HEK293-6E cell line (Figure 4.4D). These expression constructs were engineered to be transformed or transfected into the expression host organism. However, periplasmic expression in *E. coli* XL10 Gold was unsuccessful and the yield with the secretory expression system in HEK293-EBNA was poor. In contrast, expression via the pTT expression vector in HEK293-6E cells was successful.

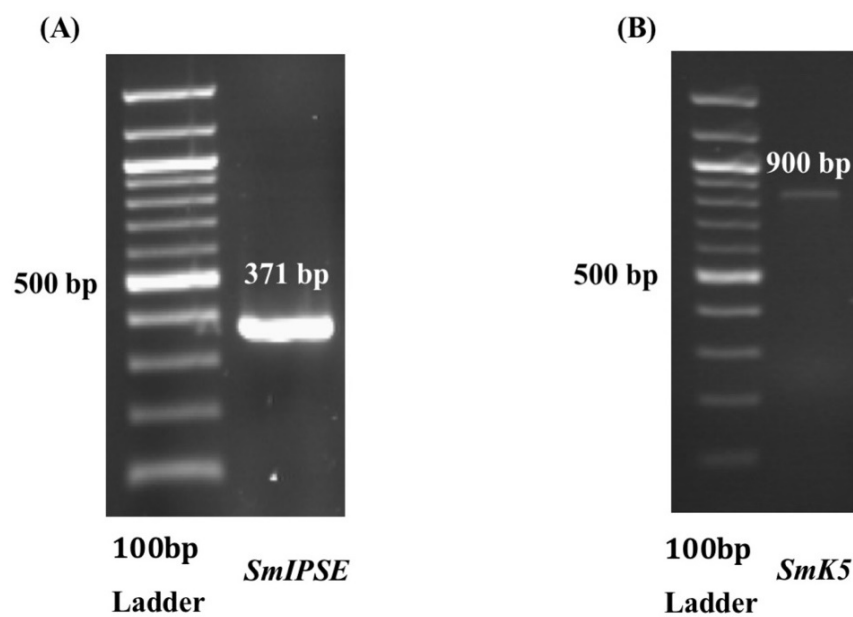


Figure 4.1: Amplification of IPSE/alpha-1 and *Smk5* fragment from *S. mansoni* egg cDNA 1% agarose gel electrophoresis and a 100 bp DNA ladder (A) Amplification of IPSE/alpha-1 from cDNA using a His tagged PCR reverse primer (≈ 371 bp). (B) Amplification of *Smk5* from cDNA using a His tagged PCR reverse primer (≈ 900 bp).

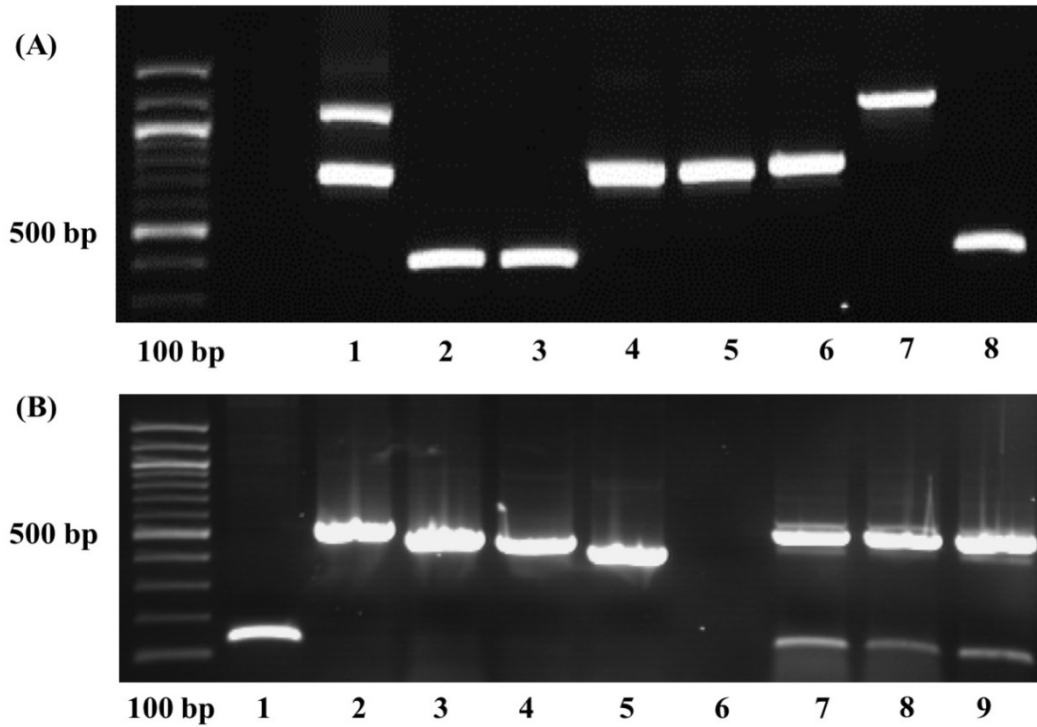


Figure 4.2: Representative verification of IPSE/alpha-1 insertion into the expression vectors pOPE101 and pCEP4

1% agarose gel electrophoresis and a 100bp DNA ladder. Vector-specific primers were used for each plasmid in a colony PCR screen after transformation. (A) IPSE/alpha-1 into pOPE101 and (B) IPSE/alpha-1 into pCEP4; successful insertion results are shown in lane 4 – 6 (~741bp) and 2 (~561bp), respectively.

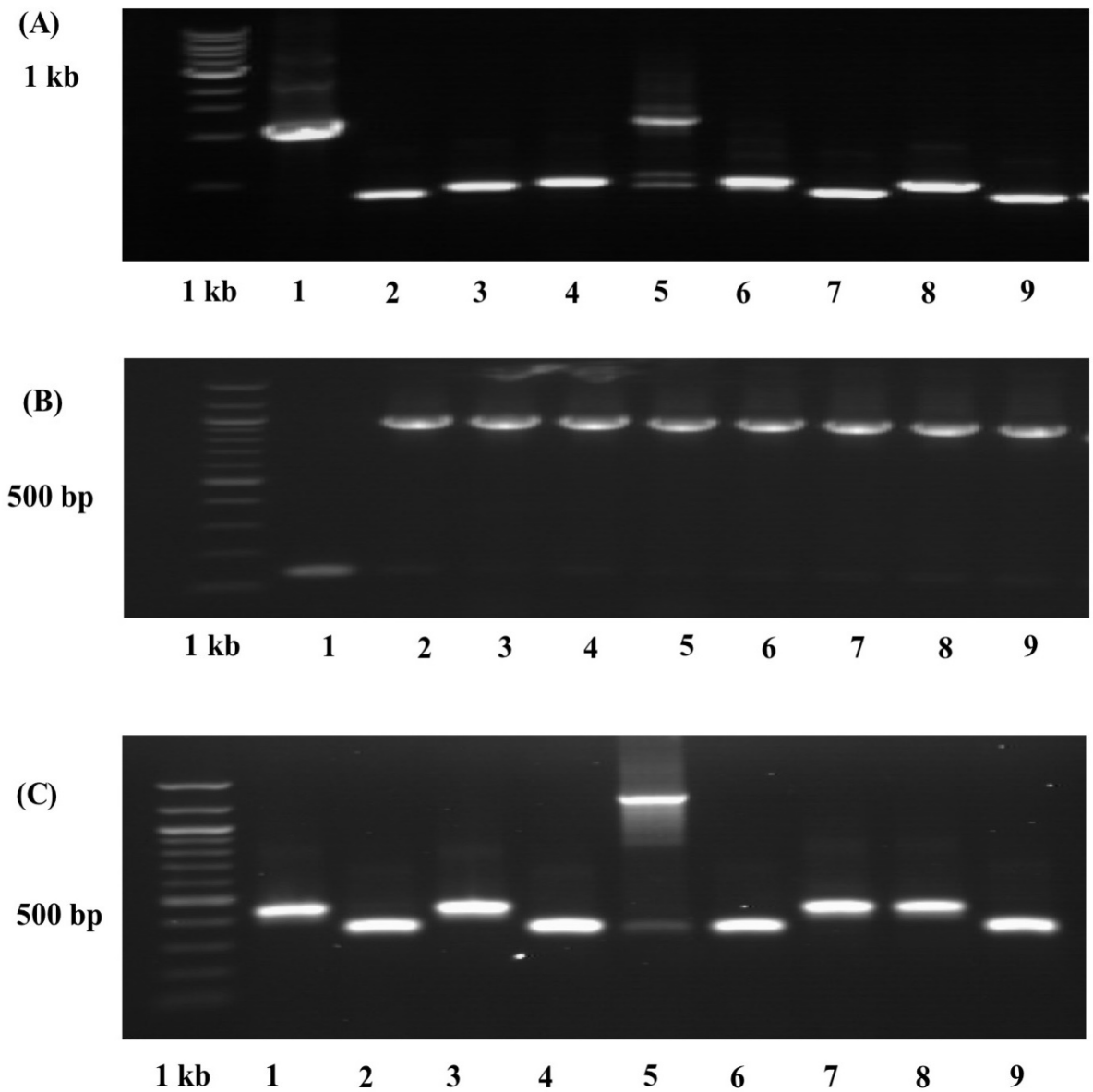


Figure 4.3: Representative verification of *Smk5* insertion into the expression vectors pOPE101, pCEP4 and pTT5

1% agarose gel electrophoresis and a 100 bp DNA ladder. Vector-specific primers were used for each plasmid in a colony PCR screen after transformation. (A) *Smk5* into pOPE101, (B) *Smk5* into pCEP4, (C) and *Smk5* into pTT5; successful insertion results are shown in lane 5 ~ 1,296bp, most lanes ~971bp, 5 ~1,328bp, respectively.

4.3.2 Expression

IPSE/alpha-1, ShIPSE03 and Smk5 proteins which were secreted into the supernatant of HEK293-6E medium, were harvested after 7 days, followed by protein purification as described in Section 4.2.2.4.

4.3.2.1 Recombinant Expression of IPSE/alpha-1 and ShIPSE03

The recombinant protein of wild-type IPSE/alpha-1 was obtained from Luke Pennington, whereas the recombinant protein of wild-type ShIPSE03 and mutant IPSE/alpha-1 and ShIPSE03 were expressed and purified in our laboratory. Figure 4.4 shows the results for these proteins when analysed by both Coomassie blue-stained SDS-PAGE (left) and Western blot (right). The band size for both IPSE lanes appeared to match the expected size. There was a dimeric protein at around 40 kDa under non-reducing sample buffer (NRSB) conditions for both IPSEs and two bands at 18 and 20 kDa under reducing sample buffer (RSB) conditions, which appeared to match the expected size.

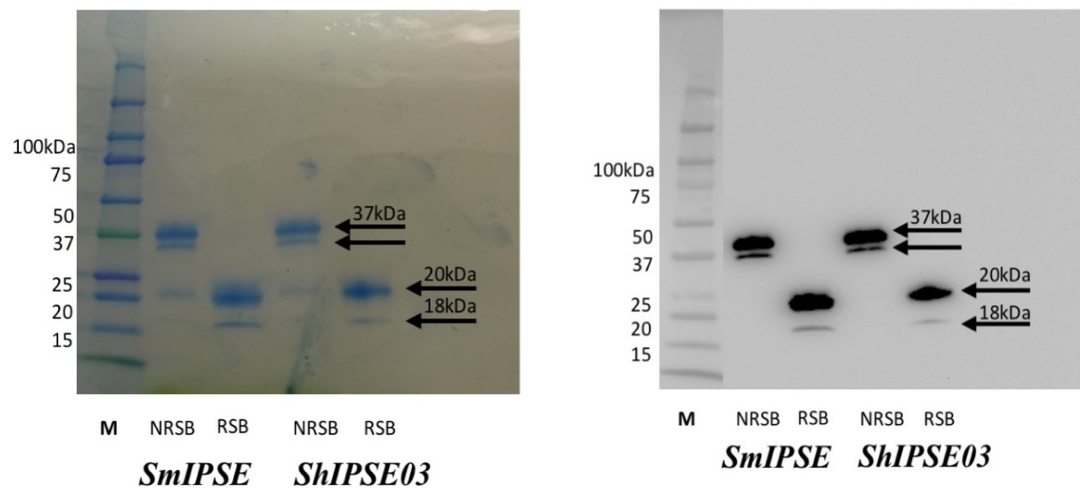


Figure 4.4: Analysis of recombinant IPSE/alpha-1 and ShIPSE03

Samples were separated by SDS-PAGE on a Mini-PROTEAN TGX 4–20% gel. Lane designations are as follows: M, marker (Precision Plus Protein™ kaleidoscope from BioRad); NRSB, non-reducing sample buffer; RSB, reducing sample buffer. Mouse

anti-His antibody (GE Healthcare) was used as the primary antibody (1:1000) in the Western blot.

4.3.2.2 Recombinant Expression of *Smk5*

The recombinant protein of wild-type *Smk5*, which was secreted into the supernatant of HEK293-6E medium was purified and Figure 4.5 shows the analysis by silver stained SDS-PAGE (left) and Western blot (right). A single predominant band was observed after silver staining and Western blotting for the purified protein; this is a strong band close to 75 kDa and 37 kDa under NRSB and RSB conditions, respectively.

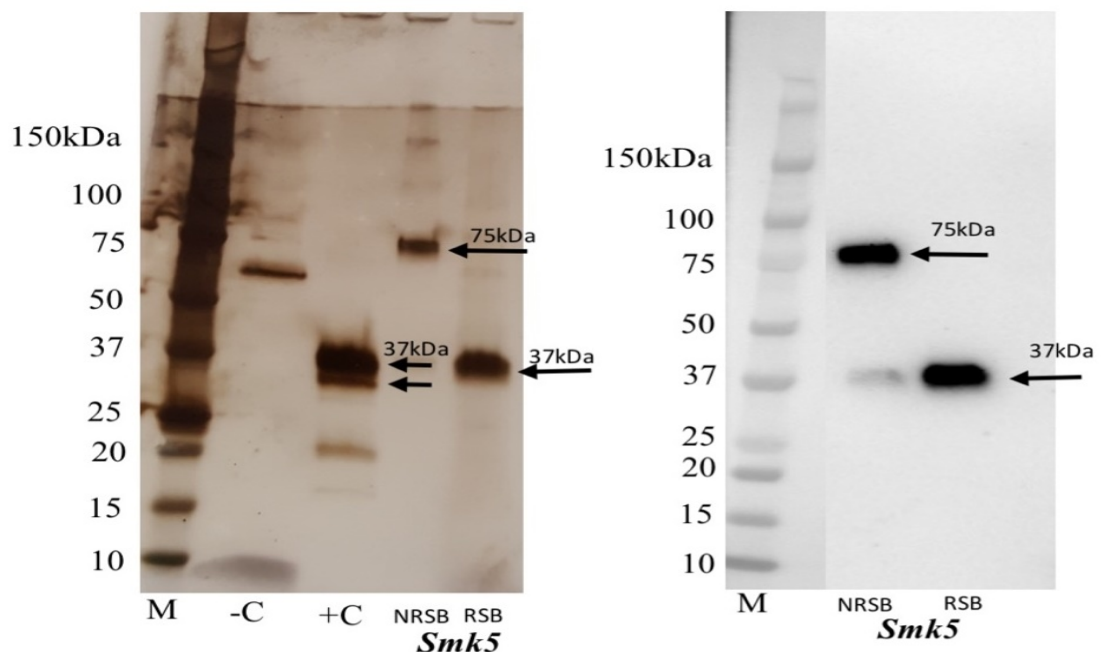


Figure 4.5: Analysis of recombinant *Smk5*

Samples were separated by SDS-PAGE on a Mini-PROTEAN TGX 4–20% gel. lane designations are as follows: M, marker (Precision Plus Protein™ kaleidoscope from BioRad); -C, negative control (HEK293Freestyle F17 media); +C, positive control (wild-type ShIPSE03) and NRSB, non-reducing sample buffer; RSB, reducing sample buffer. Mouse anti-His antibody (GE Healthcare) was used as the primary antibody (1:1000) in the Western blot.

4.3.2.3 Recombinant *FhGST-si* and *FhH2A*

Recombinant *FhGST-si* and *FhH2A* was expressed by our collaborator Robin J Flynn (School of Veterinary Medicine & Science, University of Nottingham) in *E. coli* cells

(BL21) using the expression vector pET28a (Novagen, UK). Recombinant FhGST-si was analysed for quality control purposes via Coomassie staining and Western blot, (Figure 4.6A and B). There were two strong bands close to 26 kDa under NRSB conditions and 23 kDa under RSB conditions for FhGST-si, whilst for FhH2A there was a strong band between 15–18 kDa under both NRSB and RSB conditions (Figure 4.6A and C). The expected size of FhGST-si and FhH2A are 26–28 kDa and 15–18 kDa, respectively (105, 109, 297, 311).

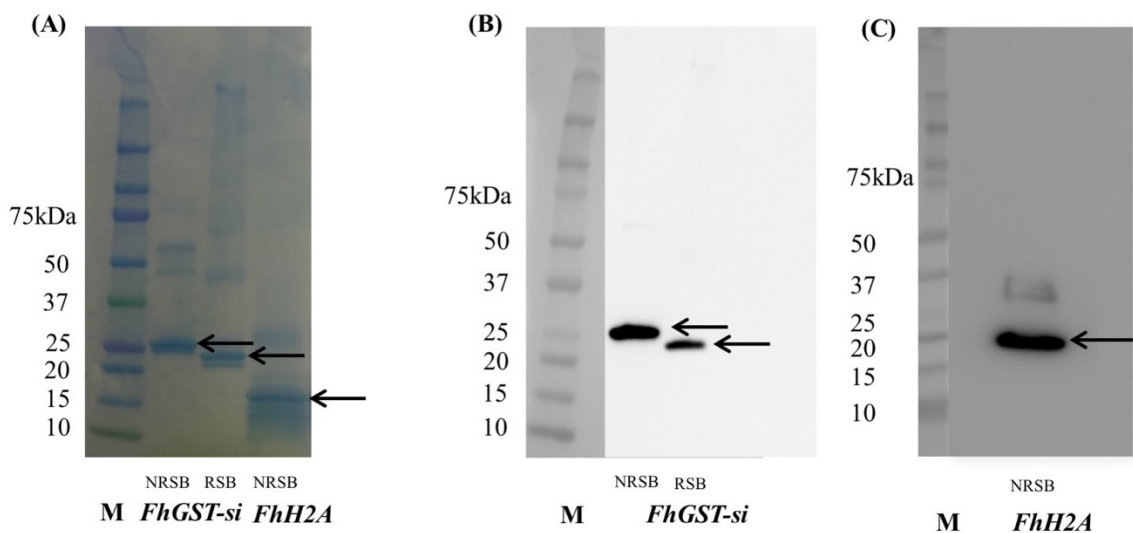


Figure 4.6: Analysis of recombinant FhGST-si and FhH2A

Samples were separated by SDS-PAGE on a Mini-PROTEAN TGX 4–20% gel. Lane designations are as follows: M, marker (Precision Plus Protein™ kaleidoscope from BioRad); NRSB, non-reducing sample buffer; RSB, reducing sample buffer. (A) Coomassie staining of FhGST-si and FhH2A, (B) Western blotting of FhGST-si and (C) Western blotting of FhH2A; mouse anti-His antibody (GE Healthcare) was used as the primary antibody (1:1000) in the Western blot.

4.4 Discussion

The objective of this part of the study was to clone, express and purify recombinant infiltrins in order to generate sufficient amounts for use in downstream experiments. Previous investigations have shown that IPSE/alpha-1 expression in *E. coli* (BL21) can

be induced using the pProEXHTb expression vector(223). Functional IPSE/alpha-1 has three intramolecular and one inter-chain disulphide bonds and these might not fold properly in the cytoplasm of *E.coli*, which is a reducing environment (236). Therefore, it should be expressed either in the periplasm, which is associated with low yields, or in specific bacterial strains in which the reducing glutathione reductase enzymes have been deleted (312). Thus, periplasmic expression in *E.coli* XL10 Gold cells was attempted. IPSE/alpha-1 and *Smk5* fragments were successfully cloned into pOPE101 (301); however, periplasmic expression was unsuccessful. This change from cytosolic to periplasmic expression was required to avoid the need for a refolding step because the solubilised protein may cause a change in the biological activity of the protein (313). Proteins generated in mammalian cells are usually folded correctly and are functionally active (314). IPSE/alpha-1 has previously been expressed in HEK293 cells using the pMSII expression vector, but no information about the type of expression vector has been provided for *Smk5* (222, 250).

For expression in mammalian cells, the first attempt to express recombinant IPSE/alpha-1 and *Smk5* was made using HEK293-EBNA cells and the expression vector pCEP4. This vector contains an EBV origin of replication (OriP) that enables replication of plasmid DNA and the functional domains of EBNA-1 (275). Therefore, both IPSE/alpha-1 and *Smk5* fragments were cloned into pCEP4 and then transfected into HEK293-EBNA cells, which are amenable to stable transfection and expression. Disappointingly, the yield with this expression system was low. Therefore, a switch was made to using the pTT mammalian expression vector because the expression level achieved with this vector has been shown by others to be increased to more than three times that achieved with pCEP4

(315). Total protein yields were determined using a BCA assay kit (Thermo Fisher Scientific, UK) and the yields were between 6 and 10 mg/L.

Previous purification data has shown the secretion of IPSE/alpha-1, ShIPSE03 and Smk5 from HEK293-6E cells. It can be seen in Figure 4.5 that IPSE/alpha-1 and ShIPSE03 are represented at the same molecular weight. As shown in Figure 3., there is 63.4% identity between IPSE/alpha-1 and ShIPSE03. It is known that native IPSE/alpha-1 occurs as a dimeric protein, with a homodimer of around 40 kDa under non-reducing conditions and two bands of around 18 and 20 kDa under reducing conditions (228, 236). However, no paper has yet been reported in the literature on the expression of ShIPSE protein. There are seven cysteine residues in the IPSE/alpha-1 sequence and these are involved in creating three intramolecular and one inter-chain disulphide bonds (316, 317). This leads to dimerization of IPSE/alpha-1 that is necessary for IPSE/alpha-1's ability to induce IL-4 release by human basophils (265). Likewise, there is the same number of cysteine residues in the *ShIPSE03* sequence (Figure 8.3). *Smk5* sequences have appeared in the NCBI data bases (GenBank TM accession number AY903301), and it has been shown that Smk5, which is a dimeric protein, can be purified from SEA by soybean agglutinin affinity chromatography. Smk5 exhibits a single band of around 75 kDa under non-reducing SDS-PAGE(226) and Figure 4.5 shows a dimeric protein band at ~75 kDa under non-reducing conditions and ~37 kDa under reducing conditions. This size also matches the result from the pI/MW compute tool at ExpASy (Figure 4.7).

Compute pI/Mw

Theoretical pI/Mw (average) for the user-entered sequence:

10	20	30	40	50	60
MLQEYNLLIN	GVTLLISLSG	LICEAQSPN	DEMHATISEY	GRLYITNIHI	HYRLLIMALS
70	80	90	100	110	120
PNMKFTPGEA	DNILHKSEEE	HQVKWALNYL	NAARSTWKLE	NEDMFKKTMS	SYVGVNKTIV
130	140	150	160	170	180
PNFCMTMLQQ	SSARNWDTNI	QKDITYGCEV	LKKYSELKWG	ARKKLDLMTI	RWLNGSDENG
190	200	210	220	230	240
QSQHISDKGF	NYHSKKEYLE	CAQSVMKIHR	TKAEVDCRST	VGEFLKLQQV	KDTPSSKTQA
250	260	270	280	290	300
IQFDKINENF	NKSLVELKRR	VENLEINRIN	YLKFMNPMER	VISVIDAMEE	EVDHKEYGVYM

Theoretical pI/Mw: 7.11 / 34911.03

Figure 4.7: Compute tool for Smk5 giving 34 kDa as the theoretical pI/Mw

Translation of the DNA sequence was carried out using the Translate tool of ExPASy and synthetic peptides using the pI/MW compute tool available from the ExPASy server (http://web.expasy.org/compute_pi/)

Figure 4.6 shows the results for the recombinant FhGST-si and FhH2A proteins. A strong monomeric band appears in each lane: for FhGST-si under non-reducing conditions it is 26 kDa, under reducing conditions it is 23 kDa and for FhH2A under non-reducing conditions it is 15 kDa. The identities of these bands were confirmed by Western blot (Figure 4.6B and C), which revealed the small difference between the bands for FhGST-si at 26 kDa and 23 kDa (105, 109). For FhGST-si, a decrease of about 3 kDa in the expected size was observed between reducing and non-reducing conditions. This protein is a dimer, with one very small chain (Figure 8.1). The Western blot in Figure 4.6C shows a monomer band at ~15 kDa under non-reducing conditions which appears to match the expected size of FhH2A (297, 311), however, the Coomassie stain shown in Figure 4.6A suggests monomers and also that the protein is either impure or partially degraded.

It is proposed that infiltrins are secreted by a parasite and have the ability to enter host cells and interact with the host cell nuclear import machinery. The next chapter focuses on the uptake of each infiltrin.

Chapter 5 - Infiltrins and Nuclear Transport

5.1 Introduction

Having successfully expressed the mature sequence of IPSE/alpha-1, *ShIPSE03*, *Smk5*, *FhGST-si* and *FhH2A*, the next objective of this study was to determine whether these infiltrins possess CSS and NLS motifs that in principle confer the ability to be secreted via the classical secretory pathway or alternative pathway, and subsequently translocate into host cell nuclei following uptake by host cells. This introduction will provide an overview of CSS and NLS and then move to focus on the first infiltrin discovered in 2011, and an *in vitro* study by our group which demonstrated the nuclear import of IPSE/alpha-1 from *E. coli* with modified NLS into host cells, Huh7 and U-2 OS (265).

5.1.1 Classical and non-classical secretory pathways

Eukaryotic protein secretions are generally targeted to the ER and Golgi complex by CSS and the classical secretory pathway (294). The non-classical pathway does not require a signal sequence, whereas the classical secretory pathway does (318). The classical pathway is one way for the secretion of proteins, whereas the non-classical pathway is an alternative, less common way, and is utilised for fibroblast growth factor-1(FGF1), interleukin-1(IL-1 α/β) and viral proteins and some parasite proteins (319, 320). It has been shown that some secreted proteins from helminths, e.g. macrophage migration inhibitory factor (MIF or MMIF) is mediated by a non-classical pathway involving an ATP-binding cassette(ABC) transporter (321). The CSS sequence is a short peptide (between 5 and 30 amino acids, usually around 20), present at the N-terminal region of some secretory proteins which use the classical secretory pathway (299, 322).

The presence of CSS and NLS on the same polypeptide chain of a protein occurs very rarely, and only a limited number of studies have described proteins with dual CSS/NLS signals. Fibroblast growth factor-3 (FGF3) in mice has six amino acids positioned between the signal sequence cleavage site and bipartite NLS; however, this distance is much greater in IPSE/alpha-1 (140 amino acids) and this wide distance between the signal sequence cleavage site and the NLS leads to the CSS motif in IPSE/alpha-1 being cleaved during export (223, 224, 323). In parathyroid hormone-related protein (PTHrP), the signals are separated by 99 amino acids, and it is targeted to the ER by the CSS, and an unknown pathway for nuclear localisation, as a small amount of protein is directed to the nucleus dependent upon the cellular requirements. The Bet protein of human foamy viruses (HFV) is secreted via the non-classical pathway and is not inhibited by Brefeldin A; this protein has been observed in both the cytoplasm and nucleus after transfection and in infected cells (324, 325). The zymogens of human matrix metalloproteinase-3 (MMP-3), which is secreted into the extracellular matrix and activated by proteases, contain a NLS and is directed to the nucleus by an NLS-dependent mechanism (326, 327). In contrast, IPSE/alpha-1 is secreted via the classical pathway and has dual CSS/NLS signal. The CSS motif of IPSE/alpha-1 targets it to the ER via 'cotranslational transport', especially for protein of more than 100 amino acids.

Commonly, proteins with or without NLS not able to target the nucleus. However, proteins with dual the N-terminal CSS/NLS signals are usually able to targeted to the nucleus. In IPSE/alpha-1, signal recognition particle (SRP) interacts with N-terminal CSS and directs them to the membrane of the endoplasmic reticulum. Next, the CSS motif in

mature IPSE/alpha-1 is cleaved during export the ER lumen. The C-terminal NLS (PKRRRTY) motif has the ability to translocate to host cell nuclei (223, 224, 265, 266) .

5.1.2 Nuclear Localisation

The transport (import and export) of proteins between the nucleus and the cytoplasm is through nuclear pore complex (NPC), which are 120 nm in diameter and approximately 70 nm thick (328). NPCs are randomly distributed across the nuclear membrane and are therefore nuclear envelope structures (329). Smaller proteins up to 40 kDa can fully pass through these channels in the nuclear membrane unimpeded via passive diffusion (330). It should be noted that proteins >40 kDa, mainly NLS-cargo proteins, can also pass through NPCs (120 nm diameter), but at slower rates (331-333). Moreover, proteins >70 kDa can also be transported through NPCs, but via an energy dependent process (276, 334, 335). These proteins will usually contain a NLS (336) that enhances their uptake, which consists of a small stretch of positively charged amino acids, such as arginine (R) and lysine (K). A single continuous stretch of basic amino acids is termed monopartite whilst two adjacent stretches of basic amino acids separated by short intervening sequences of variable length are referred to as bipartite. Proteins containing either a monopartite or bipartite sequence, or both signal sequences in their primary sequence have the ability to bind to an import receptor called importin α present in the cytoplasm which enables nuclear import. The first discovered NLS was in Simian virus (Sv40) (PKKKRKV), which was a T-Antigen (monopartite), while *Xenopus* nucleoplasmin (KRPAATKKAGQAKKK) is the first described bipartite (280, 281, 334). Importin karyopherins have two receptors (importin α and importin β). The N-terminal region of importin α contains 90 amino acids which are required for binding to importin β , the

importin-beta-binding (IBB) domain (337). The NLS of a protein can be recognised by importin α , which binds to a target cargo protein carrying a NLS and interacts with importin β , although occasionally, a NLS can bind directly to importin β without the involvement of importin α (338-340). Importin β directs the translocation of the complex to the nucleus through the NPC (341). Once the import complex reaches the nucleus, importin β binds to Ran guanosine triphosphate (RanGTP), and this new interaction destabilises the trimeric import complex, resulting in the release of the cargo protein. RanGTP recycles the import receptor (importin α) back to the cytoplasm to prepare for new imports (Figure 5.1) (334, 342, 343).

In terms of export, the release of protein from the nucleus is based on the presence of nuclear export signals (NESs) which have been grouped into three different classes (344). First are exportins (or CRM1) which possess a NES rich in hydrophobic residues (commonly leucine) which can interact with importin β (345, 346). Second are transportins, where the export of nuclear proteins occurs via a nucleocytoplasmic shuttling signal (NSS) (333, 347, 348). Finally, the NLS of a protein, which consists of a small chain of positively charged amino acids present at the C-terminus, can be used to transport proteins from the nucleus to the cytoplasm through NPCs (349). Nuclear export using a NLS appears to be via a similar mechanism to nuclear import, but there a difference concerning RanGTP. Ran in the nucleus promotes cargo protein binding to the receptor instead of the release of the cargo protein. Once the export complex reaches the cytosol, RanGTP encounters RanGAP, and this new interaction destabilises the trimeric import complex, resulting in the release of the cargo protein (350, 351).

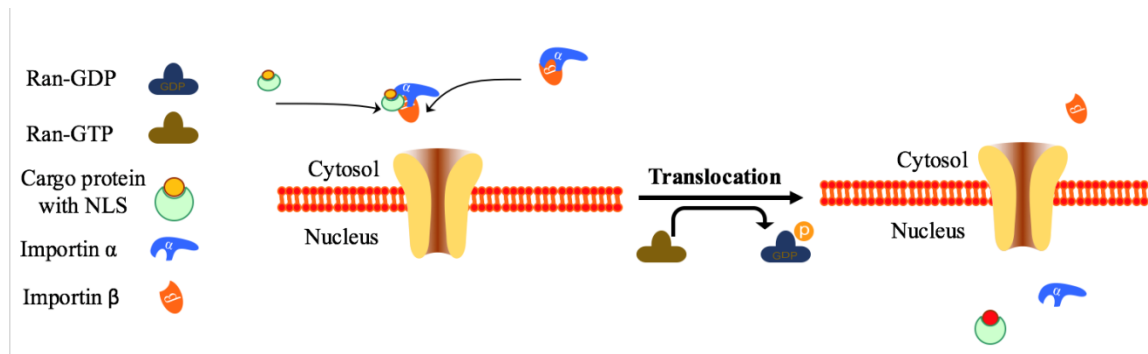


Figure 5.1: Ran-GTP nuclear transport cycle

The role of importin α , which has an N-terminal importin-beta-binding (IBB) domain, and importin β to direct the proteins with NLS between the nucleus and the cytoplasm is through nuclear pore complexes (NPCs).

5.1.3 Nuclear Localisation of IPSE/alpha-1

As mentioned earlier, IPSE/alpha-1 is considered the first example of an infiltrin (Figure 5.2). IPSE/alpha-1 contains a secretory signal of twenty amino acids at the N-terminus and a C-terminal NLS, namely, PKRRRTY, both of which have been confirmed experimentally (223, 265). The SRP involved in co-translational transport is important in directing secretory polypeptide chains to the ER lumen by recognising and binding to a CSS, even before the NLS is translated (223, 266). Therefore, proteins with dual CSS/NLS signals are not able to reach the nucleus, even if a C-terminal NLS is present(265). Conversely, a CSS is not usually present in predominantly nuclear proteins. The CSS motif in IPSE/alpha-1 is cleaved during export(223). Moreover, IPSE/alpha-1 is largely secreted from the von Lichtenberg's envelope in the subshell zone of mature *Schistosoma mansoni* eggs, and infiltrates into the surrounding tissues through channels in the egg shell (146). In 2011 it was shown in our laboratory that the C-terminal sequence, 125-PKRRRTY-131, is the NLS of mature IPSE/alpha-1, and this plays a necessary role in the process of transferring this protein into the nuclei of host cells. This was observed

in human hepatoma (Huh7) and human osteosarcoma (U-2 OS) cell lines *in vitro* (265). Therefore, IPSE/alpha-1 has both the necessary features of postulated infiltrins.



Figure 5.2: General postulated features of infiltrins as seen in IPSE/alpha-1

Infiltrins possess an N-terminal classical hydrophobic secretory signal (CSS) and at least one C-terminal NLS, which can be bipartite or monopartite, shown in A is a bipartite NLS. Our archetypal infiltrin IPSE/alpha-1 consists of twenty amino acids located at the N-terminus (CSS) and a monopartite PKRRRTY NLS close to the C-terminus. The DNA binding domain has not yet been mapped accurately in IPSE/alpha-1, but is thought to overlap at least in part with the NLS, as IPSE variants with a 10 AA C-terminal truncation do not bind DNA.

Source: (2).

Based on our definition, infiltrins (or pathogen-secreted host nuclear proteins) are putative proteins secreted by a parasite with the ability to enter host cells, where they are able to translocate into the nucleus. There, they may bind to DNA, and act e.g. as transcription factors. In the nuclei of host cells, IPSE/alpha-1 is likely to play an essential role in the modulation of the immune response(265), and this would suggest that infiltrins may be better targets for vaccination because they act as ‘master switches’ (Figure 5.3).

Therefore, this study seeks to determine whether in addition to IPSE/alpha-1, other parasite-derived secreted factors have the ability to translocate to host cell nuclei. Initially, in Chapter 3, bioinformatics analysis was used to predict the possibility of an NLS for ShIPSE03, FhGST-si and FhH2A. To confirm this bioinformatics prediction, the ability

of these potential infiltrins to translocate into HTB9 or Huh7 cells will be determined by cloning the genes into the plasmid, pAcGFP1-C3. This will result in an in-frame fusion with a gene encoding a green fluorescent protein (GFP).

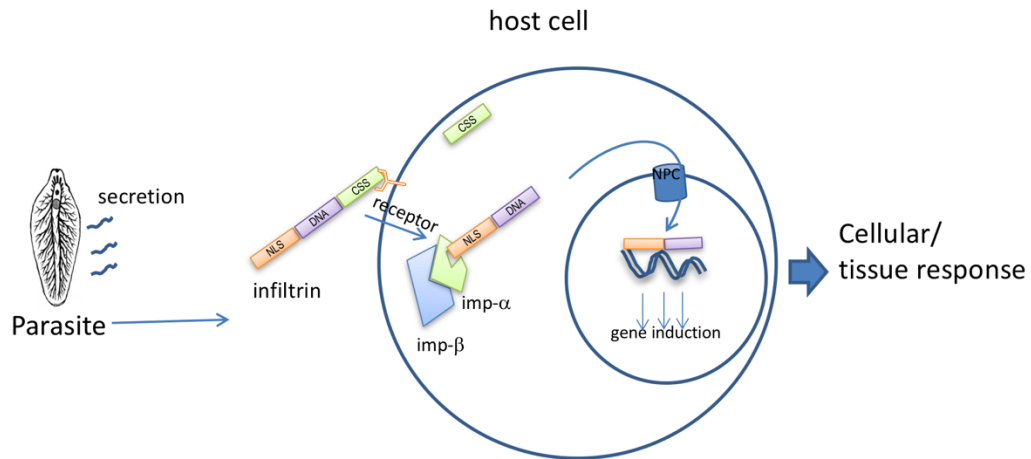


Figure 5.3: Suggested infiltrin mechanism (working hypothesis)

Infiltrins (or pathogen-secreted host nuclear proteins) are secreted by a parasite and have the ability to enter host cells via a receptor or other e.g. cell-penetrating peptide-like properties. Once inside the cytosol they can interact with the host cell nuclear import machinery, e.g. karyopherins importin α/β system (imp- α , imp- β), and translocate to the nucleus through nuclear pore complexes. Once inside the nucleus, an infiltrin can bind to DNA and act as a transcription factor, inducing an environment conducive to the parasite's survival and/or transmission.

5.2 Experimental Procedures

5.2.1 PCR Amplification and Subcloning of Infiltrins into the Vector

pAcGFP1-C3

Full length PCR fragments were amplified from cDNA of *Schistosoma* genes using Phusion® high-fidelity DNA polymerase (New England BioLabs) using a denaturation step of 98°C for 30 seconds, then 30 cycles of denaturation at 98°C for 10 seconds, annealing at 72°C for 30 seconds and extension at 72°C for 30 seconds, followed by a final extension at 72°C for 10 minutes. *F. hepatica* genes were excised with *SacI* and

KpnI from synthetic DNA templates before being purified using the Wizard® SV Gel and PCR clean-up kit (Promega), as per the manufacturer's instructions. Digested PCR products and vector DNA were separated by 1% agarose gel electrophoresis using the SYBR® Gold Nucleic Acid Gel Stain dye to visualise the DNA (under ultraviolet light). The appropriate DNA fragments were excised from the gel and purified using the Wizard® SV Gel and PCR clean-up kit (Promega) following the manufacturer's instructions. Subsequently, the fragments were cloned into a fluorescent protein fusion vector to investigate whether the mature infiltrin proteins are able to translocate into the nucleus of mammalian cells.

The PCR products were ligated into pAcGFP1-C3 (Clontech, BD Biosciences), which carries a kanamycin resistance gene, using 1 µL vector, 7 µL insert, 1 µL 10× Buffer T4-ligase and 1 U T4 DNA ligase (Promega) in a 10 µL reaction mixture. The plasmid encodes for a modified GFP from *Aequorea coerulea* which has been optimised for brighter fluorescence and has been codon-optimised for use in human cells. The ligase reaction was incubated at 16°C for 6 h. The presence and orientation of the insert was verified by plasmid DNA sequencing (using same cloning method as described in Section 4.2.1.3), using vector specific T7 sequencing primers. The same protocol was also used to clone smaller gene fragments into pAcGFP1-C3. Figure 5.4 shows the initial and progressive stages to verify and map the location of the predicted NLS for each infiltrin.

Table 5.1: Primer sequences

Primer No.	Construct Backbone	Primer Name	5'-3' Sequence
1153	pAcGFP1-c3	pAcGFP1-c3 Promoter FOR	ACTACCTGTCCACCCAGAGC
1150	pAcGFP1-c3	pAcGFP1-c3 Terminator REV	ATGTTTCAGGTTTCAGGGGGAG
1107	pAcGFP1-c3	FOR-pEGFP-C-XhoI (K-5)	CCGCCGCTCGAGATGCTCAGTCT CCTACAAACGA
1108	pAcGFP1-c3	REV-pEGFP-C-BamHI (K-5)	TATATAGGATCCTTAATGGTGAT GATGGTGGTGCATGTAGACTCCA TACTTGTGAT
1179	pAcGFP1-c3	Smk-5 pEGFP-C3 (+CAGT) For	[phos]GCAGTCGACGGTACCAGCT GCTAGCCAGTATGCTCAGTCTCC TACAAACGATGA
1168	pAcGFP1-c3	Smk-5 pEGFP-C3 Rev	[phos]AGAATTCGAAGCTTGAGCT CGAGATCTGAGTACTTGTACGCT CATCCATGCG
1188	pAcGFP1-c3	Sm k5- For primer from 1st part-SacI	CTATCGGAGCTCCAGTCTCCTAC AAACGATGAGATGCAT
1189	pAcGFP1-c3	Sm k5- Rev primer from 1st part-kpnI	GCGGCGGGTACCTAAGACTTCAC AACCATATGTTATGTCTTTTTG
1190	pAcGFP1-c3	Sm k5- For primer from 2nd part-XhoI	CCGCCGCTCGAGCTGAAGAAAT ATTCCGAGTTGAAATGG
1191	pAcGFP1-c3	Sm k5- Rev primer from 2nd part-KpnI	GCGATAGGTACCTTACATGTAGA CTCCATACTTGTGATCCAC
1180	pAcGFP1-c3	FH-GST- For primer from 1st part-SacI	CCGTACGAGCTCGACAAACAGC ATTTCAAACGTGGTA
1181	pAcGFP1-c3	FH-GST-Rev primer from 1st part-KpnI	GCCGTAGGTACCTTATACAGATC TTCGCATTCGCCAATAA
1182	pAcGFP1-c3	FH-GST-For primer from 2nd part-SacI	GCGCCAGAGCTCCGTGAAGTGT ATACCATTTTTTCGTACAC
1183	pAcGFP1-c3	FH-GST-Rev primer from 2nd part-KpnI	GCCGCCGGTACCTTAAAACGGG GTTTTTGCACGTTTTTTCA
1184	pAcGFP1-c3	FH-H2A- For primer from 1st part-SacI	TAATAAGAGCTCGCAGGCGGTA AAGCAGG
1185	pAcGFP1-c3	FH-H2A- Rev primer from 1st part-KpnI	GCCGCAGGTACCTTATTTTCAGAT CTTTGCTTGCATTACCTGC
1186	pAcGFP1-c3	FH-H2A- For primer from 2nd part-SacI	CTATCGGAGCTCGTGAACGTAT TACACCGCGT

1187	pAcGFP1-c3	FH-H2A- Rev primer from 2nd part-Kpn1	TGCGTAGGTACCTTACATACCCA GCGGTTTTGCAG
1226	pAcGFP1-c3	FHGST-C-N TERM-F-SacI	CGCGACGAGCTCCGTGAAGTGT ATACCATTTTTTCGTACACCG
1227	pAcGFP1-c3	FHGST-C-N TERM-R-BAMHI	GCCGCTGGATCCTTAGGGTTGTA AACAGAAACAGGTCACC
1228	pAcGFP1-c3	FHGST-C-C TERM-F-SacI	GTATGCGAGCTCGAAACCGTTCC GGGTTTTCTGGAAC
1229	pAcGFP1-c3	FHGST-C-C TERM-R-BAMHI	GCGGCCGGATCCTTATTAACACG GGGTTTTTCACGTTTTTTCAG
1230	pAcGFP1-c3	FHH2A-C-N TERM-F-SacI	GCAGACGAGCTCGTGAAACGTA TTACACCGCGTCATCT
1231	pAcGFP1-c3	FHH2A-C-N TERM-R-BAMHI	GCCGCTGGATCCTTAACCACCGG CAATGGTTGCTTTAATCA
1232	pAcGFP1-c3	FHH2A-C-C TERM-F-SacI	CGCGGCGAGCTCGGTGTTATTCC GCATATTCATAAAAAGCCTG
1233	pAcGFP1-c3	FHH2A-C-C TERM-R-BAMHI	GCGCCAGGATCCTTATTACATAC CCAGCGGTTTTGCAG

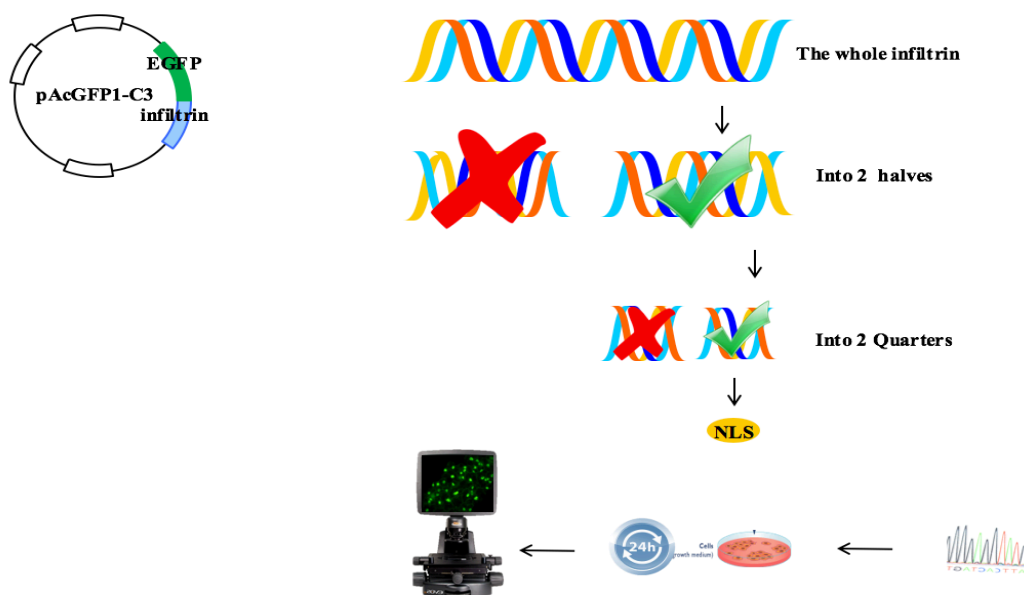


Figure 5.4: Steps involved in the amplification of the infiltrins

Truncated versions of the candidate infiltrins were generated to identify the location of the NLS for each candidate. Full length and truncated PCR fragments were amplified and subcloned into the vector, pAcGFP1-C3 and successful clones were transfected into cells. Images of the transfected cells were visualised by fluorescence microscopy after 24 h.

5.2.2 Subcloning of the Predicted NLS into the Vector pTetra-GFP

The predicted NLS for each infiltrin was subcloned into the Tetra-GFP vector (see Appendix 5) created by Christian Beetz, which carries a kanamycin resistance gene (276). This vector includes four EGFP copies and a multiple cloning site between the third and fourth EGFP into which the suspected NLS is inserted using phosphorylated oligonucleotide primers and specific restriction enzymes, which leads to a construct which codes for a tetra-EGFP fusion protein of > 100 kDa that is completely excluded from the nucleus in the absence of a functional NLS. Initially, 5'-phosphorylated pairs of matching oligonucleotides were designed (Table 5.2 and Table 5.3) to code putative NLSs containing GATC overhangs by using 1 μ L of each oligo (100 μ M) mixed with 98 μ L of EB elution buffer (Qiagen), followed by denaturation at 95°C for 7 minutes, then 3 minutes at 5°C. Next, the mixed pairs of oligonucleotides and the pTetra-EGFP vector were digested with the restriction enzyme *Bgl*III (New England Biolabs, USA), according to the manufacturer's protocol. The ends of the linearised pTetra-EGFP vector were dephosphorylated with antarctic phosphatase (New England BioLab, UK) to avoid re-ligation to itself, following the manufacturer's instructions. Ligation was performed using 1 μ L vector, 3 μ L insert, 7 μ L 10X Buffer T4-ligase, and 1 U T4 DNA ligase (Promega) in a 12 μ L reaction mixture and incubated overnight at 16°C. The next cloning step used the same methods as described in Section 4.2.1.3, by using the vector specific T7 sequencing primers (Table 5.4) for colony PCR, and confirmatory sequencing using the Tetra-EGFP-Rev primer (No. 1142).

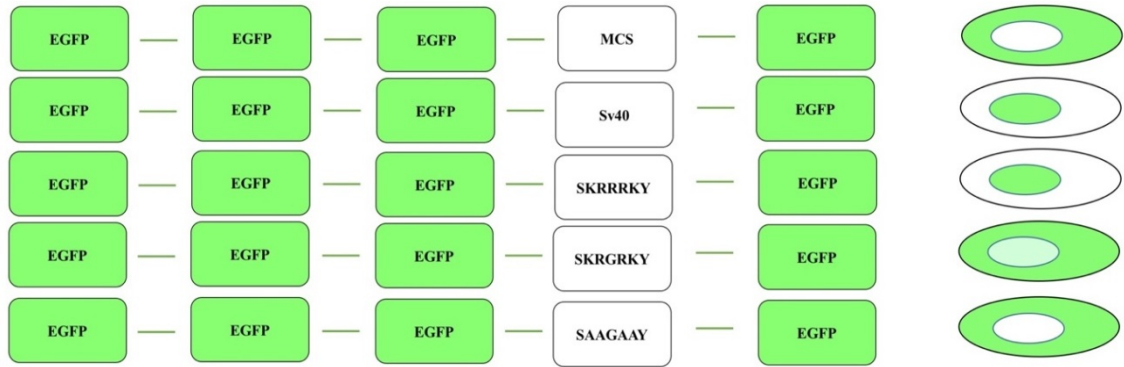


Figure 5.5: Schematic of the tetra-GFP construct and the potential NLS of *ShIPSE*

This vector includes four EGFP constructs and usually a NLS is inserted into the MCS between the third and fourth EGFP. In order from the top to the bottom: negative control (empty tetra-EGFP), positive control (Sv40), putative NLS (wild-type) and putative NLSs (mutants). The right side of the diagram shows where green fluorescence (cytoplasmic, nuclear or mixed) is expected.

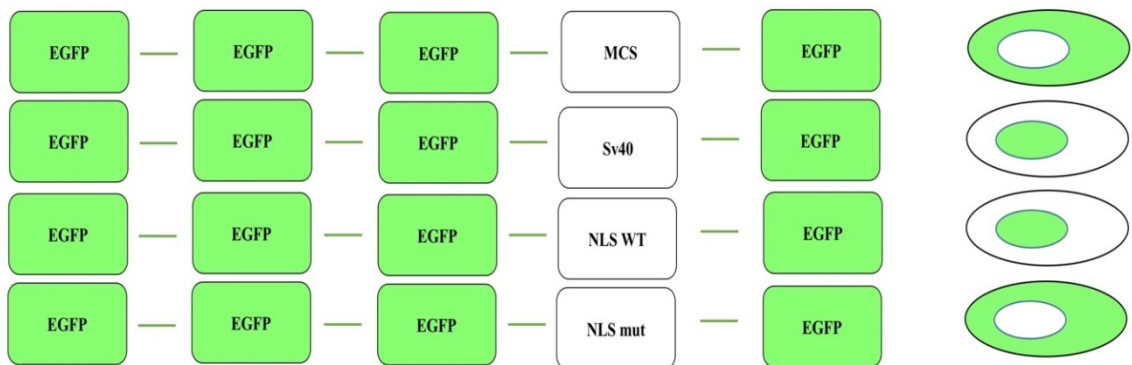


Figure 5.6: Schematic of the tetra-GFP construct with the NLS of *Smk5*, *FhGST-si* and *FhH2A*

Schematic of the tetra-GFP construct with the NLS of *Smk5*, *FhGST-si* and *FhH2A*. This vector includes four EGFP constructs and usually a NLS is inserted between the third and fourth EGFP. In order from the top to the bottom: negative control (empty tetra-EGFP), positive control (Sv40), putative NLS (wild-type) and putative NLSs (mutants). The right of the diagram shows the expected cytoplasmic or nuclear fluorescence.

Table 5.2: Oligonucleotide NLS primer sequences for Tetra-EGFP (*Schistosoma*)

Primer No.	Primer	[Phos] 5'-3' Sequence	Pairs
1119	PKKKRKY-For	GATCTCCGAAGAAGAAGAGGAAGGTAA	Sv40
1120	PKKKRKY-Rev	GATCTTACCTTCCTCTTCTTCTTCGGA	+ Control
1113	SKRGRKY-For	GATCTAGCAAGAGGGGAAGGAAGTACA	<i>ShIPSE03</i>
1114	SKRGRKY-Rev	GATCTGTA CTTCCCTCTTGCTA	1
1115	SKRRRKY-For	GATCTAGCAAGAGGAGGAGGAAGTACA	<i>ShIPSE03</i>
1116	SKRRRKY-Rev	GATCTGTA CTTCTCCTCTTGCTA	2
1117	SAA GAAY-For	GATCTAGCGCAGCAGGAGCAGCATACA	<i>ShIPSE03</i>
1118	SAA GAAY-Rev	GATCTGTATGCTGCTCCTGCTGCGCTA	3
1288	ELKRRVE-For	GATCTGAGTTGAAGAGAAGAGTGGAAA	<i>Smk5</i>
1289	ELKRRVE-Rev	GATCTTCCACTCTTCTCTTCAACTCA	1
1290	ELAAA VE-For	GATCTGAGTTGGCAGCAGCAGTGGAAA	<i>Smk5</i>
1291	ELAAA VE-Rev	GATCTTCCACTGCTGCTGCCAACTCA	2

Base pairs for binding of the restriction enzyme are shown in red. Introduced mutations are shown in blue.

Table 5.3: Oligonucleotide NLS primer sequences for Tetra-EGFP (*Fasciola hepatica*)

Primer No.	Primer	[Phos] 5'-3' Sequence	Pairs
1292	LKKRAKT -For	GATCTCTGAAAAACGTGCAAAA ACTA	<i>FhGST-si</i>
1293	LKKRAKT -Rev	GATCTAGTTTTTGCACGTTTTTTCAGA	1
1294	LAAA AKT -For	GATCTCTGGCAGCAGCAGCAAAA ACTA	<i>FhGST-si</i>
1295	LAAA AKT -Rev	GATCTAGTTTTTGCTGCTGCTGCCAGA	2
1296	IHRHLKT -For	GATCTATTCATCGTCATCTGAAA ACCA	<i>FhH2A</i>
1297	IHRHLKT -Rev	GATCTGGTTTTTCAGATGACGATGAATA	1
1298	IAA ALKT -For	GATCTATTGCAGCAGCACTGAAA ACCA	<i>FhH2A</i>
1299	IAA ALKT -Rev	GATCTGGTTTTTCAGTGCTGCTGCAATA	2

Base pairs for binding of the restriction enzyme are shown in red. Introduced mutations are shown in blue.

Table 5.4: Vector-specific primers for pTetra-GFP

Primer No.	Used with	Primer Name	5'-3' Sequence
1142	All	Tetra-EGFP-Rev	TGGATCCCGGGCCCGCGGTAC
1141	+ Control	Sv40-For	CCGGACTCAGATCTCCGAAGAAG
1138	<i>ShIPSE03-1</i>	SKRGRKY-For	AAGTCCGGACTCAGATCTAGC
1139	<i>ShIPSE03-2</i>	SKRRRKY-For	CTCAGATCTAGCAAGAGGAGG
1140	<i>ShIPSE03-3</i>	SAAGAAAY-For	GGACTCAGATCTAGCGCAGCA
1304	<i>Smk5-1</i>	ELKRRVE-For	AAGTCCGGACTCAGATCTGAGTTG
1305	<i>Smk5-2</i>	ELAAAVE-For	CTCAGATCTGAGTTGGCAGCAGCA
1306	<i>FhGST-si-1</i>	LKKRAKT-For	AAGTCCGGACTCAGATCTCTGAAA
1307	<i>FhGST-si-2</i>	LAAAANKT-For	CTCAGATCTCTGGCAGCAGCA
1308	<i>FhH2A-1</i>	IHRHLKT-For	AAGTCCGGACTCAGATCTATTCAT
1309	<i>FhH2A-2</i>	IAAALKT-For	CTCAGATCTATTGCAGCAGCA

5.2.3 Cell Culture and Transfection

The human bladder cancer cell line (HTB9) was used only with ShIPSE03, while a human hepatoma (Huh7) cell line was used for IPSE/alpha-1, *Smk5*, *FhGST-si* and *FhH2A*. Cells were grown in T75 flasks (Sarstedt, Germany), at 37°C in a humidified 5% CO₂ incubator, with Minimum Essential Medium Eagle (MEM; Sigma-Aldrich) supplemented with 5% heat-inactivated foetal bovine serum (FBS, GIBCO), 2 mM L-glutamine, 100 unit/mL penicillin and 100 µg/mL streptomycin (Sigma-Aldrich Co. Ltd., UK). Transfections were performed using X-tremeGENE9 DNA transfection reagent (Roche Applied Science, Germany) according to the manufacturer's protocol. Cells were plated onto 5mg/mL rat tail collagen I (Invitrogen, UK) -coated glass cover slips (15mm diameter, # 1 thickness) in 6-well plates, and transfected at 60-70% confluency.

5.2.4 Cell Fixation and Fluorescence Microscopy

One-day after transfection the cells were washed with Dulbecco's phosphate-buffered saline (DPBS, Gibco) and fixed in 4% paraformaldehyde (1.6 g paraformaldehyde, Fisher

Scientific, UK, heat while stirring to approximately 60 °C in 200 mL 1X PBS, add a drop of 5 M sodium hydroxide and cool at room temperature) for 10-15 mins. The cells were then washed three times with DPBS and incubated with 0.5 g/mL Hoechst 33342 stain (Sigma-Aldrich) at room temperature for 8-15 minutes, before washing three times with DPBS. Slides were mounted with mounting medium (Sigma-Aldrich), which helps preserve samples and raises the refractive index to give a good performance with fluorescence of the fusion protein. Images of the transfected cells were visualised by fluorescence microscopy (EVOS *fl*, Advanced Microscopy Group, USA) and confocal microscope (LSM510 META, ZEISS, Germany), and analysed using Zeiss LSM Image Browser software (version 4.2.0.121).

5.2.5 Cellular Uptake of Infiltrins

HTB9 and Huh7 were seeded onto Lab-Tek 8-well chambered coverglass (155411, Nalge Nunc International) at a concentration of 5×10^5 cells in order to achieve 50-60% confluency after 24 hours. Cells were then incubated with 15-0.40 nM of recombinant infiltrins (IPSE/alpha-1, *ShIPSE03*, *Smk5*, *FhGST-si* and *FhH2A*) in serum free internalisation medium (HEPES buffered HAMS-F12 media containing 10 mM NaHCO₃ and 2 mg/mL BSA (Fraction V- Biomol 01400) for 24hours, followed by fixing for 10-15 mins in 4 % paraformaldehyde solution. The cells were then washed 4-5 times with DPBS and incubated with 0.5 µg/mL Hoechst 33342 nuclear stain for 15 min and permeabilised with 0.2% Triton X-100 in DPBS for 10 min. The cells were washed 4-5 times with DPBS and incubated separately at 24°C for 30 min with two different primary antibodies diluted 1:5000: mouse anti-His antibody (GE Healthcare) (first uptake experiment) or mouse monoclonal anti-IPSE/α-1 (clone number 74 4B7), which kindly

donated by Dr. Schramm, for the second uptake experiment(223). The cells were washed three time and then labelled with the secondary antibody, 1:500 diluted Alexa Fluor 555-conjugated goat anti-mouse IgG (H+L; Molecular Probes), by incubation at 24°C for 30 min, followed by three final washes.

5.3 Results

5.3.1 Uptake of recombinant Putative Infiltrins

Bioinformatics tools are often not accurate in predicting NLSs; therefore, the presence of a putative NLS in the selected infiltrins needs to be demonstrated and mapped experimentally. In 2011, an *in vitro* study from our group demonstrated the nuclear import of IPSE/alpha-1 with a predicted NLS (125-PKRRRTY-131) into mammalian cells, Huh7 and U-2 OS(265). Similarly, recombinant infiltrins (IPSE/alpha-1, ShIPSE03, Smk5, FhGST-si and FhH2A) were examined for uptake in HTB9 or Huh7 cells. Initially, the uptake of the wildtype of IPSE/alpha-1 from HEK293 was able to access the inside of the nucleus of Huh7 cells and the result is shown in Figure 5.7. Interestingly, ShIPSE03 has the ability to translocate into the nucleus of HTB9 cells (Figure 5.8), and Smk5, FhGST-si and FhH2A also have this ability to translocate into the nucleus of Huh7 cells, with the results shown in Figure 5.9 and Figure 5.10.

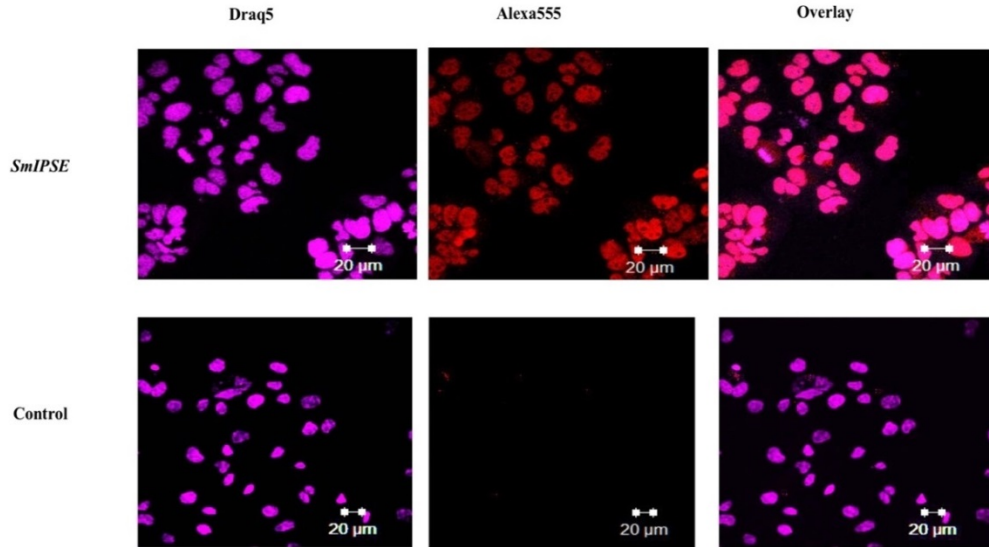


Figure 5.7: Cellular uptake of IPSE/alpha-1

Huh7 cells were stained with 5 μM DRAQ5TM (Fluorescent Probe is a far-red DNA stain, used to report nuclear DNA) for 15 minutes at room temperature (left), followed by staining with mouse anti-His antibody and goat anti-mouse IgG (H+L) and Alexa Fluor[®] 555 conjugate for 15 minutes at room temperature (middle). The images are shown overlaid (right). Cellular uptake was visualised by confocal microscopy using a 40X objective lens (Scale bar, 20 μm). A control in which the tissue is incubated without primary antibody.

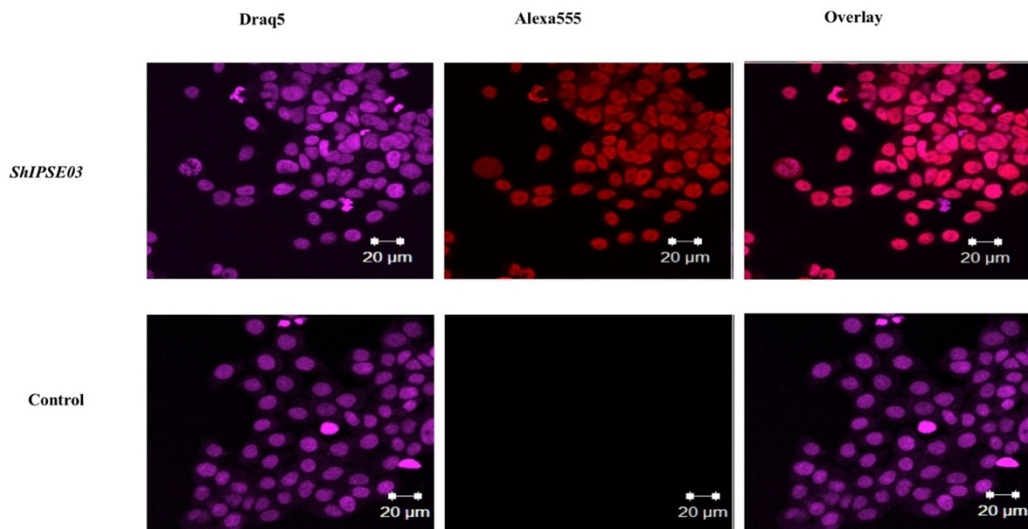


Figure 5.8: Cellular uptake of ShIPSE03

HTB9 cells were stained with 5 μM DRAQ5TM for 15 minutes at room temperature (left), followed by staining with mouse anti-His antibody and goat anti-mouse IgG (H+L) and Alexa Fluor[®] 555 conjugate for 15 minutes at room temperature (middle). The images are shown overlaid (right). Cellular uptake was visualised by confocal

microscopy using a 40X objective lens (Scale bar, 20 μm). A control in which the tissue is incubated without primary antibody.

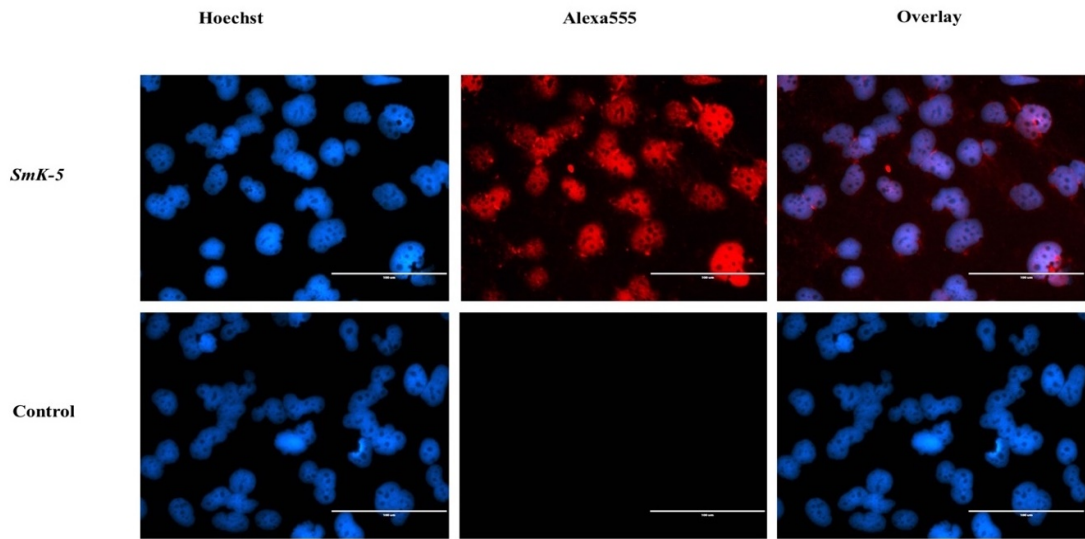


Figure 5.9: Cellular uptake of Smk5

Huh7 cells were stained with 5 μM DRAQ5TM for 15 minutes at room temperature (left), followed by staining with mouse anti-His antibody and goat anti-mouse IgG (H+L) and Alexa Fluor[®] 555 conjugate for 15 minutes at room temperature (middle). The images are shown overlaid (right). Cellular uptake was visualised by fluorescence microscopy (EVOS^{fl}) using a 40X objective lens (Scale bar, 10 μm). A control in which the tissue is incubated without primary antibody.

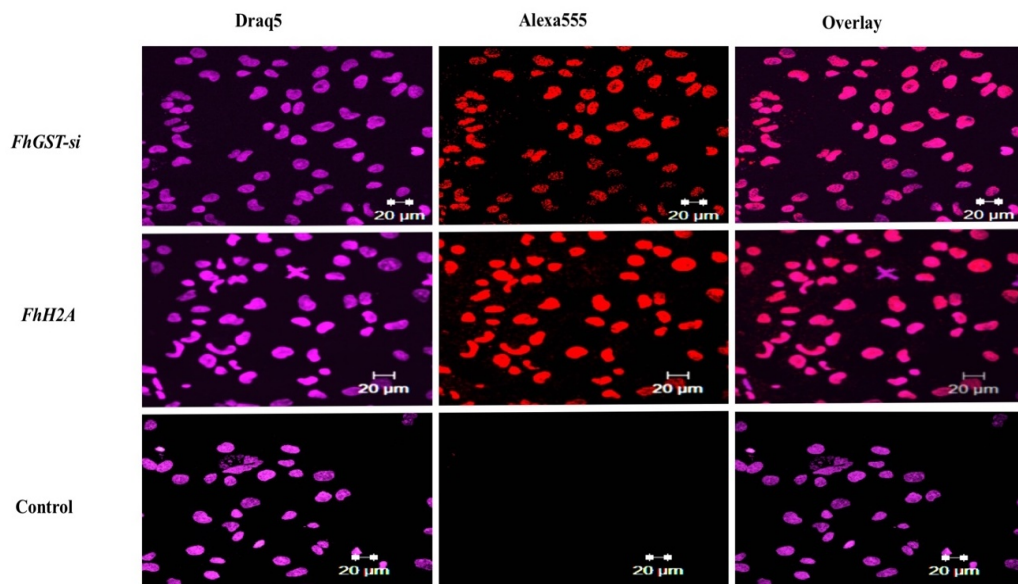


Figure 5.10: Cellular uptake of FhGST-si and FhH2A

Huh7 cells were stained with 5 μM DRAQ5TM for 15 minutes at room temperature (left), followed by staining with mouse anti-His antibody and goat anti-mouse IgG (H+L) and

Alexa Fluor® 555 conjugate for 15 minutes at room temperature (middle). The images are shown overlaid (right). Cellular uptake was visualised by confocal microscopy using a 40X objective lens (Scale bar, 10 µm). A control in which the tissue is incubated without primary antibody.

5.3.2 Analysis of the NLS of Putative Infiltrins

After the results demonstrated the uptake of recombinantly expressed infiltrins added exogenously, the potential NLSs of these infiltrins were demonstrated and mapped experimentally using full length and smaller fragments of the encoding genes cloned into pAcGFP1-C3, which resulted in an in-frame fusion with a gene encoding AcGFP. The bioinformatics tool to predict the NLS of ShIPSE03, Smk5, FhGST-si and FhH2A was presented in Chapter 3. This led to the study of the effect of nuclear translocation in Huh 7 cells, which was achieved by using different cloning step to insert the WT sequence or C-terminal or N-terminal regions of these protein into the plasmid pAcGFP1-C3, which created an in-frame fusion between the protein of interest and acGFP1 (a monomeric fluorescent protein with similar properties to EGFP). Figure 5.11 and Figure 5.12 show how AcGFP fused to wild-type FhGST-si (A), FhH2A (B) and Smk5 (C) showed complete nuclear localisation, together with AcGFP fusions with FhGST-si-C-term (F), FhH2A-N-term (G) and Smk5-C-term (J); however, fusions with FhGST-si-N-term (E), FhH2A-C-term (H) and Smk5-N-term (I) showed mixed nuclear and cytoplasmic localisation, suggesting the absence of a functional NLS. Fusions between GFP and FhGST-si-C-C-term (L) and FhH2A-N-N-term (M) showed complete nuclear localisation, while fusions with FhGST-si-C-N-term (L) and FhH2A-N-C-term (M) show mixed nuclear and cytoplasmic localisation, again suggesting the absence of a functional NLS. The results obtained by fluorescence microscopy confirmed that ShIPSE03, Smk5 and FhGST-si proteins all possess a C-terminal NLS, whereas FhH2A has a N-terminal

NLS. It was not known whether the NLS of ShIPSE03, Smk5, FhGST-si and FhH2A are functional in targeting the proteins to the nuclei of host cells. Therefore, the putative NLS motifs of these infiltrins were subcloned into the pTetra-EGFP plasmid construct.

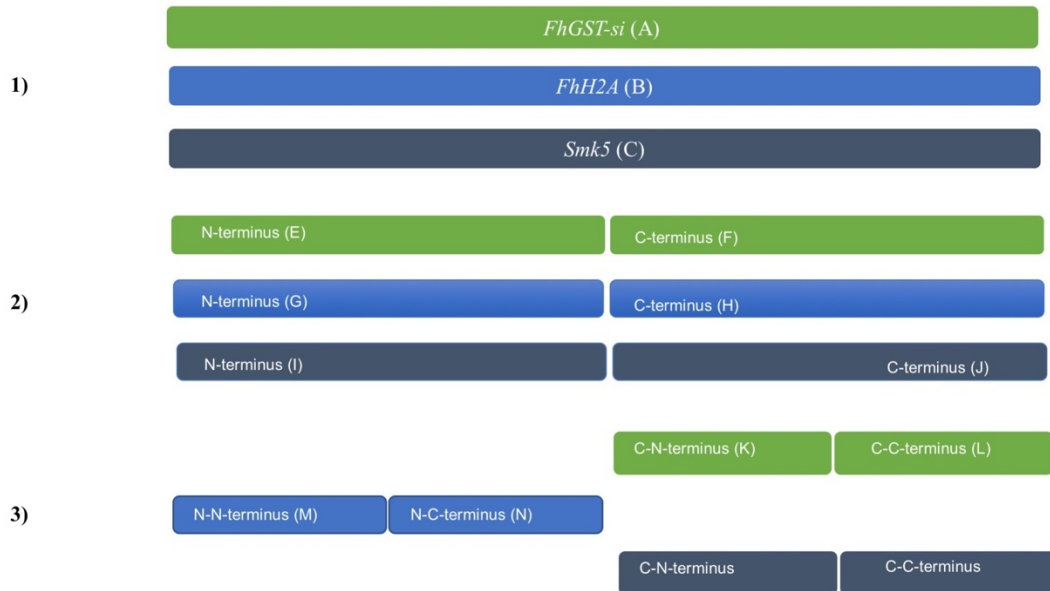


Figure 5.11: Diagram representing the different amplified infiltrins FhGST-si, FhH2A and Smk5 proteins and their sub-fragments. This scheme helps to explain the results shown in Figure 5.12.

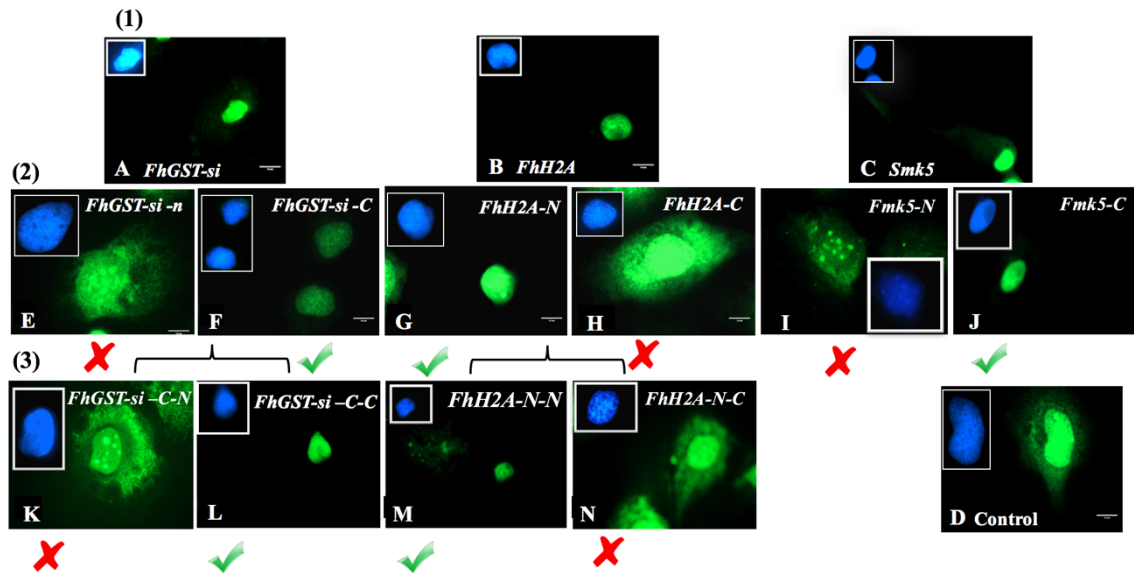


Figure 5.12: Nuclear translocation of FhGST-si, FhH2A and Smk5 in Huh7 hepatocytes AcGFP1 fusion constructs with FhGST (A), FhH2A (B) and Smk5 (C) in and FhGST-C-term (F), FhH2A-N-term (G) and Smk5-C-term (J) in were transiently transfected into Huh7 cells; fluorescence is completely localised to the nucleus. Fusion constructs with FhGST-N-term (E), FhH2A-C-term (H) or Smk5-N-term (I) and control (D) show mixed nuclear and cytoplasmic localisation. Fusion constructs FhGST-si and FhH2A, FhGST-C-C-term (L) and FhH2A-N-N-term (M) are completely localised to the nucleus, whereas FhGST-C-N-term (K) and FhH2A-N-C-term (N) show mixed nuclear and cytoplasmic localisation. All images taken 24 h after transfection with AcGFP1 as a control (D) (inserts show Hoechst nuclear stain). Scale bar, 10 μ m.

To better understand the effect of the importance of positively charged amino acids in the NLS of these infiltrins on nuclear localisation different sequences were assessed. Therefore, the pTetra-EGFP plasmid constructs contained either wild-type or various alanine-substituted NLS sequences, which were transfected into HTB9 or Huh7 cells and the fluorescence visualised via fluorescence microscopy (EVOS *fl*) after 24 h. As shown in figure Figure 5.13, Figure 5.14 and Figure 5.15, GFP fused to the NLS from wild-type *ShIPSE03* (125-SKRRRKY-131), *Smk5* (256-ELKRRVE-262), *FhGST-si* (202-LKKRAKT-208) and *FhH2A* (35-IHRHLKT-41) showed complete nuclear localisation, whereas GFP fused to NLS mutants *ShIPSE03* (SAAGAAY), *Smk5* (ELAAAVE), *FhGST-si* (LAAAAKT) and *FhH2A* (IAAALKT) showed only cytoplasmic localisation.

Moreover, careful inspection of *ShIPSE03* (SKRGRKY) showed that some fluorescent protein had remained in the cytoplasm but this had little effect on overall nuclear localisation (see Figure 5.13).

Quantitatively, using microscopy to assess at least 100 transfected cells, nuclear localisation was counted and the results are presented in Figure 5.16 and Figure 5.17. It can be seen from Figure 5.16 that *ShIPSE03* (125-SKRRRKY-131) and *ShIPSE06* (SKRGRKY) were localised into the nucleus in 97% and 60% of cells, respectively, whereas approximately only 10% of cells showed strong nuclear localisation for *ShIPSE03* (SAAGAAY). This indicates that the important amino acid residues in the *ShIPSE03* NLS are (KRRRK) and these have an essential role in translocation into the nuclei of mammalian cells. In Figure 5.17, GFP fused to wild-type *Smk5* (256-ELKRRVE-262), *FhGST-si* (202-LKKRAKT-208) and *FhH2A* (35-IHRHLKT-41) has the ability to translocate into the nucleus of Huh7 cells in 85%, 97% and 83% of cells, respectively, whereas less than 15% of the cells show nuclear localisation for the mutants *Smk5* (ELAAAVE), *FhGST-si* (LAAAAKT) and *FhH2A* (IAAALKT). This indicates that the important amino acid residues in the NLS of *Smk5*, *FhGST-si* and *FhH2A* are (KRR), (KKR) and (HRH), respectively, and these have an essential role in translocation into the nuclei of Huh7 cells.

In Section 4.3.1, wild-type and mutant *ShIPSE03* and *IPSE/alpha-1* and *Smk5* were expressed and purified from HEK293, whereas only wild-type *FhGST-si* and *FhH2A* were expressed in bacteria. Therefore, *ShIPSE03* and *IPSE/alpha-1* were examined again for uptake by HTB9 or Huh7 cells, respectively, but this time using both glycosylated *ShIPSE03* and wild-type and mutant *IPSE/alpha-1*. As shown in Figure 5.18 and

Figure 5.19, both recombinant glycosylated and wild-type IPSE were able to access the inside of the nucleus of mammalian cells. However, mutant recombinant IPSE showed cytoplasmic localisation, suggesting that the absence of KRRR leads to disabling of the NLS function. Microscopy was used to quantitatively assess nuclear localisation in at least 100 cells Figure 5.20. It was found that ShIPSE03 (125-SKRRRKY-131) and IPSE/alpha-1 (125-PKRRRTY-131) were localised to the nucleus in more than 90% of cells, whereas the mutants ShIPSE03 (SAAGAAY) and IPSE/alpha-1 (PKAAATY) showed cytoplasmic localisation.

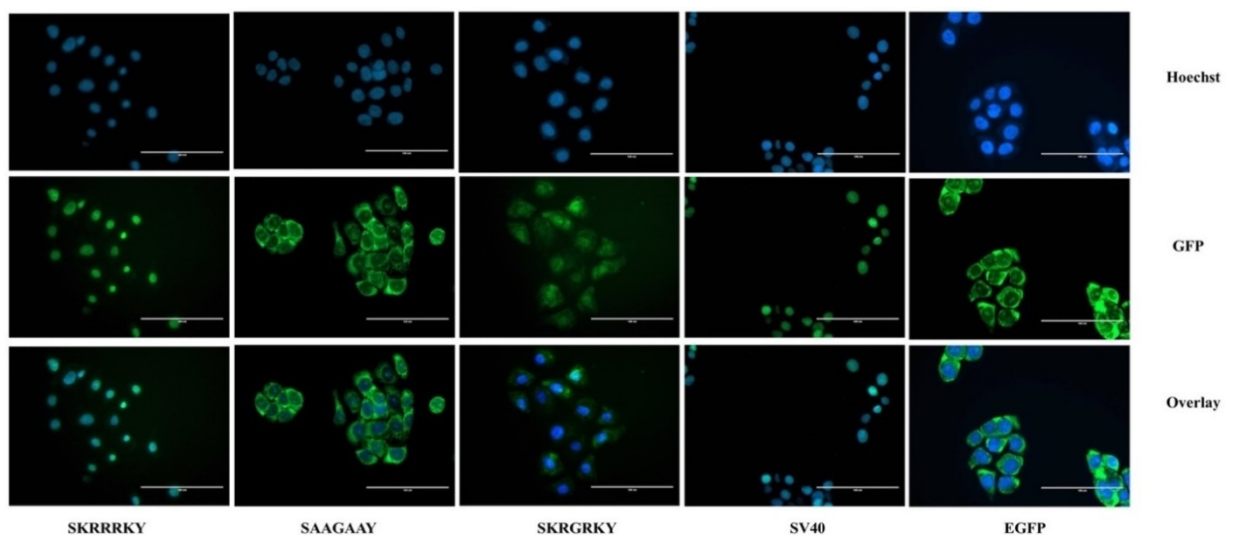


Figure 5.13: Localisation of wild-type and mutant Tetra-EGFP-ShIPSE03 NLS
 pTetra-EGFP plasmid constructs containing a positive control (Sv40), negative control (unmodified vector) and either wild-type or different alanine-substituted NLS sequences, transfected into HTB9 cells and visualised by fluorescence microscopy (EVOS *fl*) after 24 h. (Scale bar, 10 μ m)

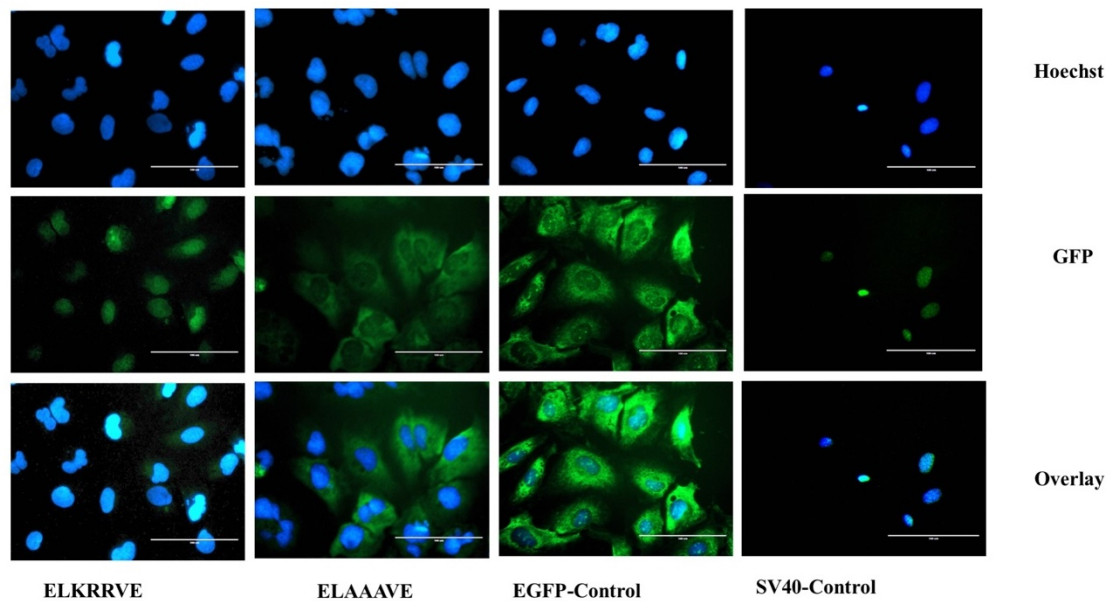


Figure 5.14: Localisation of wild-type and mutant Tetra-EGFP- Smk5 NLS
 pTetra-EGFP plasmid constructs containing a positive control (Sv40), negative control (unmodified vector) and either wild-type or different alanine-substituted NLS sequences, transfected into Huh7 cells and visualised by fluorescence microscopy (EVOS *fl*) after 24 h. (Scale bar, 10 μ m)

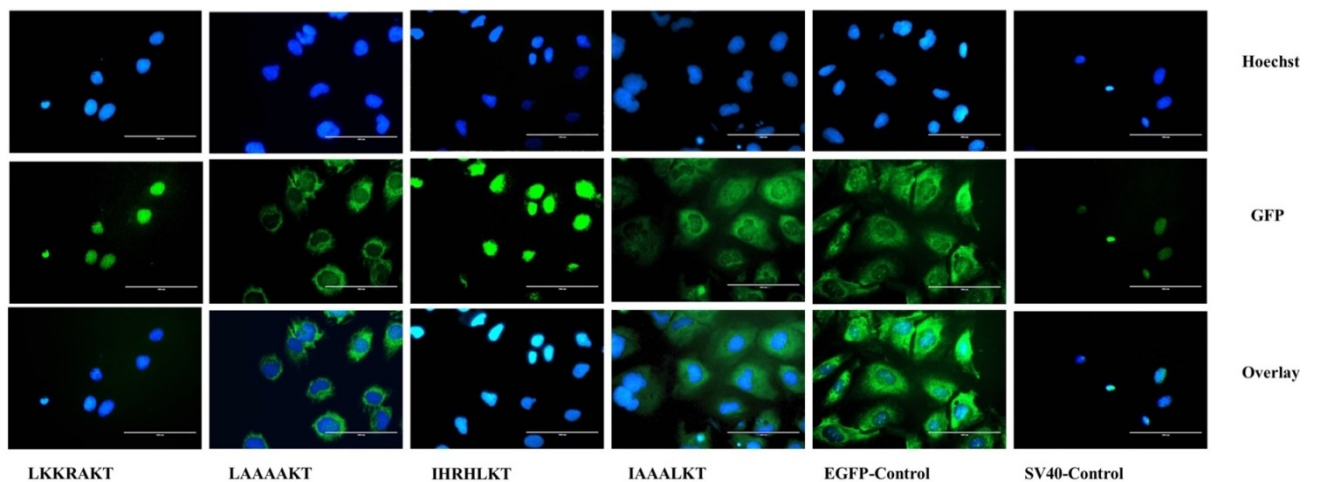


Figure 5.15: Localisation of wild-type and mutants Tetra-EGFP- FhGST-si and FhH2A NLS

Localisation of wild-type and mutants Tetra-EGFP- FhGST-si and FhH2A NLS. pTetra-EGFP plasmid constructs containing a positive control (Sv40), negative control (unmodified vector) and either wild-type or different alanine-substituted NLS sequences, transfected into Huh7 and visualised by fluorescence microscopy (EVOS *fl*) after 24 h. EGFP and Sv40 controls are the same as in Fig 5.14, and are shown here for comparison purposes. (Scale bar, 10 μ m)

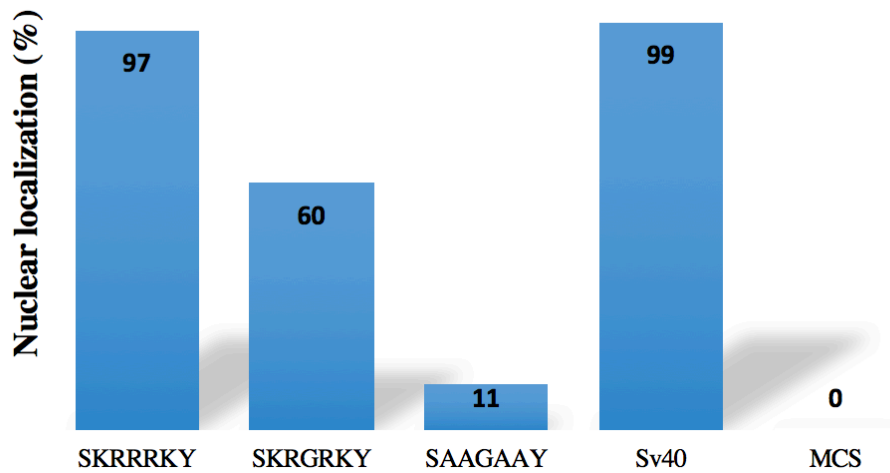


Figure 5.16: Summary of the effects of wild-type and mutants on nuclear localisation of the Tetra-EGFP-ShIPSE03 fusion protein.

100 transfected HTB9 cells were counted for each transfection and the percentage of cells displaying exclusive nuclear fluorescence calculated. Positive control (Sv40), negative control (unmodified vector).

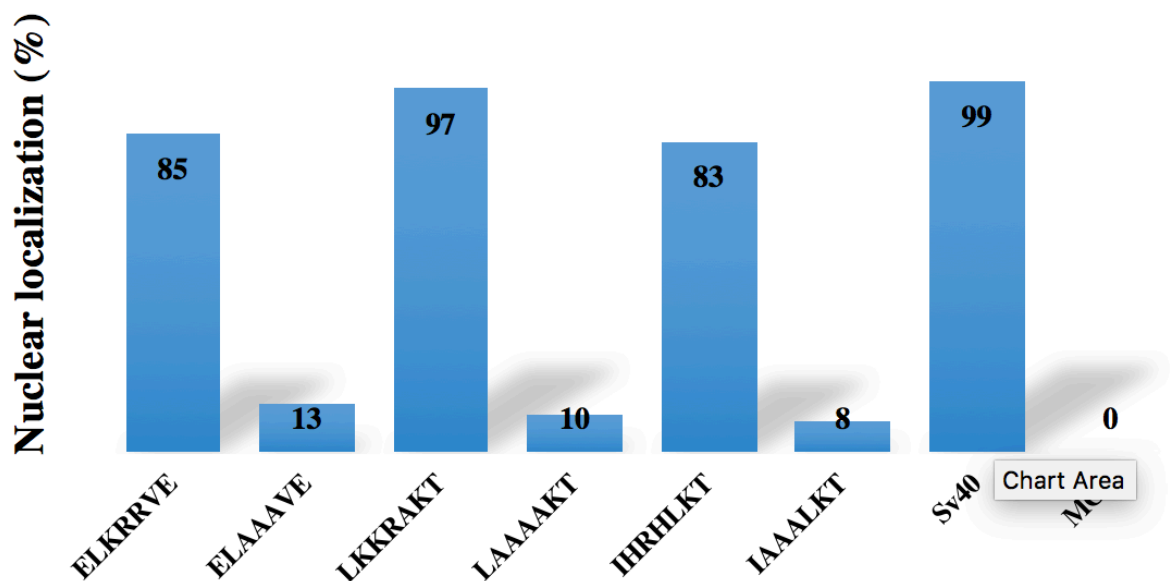


Figure 5.17: Summary of the effects of the wild-type and mutants on nuclear localisation of the Tetra-EGFP- *Smk5*, *FhGST-si* and *FhH2A* fusion protein.

100 transfected Huh7 cells were counted for each transfection and the percentage of cells displaying exclusive nuclear fluorescence calculated. Positive control (Sv40), negative control (unmodified vector).

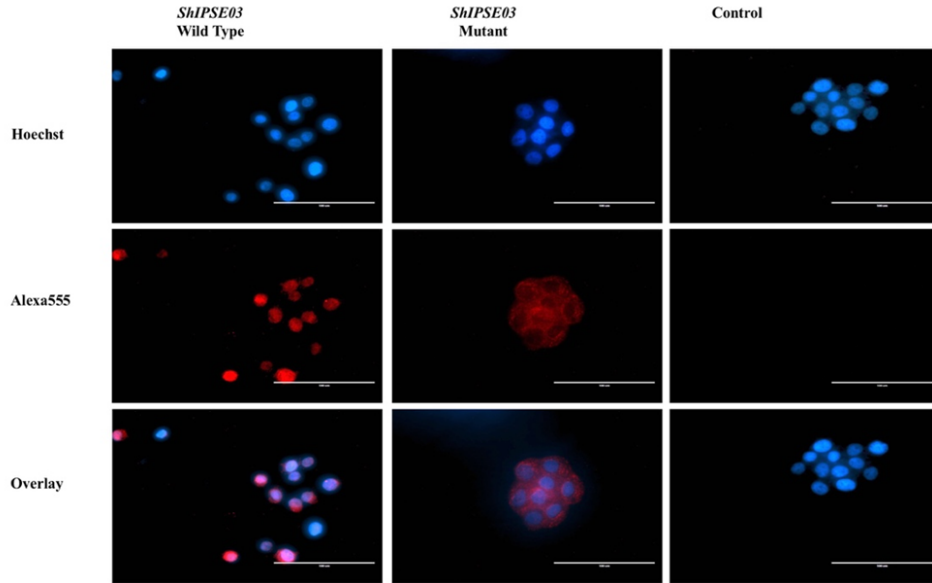


Figure 5.18: Cellular uptake of *ShIPSE* by HTB9 cells.

HTB9 cells were stained with 5 μ M DRAQ5TM for 15 minutes at room temperature (left), followed by staining with mouse anti-His antibody and goat anti-mouse IgG (H+L) and Alexa Fluor® 555 conjugate for 15 minutes at room temperature (middle). The images are shown overlaid (right). Cellular uptake was visualised by fluorescence microscopy (EVOS *fl*) using a 40X objective lens (Scale bar, 10 μ m).

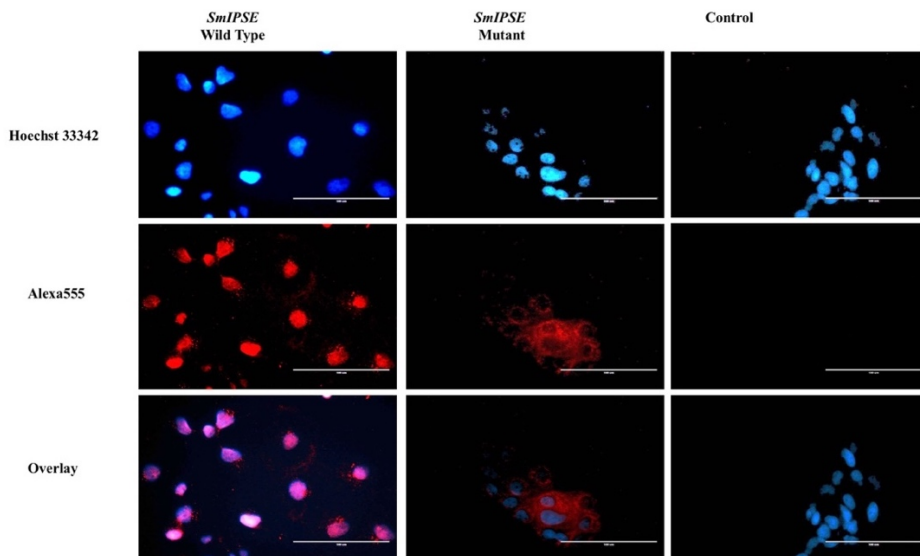


Figure 5.19: Cellular uptake of IPSE/alpha-1by Huh7 cells.

Huh7 cells were stained with 5 μ M DRAQ5TM for 15 minutes at room temperature (left), followed by staining with mouse anti-His antibody and goat anti-mouse IgG (H+L) and Alexa Fluor® 555 conjugate for 15 minutes at room temperature (middle). The images are shown overlaid (right). Cellular uptake was visualised by fluorescence microscopy

(EVOS *fl*) using a 40X objective lens (Scale bar, 10 μ m). A control in which the tissue is incubated without primary antibody.

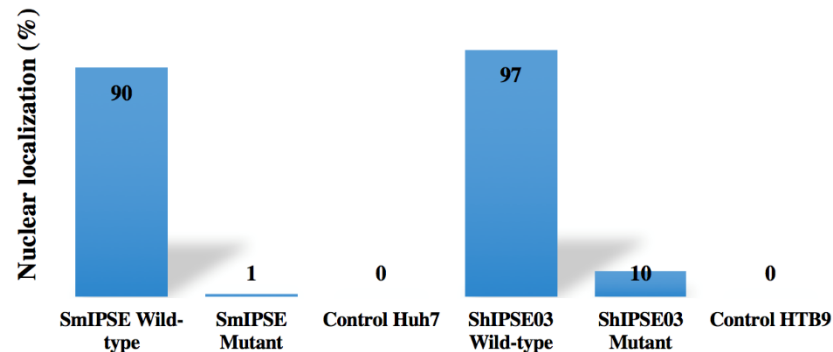


Figure 5.20: Summary of the effects of wild-type and mutants on nuclear localisation on the uptake of IPSE/alpha-1 and *ShIPSE03*.

100 transfected HTB9 cells for *ShIPSE03* and Huh7 cells for IPSE/alpha-1 were counted for each transfection and the percentage of cells displaying exclusive nuclear fluorescence calculated. Positive control (Sv40), negative control (unmodified vector).

5.4 Discussion

This chapter describes the experimental validation of the predicted NLS for each infiltrin (*ShIPSE03*, *Smk5*, *FhGST-si* and *FhH2A*) which are secreted by *S. haematobium*, *S. mansoni* or *F. hepatica*. These infiltrins have the ability to enter host cells, as demonstrated for recombinant IPSE/alpha-1 in several mammalian cell lines(265), using a human bladder carcinoma cell line (HTB9) for *ShIPSE03* and a human hepatoma cell line (Huh7) for *Smk5*, *FhGST-si* and *FhH2A*. An adult *S. haematobium* worm mates in the venous plexuses around the urinary bladder and the female worm lays its eggs which travel into the wall of the bladder (134). The adult *S. mansoni* worm mates in the portal vein and the female worm lays its eggs in the mesenteric veins, which move progressively towards the lumen of the intestine (144). Furthermore, *FhGST-si* and *FhH2A* proteins are secreted by *Fasciola* adult worms in the liver (105, 297, 298). As reported in

Section 5.3.1, recombinant wild-type infiltrins were examined for uptake *in vitro* and the results revealed that these infiltrins were able to access HTB9 or Huh7 cells and translocate into the nucleus.

This uptake was the motivating factor for the experiments reported in section 5.3.2. IPSE/alpha-1 was cloned into the vector pEGFP-C1 with intact and truncated NLS as a transfection marker(265). In this study the pEGFP-C3 vector was used to visualise infiltrins, enabling assessment of subcellular localisation using fluorescence microscopy, without the need for antibodies. These infiltrins were generated through a series of truncated constructs fused with AcGFP-C3 and mapped experimentally using cloned full length DNA and fragments. The results obtained by fluorescence microscopy, confirm that both *Fasciola* proteins and Smk5 have a functional NLS; a C-terminal NLS in FhGST-si and Smk5 and a N-terminal NLS in FhH2A. The NLS ShIPSE was not characterised through a series of truncated constructs fused with AcGFP-C3 because the NLS of *ShIPSE* of its homology with IPSE/alpha-1, which has been characterised in detail. ShIPSE03, Smk5 and FhGST-si, all contain a monopartite NLS at the C-terminal, which is a defining feature of infiltrins.

FhH2A, a histone protein, is one of four core histones, and is important for cell division, DNA packaging, regulation of transcription, and DNA repair (110, 111). Furthermore, FhH2A has the ability to be secreted via the non-classical pathway by using the alternative pathway (237, 297, 298). Parasites histones, including H2A enable the formation and stabilisation of higher order chromatin structures. They are able to be transported from the cytoplasm into the nucleus by the NLS and via receptor-mediated and energy-dependent pathways in eukaryotes (352). Histone synthesis in parasites is linked to DNA

replication through a mechanism of post-transcriptional regulation which operates at the level of translation (353). Histone H2A is already known to be a nuclear protein that contains a NLS (352), and this is necessary and sufficient for the process of transferring this protein into the nuclei of mammalian cells. It has been shown that H2A does not pass through channels in the nuclear membrane unimpeded simply by passive diffusion and that the N-terminal domains of the core or remaining histone H2A play a role (354). However, there is a belief that the NLS of histone H2A is not used as the transport process as in other proteins with a classical-type NLS (354). For example, *Leishmania* secreted histone H2A play an important role in the regulation of chromatin structure and gene transcription in eukaryotes. Furthermore, it has been shown that both amino-terminal ends of histone H2A consist of the most immunodominant epitopes. This H2A is more immunogenic than H3, H2B and H4 in sera from *Leishmania* infected dogs (355). In addition, our laboratory has shown that secreted histone H2A in *S. mansoni*, also known as Smp_035980, contains both NLS and CSS motifs. We postulate that secreted histone H2A in *S. mansoni* may have an essential role in the immune responses or cell death. This is because, histone may play an influential role in the activation and release of adrenocorticotrophic hormone (ACTH) (356) and prolactin (357) due to its direct action on perfused pituitary cells. Therefore, we believe the extracellular histones could result in inflammatory and cell injury responses.(358).

As mentioned earlier, a small protein of about 40 kDa can fully pass through channels in the nuclear membrane unimpeded by passive diffusion (330). In section 4.3.2.3, *FhGST-si* and *FhH2A* were reported to be approximately 26 kDa and 18 kDa in size, respectively, and localisation of these may be related to the passive diffusion process, with the presence

of a NLS enhancing their uptake. Moreover, proteins > 70 kDa can also be transported through NPCs, but in an energy dependent process (276, 334, 335). The size of ShIPSE03 and Smk5 is around 40 kDa and 75 kDa, respectively, and these infiltrins contains a NLS (336) that enhances their uptake. Interestingly and perhaps importantly, Kaur et al. [2011] showed that a non-EGFP fused cytosolic IPSE/alpha-1 in which ten amino acids including the NLS at the C-terminal have been removed (called IPSE/alpha-1 Δ NLS), despite being monomeric and small (~13 kDa), appeared to be retained in the cytosol with no evidence of any nuclear localisation. This can be attributed either to a strong competing NES, which could not be identified in IPSE/alpha-1, or to interactions with cytosolic components; both cases point to the importance of an NLS in smaller proteins which based on their size could cross the NPC by diffusion(265). This does not always appear to be the case.

After demonstrating the NLS experimentally, the vector pTetra-GFP was used to more precisely localise the position of each NLS, and to show that this NLS is able to redirect a large heterologous protein to the nucleus. In the classical nuclear import of proteins pathway, a stretch of positively charged amino acids (lysine (Lys, K), arginine (Arg, R) or histidine (His, H)) in the NLS sequence motif, which can be bipartite or monopartite, can be recognised by importin α , and importin α binds and interacts with importin β , although occasionally, the NLS can bind directly to importin β (338, 339, 359). The expected monopartite NLS motifs in ShIPSE03 (125-SKRRRK $\underline{\underline{Y}}$ -131), *Smk5* (256-ELKRR $\underline{\underline{VE}}$ -262), *FhGST-si* (202-LKK $\underline{\underline{RAKT}}$ -208) and *FhH2A* (35-IHR $\underline{\underline{HLKT}}$ -41) are functional in directing infiltrins to the nuclei of mammalian cells, and positively charged amino acids (Lys, Arg and His) in the NLS assist in nuclear uptake (360). As a simple illustration of this, Lys, Arg and potentially His residues are essential for the interaction

between a cargo protein and importin α for nuclear import (334, 361). This means that the residues underlined in the NLS sequence of the selected infiltrins are able to directly transport large heterologous proteins into the nucleus, as seen in Figure 5.13, Figure 5.14 and Figure 5.15.

The NLS of ShIPSE03, Smk5 and FhGST-si were also found to be in agreement with the basic core consensus sequence (362, 363). The monopartite Sv40 NLS PKKKRKV was used as a positive control because it has the ability to bind to importin α (364, 365). Human importin α contains two binding sites and several armadillo (ARM) repeats, which produce a curving structure with these sites. Moreover, a major site close to the N terminus located on ARM repeats 2–4 and a minor site close to the C terminus located on ARM repeats 6–8, and a bipartite NLS can bind to both the major site and minor site of importin α , whereas a monopartite NLS can bind to either the major site or the minor site (Figure 5.21) (334, 360).

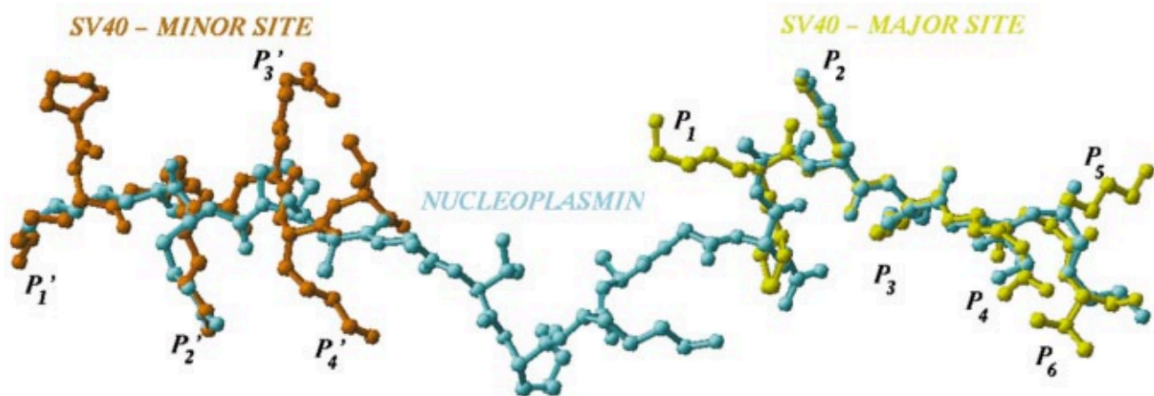


Figure 5.21: Binding between a bipartite or monopartite NLS and importin α .

The structure of importin α contains two binding sites: a major site close to the N-terminus P 1-P6 and a minor site P1- P4. A bipartite NLS can bind to both the major site and minor site of importin α , whereas a monopartite (Sv40) can bind to either the major site or the minor site (334).

Previous studies from our group have shown that the presence of NLS 125-PKRRRTY-131 at the C-terminus plays a necessary and sufficient role in the process of transferring IPSE/alpha-1 into the nuclei of mammalian cells. However, a NLS motif in the IPSE/alpha-1 sequence has been identified by our group and the three-dimensional structure (3D) has been described very recently by Mishra and others (366). However, the structure does not include the NLS, because its presence interfered with crystallisation, thus they only studied crystals of (monomeric) IPSE Δ NLS (366). Nevertheless, it has been proposed that the monopartite NLS 125-PKRRRTY-131 can bind to either the major site or minor site, as shown above for binding of the monopartite Sv40 NLS PKKKRKV and importin α ; therefore, the NLS of ShIPSE03, Smk5 and FhGST-si can be proposed. The quantitative results (Figure 5.16 and Figure 5.17) for the expected monopartite NLS motif in ShIPSE03 (125-SKRRRKY-131), Smk5 (256-ELKRRVE-262), *FhGST-si* (202-LKKRAKT-208) and FhH2A (35-IHRHLKT-41) demonstrate localisation into the nucleus in 97%, 85%, 97% and 83% of cells. This result indicates that the monopartite NLS of ShIPSE03, Smk5, FhGST-si and FhH2A are able to transport infiltrins into the nucleus, while the Ala mutants are not. This means that the Lys, Arg and His in these monopartite NLSs are essentially required for the interaction between the cargo protein and importin α for nuclear import (334, 361). However, it would be good in the future to use western blotting as additional confirmation to microscopy.

Mutating Lys, Arg and His to Alanine (Ala, A) is usually the simplest way to disrupt nuclear import (367). *ShIPSE03* (SAAGAAY), *Smk5* (ELAAAVE), *FhGST-si* (LAAA~~A~~KT) and *FhH2A* (IAAALKT) showed cytoplasmic localisation. In figure 5.16, Arg188 in the NLS *ShIPSE03* (125-SKRRRRKY-131) was replaced by Glycine

(SKRGRKY, this sequence occurs in a variant called *ShIPSE06*), and as expected, a small amount of fluorescent protein remained in the cytoplasm, but had little overall effect on nuclear localisation (368). It is believed that this may be the result of the time point chosen, suggesting that SKRGRKY is a less efficient NLS than the PKRRRTY IPSE/alpha-1 counterpart; in other words, a weaker NLS takes longer in directing all cytosolic proteins to the nucleus, but will eventually result in all protein being translocated. Alternatively, equilibrium is achieved between nuclear entry and nuclear exit, and this equilibrium is to some degree shifted towards cytosolic localisation (i.e. nuclear export) for weaker NLSs.

The vector pTetra-GFP was used to demonstrate the functionality of the monopartite NLS motif or its ablation in ShIPSE03 (125-SKRRRKY-131), Smk5 (256-ELKRRVE-262), FhGST-si (202-LKKRAKT-208), FhH2A (35-IHRHLKT-41), ShIPSE06 (SKRGRKY), ShIPSE06 mut (SAAGAAY), Smk5 mut (ELAAAVE), FhGST-si mut (LAAA AKT) and FhH2A mut (IAAALKT). Therefore, the NLS sequence (wild-type) of the selected infiltrins is able to direct the transport of heterologous proteins into the nucleus.

As already mentioned, the candidate infiltrins which contain the monopartite NLS motif (wild-type) were examined for uptake by HTB9 or Huh7 cells, and the results show that these infiltrins were able to access the cells. However, in Section 5.3.2, only two candidate infiltrins, IPSE/alpha-1 and ShIPSE03, were investigated. Parasite secreted proteins can be taken up into host cells via several mechanisms. It has been reported that glycoproteins and C-type lectin receptors (CLRs) on host immune cells are responsible for the modulatory effects of SEAs or parasite antigens through antigen presenting cells (APCs) (369). Glycoproteins, which contain glycan motifs recognised and mediated by CLRs, are

taken up via receptors such as dendritic cell-specific intercellular adhesion molecule-3-grabbing non-integrin (DC-SIGN), mannose receptors (MRs) and macrophage galactose-type lectin (MGL) (247). DC-SIGN recognises a wide range of fucose pathogen-associated molecular patterns (PAMPs), and is involved in DC-SIGN-SEA binding of two antigens, Lewis X (LeX) from *S. mansoni* and fucosylated *N,N'*- diacetyllactosamine (LDN-F) from *F. hepatica* (370). Moreover, LDN and LDN-F bind MGL ligands on SEAs or parasite antigens and MRs might bind LDN-F motifs (371, 372). For example, HEK-IPSE/alpha-1 or native IPSE/alpha-1, which are glycosylated, are taken up via receptors such as DC-SIGN and MRs, while *E.coli* IPSE should not be taken up (369, 373). However, it has been shown that non-glycosylated IPSE can also be taken up by cells, i.e. there are other possible pathways, but they are unlikely to be via the transferrin route. Previous studies from our group have shown that the uptake of IPSE/alpha-1 protein in CHO cells might be internalised by a Tf/TfR-independent pathway(291). It is believed that ShIPSE03 has the same ability, however, putative NLS mutants also showed cytoplasmic localisation. As expected, a small amount of fluorescent protein remained in the cytoplasm but this had little effect on nuclear localisation (368).

The DNA binding domain has not yet been accurately mapped for IPSE/alpha-1, but it is thought to overlap at least in part with the NLS, as IPSE variants with a 10 amino acid C-terminal truncation does not bind DNA (267). Unexpectedly, one study has reported that IPSE/alpha-1, which is an infiltrin, is hepatotoxic as Omega-1 (249), another protein secreted by mature Schistosome eggs. Therefore, the next chapter investigates whether IPSE/alpha-1 is hepatotoxic, and whether this hepatotoxicity is related to its nuclear translocation and transcriptional activities via its DNA binding domain.

Chapter 6 - Effects of Sm-IPSE (or IPSE/alpha-1) on Intestinal Epithelium cell Model

6.1 Introduction

Having successfully demonstrated the candidate infiltrins which contain the monopartite NLS motif (wild-type) were examined for uptake by HTB9 or Huh7 cells, and the results show that these infiltrins were able to access the cells. However, this study has focused on IPSE/alpha-1 which was discovered as the first infiltrin (see section 6.1.5). At the beginning of the introduction of this chapter will address the transporting macromolecules across epithelial mucosa and the role of cytokines in intestinal epithelial cells (see section 6.1.1), using Calu-3 and Caco-2 cells as intestinal epithelial model *in vitro* (see section 6.1.2), and also using humanised rat basophilic leukaemia reporter cell lines (see section 6.1.3). Moreover, this introduction will be also address the relationship between *S. mansoni* eggs and host (see section 6.1.4).

6.1.1 The Transporting Macromolecules Across Mucosal Epithelium

6.1.1.1 The Mucus Barrier and Pathways for Crossing

Epithelial barriers on mucosal surfaces are found in different areas of the body, such as intestinal, respiratory and reproductive tissues. These barriers play an important role in the protection of the mucosal surfaces in these organs from foreign particles, such as bacteria, viruses and allergens (374, 375). It has been published that the majority of proteins and large antibodies possess the ability to diffuse through mucus as fast as they

are able to diffuse through water. Most proteins are of a much lower physical size compared to the mesh of mucin fibres within mucus which are around 1 μ m (376-378).

There are three potential pathways for transporting macromolecules across epithelial barriers (379). Small amphipathic molecules are able to pass through the mucosal cell layer without a specific transport system (Figure 6.1A) (380), while smaller macromolecules and hydrophilic molecules are able to pass between adjacent epithelial cells via TJs, which is known as the paracellular pathway (see Figure 6.1B) (381, 382). The transcytotic vesicle transport pathway is used for transporting larger macromolecules, and these bind to specific receptors which transfer these macromolecules from the cell surface to inside the cell (Figure 6.3C) (379, 381, 383). These transport pathways are in part the result of the unusually tight connections between mucosal epithelial cells – the tight junctions.

6.1.1.2 Intercellular Tight Junctions and Epithelial Cells

TJs contain a complex combination of proteins, which act as linkers between the cells in mucosal tissue. Furthermore, these proteins play an important role in the formation of the TJs and include the zonula occludens (ZO) protein family, which are mediated by claudins, occluding and junctional adhesion molecules (JAMs) (384-386) (Figure 6.2). TJs, especially ZO-2 and ZO-3, are key structures which regulate and control the transport of proteins, lipids, water and ions via the paracellular pathway (386-388). Maintenance of the function and structure of TJs frequently occurs following interactions between the actin cytoskeleton and TJ proteins. Moreover, TJs are associated with the myosin light-chain (MLC), which is phosphorylated by myosin light chain kinase (MLCK) and Rho-associated kinase (ROCK). This causes the contraction of the actin, resulting in the

opening of the paracellular pathways through regulation of TJ dynamic structures, and consequently permits epithelial permeability (389-391) (392). TJs also reduce the spread of proteins and lipids between the apical and basolateral plasmalemmal domains, which are linked to the cytoskeleton and recruit cell signalling proteins that control cell differentiation, growth, polarity and apoptosis (393, 394). The average globular diameter of the paracellular space in a TJ is 15 Å and any molecule with a molecular weight of more than 3.5 kDa may be unable to pass through this space (395, 396).

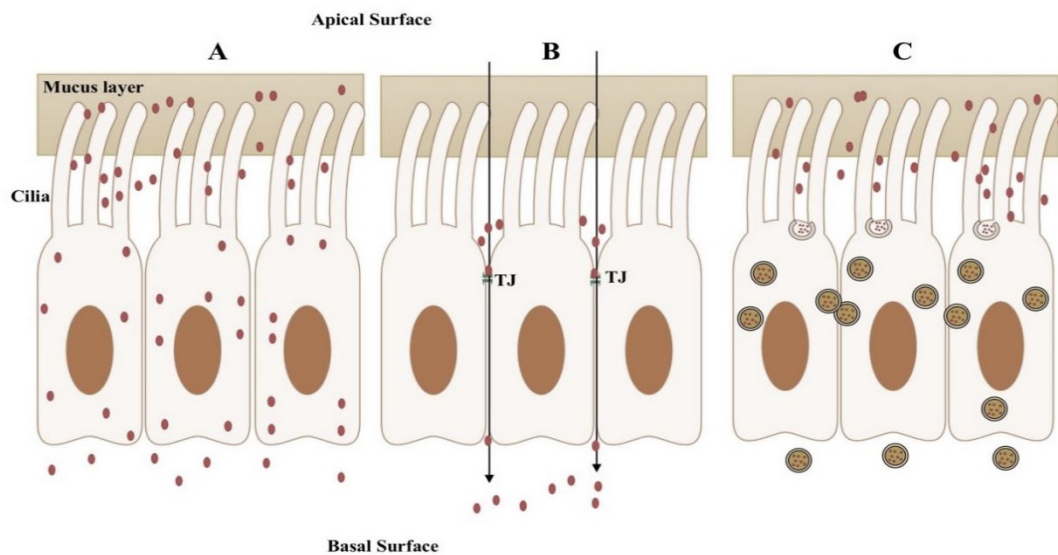


Figure 6.1 The three potential pathways for crossing the epithelial barriers

(A) Transcellular route, (B) paracellular pathway, and (C) transcytotic vesicle transport pathway.

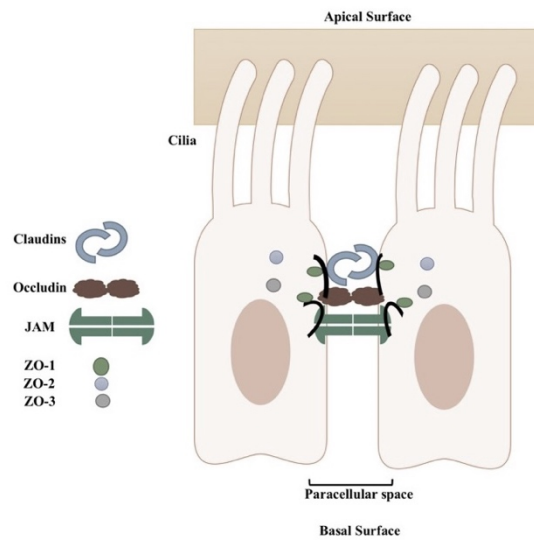


Figure 6.2 The structure of a tight junction between epithelial cells

The tight junction complex is composed of several proteins, such as claudins, occluding and junctional adhesion molecules (JAMs), which interact in the paracellular space with proteins on adjacent cells. TJs also include zonula occludens (ZO) proteins (ZO-1, ZO-2, ZO-3), which play an important role as transmembrane proteins for the actin cytoskeleton.

6.1.1.3 Proteins and Cytokines and the Regulation of Tight Junctions

Occludin, claudins, the ZO protein family, JAMs and cytokines play an important role in the regulation of TJs (Figure 6.2). Therefore, a simple summary of the role of proteins and cytokines in TJ regulation is presented. There are three types of ZO proteins (ZO-1, ZO-2 and ZO-3), which are associated with the guanylate kinase homologue (MAGUK) protein family (397). These are multi-domain ZO proteins which contain three post-synaptic density-95/Drosophila disc large/zona-occludens (PDZ) domains, a src homology-3 (SH3) domain, and a region of homology to GUK (guanylate kinase) at the side of the N-terminus. Binding and interactions between these multi-domains and TJ proteins leads to the maintenance and regulation of the TJ structure (398). Moreover, the ZO protein family may mediate the assembly of TJ proteins into cell-cell contacts during

the early stages (399). Figure 6.3 shows the three groups of ZO proteins; claudins can bind to the PDZ1 domain of ZO-1, while the PDZ2 domain is involved in interactions between ZO-2 and ZO-3, and occludin binds to the PDZ3 and GUK domains. Claudins also bind the PDZ1 of ZO-2, while the PDZ2 domain is used for interactions between ZO-2 and ZO-3 proteins, and claudins bind the PDZ1, PDZ2, PDZ1 and GUK domains. Finally in ZO-3 claudins bind the PDZ-1 domain, while PDZ2 is involved in interactions with ZO-1, and claudins bind PDZ1, PDZ2, PDZ1 and GUK domains (400).

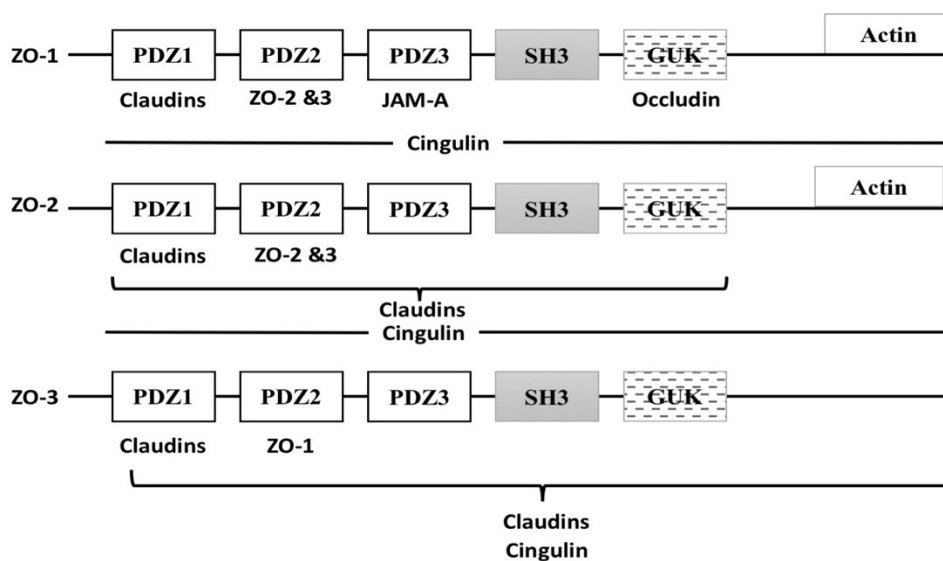


Figure 6.3 The interaction of TJ proteins – the ZO protein family

ZO proteins have three post-synaptic density-95/Drosophila disc large/zona-occludens (PDZ) domains a srchomology-3 (SH3) domain, and a region of homology to GUK near the N-terminus. Cytoskeletal actin and TJ proteins interact with ZO proteins (399).

Another important protein of TJs is occludin (approximately 65 kDa), which was first determined to be an integral membrane protein of TJs in 1993, and has a long binding domain at the C-terminus which interacts with TJ proteins in the epithelia (401, 402). This interaction is necessary to bind occludin to the actin cytoskeleton (402). Both *in vitro* and

in vivo studies have shown that occludin has a role in the intestinal epithelium (403, 404). There is no similarity between occludin and claudins in terms of sequence. Claudin is between 20–27 kDa and is a tetraspanin membrane protein with N and C-terminals, one intracellular and two extracellular loops (405). These extracellular loops create heterophilic and homophilic interactions with adjacent cells, which form either pores allowing the passage of molecules or barriers against which prevent and control the movement of molecules in the intercellular space between epithelial cells (406-408).

The final TJ protein is JAM, which is a member of the immunoglobulin superfamily. This protein possesses two extracellular Ig domains, a transmembrane domain, and an intracellular domain at the C-terminus that interacts with ZO-1 and Par3 proteins, with the latter being a cell-polarity protein that regulates the formation of TJs (409, 410).

Cytokines are small proteins or glycoproteins (between 5 and 40 kDa) that are synthesised and secreted by different cell types, mostly immune cells (411, 412). There are two types of cytokines produced by T-helper 1 cells, TNF- α and IFN- γ , while T-helper 2 cells produce IL-4, IL-10, IL-6, IL-9, IL-5 and IL-13 (413). The cytokine-mediated perturbation of the TJ barrier, resulting in stimulation of the immune system via subepithelial lymphoid tissue and the (inflamed) tissues, is considered to be key in the initiation and promotion of intestinal and systemic disease (374, 414, 415). In contrast, epidermal growth factor (EGF) plays an important role in the maintenance and protection of TJ integrity (399, 400). Table 6.1 illustrates the functionality of cytokines and their targets cells. A summary of the role of each cytokine except for IL-4, IL-13 and TNF- α is presented in Appendix 6, whilst IL-4, IL-13 and TNF- α are addressed in more detail in later sections.

Table 6.1: Functionality of cytokines and their target cells

Information taken from (416)

The function of epithelial	Regulatory cytokines	Target cells	Ref.
Barrier	interferons (IFN- γ), Tumor necrosis factor (TNF- α), IL-1 β , IL-10, IL-6, IL-22, IL-4, IL-13	Intestinal epithelial cell (IECs)	(417-430)
Leukocyte recruitment	IL-8, MCP-1, CCL20	Leukocytes	(417, 421-424)
Antigen presentation	IFN- γ , TSLP, APRIL	IECs, dendritic cells, B cells	(417, 419, 424, 431)
Homeostasis	IL-10, TGF β , TSLP, APRIL, IL-25, IL-22	IECs, dendritic cells, macrophages, B cells	(417, 419, 424-427, 431, 432)
Proinflammatory response(s)	IFN- γ , TNF- α , IL-1b, IL-8	IECs, leukocytes	(417, 418, 421, 430)
Regulation of solute, water and transport	IFN- γ , IL-4, IL-13	IECs	(417, 428, 429)

6.1.1.4 Interleukin-4 and Interleukin-13

Interleukins were considered to be one of the main sources of inflammation and irritation of the epithelial membrane (433, 434). An interesting exception is IL-4 and IL-13, which are two proinflammatory cytokines produced by Th2 cells, and play an important role in the regulation of the epithelial paracellular pathway, especially when combined with TNF- α , thus leading to increase the mechanisms of mucosal transport during inflammatory disorders, (432, 434-436). IL-4 and IL-13 share a common receptor, and they also have similar overlapping functions, such as the attenuation of the barrier function, have the ability to associate with the novel receptors IL-4R α 1 and IL-13 α 1 and 2, and are involved in the active inflammatory response in many diseases (436-440). For example, the permeability of the cell layer in the intestinal epithelium can be increased by IL-4 and IL-13, resulting in the opening of paracellular pathways by down-regulation of occludins and ZO-1 proteins (432, 435) Moreover, both cytokines stimulate the

production of anti-inflammatory cytokines and demonstrate increased proinflammatory actions in other conditions (428). For example, during infection with the trematode *S. mansoni*, IL-4 and IL-13 play essential biological roles in the function of alternatively activated macrophages. This is to reduce liver intestinal injury through down-regulation of schistosome eggs-induced inflammation (258). IL-4 and IL-13, which are released from mast cells following activation, may play important biological roles in the impairment of the intestinal barrier observed (441). In the context of nematode infection, it has been reported that IL-13 plays a significant role in the expulsion of parasites from the gut, e.g. by enhancing production of mucus from goblet cells, and also enhances the maintenance of epithelial cells and protects against injury (429).

6.1.1.5 Tumour Necrosis Factor-Alpha

TNF- α has previously been classified as a low molecular weight proinflammatory cytokine (442), and is secreted by Th1 cells and macrophages (400, 443). Most importantly perhaps in the context of this work, it is also pre-formed and stored in the granules of mast cells and also occurs in the RBL-2H3 cell line and its derivatives (444, 445). TNF- α encourages apoptotic mediators and inflammatory responses in IEC, and impairs the intestinal TJ barrier through initiating the dysfunction of TJs (430). TNF- α down-regulates ZO-1 protein expression in TJs, which may be through activating nuclear factor kappa-light-chain-enhancer of activated B cells (NF- κ B) by the expression of MLCK (403, 432). As mentioned earlier, TNF- α usually requires other cytokines, such as IL-4 and IL-13, which are released from mast cells following activation, in order to impair intestinal barrier integrity (432). In recent years it has been shown that TNF- α , which is

significantly induced by the eggs of *S. mansoni* (446), can modulate granulomatous inflammation (447, 448).

6.1.2 Using Calu-3 and Caco-2 cells as intestinal epithelial model *in vitro*

Cell culture-based *in vitro* intestinal epithelial models has been used by several research to study intestinal disease processes. Caco-2 cells were considered the most were used for this model. Moreover, it has also been shown that Caco-2 cells were grown on basement membrane (BM) proteins as a specialised form of extracellular matrix (279). These BM proteins, which were obtained from airway epithelial cells (Calu-3), form a thin extracellular matrix network and are important in many biological processes, such as cell differentiation, migration and proliferation (449-451). This BM results in the growth of a more physiological Caco-2 epithelial cell layer(279). The advantage of this model can be easily used and controled in the laboratory and under any conditions, as well as assist on reduce use of experimental animals.

6.1.3 Using Humanised Rat Basophilic Leukaemia Reporter Cell Lines

Basophils and mast cells play the main role in allergic reactions and the activation of these cells by Fc ϵ RI crosslinking of IgE molecules (Figure 6.4B-1) leads to cell degranulation (Figure 6.4B-2) with impressive, fast cellular responses. There are several chemical mediators released during inflammation, such as chemokines, leukotrienes, prostaglandins, cytokines and histamine (Figure 6.4B-3) (452, 453). Humanised rat basophilic leukaemia reporter (Fc ϵ RI) (RBL) cell lines are a modern method used for detecting allergen-specific IgE in allergic patients. Human Fc ϵ RI α , (α_H) in human mast cells and basophils is able to bind human IgE, whereas the rat Fc ϵ RI α chain (α_R) does not bind human IgE (Figure 6.4A) (454, 455). Over the last twenty years, a number of studies

have performed the transfection of human FcεRI α or all three human FcεRI α, β, and γ chains into RBL cell lines. These studies were recently summarised by Falcone et al. (456) and are shown in Table 6.2. Recently, RBL reporter systems have been developed for the assessment of allergic sensitisation.

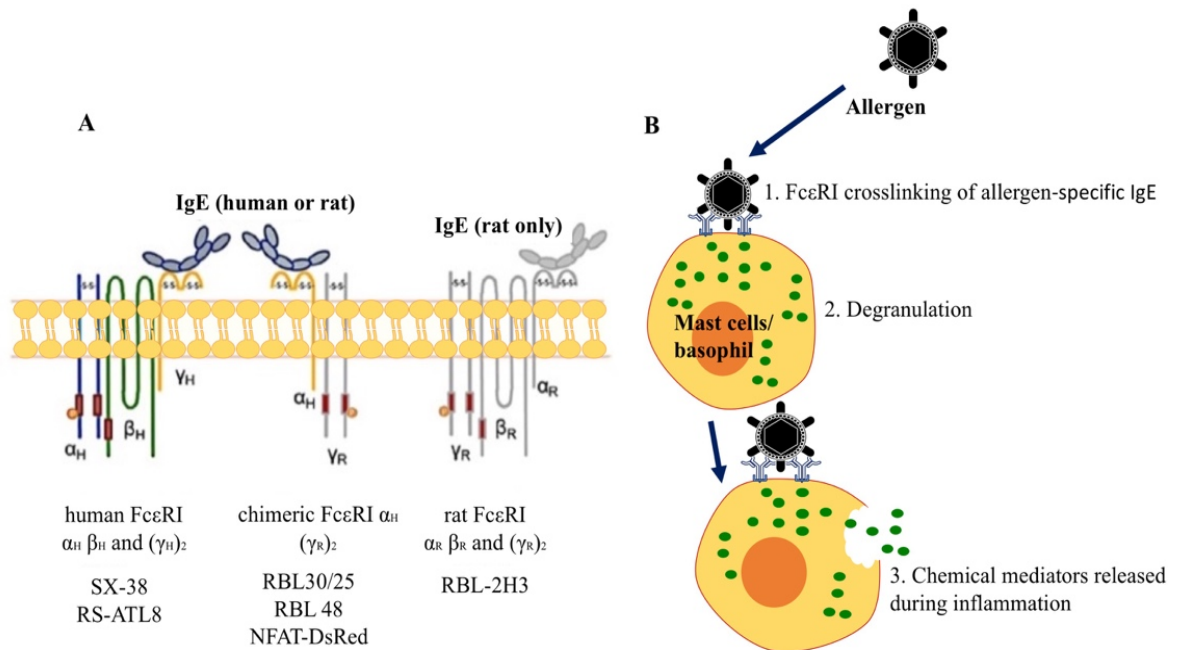


Figure 6.4 Human and rat receptor (FcεRI) and mast cells/ basophil activation due to FcεRI crosslinking.

Human and rat FcεRI α, β, and γ chains in the different RBL-derived humanised reporter systems (A). Mechanism of activation of mast cells/ basophil activation by FcεRI crosslinking of IgE molecules (B).

Table 6.2 Transfection of human FcεRI into RBL cell lines

Humanised RBL Cell lines	Trans gene	αH/cell	Detection	Application tested	Ref.
SX-38	αβγ	100,000	5-Hydroxy-tryptamine Beta-hex	sIgE detection Allergen characterisation	(457- 459)
RBL-30/25	α	not determine d (n.d.)	Beta-hex (50 % D2O)	Allergen standardisation	(460)
RBL- 2H3.E5.D12.8	α	n.d.	Beta-hex	sIgE detection	(461)
I5/3/C	α	1800	[3H] 5-HT	sIgE detection	
H 2121C		3200			
H 7/1/A		2500			
RBL-hE1a- 2B12	α	n.d.	Beta-hex	sIgE detection	(462)
RBL 48	α	25,000	Histamine, AA	sIgE detection	(463)
RBL T8	α	4100	Calcium influx	IgE dependent activation	(464)
RBL NFAT DsRed	α	n.d.	DsRed (fluorescence)	sIgE detection	(465, 466)
RS-ATL8	αβγ	n.d.	Luciferase	sIgE detection; allergenicity assessment	(467)

6.1.4 Translocation of Eggs to the Gut Lumen

A number of previous studies have shown that movements of *S. mansoni* eggs inside the host reach the gut lumen and then go out with feces. One suggested that *S. mansoni* egg does not depend on the large lateral spine in its shell to pass through gut wall because eggs from other Schistosoma species, not containing any lateral spine, are also able to pass through gut wall and exit the host (468). Furthermore, *S. mansoni* egg does not depend on the miracidium and its collagenase, to pass through gut wall because this miracidium is not fully developed during the initial phases of the translocation process (468). However, briefly, approximately 5-6 weeks after infection, adult *S. mansoni* worms

mate in the portal vein system and the female worms pass through the venule and lays its immature eggs in mesenteric veins (144). It is estimated that approximately 200-300 eggs are released daily into human veins by a single female worm (146, 469). About half of this eggs, especially the freshly laid ones, usually be coated with the residue and secretion from worm uteri and are able to activate the epithelial cells by secreting proteolytic enzymes; this can lead to facilitate movement of the eggs across the vascular endothelium, intestinal mucosa (see Figure 6.5), and reach the gut lumen in order to complete the life cycle (470).

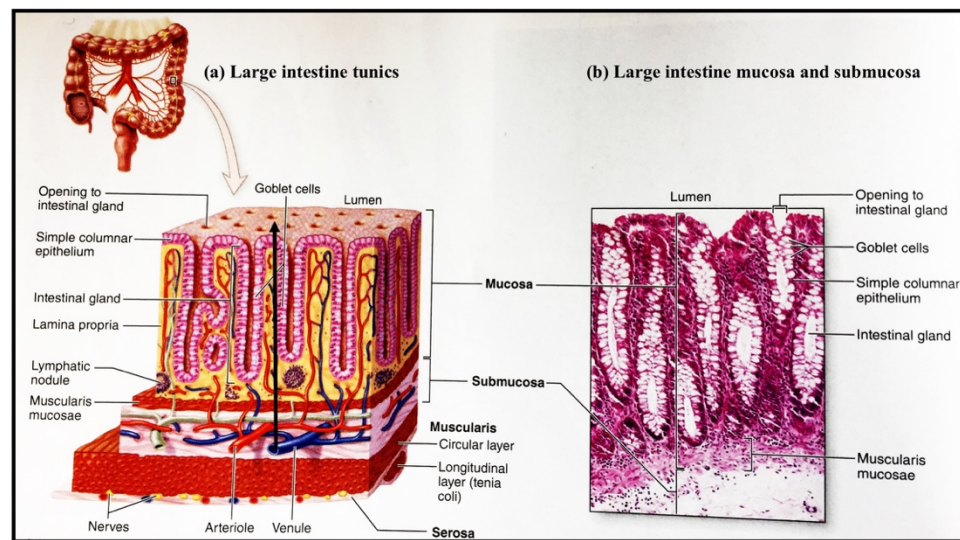


Figure 6.5 Diagram showing the wall of the large intestine composed of the four typical layers.

(1) The mucosa (the innermost layer) is made of simple columnar epithelial tissues. (2) There are large number of tissue with vessels in the submucosa, which supports the other layers. (3) There is thin layer of smooth muscle cells in the muscularis layer. (4) The serosa layer forms the outermost layer. (a) Large intestine tunics, and (b) Large intestine mucosa and submucosa. Black arrow in the middle of the first shape illustrates the direction of eggs via the vascular endothelium, intestinal mucosa, and reach the gut lumen, but this movement is still not knowing how?

Source: Mescher AL: *Junqueira's Basic Histology: Text and Atlas*, 14th ed. (Pag.324)
 Copyright © 2016 The McGraw-Hill Companies, Inc. All right reserved

The other half of eggs laid by the female worms are remaining in the host tissues. These eggs carried away by the direction of the blood flow, and remain entrapped in the intestinal lumen, lung or liver (see section 1.4.1) (152-154), causing granulomatous inflammation by secreted antigens from eggs in the host, the main pathology observed (149-151). In chronic infections this can lead to liver fibrosis and portal hypertension (152-154) and allergic responses (156). More recently Turner et al in 2012 show that the Peyer's patches (see Figure 6.6) (471), which are an important component of mammalian gut-associated lymphoid tissues in the wall of the small intestine, play an important role to facilitate movement *S. mansoni* eggs to the intestinal lumen (471).

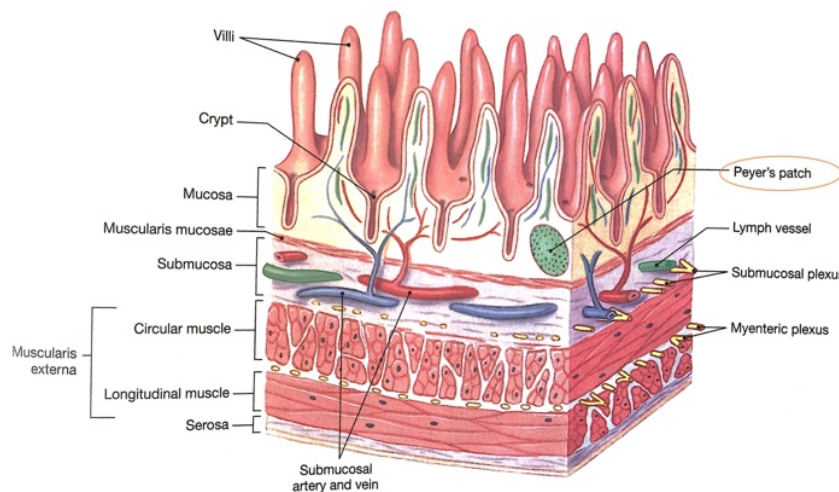


Figure 6.6 Diagram showing the sectional view of the small intestine wall and the red circle shows Peyer's patches.

Source: Silverthorn DU: *Human Physiology An Integrated Approach*, 7th ed. (Pag.681)
 Copyright © 2016 Pearson Education, Inc. All right reserved

6.1.5 Importance of IPSE/alpha-1 in this study

Previously, it has been published that only mature eggs are capable of releasing ESP, such as IPSE/alpha-1, and that *S. mansoni* egg is a stage of the life cycle during which most of the immunological changes occur (215, 223, 224). As mentioned above in section 1.4.4, in the chronic stage of these parasitic infections, secretory proteins released by the eggs, which will include IPSE/alpha-1 interact with immune cells a result in a Th2 response, which is triggered following the down-regulation of an initial Th1-type response. This response by regulatory IL-10, has a central function for alternatively activated macrophages (AAMs), and is stimulated by IL-13, IL-4 (98, 258, 472). Furthermore, during the same stage, levels of Tregs, IL-4, IL-13 and TGF- β rise. In the liver, this leads to an increase in collagen deposition, which leads to progressive fibrosis and the destruction or loss of liver (217, 218).

A Th2 response is characterised by the production of cytokines, namely IL-4, IL-10, IL-13 and IL-5, which stimulate the secretion of IgE antibodies (99, 214). Th2 responses, have the ability to repair damaged tissues and Th2 type cytokines, when induced by parasite-secreted products, balance the cellular immune responses between parasites and the host (96, 473-476). As we will argue in this chapter, IPSE/alpha-1, which owes its name due to its ability to induce IL-4 and IL-13 release from human basophils, may be able to facilitate and accelerate the transfer of eggs to the gut lumen. IL-4 and IL-13, in combination with mast cell derived TNF-alpha, which would normally have host-protective effects, as these cytokines have the ability to repair damaged tissues (477), and also can modulate granulomatous inflammation (447, 448) may play an important role in promoting egg translocation across the gut wall. Furthermore, IPSE/alpha-1 function in

RBL cells, it is well known that helminth infection and allergic diseases share common features, involve similar cytokines present in the milieu, such as IL-4, IL-5 and IL-13, and most importantly, demonstrate the up-regulation of IgE (3, 478). For example, in 2014 it was shown in our laboratory that IPSE/alpha-1 from wheat germ, expressed or expressed and refolded in *E. coli*, was able to activate the basophil reporter cell line RS-ATL8 and dose-dependently stimulated the gene expression of this reporter (466).

From the point of view of parasite development however, schistosome eggs have to reach the gut in order to complete the life cycle. The encapsulation and compartmentalisation in tissues is a dead end from the parasite's perspective (479). Despite this fact, not much is known about the molecular mechanisms resulting ultimately in egg expulsion into the lumen, except for the fact that these include a host inflammatory immune response. Much less attention has been paid to the direct effects of ESPs, particularly IPSE/alpha-1, e.g. on non-immune cells, such as fibroblasts, or epithelial cells (480). How the small schistosome eggs are able to cross much thicker layers of tissues, including tough muscular tissue and a tight epithelium, is currently not understood, in particular regarding the roles of ESPs in this process. It is therefore necessary to understand the mechanism of eggs passing from the intestinal vasculature to the gut lumen in this chapter.

6.2 Experimental Procedures

6.2.1 Activation of the RS-ATL8 reporter system by IgE binding to IPSE/alpha-1

One day before the experiment commenced, RS-ATL8 cells were cultured in 96-well clear polystyrene plates at 1.5×10^5 cells/well (Corning, USA). These cells were sensitised with 1mg/mL myeloma human IgE (AbD Serotec, UK) (1:1000 dilution = 1 μ g/mL final concentration) or 1/50 diluted human serum, and incubated at 37°C overnight at 5% CO₂. The following morning, the medium was removed from the wells and the cells were stimulated with 1 μ g/mL, 100ng/mL, 10ng/mL and 1ng/mL wild type and recombinant IPSE/alpha-1 (50 μ L per well), while 1 μ g/mL anti-human IgE (50 μ L per well) (Vector Labs, UK) was used as a positive control. The cells were incubated for 4 hours, before adding 50 μ L ONE-Glo Luciferase Assay System (Promega, Madison, Wisconsin, USA) solution to each well according to the manufacturer's instructions. After 2-4 minutes of lysis, the mixture was transferred to a 96-well flat-bottomed plate (white) (Nunc, Denmark), and the luminescence in each well measured using a Tecan Spark 10M.

6.2.2 Effect of IPSE/alpha-1 on Model Gut Epithelial Membrane Integrity

TEER was used to measure the effect of IPSE/alpha-1 on model gut epithelial membrane integrity (Caco-2) and the paracellular pathway. Calu-3 and Caco-2 cells were cultured in transwell plates (279). Calu-3 cells, which were added as a scaffold layer, were seeded onto the apical side of a 12-well Transwell plate (3460, Costar, MA, USA) at 100.000

cells/well (1.1 cm^2 filter area) with 0.5 mL culture medium Dulbecco's Modified Eagle's medium (DMEM) and a further 1.5 mL of culture medium added to the basolateral side. The cells were incubated in liquid-liquid conditions until the TEER $>800\Omega\cdot\text{cm}^2$ (approximately 13-14 days), replacing the media every 2-3 days (Figure 6.7-1). In order to create air-interface culture (AIC) conditions, once the TEER $>800\Omega\cdot\text{cm}^2$, the medium in the apical side was removed, ensuring no air bubbles were trapped beneath the transwell membrane, and the culture medium on the basolateral side was replaced with 0.5 mL culture medium instead of 1.5 mL. Calu-3 cells were cultured under AIC conditions for a further 4-7 days, replacing the media every 2-3 days. The media was then aspirated and sterile distilled water added (2 mL/well of 12-well plate). The plate was left at room temperature for 20 min, aspirated, and then the cells were stripped (decellularisation process) from the substrate deposited on the basement membrane using sterile 20 mM ammonium hydroxide for 20 min at room temperature (2 mL/well of 12-well plate). The cell lysates were aspirated, and the transwells gently washed twice (or more) with PBS (2 mL/well of 12-well plate) to ensure complete cell removal and also the removal of ammonium hydroxide (Figure 6.7-2). After decellularisation, Caco-2 cells were seeded on top of the basement membrane deposited by the Calu-3 cells, i.e. on the apical side of the 12-well Transwell plate at a starting density of 100,000 cells/well. 0.5 mL culture medium (DMEM) was added to the apical side and on the basolateral side 1.5 mL culture medium. Culture medium was replaced every 3 days, and Caco-2 cells were incubated in culture medium (DMEM) for 21 days until TEER $>1000\Omega\cdot\text{cm}^2$ (Figure 6.7-3). Next, 2.5 $\mu\text{g}/\text{mL}$ wild-type IPSE/ α -1 (PKRRRTY) or mutant IPSE/ α -1 (PKAAATY) or 25 ng/mL recombinant human TNF- α were added to the apical side of the Calu-3 cells

scaffold layer and confluent cell layers of Caco-2, together with fresh culture medium. Cells were incubated with wild-type and mutant IPSE/alpha-1 for 48 hours and TEER measurements conducted once a day (Figure 6.7-4). IPSE/alpha-1 with a triple Alanine mutant NLS, and which does neither translocate to the nucleus nor bind to DNA, was used to assess whether any effects were associated with nuclear translocation by comparing with wild type IPSE/alpha-1.

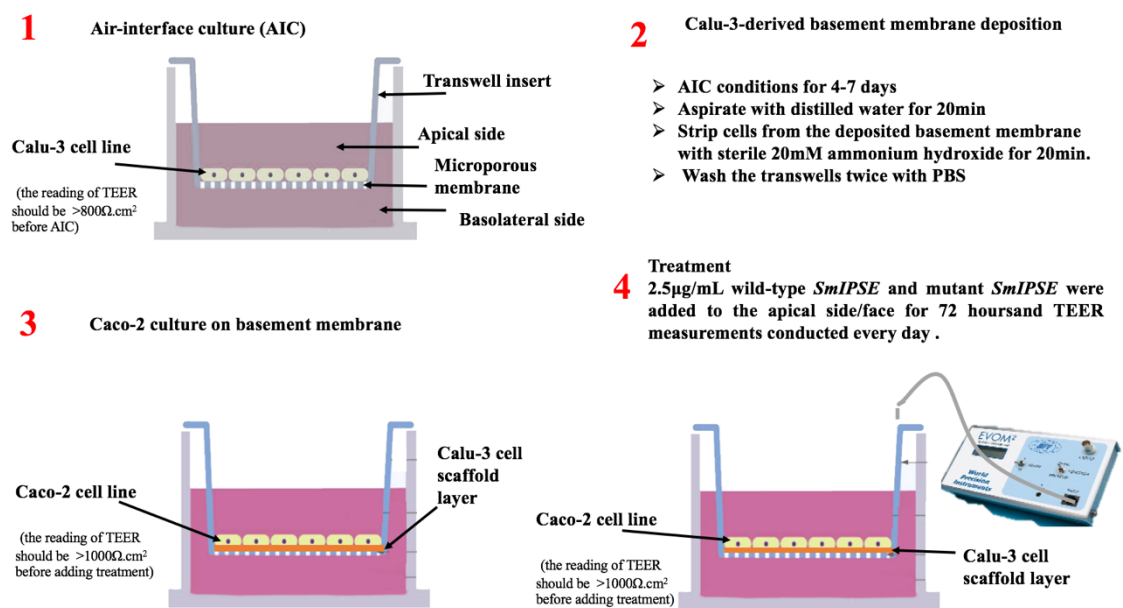


Figure 6.7 Culture of Caco-2 cells on Calu-3-derived basement membranes

Four steps are involved in preparing this type of transwell plate: 1&2) Calu-3 cells, which are added to the apical side/face as a scaffold layer, are seeded onto the apical side of a 12-well Transwell plate. 3) Caco-2 cells are grown on the substrate deposition on the basement membrane (above the scaffold layer). 4) Treatment and measuring influence.

6.2.3 Effect of the NFAT-DsRed on Model Gut Epithelial Membrane

Integrity after Activation by IPSE/alpha-1

In the first instance, Transwell plates were prepared in the same way as above (Figure 6.71-3). One day before the experiment commenced, nuclear factor of activated Tcells-

DsRed fluorescent protein (NFAT DsRed) reporter cells were cultured on the basolateral side of a 12-well Transwell plate (3460, Costar, MA, USA) at 3.8×10^5 cells per well. These cells were sensitised with 1/50 human serum and incubated at 37°C overnight with 5% CO₂. The following morning, the medium was removed from the wells and cells were stimulated with either 1 µg/mL wild type IPSE/alpha-1 (750 µL per well), 1 µg/mL mutant recombinant IPSE/alpha-1 (750 µL per well), 25 ng/mL TNF-α (750 µL per well) or 1 µg/mL anti-IgE (750 µL per well), with these last two acting as positive controls (Figure 6.8). Recombinant wild type and mutant IPSE/alpha-1 were used in these experiments from HEK293 cells.

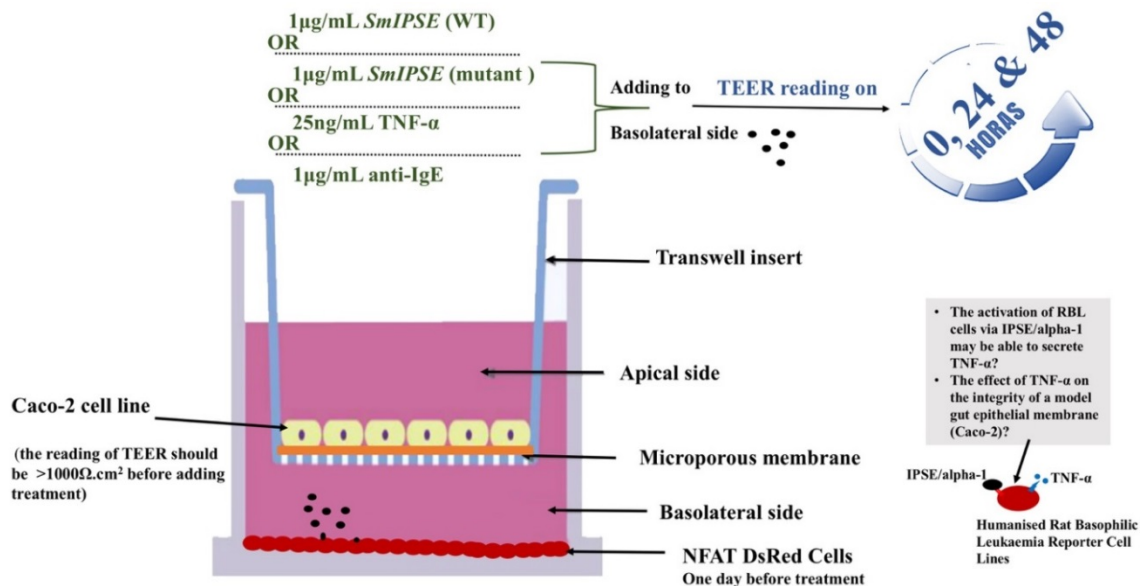


Figure 6.8 Activation of basophils and the impact on the integrity of a model gut epithelial membrane

IPSE/alpha-1 is able to activate basophils in an IgE-dependent, but non-antigen specific manner. Humanised NFAT-DsRed RBL cells were included as a model of resident mast cells that can be activated via IgE by IPSE/alpha-1. The aim here is to model the potential effects of IPSE/alpha-1 on the integrity of a model gut epithelial membrane (Caco-2), assessed by measuring TEER, either directly or in the presence of mast cells as a source of TNF-α, as would be the case in the gut tissue where mast cells are resident in the connective tissue underneath the epithelium.

Cells were incubated with wild-type and mutant IPSE/alpha-1 and positive controls for 48 hours and the integrity of a model gut epithelial membrane (Caco-2) measured using TEER every day. Activated NFAT DsRed cells, which were cultured on the basolateral side of a 12-well Transwell plate, were then incubated for 48 hours before adding 0.5mL lysis buffer (1% v/v Triton X-100 in DPBS) to each well. After one minute of lysis, lysates were transferred to black, flat-bottomed, untreated 96-well polystyrene plates (Corning, USA), and the fluorescence measured using a Tecan Spark 10M using 530nm excitation and 590nm emission. This step was performed to ensure that RBL cells had been activated by IPSE/alpha-1, a step which would result in secretion of preformed TNF- α .

6.3 Results

The outcome of IPSE/alpha-1 on epithelial cell integrity in the absence or presence of mast cells (using RBL cells as surrogate for mast cells). First, we needed to show that IPSE/alpha-1 is able to activate the RS-ATL8 RBL reporter cells after sensitisation with human IgE-containing serum. As shown in Figure 6.9, IPSE showed dose-dependent activation of RS-ATL8 cells (measured as induction of the luciferase reporter). The positive control was anti IgE and the negative control consisted of only serum, and these gave readings of 1691 and 574 relative luminescence units, respectively. The highest concentration of IPSE/alpha-1 (WT) showed a more than 3-fold increase in the activation of the RS-ATL8 reporter system above background. The highest IPSE/alpha-1 concentration resulted in activation of the same magnitude as the positive control with anti-IgE antibody.

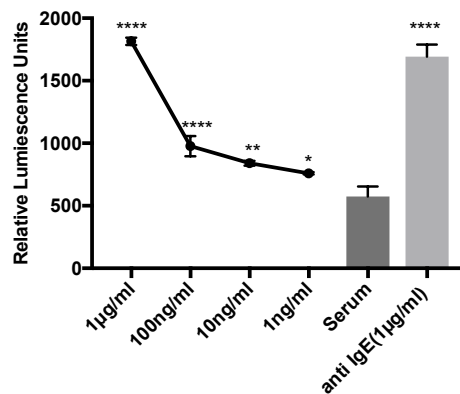


Figure 6.9 Activation of the RS-ATL8 reporter system by IgE binding to IPSE/alpha-1 expressed in HEK-293 cells

All cells (excluding serum only) were sensitised with 1/50 human serum and then incubated at 37°C overnight at 5% CO₂. Cells were then stimulated with 1 mg/mL anti-human IgE (positive control) and different concentrations of IPSE/alpha-1 (WT).

Having shown that IPSE/alpha-1 can activate the surrogate mast cells (RS-ATL8 RBL) and thus release preformed TNF- α , the next step was to assess the effects of IPSE/alpha-1 on the integrity of the Caco-2 cell layer. We added 2.5µg/mL IPSE/alpha-1 (WT), 2.5µg/mL IPSE/alpha-1 (mutant) or 25ng/mL TNF- α to the apical side of the transwell, and measured the TEER at 0 hours, after 24 hours and after 48 hours (Figure 6.10). IPSE/alpha-1 (WT) and TNF- α showed a gradual decrease in TEER measurements over the 48 hours, whereas that for IPSE/alpha-1 (mutant) fluctuated around the initial without statistically significant differences.

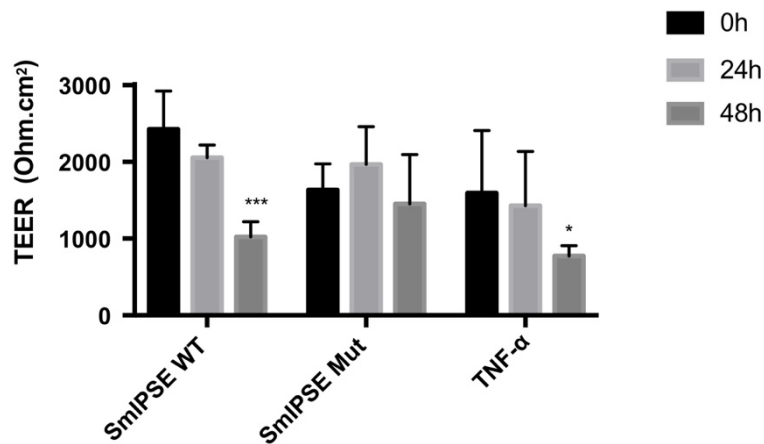


Figure 6.10 Effect of IPSE/alpha-1 on the Caco-2 cell layer via TEER.

2.5µg/mL IPSE/alpha-1 (WT), 2.5µg/mL IPSE/alpha-1 (mutant) and 25ng/mL TNF-α were added to the apical side of a transwell and TEER was measured at 0 h, 24 h and 48 h.

This result suggested that the ability to decrease electrical tightness of confluent epithelial cells is common to both IPSE/alpha-1 and TNF-α, but not shown by mutant IPSE. This suggested that IPSE-mediated effects could be due to nuclear translocation of IPSE, as the NLS mutant will not translocate to the nucleus of host cells (265).

The next results were obtained from a more complex experimental design in which 1µg/mL IPSE/alpha-1 (WT), 1µg/mL IPSE/alpha-1 (mutant), 1µg/mL anti-IgE or 25ng/mL TNF-α were added to the basolateral side of the transwells to assess whether they could activate NFAT DsRed cells (reporter system) and thereby induce TNF-α release from the cell line. TEER measurements were taken at 0 h, as well as 24 and 48 hours after activation (Figure 6.11, Figure 6.12 and Figure 6.13). Under these conditions, and in the presence of RBL cells, IPSE/alpha-1 (WT), IPSE/alpha-1 (mutant), anti-IgE

and TNF- α induced a gradual decrease in TEER measurements over the 48 hours, whereas those for untreated wells rose slightly after 24h and plateaued at 48 hours, suggesting that a stable basis had not yet been reached on day 1.

The images presented in Figure 6.13 show the ability of 1 μ g/mL IPSE/alpha-1 (WT), 1 μ g/mL IPSE/alpha-1 (mutant) and 1 μ g/mL anti-IgE (positive control for cell activation) to induce the production of red fluorescence in the cytosol of the reporter cell line NFAT DsRed cells, 48 hours after stimulation. In these and other experiments, 25ng/mL TNF- α was used as positive control for TJ disruption, but this cytokine does not lead to NFAT-DsRed cell activation. DsRed cells stimulated with anti-IgE demonstrated the highest level of fluorescence 48 hours after stimulation, followed by IPSE/alpha-1 (WT) and then IPSE/alpha-1 (mutant), while cells treated with TNF- α and non-treated cells showed very little fluorescence, as expected. Technically, cell lysis was required to obtain the optimal signal strength of relative fluorescence following the activation of NFAT DsRed cells by the various stimuli. Figure 6.12 shows the relative fluorescence following cell lysis; anti-IgE and IPSE/alpha-1 (WT) showed a more than 6-fold increase in the activation of the NFAT DsRed reporter system compared to non-treated (control) cells, while IPSE/alpha-1 (mutant) showed a more than 2-fold increase, while no change was observed for TNF- α . Figure 6.13 confirms these findings by showing red fluorescence in NFAT DsRed cells activated by IPSE/alpha-1 (WT and mut) and anti-IgE, but not by TNF- α .

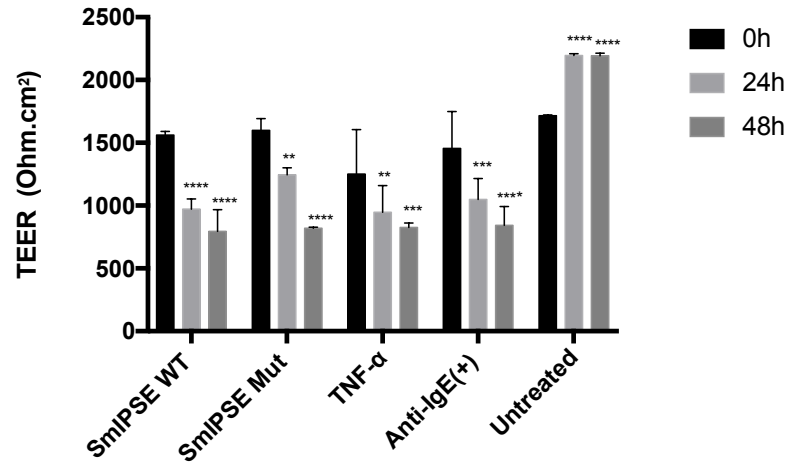


Figure 6.11 Activation of the NFAT DsRed reporter system by IPSE/alpha-1 and the effect on TEER of the Caco-2 cell layer.

1µg/mL IPSE/alpha-1 (WT), 1µg/mL IPSE/alpha-1 (mutant), 1µg/mL anti-IgE (positive control) and 25ng/mL TNF-alpha (2nd positive control) were added to the basolateral side of a transwell. Activation of NFAT DsRed cells was measured by TEER at 0 h, 24 h and 48 h. Statistical analysis via two-way ANOVA. **: P≤0.01, ***: P≤0.001, ****: P≤0.0001.

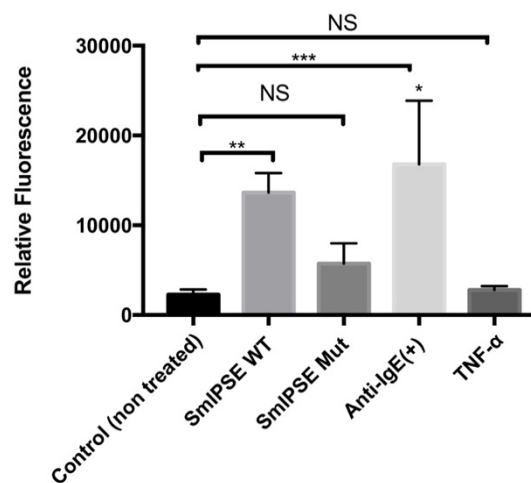


Figure 6.12 Activation of the NFAT DsRed reporter system by IgE binding factor IPSE/alpha-1 expressed in HEK293

Relative fluorescence after activation of NFAT DsRed cells by 1µg/mL IPSE/alpha-1 (WT), 1µg/mL IPSE/alpha-1 (mutant), 1µg/mL anti-IgE (positive control) and 25ng/mL TNF-α (2nd positive control) after 48 hours. Data are mean ± SD of the readings from two plates. NS: not significant, **: P≤0.01, ***: P≤0.001. (ANOVA followed by Dunnett's multiple comparisons test)

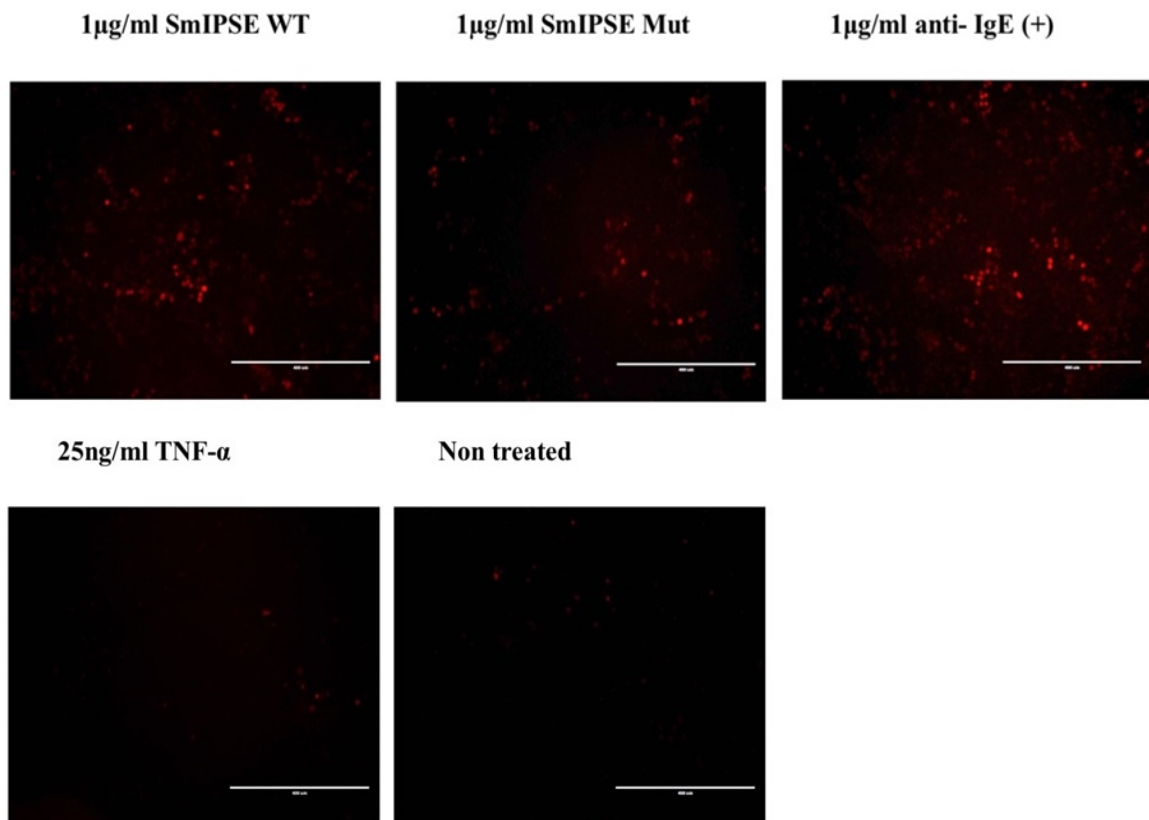


Figure 6.13 DsRed cells as a reporter system 48 hours after stimulation

To the basolateral side of a transwell 1µg/mL IPSE/alpha-1 (WT), 1µg/mL IPSE/alpha-1 (mutant), 1µg/mL anti-IgE (positive control) and 25ng/mL TNF-alpha (2nd positive control) was added. IPSE/alpha-1 (WT), IPSE/alpha-1 (mutant) and anti-IgE have the ability to activate NFAT DsRed cells. Images of the activated cells were visualised by fluorescence microscopy 48 h after stimulation.

6.4 Discussion

As mentioned earlier, Peyer's patches have been suggested to play an important role in the movement of eggs to the intestinal lumen. It has been suggested that a large number of *S. mansoni* eggs, which are supplied by the high endothelial venules (HEV) of Peyer's patches, accumulate in lymphoid tissues. Consequently, the fibroblast in Peyer's patches could be damaged by egg secretions, which are cytotoxic, leading to reduce stromal and lymphocyte cellularity. This could facilitate and accelerate the transfer of eggs to the gut lumen (471). However, it has been shown that Peyer's patches are part of the structures of the ileum region of the small intestine wall while much of the pathology in human schistosomiasis is found in the colon (481, 482). Moreover, the accumulation of eggs in lymphoid tissues and then secretions of eggs requires more than ten weeks (see Figure 1.7). However, seven to nine weeks after infection, a large amount of *S. mansoni* eggs can pass through the relatively thick colonic wall and can be found in the faeces of mice (483). Taking into consideration the long development from transformed cercaria to adult worms, this means that these eggs require only a relatively short time of up to a week, to reach the lumen of the gut.

It has been suggested that the molecular mechanisms leading to translocation of the eggs across the gut are still insufficiently understood. Here, this study is going to discuss the potential role of IPSE/alpha-1, as a major secretory protein specific to mature eggs, in this process. This role includes the release of TNF- α and Th2 cytokines (IL-4 and IL-13) from gut mast cells. To explore this in more detail, it is first necessary to explain the mast cell model used in this study.

Using a humanised rat basophil cell line, such as the RS-ATL8 and NFAT DsRed cell lines, has several benefits (467, 484). FcεRI α, β, and γ chains (α, β, and γ R) in human mast cells and basophils are able to bind to human IgE, however the rat FcεRI α chain (αR) cannot bind to human IgE (Figure 6.4A) (454, 455). Consequently, over the last twenty years a number of studies have investigated transfected human FcεRI α or all three human FcεRI α, β, and γ chains into RBL cell lines. These modified cells are easier and cheaper to obtain than from example human peripheral blood basophils (466) or mast cells, which would need to be isolated from human tissues (usually from mastectomies). This provides us with a cellular model with an easy activation readout which is responsive to IgE-dependent stimulation, and could be used to model the presence of mast cells present in gut tissues.

The dimeric structure of IPSE from *S. mansoni* eggs is able to activate basophils in an IgE-dependent manner, but not through an antigen specific mechanism, resulting in the production of IL-4 and IL-13 (250, 255). In 2014 an *in vitro* study by our group demonstrated that IPSE/alpha-1 recombinantly expressed in wheat germ lysates or expressed and refolded in *E. coli*, was able to activate a basophil reporter (RS-ATL8) cell line (466). However, it needed to be shown that IPSE/alpha-1 obtained from HEK293 cells was equally able to activate this basophil reporter (RS-ATL8) cell line. It has been shown that for this activity it is crucial that IPSE/alpha-1 occurs as a homodimers, as IPSE/alpha-1 monomers do not activate basophils.

Figure 6.9 shows that 1µg/mL of IPSE/alpha-1 (WT) results in a more than 3-fold increase in the activation of the reporter system compared to serum only (control). The same protein was used with NFAT DsRed cells and demonstrated a more than 6-fold increase

in the activation of this reporter system compared to non-treated (control) cells. In Figure 6.13 the activated NFAT DsRed cells were visualised by fluorescence microscopy. These cells had been activated by 1µg/mL of IPSE/alpha-1 (WT); however, fluorescence levels were not as high as expected (based on other experiments) and this may be due to the delay in taking images 48 h after stimulation rather than after 24 h.

This suggests that the activation of RBL cells via IPSE/alpha-1 may be able to trigger the release of TNF- α , a cytokine which is known to be stored in this cell type and mast cells in general, and which plays an important role in affects TJ proteins. As stated above, IPSE/alpha-1 induces the production of IL-4 and IL-13 from human basophils (250, 255), and these cytokines can increase the permeability of the cell layer in the intestinal epithelium, resulting in the opening of paracellular pathways via down-regulation of occludins and ZO-1 proteins (432, 435). Therefore, we can postulate that in the gut, mature eggs releasing IPSE/alpha-1 may promote their own translocation across the epithelium by activating mast cells via the IgE receptor, releasing IL-4, IL-13 and preformed TNF- α .

This study requires to model these suggested effects on the epithelial integrity *in vitro*. Two different experiments were employed to measure the effect of IPSE/alpha-1 on model gut epithelial membrane integrity (Caco-2) by measuring the TEER. In the first experiment, wild-type IPSE/alpha-1 was added to the apical transwell chamber medium and the TEER measured for 48 hours (Figure 6.10). There was a gradual decrease to half the original for the TEER measurements over the 48 hours, and this result was close to the values obtained with 25ng/mL TNF- α . TNF- α down-regulates ZO-1 protein expression in TJs, potentially through activating NF- κ B by inducing expression of

Myosin light-chain kinase (MLCK) (403, 432). The effect of TNF- α on epithelial cells usually are increased in the presence of other types of cytokines, such as IL-4 and IL-13, which are released from mast cells upon activation and impair intestinal barrier integrity (432). IL-4 is a proinflammatory cytokine produced by Th2 cells, which plays an important role in the regulation of the epithelial paracellular pathway and thus leads to increased mucosal transport during inflammation (432, 434-436).

There is an incomplete picture for the crossing of eggs into the intestinal lumen for evacuation from an infected host. The eggs would be surrounded by connective tissue with colonic granulomatous infiltrations of immune cells, which would also include mast cells, eosinophils and T lymphocytes (165, 485). During the stages of granuloma formation, the production of fibres and internal cohesive organisation has the ability to repair damaged tissues. Moreover, when eggs pass through the intestinal wall then this affects its integrity, hence IL-4 and IL-13 may also have host-protective effects, as these cytokines are involved in the repair of damaged tissues (477). The next barriers to cross on the way to the gut lumen would be the basal membrane and, toughest of all, the tightly connected epithelial cell layer. TNF- α , particularly in combination with IL-4 and IL-13, has been described as being able to weaken epithelial cell junctions (436), and as mast cells are known to contain preformed TNF- α (486), this suggests that IPSE/ α -1 may promote egg egress into the gut lumen by activating mast cells and inducing the release of TNF- α and the Th2 cytokines IL-4 and IL-13, possibly in addition to its nuclear, infiltrin-like effects on gene transcription. This would imply that an intact functional NLS plays an important role in the down-regulation of intestinal membrane integrity, suggesting that nuclear translocation and/or DNA binding may be involved.

In the second experiment, IPSE/alpha-1 was added to the basolateral transwell chamber medium which also contained our mast cell surrogate, the NFAT DsRed cells; the TEER was measured for 48 hours (Figure 6.11). This experiment was performed to take into account the spatial distribution of cells that schistosome eggs would encounter during their translocation to the lumen of the gut. Eggs would be surrounded by connective tissue with colonic granulomatous infiltrations of immune cells and would need to cross the basal membrane and tightly connected epithelial cell layer. Mast cells found be found in the connective tissue, particularly in close proximity of blood vessels. Any TNF- α released by tissue mast cells, would reach the epithelium from the basal or baso-lateral side. Thus adding this cytokine to the bottom wells, is a better approximation of what may happen *in vivo*. Consistent with this hypothesis, there was a gradual decrease to around half the original levels for the TEER measurements over the 48 hours, and mutant IPSE/alpha-1, anti-IgE and TNF- α showed the same result as wild-type IPSE/alpha-1.

It is difficult to draw any firm conclusions from these experiments. IPSE/alpha-1 may act directly on target host cells (e.g. on the epithelium) via its nuclear translocation and transcriptional (i.e. infiltrin-like) activities, as well as indirectly by inducing TNF- α and Th2 cytokines from resident mast cells. These direct and indirect effects are not necessarily mutually exclusive, as they may occur together. However, at the molecular level, IPSE/alpha-1 is either binding to IgE (followed by internalisation of the IgE/Fc ϵ RI/IPSE complex) or is taken up into host cells, where it translocates from the cytosol to the nucleus, and these pathways would appear to be mutually exclusive.

In this context, it is interesting to note that TNF- α has been previously described by Amiri *et al.* to be a key cytokine promoting *S. mansoni* fertility by boosting egg deposition by

females, and also by increasing excretion of eggs from the host (447). The results presented in this chapter cannot be easily mapped onto those obtained by Amiri et al. as TNF- α will also play a major role in recruiting inflammatory cells, such as granulocytes and macrophages to the granuloma, or up-regulating adhesion molecules on endothelial cells, and increasing extravasation of inflammatory immune cells to the granuloma, although this latter effect may be less prominent once eggs have left the endothelium and are preparing to cross the epithelium. There is a vast body of literature confirming the importance of the egg-induced granulomatous response in host protection (reducing egg hepatotoxicity) (487, 488) and in allowing eggs to cross the gut wall, via proteolytic and other activities of mediators produced during inflammation(489, 490). The data in this chapter merely suggests that TNF- α , derived from mast cells activated by IgE, through the action of IPSE/alpha-1 binding to IgE their surface, might contribute to the translocation of eggs into the gut lumen.

More importantly perhaps, it suggests a cellular source of TNF- α and a mechanism for its release via a protein (IPSE/alpha-1) abundantly secreted by mature eggs on their way to the gut lumen, however this has not been described in the literature. Whether the IgE binding/mast cell activating properties of IPSE/alpha-1 or its nuclear activities are more important remains to be demonstrated. Our collaborators at George Washington University are currently aiming to assess these effects by using CRISPR/Cas9 technology to delete the IPSE gene in schistosome eggs.

There are also a few intrinsic assumptions that were made in these experiments. The Caco-2 cells used as a model of the gut epithelium are of human origin. The RBL cells, used as a model of resident mast cells, carried a human IgE receptor able to bind human IgE;

however, the TNF- α (and IL-4 or IL-13 released) will be the rat homologue of this cytokine. Thus it is assumed that rat TNF- α is able to bind to and activate the human TNF- α receptor. For example, it has been shown that Human TNF- α binds only to the type I (p55) rat receptor, whereas mouse TNF- α binds to p55 and p75 rat TNF receptors (491, 492). Moreover, human and murine TNF- α both bind to p60 human TNF receptors (492, 493). Interestingly, after adding IPSE/alpha-1 (WT) and TNF- α to the apical or the basolateral side of a transwell, both treatments showed a gradual decrease in TEER measurements over 48 hours. Indeed, the positive control was human TNF- α , and it would probably have been better or more consistent to use rat TNF- α . An antibody could have been used to block TNF- α binding to validate this result.

The second assumption made is that Caco-2 cells, or more generally, polarised epithelial cells, express TNF- α receptors on their basolateral side. The changes induced by human TNF- α seem to suggest that this is the case, as it was noted that TNF- α receptors are on the basolateral side of the epithelium (494). Bearing in mind that schistosomes also possess a TNF- α receptor, which is capable of binding human TNF- α , the data in this chapter adds to the complex picture depicting the central role of TNF- α in the schistosome-host molecular cross-talk and highlights the potential importance of IPSE/alpha-1 as a key inducer of TNF- α (495).

Chapter 7 - IPSE/Alpha-1 and Alanine Transaminase (ALT)

7.1 Introduction

In the previous chapter, the results showed that IPSE/alpha is able to activate humanised basophil reporter cell lines, and also may have an effect on TJ proteins and gut epithelial membrane integrity. However, another consideration of IPSE/alpha-1 is that it has been said to have more hepatotoxicity than any other type of ESP. Therefore, one possible hypothesis could be that egg egress is caused by direct cytotoxic effects on the epithelium. The alanine transaminase (ALT) enzymatic activity test, which measures the level of ALT enzyme in the blood, also known as serum glutamic pyruvic transaminase (SGPT). This enzyme is commonly used as an indicator of hepatic cell injury and can therefore be used to characterise the hepatotoxicity of egg components of *Schistosoma* in mice *ex vivo* using primary hepatocyte cultures for 72 hours, as done by others (249). Based on the ALT test results, IPSE/alpha-1 in Abdulla et al.'s work appeared to be directly hepatotoxic. This was corroborated by using a specific monoclonal antibody that neutralised IPSE/alpha-1 toxicity, whilst also decreasing the level of cell injury due to ESP and SEA through a combination of monoclonal antibodies. These targeted both Omega-1 and IPSE/alpha-1, indicating that approximately 60% of the toxicity of the egg-derived material was due to these two proteins (249). Previous studies have shown that Omega-1 is a monomeric glycoprotein released from *S. mansoni* eggs (229), and this protein is a functional RNase T2 (248). Omega-1 has been confirmed as a hepatotoxin by different studies (249, 496, 497), whereas IPSE/alpha-1 was considered to be a hepatotoxin in a single study, using only the ALT test (249). Bearing in mind the nuclear translocation of IPSE/alpha-1

described in this study, an alternative hypothesis could be that the effects on ALT are not due to cytotoxicity, but are a direct consequence of transcriptional activities of this infiltrin. Thus, there is a need to confirm IPSE/alpha-1 hepatotoxicity (or cytotoxicity in general) using less indirect methods. Therefore, the toxicity of IPSE/alpha-1 will be measured via MTT, LDH and resazurin assays, together with ALT (a.k.a. serum glutamic-pyruvic transaminase, SGPT) mRNA measurements.

7.1.1 qRT-PCR for assessment of changes in ALT mRNA expression

ALT and SGPT are both names used for the same transaminase enzyme which has been known since the mid-1950s (498, 499). The ALT enzymatic activity test has been used as a marker of hepatic liver injury in humans (249, 500). However, there are several factors that can lead to an increase in ALT levels, such as a viral hepatitis infection, diabetes mellitus, obesity, some medications, and hyperlipidemia (501-505); the natural factors of gender and age may also play a role in ALT elevation (506, 507). Therefore, not all factors affecting ALT levels are a reflection of direct hepatotoxicity. Bearing in mind the nuclear infiltrin-like properties of IPSE/alpha-1, the increase in ALT activity measured after 72 hours could also be a result of the increased gene expression after IPSE/alpha-1 nuclear translocation, rather than a true reflection of hepatotoxicity. Therefore, the mRNA expression levels of ALT after treating hepatic cells with IPSE/alpha-1 should be assessed and considered by fluorescence based quantitative real-time PCR (qRT-PCR). To normalise the data, suitable housekeeping genes (reference gene), such as PSMB2 and RPL32, which are known to be stably expressed at a level of expression comparable to those of the target genes (508), have to be used. The outcome of this qRT-PCR should show us whether IPSE/alpha-1 can lead to a transcriptional upregulation of ALT levels.

7.2 Experimental Procedures

7.2.1 Evaluation of Cytotoxicity

Three different techniques were used to assess whether IPSE/alpha-1 has any cytotoxic properties: LDH test, MTT test and a resazurin assay. The basis of cytotoxicity tests was explained in section 2.3. 1×10^4 Huh7 cells/well were incubated in a 96-well plate with different concentrations of wild type IPSE/alpha-1 (10 μ g/mL, 5 μ g/mL, 1 μ g/mL and 0.1 μ g/mL) for 72 h, followed by an evaluation of cytotoxicity using the MTT (In Vitro Toxicology Assay Kit, Sigma-Aldrich), LDH (Lactate Dehydrogenase Kit, Sigma-Aldrich) and resazurin (resazurin sodium salt, Sigma-Aldrich) assays, following the manufacturer's protocol for each. The result of the MTT assay was measured at OD 590 nm with a reference filter of 620 nm using a MRX plate reader (Dynex technologies, USA), the change of absorbance at 490 nm was measured for the LDH assay using the same plate reader, and the fluorescence intensity of the resazurin assay was assessed at excitation 540nm and emission 590nm using a microtitre plate fluorometer (MFX Microtitre Plate Fluorometer; Dynex Technologies). Human hepatoma (Huh7) cells were used for hepatotoxicity assessment.

7.2.2 Effect of IPSE/alpha-1 on Gene Expression

Huh7 cells were seeded in 12-well tissue-culture plates and, once 70% confluence was reached, incubated with or without 10 μ g recombinant IPSE/alpha-1. At different time points (2 and 4 h) cells were lysed and RNA purified using a GenElute Mammalian Total

RNA Extraction Kit (Sigma–Aldrich, Dorset, UK), following the manufacturer’s instructions. The mRNA was converted to cDNA using a GeneAmp RNA PCR Core Kit (Applied Biosystem, USA) following the manufacturer’s protocol, using oligodT for priming. qRT-PCR is a highly sensitive technique for measuring mRNA levels, and is also used for determining the covariance, quantification and detection of gene expression levels (509, 510). RT-PCR was performed using KAPA SYBR® FAST qPCR Kit (KAPA Biosystems, USA) following the manufacturer’s protocol. Each sample or standard was run in a total volume of 10µl in a transparent tube (0.1- mL Strip Tubes and Caps; Qiagen) using a Rotor-GeneQ Real-Time PCR system (Qiagen). The cycling conditions used were: step 1, 95°C for 2 minutes; step 2, 95°C for 5 seconds, 60°C for 30 seconds for 40 times; step 3, 95°C for 5 seconds; ending with a cycle of 65°C for 5 seconds and 95°C for 5 seconds to determine the melt curve for each sample. HsRPL32 primers, which were designed by Dr Franco Falcone, (Table 7.1) were used as the internal reference gene and also the ready primer for the ALT or GPT gene (PrimePCR™ PreAmp for SYBR® Green Assay: GPT, Human) from Bio-Rad (Assay ID: qHsaCED0006809). E = 2 was assumed as the real time-PCR efficiencies for both the target and reference genes was close to 100%. The Pfaffl equation below was used to calculate the fold induction between the reference control gene and the target gene of interest (511).

$$\text{Relative expression ratio} = \frac{(\text{Efficiency target})^{\Delta\text{CT target (Control CT value - Sample CT value)}}}{(\text{Efficiency reference})^{\Delta\text{CT reference (Control CT value - Sample CT value)}}$$

Table 7.1: RPL32 primers

Primer No.	Primer	5’-3’ Sequence
906	Hs SYBR RPL32 FOR	TGTCAAATTAAGCGTAACTGG
907	Hs SYBR RPL32 REV	TAACCAATGTTGGGCATCAA

7.3 Results

The cytotoxic effects of IPSE/alpha-1 (WT) were investigated in Huh7 cells using different concentrations (10, 5, 1 and 0.1 µg/mL) and assessed after 72 h via three different cytotoxic assays which measured metabolic activity (MTT, resazurin) or membrane integrity (LDH). Figure 7.1 indicates the LDH (%), the different concentrations of IPSE/alpha-1 (WT) did not induce a significant decline of the cell viability.

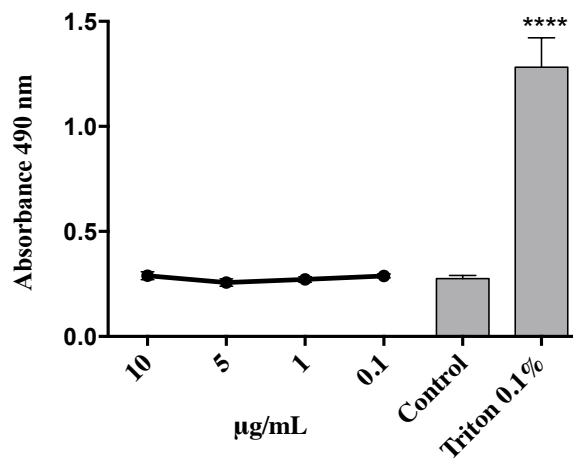


Figure 7.1: LDH activity of Huh7 cells cultured in the presence of different concentrations of IPSE/alpha-1 (WT) for 72h. N=3 experiments.

Data were determined by one-way ANOVA using Prism 7. ****P<0.0001 represents statistical significance of differences between control and treatment group.

The effects of IPSE/alpha-1 (WT) were also estimated by assessment of metabolic activity via a MTT assay. Absorbance is used as the assay readout. There was a relatively small, but statistically significant decrease in absorbance compared to the control (non-treated cells) for IPSE/alpha-1 (WT) for all tested concentrations above 0.1 µg/mL, but this did not appear to be dose-dependent (Figure 7.2).

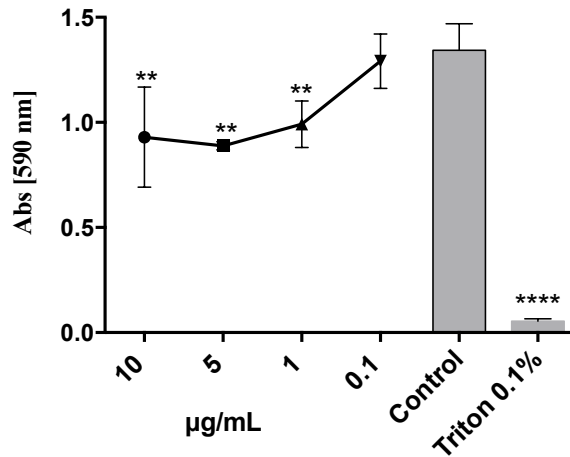


Figure 7.2: MTT activity of Huh7 cells cultured with different concentrations of IPSE/alpha-1 (WT) for 72h.

Data were analysed by one-way ANOVA using Prism 7. **P<0.005; ****P<0.0001 represents statistical significance of differences between control and treatment group. N=3 experiments.

As these experiments suggested a small negative but statistically significant effect on metabolic activity, we sought to verify these results by assessing the effects of IPSE/alpha-1 (WT) using a different metabolic assay. Resazurin assay does not show significant differences in fluorescence with the different concentrations of IPSE/alpha-1 (WT) (Figure 7.3).

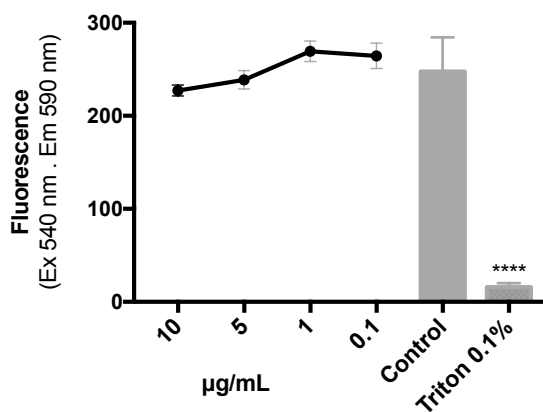


Figure 7.3: Resazurin activity of Huh7 cells cultured with different concentrations of IPSE/alpha-1 (WT) for 72h.

Data were determined by one-way ANOVA using Prism 7. ****P<0.0001 represents statistical significance of differences between control and treatment group. N=3 experiments.

Having established that IPSE/alpha-1 has no or only small effects on cell viability, we next wanted to assess the impact of IPSE/alpha-1 on ALT level. As previous authors had shown increased ALT (whose official HGNC gene name is GPT) enzymatic activity in hepatocytes treated with IPSE/alpha-1, suggesting potential cytotoxicity, we wanted to assess whether these could have been caused by a transcriptional effect of IPSE/alpha-1. In this case, IPSE/alpha-1 would cause an increase in GPT mRNA levels, but not the IPSE/alpha-1 NLS mutant, as the latter will neither enter nuclei nor bind to DNA (265).

Table 7.3 shows the changes in gene expression following stimulation of Huh7 cells with IPSE/alpha-1 (WT) and IPSE/alpha-1 (mutant) and the marked up-/down-regulated patterns as detected by qRT-PCR. Experimentally, after treating hepatic cells with 10µg of IPSE/alpha-1 (WT) showed up-regulation in the relative GPT or ALT - mRNA expression levels at 8.66 (condition No.1) and 8.78 (No.2) after two hours and four hours, respectively; whereas hepatic cells treated with 10µg of IPSE/alpha-1 (mutant) showed similar up-regulation at 8.24 (No.3) after two hours and observed significant decrease in the relative GPT or ALT mRNA expression levels to 3.31 (No.4) after four hours. There was no difference in GPT/ALT mRNA levels between IPSE/alpha-1 WT vs mut treated cells (1.04; No.5). Thus, it can be stated that IPSE/alpha-1 leads to a fast upregulation of GPT/ALT mRNA, which does not appear to depend on the presence of a functional NLS. The drop in GPT/ALT mRNA levels in IPSE/alpha-1 mut treated cells after 4 hours is difficult to explain, and could be due to an unknown experimental error.

Table 7.2: Average GPT and RPL32 gene expression as assessed via qRT-PCR (see Appendix 7)

<u>GPT</u> (Ct values, average of 4 samples)	<u>RPL32</u> (Ct values, average of 4 samples)
IPSE/alpha-1 WT 10µg after 2h = 28.98	IPSE/alpha-1 WT 10µg after 2h = 23.48
IPSE/alpha-1 Mut 10µg after 2h = 28.91	IPSE/alpha-1 Mut 10µg after 2h = 23.35
IPSE/alpha-1 WT 10µg after 4h = 28.79	IPSE/alpha-1 WT 10µg after 4h = 23.31
IPSE/alpha-1 Mut 10µg after 4h = 29.70	IPSE/alpha-1 Mut 10µg after 4h = 22.82
Control=33.14	Control= 24.53

Table 7.3: Fold induction of gene of interest (GPT) after normalisation with reference control gene (RPL32)

No.	Treatment	Relative expression ratio
1	IPSE/alpha-1 (WT) 10µg after 2h vs untreated control	$= \frac{2^{(33.14-28.98)}}{2^{(24.53-23.48)}} = 8.63$
2	IPSE/alpha-1 (WT) 10µg after 4h vs untreated control	$= \frac{2^{(33.14-28.79)}}{2^{(24.53-23.31)}} = 8.75$
3	IPSE/alpha-1 (Mut) 10µg after 2h vs Control	$= \frac{2^{(33.14-28.91)}}{2^{(24.53-23.35)}} = 8.28$
4	IPSE/alpha-1 (Mut) 10µg after 4h vs untreated control	$= \frac{2^{(29.70-33.14)}}{2^{(22.82-24.53)}} = 0.30$
5	IPSE/alpha-1 (WT) 10µg after 2h vs IPSE/alpha-1 (Mut) 10µg after 2h	$= \frac{2^{(28.91-28.98)}}{2^{(23.35-23.48)}} = 1.04$
6	IPSE/alpha-1 (WT) 10µg after 4h vs IPSE/alpha-1 (Mut) 10µg after 4h	$= \frac{2^{(28.70-29.79)}}{2^{(22.82-23.31)}} = 2.64$

7.4 Discussion

Abdullah et al. (2011) suggested that IPSE from *S. mansoni* eggs is a toxic protein by using an ALT test which showed that enzyme activity was significantly increased, suggesting a hepatotoxic effect. However, based on our knowledge of IPSE/alpha-1 uptake and nuclear translocation, the increase in ALT activity measured after 72 hours could also be a result of increased gene expression after IPSE/alpha-1 nuclear translocation, rather than a true reflection of hepatotoxicity. Experimentally, previous results (Fig. 7.4) showed that treatment of host cells with IPSE/alpha-1 has a strong effect

on mRNA levels of proteins involved in cell adhesion. However, these results were obtained using human monocyte derived dendritic cells (Falcone, unpublished). The results obtained after treating hepatic cells with 10µg of IPSE/alpha-1 (WT) showed up-regulation of GPT or ALT - mRNA expression levels with a more than eight-fold increase after two hours and four hours, similarly to hepatic cells treated with 10µg of IPSE/alpha-1 (mutant) after two hours; however, a significant decrease in the relative GPT or ALT mRNA expression levels occurred after four hours.

As shown in these results, after two hours, both wild-type and mutant recombinant IPSE/alpha-1 showed up-regulation in their respective GPT or ALT - mRNA expression levels with a more than eight-fold increase. As shown by Kaur et al. in 2011 that PKRRRTY plays a crucial and sufficient role in the process of transferring IPSE/alpha into the nucleus of various mammalian cells. The internalization of IPSE/alpha into various mammalian host cell can also be mediated by receptor-independent pathway. However, after four hours, mutant IPSE/alpha-1 showed up-regulation, but this up-regulation was lower in the relative GPT or ALT mRNA expression levels after two hours. The induction of GPT mRNA by IPSE/alpha-1 does not appear to depend on the integrity of the NLS, as both the PKRRRTY wildtype and the PKAAATY mutant proteins showed the same induction. It appears therefore unlikely that this effect is mediated via nuclear activities, as IPSE/alpha-1 mutant is excluded from the nucleus and does not bind to DNA (265). As we have not seen any major cytotoxicity, we can only hypothesise that the effects on GPT mRNA levels are due to actions on yet to be described cell receptors. This is supported by the fact that binding

of C-type lectin receptors such as DC-SIGN or the mannose receptor by glycosylated, native IPSE/alpha-1 has been described for dendritic cells(232).

According to gene array data supplied by F.H. Falcone, IPSE/alpha-1 (WT) was tested by two types of cells: Dendritic cells (derived from monocyte in vitro) and HUVEC cells (these are venous endothelial cells), and this IPSE was incubated with these cells for 2 hours. Therefore, IPSE/alpha-1 (WT) can affect gene expression in human DCs (Figure 7.4), revealing the up-regulation of 624 genes.

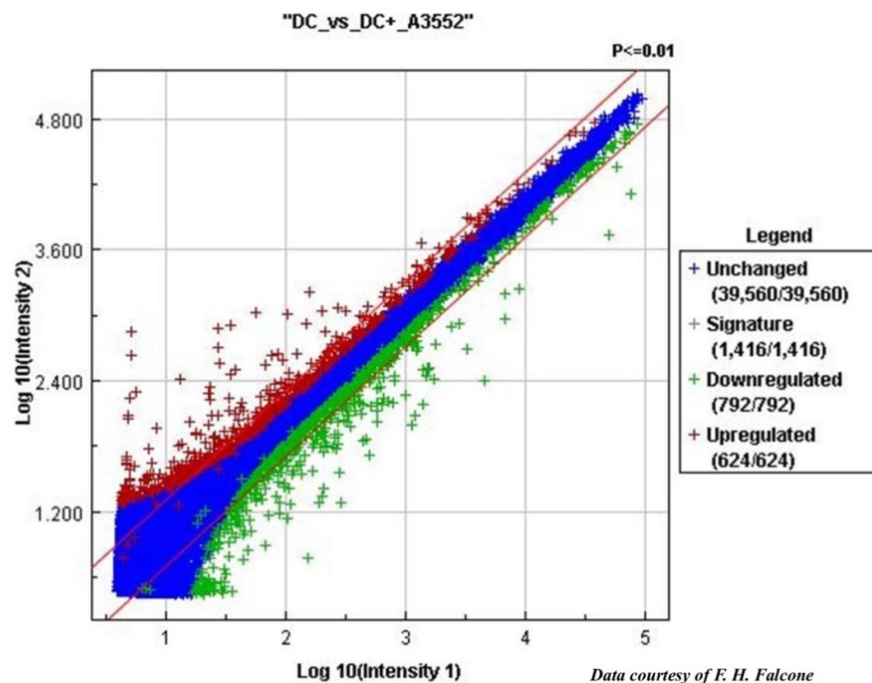


Figure 7.4: IPSE/alpha-1 has a profound effect on gene expression in human dendritic cells Log_{10} of red fluorescence indicates the up-regulation of 624 genes, and down-regulation of 792 genes, while the expression of 39,560 genes is unchanged.

Moreover, there are two GPT genes in humans, GPT and GPT2, but there appear to be no upregulation in any of them (the highest is 1.5fold for GPT2; probably not real) (see Appendix 8). This may be because the effects of this IPSE on these cells were looked at one very early time point of 2 hours and this would need to do full time course (or at least

after four and eight hours). Furthermore, DCs and HUVECs cells were not hepatocytes, and these cells might affect the gene expression patterns, if receptors are involved in uptake. Analysis of the same microarray data in the dissertation by Hwey Shan Goh (2010) from our laboratory, demonstrated that IPSE/alpha-1 had a powerful effect on genes involved in cell-to cell-contact and cell-to-extracellular matrix binding, amongst others. However, the samples for the gene array were obtained 2 hours after incubation with IPSE, thus anything changing the modality of transcription in the host cell that occurs later (e.g. 48-72 hours) will not have been picked up in this experiment if it is transient in nature. Thus more experiments are required, such as time courses and validation at the protein level.

In terms of toxicity, using three different assays (LDH assay, MTT assay and resazurin assay) proved the absence of cytotoxic activities on Huh7 cells with different concentrations of IPSE/alpha-1 (WT) at 72 h. As mentioned in the results section, the three assays did not show significant cell toxicity; however, the MTT assay showed a significant difference compared to the control (non-treated cells) for IPSE/alpha-1 (WT) concentrations of 1µg/mL, 5µg/mL and 10µg/mL. The reason for this discrepancy remains unclear and may potentially be due to natural variation in cellular metabolism. However, these results were not enough to confirm that IPSE/alpha-1 is not hepatotoxic. Therefore, future work should explore quantitative measurements of enzymatic activities, and also to determine whether IPSE/alpha-1 is hepatotoxic as Omega-1 or not. This could be carried out by inhibitory assay of the biomarker (ALT). The lysate and supernatant can be probed on western blot to measure the level of expression. Likewise, ALT levels in the supernatant can be quantified specific enzymatic activity assays. These experiments will

compare both wild-type and/or mutant IPSE/alpha-1 with untreated control cells to further ascertain the hepatotoxic effect.

Chapter 8 - General Discussion and Conclusions

8.1 Infiltrins

In previous studies virus-derived capsids, which are the protein shell of a virus, have been found to translocate into the nucleus, bind to DNA and play an important role in changing the modality of transcription within a host cell. For example, Venezuelan equine encephalitis virus (VEEV) translocates into the nucleus after invading host cells, leading to down-regulation of cellular gene transcription and then cell death (512, 513). Viruses are small in size, they are measured in nanometres, and are able to enter host cells. In contrast, parasitic helminths (worms) are not able to enter host cells because they are large multicellular organisms; however, secreted parasite proteins may achieve similar effects by entering cells and translocating into the nucleus of mammalian cells.

There are plenty of similar viral examples, such as the trans-activator of transcription (Tat) from HIV-1, which also has important nuclear activities. While such functions are easy to understand and highly plausible for viruses, they are much smaller than a host cell, rely completely on the cellular machinery for reproduction, and have an obligatory intracellular lifestyle, there are no clear examples of similar regulatory principles operating in the host-pathogen relationship between large, multicellular organisms and host cells. However, as argued in this dissertation, a case can be made that helminth parasites could also benefit from controlling host responses by translocating into the nuclei of host cells, where they manipulate the host response in order to promote helminth survival.

It is therefore suggested that infiltrins (or pathogen-secreted host nuclear proteins) are a new class of proteins. Based on our definition, infiltrins are parasite-secreted proteins with the ability to invade host cells, which can be further subdivided into cytosolic infiltrins (such as *S. mansoni* omega-1) and nuclear infiltrins (exemplified by *S. mansoni* IPSE/alpha-1). Once inside a host cell, the latter proteins can translocate into the nucleus, bind to DNA, and act as transcription factors, potentially creating an environment conducive to parasite survival, transmission and/or immune evasion. For example in the nuclei of host cells, IPSE/alpha-1 is likely to play an essential role in the host-parasite relationship (265), perhaps promoting translocation of eggs into the gut lumen, a key event in the parasite life cycle. This would suggest that infiltrins may be attractive targets for vaccination because they act as ‘master switches’.

Four potential infiltrins were identified using a bioinformatics approach, FhGST-si and FhH2A in the liver fluke *F. hepatica*, ShIPSE03 from *S. haematobium* eggs, and Smk5 from *S. mansoni* eggs. However, it is still necessary to determine whether these putative infiltrins have the ability to enter host cells, as demonstrated for recombinant IPSE/alpha-1 in mammalian cells.

Many studies have shown that proteins are secreted by *Fasciola* adult worms in the liver, including FhGST-si and FhH2A, and by the eggs of *Schistosoma* spp., such as ShIPSE03 from *S. haematobium* eggs (105, 167, 226, 297, 298). However, these proteins were predicted using different tools, as reported in Chapter 3. FhH2A is central role as a core histone nuclear protein, and it has the ability to be imported into the nucleus via a classical NLS (300). To date, there have been no experimental studies on the NLS motifs of FhGST-si and there is also no NLS prediction for Smk5. However, it is important to show

experimentally the functionality of these NLS motifs for each protein. Therefore, the presence of a putative NLS in these secreted proteins must be demonstrated and mapped. The results obtained by fluorescence microscopy confirmed that these infiltrins have monopartite NLS motifs and they have the ability to be imported into the nucleus. However, in this study, it has been focused on IPSE/alpha-1, which was discovered as the first infiltrin, to do further studies.

8.2 Egg Translocation and Function of IPSE/Alpha-1

It has been shown that Schistosome eggs have to reach the gut lumen in order to complete the life cycle, but before they enter the gut they pass through different layers, such as the adventitia/serosa, muscularis mucosae (comprising longitudinal and circular muscle), submucosa and finally the epithelium. It takes approximately a week to cross the gut wall into the gut lumen, which occurs via proteolytic and other activities of mediators produced during inflammation (489, 490). In section 6.5 we suggest that the involvement of Peyer's in facilitating movement *S. mansoni* eggs to the intestinal lumen is unclear, as these are not located in the colon, where most of the pathology caused by eggs is found. However, there are also many studies trying to explain how eggs move through the intestinal wall, and then into gut lumen. Initially, approximately 6-8 weeks after mouse infestation, the enzyme mouse mast cell protease-1 (mMCP-1) are expressed in a population of mucosal mast cells (MMC) (514, 515). However, the role of MMC in the intestines with schistosome eggs remains unknown, whereas mMCP-1 is up-regulated during infection, and consequently permits epithelial permeability, and also modifies TJ proteins (384, 397). For example, in nematode infections, It has been found that *Trichinella spiralis* is associated with the production of IgE, and subsequently with an expanded intestinal MC

population; thus, the level of MCs-associated mMCP-1 increase into the circulation and also increase intestinal permeability and then the expulsion of the parasites from the intestine (516, 517). However, there was a belief that mMCP-1 plays an important role in facilitating and excretion of schistosome eggs into the gut lumen, but these eggs do not depend on the mMCP-1 in mice to cross the gut wall (441). Moreover, it has been shown in another study that egg deposition plays an important role in the development of regulatory T cell mediated immune responses (518). Briefly, this experiment showed that T-cell deprived mice have slightly low number of eggs deposited and around two third of eggs were retained in the mice (host), and this was compared with control mice; however, after treatment in infected deprived mice with sera from chronically infected mice, they regained part of their ability to secrete eggs. Furthermore, in the infected severe compromised immunodeficient (SCID) mice, there was a delay in egg production in the stool and also failure to develop granulomas, a phenotype that could be reverted via the role of TNF- α (447, 519). This again explains how TNF- α could play a major role in recruiting inflammatory cells, and also by increasing excretion of eggs from the host, as described in Section 6.5.

8.3 Infiltrins and Future Vaccine development

Most research to develop anti-schistosomal vaccines has been empirical, with no detailed understanding of how the candidates activate the host's immune system. The essential parameters of long-term vaccine efficacy dependson persisting antibodies and immune memory for protection against infection of re-infection. One issue which may be the underlying reason for our persistent lack of efficient anti-helminthic vaccines is that parasitic antigens as vaccine candidates are traditionally assessed one by one. However,

it is reasonable to assume that a full protection will only be achieved by using multiple targets for vaccination, i.e. multiple vaccine antigens. This however has an impact on vaccine development and cost, as each antigen has to be validated and later given regulatory approval individually. As infiltrins are proteins potentially endowed with transcriptional activities, targeting the infiltrins may have an impact on many other gene products modulated by the infiltrin. This may amplify the effects on multiple aspects of the host-parasite interplay, while still targeting one single protein. The motivation for this research was to identify new targets which may provide a strategic method to develop more efficient vaccines against helminthic parasites.

Drugs are not sufficient for the prevention of the risk of parasitic disease. Currently, the drugs of choice for the treatment of *Fasciola* spp. and *Schistosoma* spp. infestations are praziquantel and triclabendazole, respectively. However, recent reports have indicated the rise of resistance of *Schistosoma* spp. and *Fasciola* spp. to these drugs (192, 520). In some endemic areas, animals infested with the latter parasites have also demonstrated resistance to treatment with these drugs (521); consequently, the treatment of these diseases may become more difficult in the future. Therefore, it is proposed that a combined approach of vaccination for control and drugs for treatment are required for the management of schistosomiasis and fascioliasis. However, current experimental vaccines targeting proteins such as helminth defence molecule (FhHDM) and peroxiredoxin (FhPrx) do not offer sufficient protection against parasitic infection, with efficacies reported at between 30% and 60% (94, 95). A similar situation is seen for anti-schistosomiasis vaccines, with many candidate vaccine antigens failing to reach the 40% threshold set as a benchmark by the WHO, and even the most promising candidate, Sm Tsp-2, has only achieved 57%

and 64% in terms of the reduction in adult worm and liver egg burdens, respectively (196). A host's immune system is influenced by proteins secreted by the parasite and the expression of its carbohydrate molecules (522). Some of these proteins could be used as vaccines for the prevention of parasitic diseases (523). Attempts have been made to use some of these secreted proteins, such as glutathione-S transferase (GST) and cathepsin B (CB 1-10) from *F. hepatica* as vaccines (96); however, in Table 1.4, there are three vaccines in clinical trials, but these vaccines did not have a chance yet to get tangible results in affected countries (195). Indeed, IPSE/alpha-1 could play an important role in the disruption of intestinal membrane integrity and in promoting translocation of eggs into the gut lumen, a complex, key event in parasite transmission. Therefore, this led to an investigation in order to *understand* the effect of the wild-type NLS in IPSE/alpha-1 on the integrity of a model gut epithelial membrane and RBL reporter systems. It was also sought to determine whether potential infiltrins, based on the simultaneous presence of a dual CSS/NLS signal, can be found in other related trematode parasites.

8.4 Conclusions and Future Work

Through the experimental work presented, the results obtained by fluorescence microscopy confirms that other parasite-derived secreted factors have the ability to translocate to host cell nuclei. FhGST-si and FhH2A from *F. hepatica*, ShIPSE03 from *S. haematobium* eggs, and Smk5 from *S. mansoni* eggs, which all have monopartite NLS motifs, are postulated to be new candidate infiltrins. Moreover, this study has demonstrated that recombinant IPSE/alpha-1 does not have a cytotoxic effect on host cells, at least in vitro, but more experiments for quantitative measurement of enzymatic activities are required, such as chemical analysis and inhibitory assay. As has been

suggested in this thesis, IPSE/alpha-1 can play an important role to facilitate and accelerate the transfer of eggs to the gut lumen, but the mechanisms require further studies to be fully understood. Future research should focus on the functionality of each infiltrin and also on studying the interactions between them and host cells, also in the *in vivo* context. In the longer term, the results of this study are expected to facilitate the development of effective strategies for the prevention and control of these diseases using a combined approach of both drug treatment and vaccination, but also a better understanding of the host-parasite relationship at the cellular and molecular level. Due to their postulated important role in the host-parasite relationship, it is possible that using one or more infiltrin as targets would help in the development of more efficient vaccines for protection against these diseases. Overall, this new class of protein (infiltrin) may be better targets for vaccination and represent the foundation for future translational research.

References

1. Paracer S, Ahmadjian V. Symbiosis: an introduction to biological associations: Oxford University Press; 2000.
2. van Crevel R, van de Vijver S, Moore DA. The global diabetes epidemic: what does it mean for infectious diseases in tropical countries? *The Lancet Diabetes & Endocrinology*. 2016 Aug 4.
3. Yazdanbakhsh M, Kremsner PG, Van Ree R. Allergy, parasites, and the hygiene hypothesis. *Science*. 2002;296(5567):490-4.
4. Howard S, Donnelly C, Chan M-S. Methods for estimation of associations between multiple species parasite infections. *Parasitology*. 2001;122(02):233-51.
5. Pozio E, Murrell KD. Systematics and epidemiology of *Trichinella*. *Advances in parasitology*. 2006;63:367-439.
6. Burdakova E, Yastrebova I, Yastrebov M. The oral sucker muscles of six representatives of the order Paramphistomatida (Plathelminthes, Trematoda). *Biology Bulletin*. 2015;42(2):108-16.
7. Cai X, Liu G, Song H, Wu C, Zou F, Yan H, et al. Sequences and gene organization of the mitochondrial genomes of the liver flukes *Opisthorchis viverrini* and *Clonorchis sinensis* (Trematoda). *Parasitology research*. 2012;110(1):235-43.
8. Toledo R, Fried B. Digenetic trematodes: Springer; 2014.
9. Taylor LH, Latham SM, Mark E. Risk factors for human disease emergence. *Philosophical Transactions of the Royal Society of London B: Biological Sciences*. 2001;356(1411):983-9.
10. Daczkowski CM. Optimization of Culture Conditions for in Vitro Fertilization of the Microphallid Trematodes *Gynaecotyla Adunca* and *Microphallus Turgidus*. 2014.
11. Organization WH. First WHO report on neglected tropical diseases: working to overcome the global impact of neglected tropical diseases. First WHO report on neglected tropical diseases: Working to overcome the global impact of neglected tropical diseases: WHO; 2010.
12. Ball M, Parker G, Chubb J. The evolution of complex life cycles when parasite mortality is size- or time-dependent. *Journal of theoretical biology*. 2008;253(1):202-14.
13. Parker GA, Chubb JC, Ball MA, Roberts GN. Evolution of complex life cycles in helminth parasites. *Nature*. 2003;425(6957):480-4.
14. Norseth HM, Ndhlovu PD, Kleppa E, Randrianasolo BS, Jourdan PM, Roald B, et al. The Colposcopic Atlas of Schistosomiasis in the Lower Female Genital Tract Based on Studies in Malawi, Zimbabwe, Madagascar and South Africa. *PLoS neglected tropical diseases*. 2014;8(11):e3229.
15. Uglem G, Lewis M, Larson O. Niche segregation and sugar transport capacity of the tegument in digenean flukes. *Parasitology*. 1985;91(01):121-7.
16. Cioli D, Pica-Mattoccia L, Basso A, Guidi A. Schistosomiasis control: praziquantel forever? *Molecular and biochemical parasitology*. 2014;195(1):23-9.
17. Prakash M, Krishnamurthy D. The deadly swimming of Cercariae: an unusual Stokesian swimmer. In APS Division of Fluid Dynamics Meeting Abstracts . 2014;59.

18. Organization WH. Report of the WHO expert consultation on foodborne trematode infections and taeniasis. (2011).
19. Lotfy W, El-Morshedy H, El-Hoda MA, El-Tawila M, Omar E, Farag H. Identification of the Egyptian species of *Fasciola*. *Veterinary parasitology*. 2002;103(4):323-32.
20. Roberts EW. Studies on the life-cycle of *Fasciola hepatica* (Linnaeus) and of its snail host, *Limnaea* (*Galba*) *truncatula* (Müller), in the field and under controlled conditions in the laboratory. *Annals of Tropical Medicine & Parasitology*. 1950;44(2):187-206.
21. Keiser J, Utzinger J. Emerging foodborne trematodiasis. *Emerging infectious diseases*. 2005;11(10):1507.
22. Mas-Coma S, Bargues MD, Valero M. Fascioliasis and other plant-borne trematode zoonoses. *International journal for parasitology*. 2005;35(11):1255-78.
23. Chen M, Mott K. Progress in assessment of morbidity due to *Fasciola hepatica* infection: a review of recent literature. *Tropical diseases bulletin*. 1990;87(4):R1-R38.
24. Mas-Coma S, Valero MA, Bargues MD. *Fasciola*, lymnaeids and human fascioliasis, with a global overview on disease transmission, epidemiology, evolutionary genetics, molecular epidemiology and control. *Advances in parasitology*. 2009;69:41-146.
25. Mas-Coma M, Esteban J, Bargues M. Epidemiology of human fascioliasis: a review and proposed new classification. *Bull World Health Organ*. 1999;77(4):340-46.
26. Mas-Coma S, Agramunt VH, Valero MA. Neurological and ocular fascioliasis in humans. *Adv Parasitol*. 2014;84(84):27-149.
27. MAS CS, Bargues M. Human liver flukes: a review. (1997).
28. Fried B, Graczyk TK, Tamang L. Food-borne intestinal trematodiasis in humans. *Parasitology Research*. 2004;93(2):159-70.
29. Gulsen M, Savas M, Koruk M, Kadayifci A, Demirci F. Fascioliasis: a report of five cases presenting with common bile duct obstruction. *The Netherland Journal of Medicine*. 2006;64(1):17-9.
30. González-Díaz H, Prado-Prado F, Ubeira FM. Predicting antimicrobial drugs and targets with the MARCH-INSIDE approach. *Current topics in medicinal chemistry*. 2008;8(18):1676-90.
31. FAO., Food, Nations AOotU, OAA. Diseases of domestic animals caused by flukes: Food and Agriculture Organization of the United Nations; 1994.
32. Cwiklinski K, de la Torre-Escudero E, Trelis M, Bernal D, Dufresne PJ, Brennan GP, et al. The extracellular vesicles of the helminth pathogen, *Fasciola hepatica*: biogenesis pathways and cargo molecules involved in parasite pathogenesis. *Molecular & Cellular Proteomics*. 2015;14(12):3258-73.
33. Claridge J, Diggle P, McCann CM, Mulcahy G, Flynn R, McNair J, et al. *Fasciola hepatica* is associated with the failure to detect bovine tuberculosis in dairy cattle. *Nature communications*. 2012;3:853.
34. Spithill T, Smooker P, Copeman D. *Fasciola gigantica*: epidemiology, control, immunology and molecular biology. *Fasciolosis*. 1999. p. 465-525.
35. Cancela M, Ruétalo N, Dell'Oca N, da Silva E, Smircich P, Rinaldi G, et al. Research article Survey of transcripts expressed by the invasive juvenile stage of the liver fluke *Fasciola hepatica*. *BMC genomics*. 2010.

36. Mas-Coma S, Bargues M, Valero M. Diagnosis of human fascioliasis by stool and blood techniques: update for the present global scenario. *Parasitology*. 2014;141(14):1918-46.
37. Duthaler UP. Artemisinins for the treatment of fascioliasis: Progress in preclinical and diagnostic research: (Doctoral dissertation, University of Basel) ; 2012.
38. Yılmaz H, Gödekmerdan A. Human fasciolosis in Van province, Turkey. *Acta tropica*. 2004;92(2):161-2.
39. Esteban J, Bargues M, MAS CS. Geographical distribution, diagnosis and treatment of human fascioliasis: a review. (1998).
40. Novobilský A, Sollenberg S, Höglund J. Distribution of *Fasciola hepatica* in Swedish dairy cattle and associations with pasture management factors. *Geospatial health*. 2015;9(2):293-300.
41. Organization WH, Infections WSGotCoFT. Control of foodborne trematode infections: report of a WHO study group: World Health Organization; 1995.
42. Organization WH. Report of the WHO Informal Meeting on use of triclabendazole in fascioliasis control. World Health Organization, Headquarters Geneva. 2006:17-8.
43. Keiser J, Utzinger J. Food-borne trematodiasis: current chemotherapy and advances with artemisinins and synthetic trioxolanes. *Trends in Parasitology*. 2007;23(11):555-62.
44. Bargues MD, Malandrini JB, Artigas P, Soria CC, Velásquez JN, Carnevale S, et al. Human fascioliasis endemic areas in Argentina: multigene characterisation of the lymnaeid vectors and climatic-environmental assessment of the transmission pattern. *Parasites & vectors*. 2016;9(1):1.
45. Ashrafi K, Valero MA, Peixoto RV, Artigas P, Panova M, Mas-Coma S. Distribution of *Fasciola hepatica* and *F. gigantica* in the endemic area of Guilan, Iran: Relationships between zonal overlap and phenotypic traits. *Infection, Genetics and Evolution*. 2015;31:95-109.
46. Periago M, Valero M, Panova M, Mas-Coma S. Phenotypic comparison of allopatric populations of *Fasciola hepatica* and *Fasciola gigantica* from European and African bovines using a computer image analysis system (CIAS). *Parasitology research*. 2006;99(4):368-78.
47. Mas-Coma S. Human fascioliasis: epidemiological patterns in human endemic areas of South America, Africa and Asia. *Southeast Asian J Trop Med Public Health*. 2004;35(Suppl 1):1-11.
48. Tran VH, Tran TK, Nguye HC, Pham HD, Pham TH. Fascioliasis in Vietnam. *The Southeast Asian journal of tropical medicine and public health*. 2000 Dec;32:48-50.
49. Robinson MW, Dalton JP. Zoonotic helminth infections with particular emphasis on fasciolosis and other trematodiasis. *Philosophical Transactions of the Royal Society of London B: Biological Sciences*. 2009;364(1530):2763-76.
50. Torgerson P, Claxton J. *Epidemiology and control. Fasciolosis*; (1999): 113-149.
51. Rapsch C, Schweizer G, Grimm F, Kohler L, Bauer C, Deplazes P, et al. Estimating the true prevalence of *Fasciola hepatica* in cattle slaughtered in Switzerland in the absence of an absolute diagnostic test. *International journal for parasitology*. 2006;36(10):1153-8.

52. Byrne AW, McBride S, Lahuerta-Marin A, Guelbenzu M, McNair J, Skuce RA, et al. Liver fluke (*Fasciola hepatica*) infection in cattle in Northern Ireland: a large-scale epidemiological investigation utilising surveillance data. *Parasites & vectors*. 2016;9(1):1.
53. Valero MA, Panova M, Comes AM, Fons R, Mas-Coma S. Patterns in size and shedding of *Fasciola hepatica* eggs by naturally and experimentally infected murid rodents. *Journal of Parasitology*. 2002;88(2):308-13.
54. Tolan RW. Fascioliasis due to *Fasciola hepatica* and *Fasciola gigantica* infection: an update on this 'neglected' neglected tropical disease. *Laboratory Medicine*. 2011;42(2):107-16.
55. Taira K, Saitoh Y. Estimated egg production of *Fasciola gigantica* (Japanese strain) in goats experimentally infected with 50 metacercariae. *Helminthologia*. 2010;47(4):199-203.
56. Periago M, Valero M, El Sayed M, Ashrafi K, El Wakeel A, Mohamed M, et al. First phenotypic description of *Fasciola hepatica*/*Fasciola gigantica* intermediate forms from the human endemic area of the Nile Delta, Egypt. *Infection, Genetics and Evolution*. 2008;8(1):51-8.
57. Santos TRMd. Genetic characterization of Portuguese *Fasciola hepatica* isolates: Faculdade de Ciências e Tecnologia; 2012.
58. Esteban J, Flores A, Angles R, Strauss W, Aguirre C, Mas-Coma S. A population-based coprological study of human fascioliasis in a hyperendemic area of the Bolivian Altiplano. *Tropical Medicine & International Health*. 1997;2(7):695-9.
59. Mas-Coma S, Angles R, Esteban J, Bargues M, Buchon P, Franken M, et al. The Northern Bolivian Altiplano: a region highly endemic for human fascioliasis. *Tropical Medicine & International Health*. 1999;4(6):454-67.
60. Khandelwal N, Shaw J, Jain MK. Biliary parasites: diagnostic and therapeutic strategies. *Current treatment options in gastroenterology*. 2008;11(2):85-95.
61. Mochankana ME. Epidemiological Studies on Bovine Fasciolosis in Botswana. (Doctoral dissertation, Murdoch University). 2014.
62. Dalton JP. Fasciolosis: CAB International; 1998.
63. Krull W. The number of cercariae of *Fasciola hepatica* developing in snails infected with a single miracidium. *Proceedings of the Helminthological Society of Washington*. 1941;8(2):55-8.
64. Andrews S. *The Life Cycle of Fasciola hepatica*. 1–29. CAB International; 1999.
65. Rapsch C, Dahinden T, Heinzmann D, Torgerson PR, Braun U, Deplazes P, et al. An interactive map to assess the potential spread of *Lymnaea truncatula* and the free-living stages of *Fasciola hepatica* in Switzerland. *Veterinary parasitology*. 2008;154(3):242-9.
66. Rana SS, Bhasin DK, Nanda M, Singh K. Parasitic infestations of the biliary tract. *Current gastroenterology reports*. 2007;9(2):156-64.
67. Kaewkes S. Taxonomy and biology of liver flukes. *Acta tropica*. 2003;88(3):177-86.
68. Corporation MC. *Diseases and Disorders*: Marshall Cavendish; 2007.
69. Dalton JP. Fasciolosis: CAB International; 1999.
70. Hanna R, Edgar H, Moffett D, McConnell S, Fairweather I, Brennan G, et al. *Fasciola hepatica*: histology of the testis in egg-producing adults of several laboratory-

- maintained isolates of flukes grown to maturity in cattle and sheep and in flukes from naturally infected hosts. *Veterinary parasitology*. 2008;157(3):222-34.
71. Phalee A, Wongsawad C, Rojanapaibul A, Chai J-Y. Experimental life history and biological characteristics of *Fasciola gigantica* (Digenea: Fasciolidae). *The Korean journal of parasitology*. 2015;53(1):59.
 72. Arjona R, Riancho JA, Aguado JM, Salesa R, González-Macías J. Fascioliasis in developed countries: a review of classic and aberrant forms of the disease. *Medicine*. 1995;74(1):13-23.
 73. Mas-Coma S, Bargues M, Valero M. Fascioliasis. *Helminth Infections and their Impact on Global Public Health*: Springer; 2014. p. 93-122.
 74. Haswell-Elkins M, Levri E. Food-borne trematodes. Chapter. 2003;81:1471-86.
 75. Soliman O, El-Arman M, Abdul-Samie E, El-Nemr H, Massoud A. Evaluation of myrrh (Mirazid) therapy in fascioliasis and intestinal schistosomiasis in children: immunological and parasitological study. *Journal of the Egyptian Society of Parasitology*. 2004;34(3):941-66.
 76. Duthaler U, Rinaldi L, Maurelli MP, Vargas M, Utzinger J, Cringoli G, et al. *Fasciola hepatica*: comparison of the sedimentation and FLOTAC techniques for the detection and quantification of faecal egg counts in rats. *Experimental parasitology*. 2010;126(2):161-6.
 77. El-Shabrawi M, El-Karakasy H, Okasha S, El-Hennawy A. Human fascioliasis: clinical features and diagnostic difficulties in Egyptian children. *Journal of tropical pediatrics*. 1997;43(3):162-6.
 78. Boray J. Studies on experimental infections with *Fasciola hepatica*, with particular reference to acute fascioliasis in sheep. *Annals of Tropical Medicine & Parasitology*. 1967;61(4):439-50.
 79. Hoyle D, Taylor D. The immune response of regional lymph nodes during the early stages of *Fasciola hepatica* infection in cattle. *Parasite immunology*. 2003;25(4):221-9.
 80. Adarosy H, Gad Y, El-Baz S, El-Shazly A. Changing pattern of fascioliasis prevalence early in the 3rd millennium in Dakahlia Governorate, Egypt: an update. *Journal of the Egyptian Society of Parasitology*. 2013;43(1):275-86.
 81. Gonzalo-Orden M, Millán L, Alvarez M, Sánchez-Campos S, Jiménez R, González-Gallego J, et al. Diagnostic imaging in sheep hepatic fascioliasis: ultrasound, computer tomography and magnetic resonance findings. *Parasitology research*. 2003;90(5):359-64.
 82. Saba R, Korkmaz M, Inan D, Mamikoğlu L, Turhan Ö, Günseren F, et al. Human fascioliasis. *Clinical microbiology and infection*. 2004;10(5):385-7.
 83. Espino AM, Finlay C. Sandwich enzyme-linked immunosorbent assay for detection of excretory secretory antigens in humans with fascioliasis. *Journal of Clinical Microbiology*. 1994;32(1):190-3.
 84. Espino AM, Duménigo BE, Fernández R, Finlay CM. Immunodiagnosis of human fascioliasis by enzyme-linked immunosorbent assay using excretory-secretory products. *The American journal of tropical medicine and hygiene*. 1987;37(3):605.
 85. Adela Valero M, Victoria Periago M, Pérez-Crespo I, Rodríguez E, Jesús Perteguer M, Gárate T, et al. Assessing the validity of an ELISA test for the serological

- diagnosis of human fascioliasis in different epidemiological situations. *Tropical Medicine & International Health*. 2012;17(5):630-6.
86. Cabada MM, White Jr AC. New developments in epidemiology, diagnosis, and treatment of fascioliasis. *Current opinion in infectious diseases*. 2012;25(5):518-22.
 87. McMullen DB. Schistosomiasis Control in Theory and Practice (the 27th Charles Franklin Craig Lecture). *American Journal of Tropical Medicine and Hygiene*. 1963;12(3):288-95.
 88. Sunita K, Kumar P, Singh D. Fasciolosis Control: Phytotherapy of Host Snail *Lymnaea acuminata* by Allicin to Kill *Fasciola gigantica* Larvae. 2013.
 89. Adewunmi C. Water extract of *Tetrapleura tetraptera*: an effective molluscicide for the control of schistosomiasis and fascioliasis in Nigeria. *Journal of Animal Production Research (Nigeria)*. 1984.
 90. Keiser J, Engels D, Büscher G, Utzinger J. Triclabendazole for the treatment of fascioliasis and paragonimiasis. *Expert opinion on investigational drugs*. 2005;14(12):1513-26.
 91. Villegas F, Angles R, Barrientos R, Barrios G, Valero MA, Hamed K, et al. Administration of triclabendazole is safe and effective in controlling fascioliasis in an endemic community of the Bolivian Altiplano. *PLoS Negl Trop Dis*. 2012;6(8):e1720.
 92. Cabada MM, Lopez M, Cruz M, Delgado JR, Hill V, White Jr AC. Treatment failure after multiple courses of triclabendazole among patients with fascioliasis in Cusco, Peru: a case series. *PLoS Negl Trop Dis*. 2016;10(1):e0004361.
 93. Fernández V, Cadenazzi G, Miranda-Miranda E, Larsen K, Solana H. A Multienzyme Response is involved in the Phenomenon of *Fasciola hepatica* Resistance to Triclabendazole. *J Drug Metab Toxicol*. 2015;6(192):2.
 94. Kaufmann SHE, Rouse BT, Sacks DL. *The Immune Response to Infection*: ASM Press; 2010.
 95. Mas-Coma S, Valero M, Bargues M. 4.2 Systematics and Morphology of Casual Agents. *Digenetic Trematodes*. 2014:77.
 96. Dalton JP, Robinson MW, Mulcahy G, O'Neill SM, Donnelly S. Immunomodulatory molecules of *Fasciola hepatica*: candidates for both vaccine and immunotherapeutic development. *Veterinary parasitology*. 2013;195(3):272-85.
 97. Toet H, Piedrafita DM, Spithill TW. Liver fluke vaccines in ruminants: strategies, progress and future opportunities. *International journal for parasitology*. 2014;44(12):915-27.
 98. Brady MT, O'Neill SM, Dalton JP, Mills KH. *Fasciola hepatica* suppresses a protective Th1 response against *Bordetella pertussis*. *Infection and Immunity*. 1999;67(10):5372-8.
 99. van Riet E, Hartgers FC, Yazdanbakhsh M. Chronic helminth infections induce immunomodulation: consequences and mechanisms. *Immunobiology*. 2007;212(6):475-90.
 100. Allen JE, Maizels RM. Diversity and dialogue in immunity to helminths. *Nature Reviews Immunology*. 2011;11(6):375-88.
 101. Henry EK, Sy CB, Inclan-Rico JM, Espinosa V, Ghanny SS, Dwyer DF, et al. Carbonic anhydrase enzymes regulate mast cell-mediated inflammation. *The Journal of experimental medicine*. 2016;213(9):1663-73.

102. Serradell MC, Guasconi L, Cervi L, Chiapello LS, Masih DT. Excretory-secretory products from *Fasciola hepatica* induce eosinophil apoptosis by a caspase-dependent mechanism. *Veterinary immunology and immunopathology*. 2007;117(3):197-208.
103. Grzych J-M, Pearce E, Cheever A, Caulada Z, Caspar P, Heiny S, et al. Egg deposition is the major stimulus for the production of Th2 cytokines in murine schistosomiasis mansoni. *The Journal of Immunology*. 1991;146(4):1322-7.
104. O'Neill SM, Brady MT, Callanan JJ, Mulcahy G, Joyce P, Mills KH, et al. *Fasciola hepatica* infection downregulates Th1 responses in mice. *Parasite immunology*. 2000;22(3):147-55.
105. Dowling DJ, Hamilton CM, Donnelly S, La Course J, Brophy PM, Dalton J, et al. Major secretory antigens of the helminth *Fasciola hepatica* activate a suppressive dendritic cell phenotype that attenuates Th17 cells but fails to activate Th2 immune responses. *Infection and immunity*. 2010;78(2):793-801.
106. Chemale G, Morpew R, Moxon JV, Morassuti AL, LaCourse EJ, Barrett J, et al. Proteomic analysis of glutathione transferases from the liver fluke parasite, *Fasciola hepatica*. *Proteomics*. 2006;6(23):6263-73.
107. LaCourse EJ, Hernandez-Viadel M, Jefferies JR, Svendsen C, Spurgeon DJ, Barrett J, et al. Glutathione transferase (GST) as a candidate molecular-based biomarker for soil toxin exposure in the earthworm *Lumbricus rubellus*. *Environmental Pollution*. 2009;157(8):2459-69.
108. LaCourse EJ, Hoey E, Zafra R, Buffoni L, Pérez Arévalo J, Brophy PM, et al. The Sigma class glutathione transferase from the liver fluke *Fasciola hepatica*. *PLoS neglected tropical diseases*. 2012;6(5):e1666.
109. LaCourse EJ, Perally S, Morpew RM, Moxon JV, Prescott M, Dowling DJ, et al. The Sigma class glutathione transferase from the liver fluke *Fasciola hepatica*. *PLoS Negl Trop Dis*. 2012;6(5):e1666.
110. Geyer KK, Hoffmann KF. Epigenetics: A key regulator of platyhelminth developmental biology? *International journal for parasitology*. 2012;42(3):221-4.
111. Luger K, Rechsteiner TJ, Flaus AJ, Wayne MM, Richmond TJ. Characterization of nucleosome core particles containing histone proteins made in bacteria. *Journal of molecular biology*. 1997;272(3):301-11.
112. de Carvalho LP, Soto M, Jerônimo S, Dondji B, Bacellar O, Luz V, et al. Characterization of the immune response to *Leishmania infantum* recombinant antigens. *Microbes and infection*. 2003;5(1):7-12.
113. Probst P, Stromberg E, Ghalib HW, Mozel M, Badaro R, Reed SG, et al. Identification and characterization of T cell-stimulating antigens from *Leishmania* by CD4 T cell expression cloning. *The Journal of Immunology*. 2001;166(1):498-505.
114. Soto M, Requena JM, Quijada L, García M, Guzman F, Patarroyo ME, et al. Mapping of the linear antigenic determinants from the *Leishmania infantum* histone H2A recognized by sera from dogs with leishmaniasis. *Immunology letters*. 1995;48(3):209-14.
115. Shebel HM, Elsayes KM, El Atta HMA, Elguindy YM, El-Diasty TA. Genitourinary Schistosomiasis: Life Cycle and Radiologic-Pathologic Findings. *Radiographics*. 2012;32(4):1031-46.

116. Ruffer MA. Note on the presence of “*Bilharzia haematobia*” in Egyptian mummies of the twentieth dynasty [1250-1000 BC]. *British Medical Journal*. 1910;1(2557):16.
117. Peterson RK. Insects, disease, and military history. *American Entomologist*. 1995;41(3):147-61.
118. Farooq M. Historical development. *Epidemiology and Control of Schistosomiasis (bilharziasis)*: Karger Publishers; 1973. p. 1-16.
119. Baba T, Hosoi M, Urabe M, Shimazu T, Tochimoto T, Hasegawa H. *Liolope copulans* (Trematoda: Digenea: Liolopidae) parasitic in *Andrias japonicus* (Amphibia: Caudata: Cryptobranchidae) in Japan: Life cycle and systematic position inferred from morphological and molecular evidence. *Parasitology International*. 2011;60(2):181-92.
120. Katz N. The discovery of *Schistosomiasis mansoni* in Brazil. *Acta Tropica*. 2008;108(2):69-71.
121. Jordan P. From Katayama to the Dakhla Oasis: the beginning of epidemiology and control of bilharzia. *Acta tropica*. 2000;77(1):9-40.
122. Loker ES. A comparative study of the life-histories of mammalian schistosomes. *Parasitology*. 1983;87(02):343-69.
123. Gray DJ, Ross AG, Li Y-S, McManus DP. Diagnosis and management of schistosomiasis. *BMJ*. 2011;342(may16_2):d2651-d.
124. King CH. *Epidemiology of schistosomiasis: determinants of transmission of infection*. Schistosomiasis Imperial College Press, London, United Kingdom. 2001:115-32.
125. Song L, Wu X, Ren J, Gao Z, Xu Y, Xie H, et al. Assessment of the effect of treatment and assistance program on advanced patients with schistosomiasis japonica in China from 2009 to 2014. *Parasitology research*. 2016;115(11):4267-73.
126. Steinmann P, Keiser J, Bos R, Tanner M, Utzinger J. Schistosomiasis and water resources development: systematic review, meta-analysis, and estimates of people at risk. *The Lancet infectious diseases*. 2006;6(7):411-25.
127. Peak E, Chalmers IW, Hoffmann KF. Development and validation of a quantitative, high-throughput, fluorescent-based bioassay to detect schistosoma viability. *PLoS neglected tropical diseases*. 2010;4(7):e759.
128. Milligan JN, Jolly ER. Identification and characterization of a Mef2 transcriptional activator in schistosome parasites. *PLoS neglected tropical diseases*. 2012;6(1):e1443.
129. Colley DG, Bustinduy AL, Secor WE, King CH. Human schistosomiasis. *The Lancet*. 2014;383(9936):2253-64.
130. Murray CJ, Vos T, Lozano R, Naghavi M, Flaxman AD, Michaud C, et al. Disability-adjusted life years (DALYs) for 291 diseases and injuries in 21 regions, 1990–2010: a systematic analysis for the Global Burden of Disease Study 2010. *The lancet*. 2013;380(9859):2197-223.
131. Fallon PG, Mangan NE. Suppression of TH2-type allergic reactions by helminth infection. *Nature Reviews Immunology*. 2007;7(3):220-30.
132. Berriman M, Haas BJ, LoVerde PT, Wilson RA, Dillon GP, Cerqueira GC, et al. The genome of the blood fluke *Schistosoma mansoni*. *Nature*. 2009;460(7253):352-8.

133. WHO. Schistosomiasis 2013 [Available from: http://search.who.int/search?q=schistosoma&ie=utf8&site=who&client=en_r&proxystylesheet=en_r&output=xml_no_dtd&oe=utf8&getfields=doctype].
134. Gryseels B, Polman K, Clerinx J, Kestens L. Human schistosomiasis. *The Lancet*. 2006;368(9541):1106-18.
135. Farrar J, Hotez P, Junghanss T, Kang G, Lalloo D, White NJ. *Manson's tropical diseases*: Elsevier Health Sciences; 2013.
136. Webster JP, Gower CM, Knowles SC, Molyneux DH, Fenton A. One health—an ecological and evolutionary framework for tackling Neglected Zoonotic Diseases. *Evolutionary applications*. 2016;9(2):313-33.
137. SCRIMGEOUR EM, GAJDUSEK DC. INVOLVEMENT OF THE CENTRAL NERVOUS SYSTEM IN SCHISTOSOMA MANSONI AND S. HAEMATOBIIUM INFECTION A REVIEW. *Brain*. 1985;108(4):1023-38.
138. Beltran S, Cézilly F, Boissier J. Genetic dissimilarity between mates, but not male heterozygosity, influences divorce in schistosomes. *PLoS One*. 2008;3(10):e3328.
139. Granath Jr WO, Yoshino TP. Lysosomal enzyme activities in susceptible and refractory strains of *Biomphalaria glabrata* during the course of infection with *Schistosoma mansoni*. *The Journal of Parasitology*. 1983;1018-26.
140. Trail DRS. Behavioral interactions between parasites and hosts: host suicide and the evolution of complex life cycles. *American Naturalist*. 1980:77-91.
141. de Jong-Brink M, Bergamin-Sassen M, Solis Soto M. Multiple strategies of schistosomes to meet their requirements in the intermediate snail host. *Parasitology*. 2001;123(7):129-41.
142. Mahmoud A, Warren KS, Peters PA. A role for the eosinophil in acquired resistance to *Schistosoma mansoni* infection as determined by antieosinophil serum. *The Journal of experimental medicine*. 1975;142(4):805-13.
143. Miller P, Wilson R. Migration of the schistosomula of *Schistosoma mansoni* from the lungs to the hepatic portal system. *Parasitology*. 1980;80(02):267-88.
144. Lichtenberg Fv. Host response to eggs of *S. mansoni*: I. Granuloma formation in the unsensitized laboratory mouse. *The American Journal of Pathology*. 1962;41(6):711.
145. Yamabe M, Kumagai T, Shimogawara R, Blay EA, Hino A, Ichimura K, et al. Novel synthetic compounds with endoperoxide structure damage juvenile stage of *Schistosoma mansoni* by targeting lysosome-like organelles. *Parasitology International*. 2017;66(1):917-24.
146. Meevissen MH, Yazdanbakhsh M, Hokke CH. *Schistosoma mansoni* egg glycoproteins and C-type lectins of host immune cells: molecular partners that shape immune responses. *Exp Parasitol*. 2012;132(1):14-21.
147. Sturrock RF. *The schistosomes and their intermediate hosts*. Imperial College Press, London, UK. 2001:7-83.
148. Warren K, Mahmoud A, Muruka J, Whittaker L, Ouma J, Arap ST. Schistosomiasis haematobia in coast province Kenya. Relationship between egg output and morbidity. *The American journal of tropical medicine and hygiene*. 1979;28(5):864-70.
149. Boros DL, Warren KS. Delayed hypersensitivity-type granuloma formation and dermal reaction induced and elicited by a soluble factor isolated from *Schistosoma mansoni* eggs. *The Journal of experimental medicine*. 1970;132(3):488-507.

150. Zhang Y, Chen L, Gao W, Hou X, Gu Y, Gui L, et al. IL-17 neutralization significantly ameliorates hepatic granulomatous inflammation and liver damage in *Schistosoma japonicum* infected mice. *European journal of immunology*. 2012;42(6):1523-35.
151. Zhong X, Isharwal S, Naples JM, Shiff C, Veltri RW, Shao C, et al. Hypermethylation of genes detected in urine from Ghanaian adults with bladder pathology associated with *Schistosoma haematobium* infection. *PloS one*. 2013;8(3):e59089.
152. Meurs L, Mbow M, Vereecken K, Menten J, Mboup S, Polman K. Bladder morbidity and hepatic fibrosis in mixed *Schistosoma haematobium* and *S. mansoni* Infections: a population-wide study in Northern Senegal. *PLoS Negl Trop Dis*. 2012;6(9):e1829.
153. Mchedlidze T, Waldner M, Zopf S, Walker J, Rankin AL, Schuchmann M, et al. Interleukin-33-dependent innate lymphoid cells mediate hepatic fibrosis. *Immunity*. 2013;39(2):357-71.
154. Gao B, Radaeva S. Natural killer and natural killer T cells in liver fibrosis. *Biochimica et Biophysica Acta (BBA)-Molecular Basis of Disease*. 2013;1832(7):1061-9.
155. Pavlin BI, Kozarsky P, Cetron MS. Acute pulmonary schistosomiasis in travelers: case report and review of the literature. *Travel medicine and infectious disease*. 2012;10(5):209-19.
156. Ross AG, Vickers D, Olds GR, Shah SM, McManus DP. Katayama syndrome. *The Lancet infectious diseases*. 2007;7(3):218-24.
157. Khan M. IMPORTANT VECTOR-BORNE DISEASES WITH THEIR ZOONOTIC POTENTIAL: PRESENT SITUATION AND FUTURE PERSPECTIVE. *Bangladesh Journal of Veterinary Medicine*. 2016;13(2):1-14.
158. Ouma JH, Vennervald BJ, Kariuki HC, Butterworth AE. Morbidity in schistosomiasis: an update. *Trends in parasitology*. 2001;17(3):117-8.
159. Richter J, Botelho M, Holtfreter M, Akpata R, El Scheich T, Neumayr A, et al. Ultrasound assessment of schistosomiasis. *Zeitschrift für Gastroenterologie*. 2016;54(07):653-60.
160. Ranasinghe SL, Fischer K, Gobert GN, Mcmanus DP. A novel coagulation inhibitor from *Schistosoma japonicum*. *Parasitology*. 2015;142(14):1663-72.
161. Doehring E, Reider F, Schmidt-Ehry G, Ehrlich JH. Reduction of pathological findings in urine and bladder lesions in infection with *Schistosoma haematobium* after treatment with praziquantel. *Journal of infectious diseases*. 1985;152(4):807-10.
162. Olveda DU, Olveda RM, Montes CJ, Chy D, Abellera JMB, Cuajunco D, et al. Clinical management of advanced schistosomiasis: a case of portal vein thrombosis-induced splenomegaly requiring surgery. *BMJ case reports*. 2014;2014:bcr2014203897.
163. Warren KS. Pathophysiology and pathogenesis of hepatosplenic schistosomiasis *mansoni*. *Bulletin of the New York Academy of Medicine*. 1968;44(3):280.
164. Yanagisawa S, Yuasa T, Tanaka T. Clinical diagnosis of *Schistosoma japonicum* infection complicating infective endocarditis and liver cirrhosis. *Internal Medicine*. 2010;49(11):1001-5.
165. Boros D. Immunopathology of *Schistosoma mansoni* infection. *Clinical microbiology reviews*. 1989;2(3):250-69.

166. Hesse M, Modolell M, La Flamme AC, Schito M, Fuentes JM, Cheever AW, et al. Differential regulation of nitric oxide synthase-2 and arginase-1 by type 1/type 2 cytokines in vivo: granulomatous pathology is shaped by the pattern of L-arginine metabolism. *The Journal of Immunology*. 2001;167(11):6533-44.
167. Fu C-L, Odegaard JI, De'Broski RH, Hsieh MH. A novel mouse model of *Schistosoma haematobium* egg-induced immunopathology. *PLoS Pathog*. 2012;8(3):e1002605.
168. Badawi A, Mostafa M, Probert A, O'Connor P. Role of schistosomiasis in human bladder cancer: evidence of association, aetiological factors, and basic mechanisms of carcinogenesis. *European journal of cancer prevention*. 1995;4(1):45-60.
169. Roberts L, Janovy Jr J. *Nematodes: Oxyurida, the pinworms*. Foundations of parasitology Boston: McGraw Hill. 2000:433-7.
170. Markakpo US, Armah GE, Fobil JN, Asmah RH, Anim-Baidoo I, Dodoo AK, et al. Immunolocalization of the 29 kDa *Schistosoma haematobium* species-specific antigen: a potential diagnostic marker for urinary schistosomiasis. *BMC infectious diseases*. 2015;15(1):1.
171. Steinfelder S, Andersen JF, Cannons JL, Feng CG, Joshi M, Dwyer D, et al. The major component in schistosome eggs responsible for conditioning dendritic cells for Th2 polarization is a T2 ribonuclease (omega-1). *The Journal of experimental medicine*. 2009;206(8):1681-90.
172. Mott K, Baltes R, Bambagha J, Baldassini B. Field studies of a reusable polyamide filter for detection of *Schistosoma haematobium* eggs by urine filtration. *Tropenmedizin und Parasitologie*. 1982;33(4):227.
173. Hoffman WA, Pons JA, Janer JL. The Sedimentation-Concentration Method In *Schistosomiasis mansoni*. *Puerto Rico Journal of Public Health and Tropical Medicine*. 1934;9(3):283-91.
174. Abo-Madyan A, Morsy T, Motawea S. Efficacy of Myrrh in the treatment of schistosomiasis (*haematobium* and *mansoni*) in Ezbet El-Bakly, Tamyia Center, El-Fayoum Governorate, Egypt. *Journal of the Egyptian Society of Parasitology*. 2004;34(2):423-46.
175. Pontes LA, Oliveira MC, Katz N, Dias-Neto E, Rabello A. Comparison of a polymerase chain reaction and the Kato-Katz technique for diagnosing infection with *Schistosoma mansoni*. *The American journal of tropical medicine and hygiene*. 2003;68(6):652-6.
176. Barda BD, Rinaldi L, Ianniello D, Zepherine H, Salvo F, Sadutshang T, et al. Mini-FLOTAC, an innovative direct diagnostic technique for intestinal parasitic infections: experience from the field. *PLoS Negl Trop Dis*. 2013;7(8):e2344.
177. Abdel-Wahab MF, Strickland GT. Abdominal ultrasonography for assessing morbidity from schistosomiasis 2. Hospital studies. *Transactions of the Royal Society of Tropical Medicine and Hygiene*. 1993;87(2):135-7.
178. González AY, Sulbarán GS, Ballen DE, Cesari IM. Immunocapture of circulating *Schistosoma mansoni* cathepsin B antigen (Sm31) by anti-Sm31 polyclonal antibodies. *Parasitology international*. 2016;65(3):191-5.
179. Doenhoff MJ, Chiodini PL, Hamilton JV. Specific and sensitive diagnosis of schistosome infection: can it be done with antibodies? *Trends in parasitology*. 2004;20(1):35-9.

180. van Gool T, Vetter H, Vervoort T, Doenhoff MJ, Wetsteyn J, Overbosch D. Serodiagnosis of imported schistosomiasis by a combination of a commercial indirect hemagglutination test with *Schistosoma mansoni* adult worm antigens and an enzyme-linked immunosorbent assay with *S. mansoni* egg antigens. *Journal of clinical microbiology*. 2002;40(9):3432-7.
181. Vennervald BJ, Kahama A, Reimert C. Assessment of morbidity in *Schistosoma haematobium* infection: current methods and future tools. *Acta tropica*. 2000;77(1):81-9.
182. Robert J, Verweij JJ, Vereecken K, Polman K, Dieye L, van Lieshout L. Multiplex real-time PCR for the detection and quantification of *Schistosoma mansoni* and *S. haematobium* infection in stool samples collected in northern Senegal. *Transactions of the Royal Society of Tropical Medicine and Hygiene*. 2008;102(2):179-85.
183. Jothikumar N, Mull BJ, Brant SV, Loker ES, Collinson J, Secor WE, et al. Real-time PCR and sequencing assays for rapid detection and identification of avian schistosomes in environmental samples. *Applied and environmental microbiology*. 2015;81(12):4207-15.
184. Weerakoon KG, Gordon CA, Gobert GN, Cai P, McManus DP. Optimisation of a droplet digital PCR assay for the diagnosis of *Schistosoma japonicum* infection: A duplex approach with DNA binding dye chemistry. *Journal of microbiological methods*. 2016;125:19-27.
185. Eraky MA, Aly NS. Assessment of diagnostic performance of a commercial direct blood PCR kit for the detection of *Schistosoma mansoni* infection in mice compared with the pre-extracted PCR assay. *Parasitologists United Journal*. 2016;9(1):13.
186. Grimes JE, Croll D, Harrison WE, Utzinger J, Freeman MC, Templeton MR. The relationship between water, sanitation and schistosomiasis: a systematic review and meta-analysis. *PLoS Negl Trop Dis*. 2014;8(12):e3296.
187. Sokolow SH, Wood CL, Jones IJ, Swartz SJ, Lopez M, Hsieh MH, et al. Global assessment of schistosomiasis control over the past century shows targeting the snail intermediate host works best. *PLoS Neglected Tropical Diseases*. 2016;10(7):e0004794.
188. Gryseels B, Mbaye A, De Vlas S, Stelma F, Guisse F, Van Lieshout L, et al. Are poor responses to praziquantel for the treatment of *Schistosoma mansoni* infections in Senegal due to resistance? An overview of the evidence. *Tropical medicine & international health*. 2001;6(11):864-73.
189. Ismail M, Metwally A, Farghaly A, Bruce J, Tao L-F, Bennett JL. Characterization of isolates of *Schistosoma mansoni* from Egyptian villagers that tolerate high doses of praziquantel. *The American journal of tropical medicine and hygiene*. 1996;55(2):214-8.
190. Ming-Gang C. Use of praziquantel for clinical treatment and morbidity control of schistosomiasis japonica in China: a review of 30 years' experience. *Acta tropica*. 2005;96(2):168-76.
191. Hotez PJ, Bethony JM, Diemert DJ, Pearson M, Loukas A. Developing vaccines to combat hookworm infection and intestinal schistosomiasis. *Nature Reviews Microbiology*. 2010;8(11):814-26.

192. Wang W, Li H-J, Qu G-L, Xing Y-T, Yang Z-K, Dai J-R, et al. Is there a reduced sensitivity of dihydroartemisinin against praziquantel-resistant *Schistosoma japonicum*? *Parasitology research*. 2014;113(1):223-8.
193. Lotfy WM, Hishmat MG, El Nashar AS, Abu El Einin HM. Evaluation of a method for induction of praziquantel resistance in *Schistosoma mansoni*. *Pharmaceutical biology*. 2015;53(8):1214-9.
194. Wang W, Wang L, Liang Y-S. Susceptibility or resistance of praziquantel in human schistosomiasis: a review. *Parasitology research*. 2012;111(5):1871-7.
195. Hagen J, Young ND, Every AL, Pagel CN, Schnoeller C, Scheerlinck J-PY, et al. Omega-1 knockdown in *Schistosoma mansoni* eggs by lentivirus transduction reduces granuloma size in vivo. *Nature communications*. 2014;5.
196. Tran MH, Pearson MS, Bethony JM, Smyth DJ, Jones MK, Duke M, et al. Tetraspanins on the surface of *Schistosoma mansoni* are protective antigens against schistosomiasis. *Nature medicine*. 2006;12(7):835-40.
197. Ricciardi A, Ndao M. Still hope for schistosomiasis vaccine. *Human vaccines & immunotherapeutics*. 2015;11(10):2504-8.
198. Merrifield M, Hotez PJ, Beaumier CM, Gillespie P, Strych U, Hayward T, et al. Advancing a vaccine to prevent human schistosomiasis. *Vaccine*. 2016;34(26):2988-91.
199. Santini-Oliveira M, Coler RN, Parra J, Veloso V, Jayashankar L, Pinto PM, et al. Schistosomiasis vaccine candidate Sm14/GLA-SE: Phase 1 safety and immunogenicity clinical trial in healthy, male adults. *Vaccine*. 2016;34(4):586-94.
200. Pearson MS, Pickering DA, McSorley HJ, Bethony JM, Tribolet L, Dougall AM, et al. Enhanced protective efficacy of a chimeric form of the schistosomiasis vaccine antigen Sm-TSP-2. *PLoS Negl Trop Dis*. 2012;6(3):e1564.
201. Karmakar S, Zhang W, Ahmad G, Torben W, Alam MU, Le L, et al. Use of an Sm-p80-Based therapeutic vaccine to kill established adult schistosome parasites in chronically infected baboons. *Journal of Infectious Diseases*. 2014;209(12):1929-40.
202. Ahmad G, Zhang W, Torben W, Ahrorov A, Damian RT, Wolf RF, et al. Preclinical Prophylactic Efficacy Testing of Sm-p80-Based Vaccine in a Nonhuman Primate Model of *Schistosoma mansoni* Infection and Immunoglobulin G and E Responses to Sm-p80 in Human Serum Samples From an Area Where Schistosomiasis Is Endemic. *Journal of Infectious Diseases*. 2011;204(9):1437-49.
203. Mo AX, Agosti JM, Walson JL, Hall BF, Gordon L. Schistosomiasis elimination strategies and potential role of a vaccine in achieving global health goals. *The American journal of tropical medicine and hygiene*. 2014;90(1):54-60.
204. You H, Zhang W, Jones MK, Gobert GN, Mulvenna J, Rees G, et al. Cloning and characterisation of *Schistosoma japonicum* insulin receptors. *PLoS One*. 2010;5(3):e9868.
205. Burke M, Jones M, Gobert G, Li Y, Ellis M, McManus D. Immunopathogenesis of human schistosomiasis. *Parasite immunology*. 2009;31(4):163-76.
206. Sorci G, Cornet S, Faivre B. Immune Evasion, Immunopathology and the Regulation of the Immune System. *Pathogens*. 2013;2(1):71-91.
207. Mosmann TR, Sad S. The expanding universe of T-cell subsets: Th1, Th2 and more. *Immunology today*. 1996;17(3):138-46.
208. Smithers S, Gammage K. Recovery of *Schistosoma mansoni* from the skin, lungs and hepatic portal system of naive mice and mice previously exposed to S.

- mansoni: evidence for two phases of parasite attrition in immune mice. *Parasitology*. 1980;80(2):289-300.
209. Singh KP, Gerard HC, Hudson AP, Boros DL. Expression of matrix metalloproteinases and their inhibitors during the resorption of schistosome egg-induced fibrosis in praziquantel-treated mice. *Immunology*. 2004;111(3):343-52.
210. Bourke CD, Nausch N, Rujeni N, Appleby LJ, Mitchell KM, Midzi N, et al. Integrated analysis of innate, Th1, Th2, Th17, and regulatory cytokines identifies changes in immune polarisation following treatment of human schistosomiasis. *Journal of Infectious Diseases*. 2013;208(1):159-69.
211. Henri S, Chevillard C, Mergani A, Paris P, Gaudart J, Camilla C, et al. Cytokine regulation of periportal fibrosis in humans infected with *Schistosoma mansoni*: IFN- γ is associated with protection against fibrosis and TNF- α with aggravation of disease. *The Journal of Immunology*. 2002;169(2):929-36.
212. de Jesus AR, Magalhães A, Miranda DG, Miranda RG, Araújo MI, de Jesus AA, et al. Association of type 2 cytokines with hepatic fibrosis in human *Schistosoma mansoni* infection. *Infection and immunity*. 2004;72(6):3391-7.
213. Cliffe LJ, Grenicis RK. The *Trichuris muris* System: a Paradigm of Resistance and Susceptibility to Intestinal Nematode Infection. *Advances in parasitology*. 2004;57:255-307.
214. Montenegro SM, Miranda P, Mahanty S, Abath FG, Teixeira KM, Coutinho EM, et al. Cytokine production in acute versus chronic human schistosomiasis mansoni: the cross-regulatory role of interferon- γ and interleukin-10 in the responses of peripheral blood mononuclear cells and splenocytes to parasite antigens. *Journal of Infectious Diseases*. 1999;179(6):1502-14.
215. Pearce EJ, MacDonald AS. The immunobiology of schistosomiasis. *Nature Reviews Immunology*. 2002;2(7):499-511.
216. MacDonald AS, Straw AD, Dalton NM, Pearce EJ. Cutting edge: Th2 response induction by dendritic cells: a role for CD40. *The Journal of Immunology*. 2002;168(2):537-40.
217. Murray PJ, Wynn TA. Protective and pathogenic functions of macrophage subsets. *Nature reviews Immunology*. 2011;11(11):723-37.
218. Fairfax K, Nascimento M, Huang SC-C, Everts B, Pearce EJ, editors. Th2 responses in schistosomiasis. *Seminars in immunopathology*; 2012: Springer.
219. Neill P, Smith JH, Doughty BL, Kemp M. The ultrastructure of the *Schistosoma mansoni* egg. *The American journal of tropical medicine and hygiene*. 1988;39(1):52-65.
220. Ashton P, Harrop R, Shah B, Wilson R. The schistosome egg: development and secretions. *Parasitology*. 2001;122(03):329-38.
221. Meevissen MH, Balog CI, Koeleman CA, Doenhoff MJ, Schramm G, Haas H, et al. Targeted glycoproteomic analysis reveals that kappa-5 is a major, uniquely glycosylated component of *Schistosoma mansoni* egg antigens. *Molecular & Cellular Proteomics*. 2011;10(5).
222. Meevissen MH, Balog CI, Koeleman CA, Doenhoff MJ, Schramm G, Haas H, et al. Targeted glycoproteomic analysis reveals that kappa-5 is a major, uniquely glycosylated component of *Schistosoma mansoni* egg antigens. *Molecular & Cellular Proteomics*. 2011;10(5):M110. 005710.

223. Schramm G, Falcone FH, Gronow A, Haisch K, Mamat U, Doenhoff MJ, et al. Molecular characterization of an interleukin-4-inducing factor from *Schistosoma mansoni* eggs. *Journal of Biological Chemistry*. 2003;278(20):18384-92.
224. Schramm G, Falcone FH, Gronow A, Haisch K, Mamat U, Doenhoff MJ, et al. Molecular characterization of an interleukin-4-inducing factor from *Schistosoma mansoni* eggs. *The Journal of biological chemistry*. 2003;278(20):18384-92.
225. Pennington LF, Hsieh MH. *The Immunobiology of Urogenital Schistosomiasis*. 2014.
226. Schramm G, Hamilton J, Balog C, Wuhrer M, Gronow A, Beckmann S, et al. Molecular characterisation of kappa-5, a major antigenic glycoprotein from *Schistosoma mansoni* eggs. *Molecular and biochemical parasitology*. 2009;166(1):4-14.
227. Zaccone P, Cooke A. Helminth mediated modulation of Type 1 diabetes (T1D). *Int J Parasitol*. 2013;43(3-4):311-8.
228. Schramm G, Gronow A, Knobloch J, Wippersteg V, Grevelding C, Galle J, et al. IPSE/alpha-1: a major immunogenic component secreted from *Schistosoma mansoni* eggs. *Molecular and biochemical parasitology*. 2006;147(1):9-19.
229. Dunne D, Jones F, Doenhoff M. The purification, characterization, serological activity and hepatotoxic properties of two cationic glycoproteins (oc1 and QJi) from *Schistosoma mansoni* eggs. *Parasitology*. 1991;103:225-36.
230. Pearce E, Freitas T. Reverse genetics and the study of the immune response to schistosomes. *Parasite immunology*. 2008;30(4):215-21.
231. Pearce E. Priming of the immune response by schistosome eggs. *Parasite immunology*. 2005;27(7-8):265-70.
232. van den Biggelaar AH, van Ree R, Rodrigues LC, Lell B, Deelder AM, Kremsner PG, et al. Decreased atopy in children infected with *Schistosoma haematobium*: a role for parasite-induced interleukin-10. *The Lancet*. 2000;356(9243):1723-7.
233. Weerakoon KG, Gobert GN, Cai P, McManus DP. Advances in the diagnosis of human schistosomiasis. *Clinical microbiology reviews*. 2015;28(4):939-67.
234. Shariati F, Pérez-Arellano J, Lopez-Aban J, Alvarez A. ANGIOGENESIS AND HELMINTHS. *Journal of Fundamental and Applied Sciences*. 2016;8(3S):2037-58.
235. Meevissen MH, Wuhrer M, Doenhoff MJ, Schramm G, Haas H, Deelder AM, et al. Structural characterization of glycans on omega-1, a major *Schistosoma mansoni* egg glycoprotein that drives Th2 responses. *Journal of proteome research*. 2010;9(5):2630-42.
236. Wuhrer M, Balog CI, Catalina M, Jones FM, Schramm G, Haas H, et al. IPSE/alpha-1, a major secretory glycoprotein antigen from schistosome eggs, expresses the Lewis X motif on core-difucosylated N-glycans. *Febs Journal*. 2006;273(10):2276-92.
237. Cass CL, Johnson JR, Califf LL, Xu T, Hernandez HJ, Stadecker MJ, et al. Proteomic analysis of *Schistosoma mansoni* egg secretions. *Molecular and biochemical parasitology*. 2007;155(2):84-93.
238. Cass CL, Johnson JR, Califf LL, Xu T, Hernandez HJ, Stadecker MJ, et al. Proteomic analysis of *Schistosoma mansoni* egg secretions. *Molecular and biochemical parasitology*. 2007;155(2):84-93.

239. Fallon PG. Immunopathology of schistosomiasis: a cautionary tale of mice and men. *Immunology today*. 2000;21(1):29-35.
240. Ouf EA, Ojuronbe O, Akindele AA, Sina-Agbaje OR, Van Tong H, Adeyeba AO, et al. Ficolin-2 levels and FCN2 genetic polymorphisms as a susceptibility factor in schistosomiasis. *Journal of Infectious Diseases*. 2012;206(4):562-70.
241. Kumar R, Mickael C, Chabon J, Gebreab L, Rutebemberwa A, Garcia AR, et al. The causal role of IL-4 and IL-13 in *Schistosoma mansoni* pulmonary hypertension. *American journal of respiratory and critical care medicine*. 2015;192(8):998-1008.
242. McKee AS, Pearce EJ. CD25+ CD4+ cells contribute to Th2 polarization during helminth infection by suppressing Th1 response development. *The Journal of Immunology*. 2004;173(2):1224-31.
243. Hoffmann KF, Cheever AW, Wynn TA. IL-10 and the dangers of immune polarization: excessive type 1 and type 2 cytokine responses induce distinct forms of lethal immunopathology in murine schistosomiasis. *The Journal of immunology*. 2000;164(12):6406-16.
244. Vaillant B, Chiaramonte MG, Cheever AW, Soloway PD, Wynn TA. Regulation of hepatic fibrosis and extracellular matrix genes by the Th response: new insight into the role of tissue inhibitors of matrix metalloproteinases. *The Journal of Immunology*. 2001;167(12):7017-26.
245. Booth M, Mwatha JK, Joseph S, Jones FM, Kadzo H, Ileri E, et al. Periportal fibrosis in human *Schistosoma mansoni* infection is associated with low IL-10, low IFN- γ , high TNF- α , or low RANTES, depending on age and gender. *The Journal of Immunology*. 2004;172(2):1295-303.
246. Everts B, Perona-Wright G, Smits HH, Hokke CH, van der Ham AJ, Fitzsimmons CM, et al. Omega-1, a glycoprotein secreted by *Schistosoma mansoni* eggs, drives Th2 responses. *The Journal of experimental medicine*. 2009;206(8):1673-80.
247. van Liempt E, van Vliet SJ, Engering A, Vallejo JJG, Bank CM, Sanchez-Hernandez M, et al. *Schistosoma mansoni* soluble egg antigens are internalized by human dendritic cells through multiple C-type lectins and suppress TLR-induced dendritic cell activation. *Molecular immunology*. 2007;44(10):2605-15.
248. Steinfeld S, Andersen JF, Cannons JL, Feng CG, Joshi M, Dwyer D, et al. The major component in schistosome eggs responsible for conditioning dendritic cells for Th2 polarization is a T2 ribonuclease (omega-1). *The Journal of experimental medicine*. 2009;206(8):1681-90.
249. Abdulla M-H, Lim K-C, McKerrow JH, Caffrey CR. Proteomic identification of IPSE/alpha-1 as a major hepatotoxin secreted by *Schistosoma mansoni* eggs. *PLoS Negl Trop Dis*. 2011;5(10):e1368.
250. Schramm G, Mohrs K, Wodrich M, Doenhoff MJ, Pearce EJ, Haas H, et al. Cutting edge: IPSE/alpha-1, a glycoprotein from *Schistosoma mansoni* eggs, induces IgE-dependent, antigen-independent IL-4 production by murine basophils in vivo. *The Journal of Immunology*. 2007;178(10):6023-7.
251. Jang-Lee J, Curwen RS, Ashton PD, Tissot B, Mathieson W, Panico M, et al. Glycomics analysis of *Schistosoma mansoni* egg and cercarial secretions. *Molecular & Cellular Proteomics*. 2007;6(9):1485-99.

252. Paul WE, Zhu J. How are T(H)2-type immune responses initiated and amplified? *Nature reviews Immunology*. 2010;10(4):225-35.
253. Dewalick S, Bexkens ML, van Balkom BW, Wu YP, Smit CH, Hokke CH, et al. The proteome of the insoluble *Schistosoma mansoni* eggshell skeleton. *Int J Parasitol*. 2011;41(5):523-32.
254. Mayerhofer H, Schramm G, Hatzopoulos GN, Mueller-Dieckmann C, Haas H, Mueller-Dieckmann J. Cloning, expression, purification, crystallization and preliminary X-ray crystallographic analysis of interleukin-4-inducing principle from *Schistosoma mansoni* eggs (IPSE/alpha-1). *Acta Crystallographica Section F: Structural Biology and Crystallization Communications*. 2009;65(6):594-6.
255. Falcone FH, Dahinden CA, Gibbs BF, Noll T, Amon U, Hebestreit H, et al. Human basophils release interleukin-4 after stimulation with *Schistosoma mansoni* egg antigen. *European journal of immunology*. 1996;26(5):1147-55.
256. Borthwick L, Barron L, Hart K, Vannella K, Thompson R, Oland S, et al. Macrophages are critical to the maintenance of IL-13-dependent lung inflammation and fibrosis. *Mucosal immunology*. 2016;9(1):38-55.
257. Schramm G, Haas H, Falcone F, Gronow A. IMMUNOMODULATING AGENTS FROM PARASITIC WORMS AND METHOD FOR ISOLATION THEREOF. EP Patent 1,363,937; 2008.
258. De'Broski RH, Hölscher C, Mohrs M, Arendse B, Schwegmann A, Radwanska M, et al. Alternative macrophage activation is essential for survival during schistosomiasis and downmodulates T helper 1 responses and immunopathology. *Immunity*. 2004;20(5):623-35.
259. Hagen J, Scheerlinck J-PY, Young ND, Gasser RB, Kalinna BH. Chapter Three-Prospects for Vector-Based Gene Silencing to Explore Immunobiological Features of *Schistosoma mansoni*. *Advances in parasitology*. 2015;88:85-122.
260. Everts B, Perona-Wright G, Smits HH, Hokke CH, van der Ham AJ, Fitzsimmons CM, et al. Omega-1, a glycoprotein secreted by *Schistosoma mansoni* eggs, drives Th2 responses. *J Exp Med*. 2009;206(8):1673-80.
261. Mathieson W, Wilson RA. A comparative proteomic study of the undeveloped and developed *Schistosoma mansoni* egg and its contents: The miracidium, hatch fluid and secretions. *International journal for parasitology*. 2010;40(5):617-28.
262. Schramm G, Hamilton JV, Balog C, Wuhler M, Gronow A, Beckmann S, et al. Molecular characterisation of kappa-5, a major antigenic glycoprotein from *Schistosoma mansoni* eggs. *Molecular and biochemical parasitology*. 2009;166(1):4-14.
263. Larkin BM, Smith PM, Ponichtera HE, Shainheit MG, Rutitzky LI, Stadecker MJ, editors. Induction and regulation of pathogenic Th17 cell responses in schistosomiasis. *Seminars in immunopathology*; 2012: Springer.
264. Schramm G, Haas H. Th2 immune response against *Schistosoma mansoni* infection. *Microbes and Infection*. 2010;12(12):881-8.
265. Kaur I, Schramm G, Everts B, Scholzen T, Kindle KB, Beetz C, et al. Interleukin-4-inducing principle from *Schistosoma mansoni* eggs contains a functional C-terminal nuclear localization signal necessary for nuclear translocation in mammalian cells but not for its uptake. *Infection and immunity*. 2011;79(4):1779-88.

266. Rapoport TA, Jungnickel B, Kutay U. Protein transport across the eukaryotic endoplasmic reticulum and bacterial inner membranes. *Annual review of biochemistry*. 1996;65(1):271-303.
267. LaCasse EC, Lefebvre YA. Nuclear localization signals overlap DNA-or RNA-binding domains in nucleic acid-binding proteins. *Nucleic acids research*. 1995;23(10):1647.
268. Fotakis G, Timbrell JA. In vitro cytotoxicity assays: comparison of LDH, neutral red, MTT and protein assay in hepatoma cell lines following exposure to cadmium chloride. *Toxicology letters*. 2006;160(2):171-7.
269. Mosmann T. Rapid colorimetric assay for cellular growth and survival: application to proliferation and cytotoxicity assays. *Journal of immunological methods*. 1983;65(1-2):55-63.
270. Twentyman P, Luscombe M. A study of some variables in a tetrazolium dye (MTT) based assay for cell growth and chemosensitivity. *British journal of cancer*. 1987;56(3):279.
271. Decker T, Lohmann-Matthes M-L. A quick and simple method for the quantitation of lactate dehydrogenase release in measurements of cellular cytotoxicity and tumor necrosis factor (TNF) activity. *Journal of immunological methods*. 1988;115(1):61-9.
272. Braydich-Stolle L, Hussain S, Schlager JJ, Hofmann M-C. In vitro cytotoxicity of nanoparticles in mammalian germline stem cells. *Toxicological sciences*. 2005;88(2):412-9.
273. Borra RC, Lotufo MA, Gaglioti SM, Barros FdM, Andrade PM. A simple method to measure cell viability in proliferation and cytotoxicity assays. *Brazilian oral research*. 2009;23(3):255-62.
274. Moors M, Rockel TD, Abel J, Cline JE, Gassmann K, Schreiber T, et al. Human neurospheres as three-dimensional cellular systems for developmental neurotoxicity testing. *Environmental health perspectives*. 2009;117(7):1131.
275. Parham JH, Kost T, Hutchins JT. Effects of pCIneo and pCEP4 expression vectors on transient and stable protein production in human and simian cell lines. *Cytotechnology*. 2001;35(3):181-7.
276. Beetz C, Brodhun M, Moutzouris K, Kiehntopf M, Berndt A, Lehnert D, et al. Identification of nuclear localisation sequences in spastin (SPG4) using a novel Tetra-GFP reporter system. *Biochemical and biophysical research communications*. 2004;318(4):1079-84.
277. Hidalgo IJ, Raub TJ, Borchardt RT. Characterization of the human colon carcinoma cell line (Caco-2) as a model system for intestinal epithelial permeability. *Gastroenterology*. 1989;96(3):736-49.
278. Grainger CI, Greenwell LL, Lockley DJ, Martin GP, Forbes B. Culture of Calu-3 cells at the air interface provides a representative model of the airway epithelial barrier. *Pharmaceutical research*. 2006;23(7):1482-90.
279. Villasaliu D, Falcone FH, Stolnik S, Garnett M. Basement membrane influences intestinal epithelial cell growth and presents a barrier to the movement of macromolecules. *Experimental cell research*. 2014;323(1):218-31.
280. Kalderon D, Roberts BL, Richardson WD, Smith AE. A short amino acid sequence able to specify nuclear location. *Cell*. 1984;39(3):499-509.

281. Hames B, Hooper N, Houghton J. Instant notes in biochemistry. Biochemical Education. 1997;25:4.
282. Ba ANN, Pogoutse A, Provart N, Moses AM. NLStradamus: a simple Hidden Markov Model for nuclear localization signal prediction. BMC bioinformatics. 2009;10(1):1.
283. King BR, Guda C. ngLOC: an n-gram-based Bayesian method for estimating the subcellular proteomes of eukaryotes. Genome biology. 2007;8(5):1.
284. Briesemeister S, Rahnenführer J, Kohlbacher O. YLoc—an interpretable web server for predicting subcellular localization. Nucleic acids research. 2010;38(suppl 2):W497-W502.
285. Nakai K, Horton P. PSORT: a program for detecting sorting signals in proteins and predicting their subcellular localization. Trends in biochemical sciences. 1999;24(1):34-5.
286. Brameier M, Krings A, MacCallum RM. NucPred—predicting nuclear localization of proteins. Bioinformatics. 2007;23(9):1159-60.
287. Bhasin M, Raghava G. ESLpred: SVM-based method for subcellular localization of eukaryotic proteins using dipeptide composition and PSI-BLAST. Nucleic acids research. 2004;32(suppl 2):W414-W9.
288. Petersen TN, Brunak S, von Heijne G, Nielsen H. SignalP 4.0: discriminating signal peptides from transmembrane regions. Nature methods. 2011;8(10):785-6.
289. Bendtsen JD, Nielsen H, von Heijne G, Brunak S. Improved prediction of signal peptides: SignalP 3.0. Journal of molecular biology. 2004;340(4):783-95.
290. Lin J-r, Hu J. SeqNLS: nuclear localization signal prediction based on frequent pattern mining and linear motif scoring. PloS one. 2013;8(10):e76864.
291. Kaur I. Nuclear translocation and Transferrin–Transferrin receptor interaction of IPSE/ α -1, a secretory glycoprotein from *Schistosoma mansoni*. UK: The University of Nottingham; 2009.
292. Brar SS, Watson M, Diaz M. Activation-induced cytosine deaminase (AID) is actively exported out of the nucleus but retained by the induction of DNA breaks. Journal of Biological Chemistry. 2004;279(25):26395-401.
293. Heddad A, Brameier M, MacCallum RM, editors. Evolving regular expression-based sequence classifiers for protein nuclear localisation. Workshops on Applications of Evolutionary Computation; 2004: Springer.
294. Bendtsen JD, Jensen LJ, Blom N, Von Heijne G, Brunak S. Feature-based prediction of non-classical and leaderless protein secretion. Protein Engineering Design and Selection. 2004;17(4):349-56.
295. Ba ANN, Pogoutse A, Provart N, Moses AM. NLStradamus: a simple Hidden Markov Model for nuclear localization signal prediction. BMC bioinformatics. 2009;10(1):202.
296. King BR, Guda C. ngLOC: an n-gram-based Bayesian method for estimating the subcellular proteomes of eukaryotes. Genome biology. 2007;8(5):R68.
297. Robinson MW, Menon R, Donnelly SM, Dalton JP, Ranganathan S. An Integrated Transcriptomics and Proteomics Analysis of the Secretome of the Helminth Pathogen *Fasciola hepatica* Proteins associated with invasion and infection of the mammalian host. Molecular & Cellular Proteomics. 2009;8(8):1891-907.

298. De la Torre Escudero E, Manzano-Román R, Valero L, Oleaga A, Pérez-Sánchez R, Hernández-González A, et al. Comparative proteomic analysis of *Fasciola hepatica* juveniles and *Schistosoma bovis* schistosomula. *Journal of proteomics*. 2011;74(9):1534-44.
299. Gardella S, Andrei C, Ferrera D, Lotti LV, Torrisi MR, Bianchi ME, et al. The nuclear protein HMGB1 is secreted by monocytes via a non-classical, vesicle-mediated secretory pathway. *EMBO reports*. 2002;3(10):995-1001.
300. Baake M, Bäuerle M, Doenecke D, Albig W. Core histones and linker histones are imported into the nucleus by different pathways. *European journal of cell biology*. 2001;80(11):669-77.
301. Hage N, Renshaw JG, Winkler GS, Gellert P, Stolnik S, Falcone FH. Improved expression and purification of the *Helicobacter pylori* adhesin BabA through the incorporation of a hexa-lysine tag. *Protein expression and purification*. 2015;106:25-30.
302. Geisse S, Henke M. Large-scale transient transfection of mammalian cells: a newly emerging attractive option for recombinant protein production. *Journal of structural and functional genomics*. 2005;6(2-3):165-70.
303. Meyer S, Lorenz C, Baser B, Wördehoff M, Jäger V, van den Heuvel J. Multi-host expression system for recombinant production of challenging proteins. *PloS one*. 2013;8(7):e68674.
304. Baldi L, Hacker DL, Adam M, Wurm FM. Recombinant protein production by large-scale transient gene expression in mammalian cells: state of the art and future perspectives. *Biotechnology letters*. 2007;29(5):677-84.
305. Geisse S. Reflections on more than 10 years of TGE approaches. *Protein expression and purification*. 2009;64(2):99-107.
306. Pham PL, Kamen A, Durocher Y. Large-scale transfection of mammalian cells for the fast production of recombinant protein. *Molecular biotechnology*. 2006;34(2):225-37.
307. Ehrhardt C, Schmolke M, Matzke A, Knoblauch A, Will C, Wixler V, et al. Polyethylenimine, a cost-effective transfection reagent. *Signal Transduction*. 2006;6(3):179-84.
308. Forrest ML, Koerber JT, Pack DW. A degradable polyethylenimine derivative with low toxicity for highly efficient gene delivery. *Bioconjugate chemistry*. 2003;14(5):934-40.
309. Raymond C, Tom R, Perret S, Moussouami P, L'Abbé D, St-Laurent G, et al. A simplified polyethylenimine-mediated transfection process for large-scale and high-throughput applications. *Methods*. 2011;55(1):44-51.
310. Doenhoff M, Pearson S, Dunne D, Bickle Q, Lucas S, Bain J, et al. Immunological control of hepatotoxicity and parasite egg excretion in *Schistosoma mansoni* infections: stage specificity of the reactivity of immune serum in T-cell deprived mice. *Transactions of the Royal Society of Tropical Medicine and Hygiene*. 1981;75(1):41-53.
311. Hernandez-Gonzalez A, Valero M, del Pino MS, Oleaga A, Siles-Lucas M. Proteomic analysis of in vitro newly excysted juveniles from *Fasciola hepatica*. *Molecular and biochemical parasitology*. 2010;172(2):121-8.
312. De Marco A. Strategies for successful recombinant expression of disulfide bond-dependent proteins in *Escherichia coli*. *Microbial cell factories*. 2009;8(1):1.

313. Clark EDB. Protein refolding for industrial processes. *Current Opinion in Biotechnology*. 2001;12(2):202-7.
314. Kost TA, Condreay JP, Jarvis DL. Baculovirus as versatile vectors for protein expression in insect and mammalian cells. *Nature biotechnology*. 2005;23(5):567-75.
315. Durocher Y, Perret S, Kamen A. High-level and high-throughput recombinant protein production by transient transfection of suspension-growing human 293-EBNA1 cells. *Nucleic acids research*. 2002;30(2):e9-e.
316. Hokke CH, Deelder AM. Schistosome glycoconjugates in host-parasite interplay. *Glycoconjugate journal*. 2001;18(8):573-87.
317. Morgan JA, DeJong RJ, Kazibwe F, Mkoji GM, Loker ES. A newly-identified lineage of *Schistosoma*. *International Journal for Parasitology*. 2003;33(9):977-85.
318. Rabinovich GA, Conejo-García JR. Shaping the Immune Landscape in Cancer by Galectin-Driven Regulatory Pathways. *Journal of molecular biology*. 2016.
319. Olaya-Abril A, Jiménez-Munguía I, Gómez-Gascón L, Rodríguez-Ortega MJ. Surfomics: shaving live organisms for a fast proteomic identification of surface proteins. *Journal of proteomics*. 2014;97:164-76.
320. Huang W-L, Liaw C, Ho S-Y, editors. Predicting non-classical secretory proteins by using Gene Ontology terms and physicochemical properties. *Computer Science and Automation Engineering (CSAE), 2011 IEEE International Conference on*; 2011: IEEE.
321. Fliieger O, Engling A, Bucala R, Lue H, Nickel W, Bernhagen J. Regulated secretion of macrophage migration inhibitory factor is mediated by a non-classical pathway involving an ABC transporter. *FEBS letters*. 2003;551(1-3):78-86.
322. Blobel G. Protein targeting (Nobel lecture). *Chembiochem*. 2000;1(2):86-102.
323. Kiefer P, Acland P, Pappin D, Peters G, Dickson C. Competition between nuclear localization and secretory signals determines the subcellular fate of a single CUG-initiated form of FGF3. *The EMBO journal*. 1994;13(17):4126.
324. Amaya Y, Nakai T, Komaru K, Tsuneki M, Miura S. Cleavage of the ER-targeting signal sequence of parathyroid hormone-related protein is cell-type-specific and regulated in cis by its nuclear localization signal. *Journal of biochemistry*. 2008;143(4):569-79.
325. Lecellier C-H, Vermeulen W, Bachelier F, Giron M-L, Saïb A. Intra- and intercellular trafficking of the foamy virus auxiliary bet protein. *Journal of virology*. 2002;76(7):3388-94.
326. Nagase H, Suzuki K, Morodomi T, Enghild J, Salvesen G. Activation mechanisms of the precursors of matrix metalloproteinases 1, 2 and 3. *Matrix (Stuttgart, Germany) Supplement*. 1991;1:237-44.
327. Si-Tayeb K, Monvoisin A, Mazzocco C, Lepreux S, Decossas M, Cubel G, et al. Matrix metalloproteinase 3 is present in the cell nucleus and is involved in apoptosis. *The American journal of pathology*. 2006;169(4):1390-401.
328. Ribbeck K, Görlich D. Kinetic analysis of translocation through nuclear pore complexes. *The EMBO journal*. 2001;20(6):1320-30.
329. Aaronson RP, Blobel G. Isolation of nuclear pore complexes in association with a lamina. *Proceedings of the National Academy of Sciences*. 1975;72(3):1007-11.
330. Patel SS, Belmont BJ, Sante JM, Rexach MF. Natively unfolded nucleoporins gate protein diffusion across the nuclear pore complex. *Cell*. 2007;129(1):83-96.

331. Pante N, Aebi U. Sequential binding of import ligands to distinct nucleopore regions during their nuclear import. *Science*. 1996;273(5282):1729.
332. Melchior F, Gerace L. Mechanisms of nuclear protein import. *Current opinion in cell biology*. 1995;7(3):310-8.
333. Nigg EA. Nucleocytoplasmic transport: signals, mechanisms and regulation. 1997.
334. Fontes MR, Teh T, Kobe B. Structural basis of recognition of monopartite and bipartite nuclear localization sequences by mammalian importin- α . *Journal of molecular biology*. 2000;297(5):1183-94.
335. Melén K, Fagerlund R, Franke J, Köhler M, Kinnunen L, Julkunen I. Importin α nuclear localization signal binding sites for STAT1, STAT2, and influenza A virus nucleoprotein. *Journal of Biological Chemistry*. 2003;278(30):28193-200.
336. Zilman A, Di Talia S, Chait BT, Rout MP, Magnasco MO. Efficiency, selectivity, and robustness of nucleocytoplasmic transport. *PLoS computational biology*. 2007;3(7):e125.
337. Lott K, Cingolani G. The importin β binding domain as a master regulator of nucleocytoplasmic transport. *Biochimica et Biophysica Acta (BBA)-Molecular Cell Research*. 2011;1813(9):1578-92.
338. Lange A, Mills RE, Lange CJ, Stewart M, Devine SE, Corbett AH. Classical nuclear localization signals: definition, function, and interaction with importin α . *Journal of Biological Chemistry*. 2007;282(8):5101-5.
339. Kutay U, Izaurralde E, Bischoff FR, Mattaj IW, Görlich D. Dominant-negative mutants of importin- β block multiple pathways of import and export through the nuclear pore complex. *The EMBO journal*. 1997;16(6):1153-63.
340. Palmeri D, Malim MH. Importin β can mediate the nuclear import of an arginine-rich nuclear localization signal in the absence of importin α . *Molecular and Cellular Biology*. 1999;19(2):1218-25.
341. Bayliss R, Littlewood T, Stewart M. Structural basis for the interaction between FxFG nucleoporin repeats and importin- β in nuclear trafficking. *Cell*. 2000;102(1):99-108.
342. Nachury MV, Maresca TJ, Salmon WC, Waterman-Storer CM, Heald R, Weis K. Importin β is a mitotic target of the small GTPase Ran in spindle assembly. *Cell*. 2001;104(1):95-106.
343. van der Watt PJ, Chi A, Stelma T, Stowell C, Strydom E, Carden S, et al. Targeting the Nuclear Import Receptor Kpn β 1 as an Anticancer Therapeutic. *Molecular cancer therapeutics*. 2016;15(4):560-73.
344. Fischer U, Huber J, Boelens WC, Mattajt LW, Lührmann R. The HIV-1 Rev activation domain is a nuclear export signal that accesses an export pathway used by specific cellular RNAs. *Cell*. 1995;82(3):475-83.
345. Fukuda M, Asano S, Nakamura T, Adachi M, Yoshida M, Yanagida M, et al. CRM1 is responsible for intracellular transport mediated by the nuclear export signal. *Nature*. 1997;390(6657):308-11.
346. Kudo N, Matsumori N, Taoka H, Fujiwara D, Schreiner EP, Wolff B, et al. Leptomycin B inactivates CRM1/exportin 1 by covalent modification at a cysteine residue in the central conserved region. *Proceedings of the National Academy of Sciences*. 1999;96(16):9112-7.

347. Lischka P, Rosorius O, Trommer E, Stamminger T. A novel transferable nuclear export signal mediates CRM1-independent nucleocytoplasmic shuttling of the human cytomegalovirus transactivator protein pUL69. *The EMBO Journal*. 2001;20(24):7271-83.
348. Pollard VW, Michael WM, Nakielny S, Siomi MC, Wang F, Dreyfuss G. A novel receptor-mediated nuclear protein import pathway. *Cell*. 1996;86(6):985-94.
349. Bear J, Tan W, Zolotukhin AS, Taberner C, Hudson EA, Felber BK. Identification of novel import and export signals of human TAP, the protein that binds to the constitutive transport element of the type D retrovirus mRNAs. *Molecular and Cellular Biology*. 1999;19(9):6306-17.
350. Pemberton LF, Paschal BM. Mechanisms of receptor-mediated nuclear import and nuclear export. *Traffic*. 2005;6(3):187-98.
351. Soniat M, Chook YM. Nuclear localization signals for four distinct karyopherin- β nuclear import systems. *Biochemical Journal*. 2015;468(3):353-62.
352. Mosammamaparast N, Jackson KR, Guo Y, Brame CJ, Shabanowitz J, Hunt DF, et al. Nuclear import of histone H2A and H2B is mediated by a network of karyopherins. *The Journal of cell biology*. 2001;153(2):251-62.
353. Singh R, Kumar D, Duncan RC, Nakhasi HL, Salotra P. Overexpression of histone H2A modulates drug susceptibility in *Leishmania* parasites. *International journal of antimicrobial agents*. 2010;36(1):50-7.
354. Baake M, Doenecke D, Albig W. Characterisation of nuclear localisation signals of the four human core histones. *Journal of cellular biochemistry*. 2001;81(2):333-46.
355. Carrión J, Folgueira C, Alonso C. Transitory or long-lasting immunity to *Leishmania* major infection: the result of immunogenicity and multicomponent properties of histone DNA vaccines. *Vaccine*. 2008;26(9):1155-65.
356. Goya RG, Castro MG, Saphier PW, Sosa YE, Lowry PJ. Thymus—Pituitary Interactions During Ageing. *Age and ageing*. 1993;22(suppl 1):S19-S25.
357. Brown O, Sosa Y, Goya R. Histones and related nuclear preparations stimulate prolactin release in vitro. *Medical science research*. 1993;21(21):799-800.
358. Xu J, Zhang X, Pelayo R, Monestier M, Ammollo CT, Semeraro F, et al. Extracellular histones are major mediators of death in sepsis. *Nature medicine*. 2009;15(11):1318-21.
359. Cutress ML, Whitaker HC, Mills IG, Stewart M, Neal DE. Structural basis for the nuclear import of the human androgen receptor. *Journal of cell science*. 2008;121(7):957-68.
360. Conti E, Uy M, Leighton L, Blobel G, Kuriyan J. Crystallographic analysis of the recognition of a nuclear localization signal by the nuclear import factor karyopherin α . *Cell*. 1998;94(2):193-204.
361. Chaudhary SC, Cho M-G, Nguyen TT, Park K-S, Kwon M-H, Lee J-H. A putative pH-dependent nuclear localization signal in the juxtamembrane region of c-Met. *Experimental & molecular medicine*. 2014;46(10):e119.
362. Kalderon D, Richardson WD, Markham AF, Smith AE. Sequence requirements for nuclear location of simian virus 40 large-T antigen. *Nature*. 1983;311(5981):33-8.
363. Hicks GR, Raikhel NV. Protein import into the nucleus: an integrated view. *Annual review of cell and developmental biology*. 1995;11(1):155-88.

364. Weis K, Ryder U, Lamond AI. The conserved amino-terminal domain of hSRP1 alpha is essential for nuclear protein import. *The EMBO journal*. 1996;15(8):1818.
365. Moroianu J, Hijikata M, Blobel G, Radu A. Mammalian karyopherin alpha 1 beta and alpha 2 beta heterodimers: alpha 1 or alpha 2 subunit binds nuclear localization signal and beta subunit interacts with peptide repeat-containing nucleoporins. *Proceedings of the National Academy of Sciences*. 1995;92(14):6532-6.
366. Mishra A, Krishnan B, Srivastava SS, Sharma Y. Microbial $\beta\gamma$ -crystallins. *Progress in biophysics and molecular biology*. 2014;115(1):42-51.
367. Bonifaci N, Moroianu J, Radu A, Blobel G. Karyopherin $\beta 2$ mediates nuclear import of a mRNA binding protein. *Proceedings of the National Academy of Sciences*. 1997;94(10):5055-60.
368. Malek S, Huxford T, Ghosh G. I κ B α functions through direct contacts with the nuclear localization signals and the DNA binding sequences of NF- κ B. *Journal of Biological Chemistry*. 1998;273(39):25427-35.
369. Everts B, Smits HH, Hokke CH, Yazdanbakhsh M. Helminths and dendritic cells: sensing and regulating via pattern recognition receptors, Th2 and Treg responses. *European journal of immunology*. 2010;40(6):1525-37.
370. Geijtenbeek TB, Gringhuis SI. Signalling through C-type lectin receptors: shaping immune responses. *Nature Reviews Immunology*. 2009;9(7):465-79.
371. Meevissen MH, Yazdanbakhsh M, Hokke CH. Partly based on: Schistosoma mansoni egg glycoproteins and C-type lectins of host immune cells: Molecular partners that shape immune responses. *Schistosoma mansoni egg glycoproteins: glycan structures & host immune responses*. 2012:7.
372. van Vliet SJ, van Liempt E, Saeland E, Aarnoudse CA, Appelmelk B, Irimura T, et al. Carbohydrate profiling reveals a distinctive role for the C-type lectin MGL in the recognition of helminth parasites and tumor antigens by dendritic cells. *International immunology*. 2005;17(5):661-9.
373. Everts B, Husaarts L, Driessen NN, Meevissen MH, Schramm G, van der Ham AJ, et al. Schistosome-derived omega-1 drives Th2 polarization by suppressing protein synthesis following internalization by the mannose receptor. *The Journal of experimental medicine*. 2012;209(10):1753-67.
374. Turner JR. Intestinal mucosal barrier function in health and disease. *Nature Reviews Immunology*. 2009;9(11):799-809.
375. Neutra MR, Pringault E, Kraehenbuhl J-P. Antigen sampling across epithelial barriers and induction of mucosal immune responses. *Annual review of immunology*. 1996;14(1):275-300.
376. Cu Y, Saltzman WM. Stealth particles give mucus the slip. *Nature materials*. 2009;8(1):11.
377. Saltzman WM, Radomsky ML, Whaley KJ, Cone RA. Antibody diffusion in human cervical mucus. *Biophysical journal*. 1994;66(2 Pt 1):508.
378. Radomsky ML, Whaley KJ, Cone RA, Saltzman WM. Macromolecules released from polymers: diffusion into unstirred fluids. *Biomaterials*. 1990;11(9):619-24.
379. Mostov K, Su T, ter Beest M. Polarized epithelial membrane traffic: conservation and plasticity. *Nature Cell Biology*. 2003;5(4):287-93.

380. Artursson P, Palm K, Luthman K. Caco-2 monolayers in experimental and theoretical predictions of drug transport. *Advanced drug delivery reviews*. 2001;46(1):27-43.
381. Egan WJ, Lauri G. Prediction of intestinal permeability. *Advanced drug delivery reviews*. 2002;54(3):273-89.
382. Itoh M, Furuse M, Morita K, Kubota K, Saitou M, Tsukita S. Direct binding of three tight junction-associated MAGUKs, ZO-1, ZO-2, and ZO-3, with the COOH termini of claudins. *The Journal of cell biology*. 1999;147(6):1351-63.
383. Siccardi D, Turner JR, Mrsny RJ. Regulation of intestinal epithelial function: a link between opportunities for macromolecular drug delivery and inflammatory bowel disease. *Advanced drug delivery reviews*. 2005;57(2):219-35.
384. Lapiere LA. The molecular structure of the tight junction. *Advanced drug delivery reviews*. 2000;41(3):255-64.
385. Sawada N, Murata M, Kikuchi K, Osanai M, Tobioka H, Kojima T, et al. Tight junctions and human diseases. *Medical Electron Microscopy*. 2003;36(3):147-56.
386. Schneeberger EE, Lynch RD. The tight junction: a multifunctional complex. *American Journal of Physiology-Cell Physiology*. 2004;286(6):C1213-C28.
387. Walsh T, Pierce SB, Lenz DR, Brownstein Z, Dagan-Rosenfeld O, Shahin H, et al. Genomic duplication and overexpression of TJP2/ZO-2 leads to altered expression of apoptosis genes in progressive nonsyndromic hearing loss DFNA51. *The American Journal of Human Genetics*. 2010;87(1):101-9.
388. Fanning AS, Jameson BJ, Jesaitis LA, Anderson JM. The tight junction protein ZO-1 establishes a link between the transmembrane protein occludin and the actin cytoskeleton. *Journal of Biological Chemistry*. 1998;273(45):29745-53.
389. Madara JL, Moore R, Carlson S. Alteration of intestinal tight junction structure and permeability by cytoskeletal contraction. *American Journal of Physiology-Cell Physiology*. 1987;253(6):C854-C61.
390. Walsh SV, Hopkins AM, Chen J, Narumiya S, Parkos CA, Nusrat A. Rho kinase regulates tight junction function and is necessary for tight junction assembly in polarized intestinal epithelia. *Gastroenterology*. 2001;121(3):566-79.
391. Turner JR, Rill BK, Carlson SL, Carnes D, Kerner R, Mrsny RJ, et al. Physiological regulation of epithelial tight junctions is associated with myosin light-chain phosphorylation. *American Journal of Physiology-Cell Physiology*. 1997;273(4):C1378-C85.
392. Ivanov AI, Parkos CA, Nusrat A. Cytoskeletal regulation of epithelial barrier function during inflammation. *The American journal of pathology*. 2010;177(2):512-24.
393. Stevenson BR, Keon BH. The tight junction: morphology to molecules. *Annual review of cell and developmental biology*. 1998;14(1):89-109.
394. Tsukita S, Furuse M, Itoh M. Multifunctional strands in tight junctions. *Nature reviews Molecular cell biology*. 2001;2(4):285-93.
395. Salama NN, Eddington ND, Fasano A. Tight junction modulation and its relationship to drug delivery. *Advanced drug delivery reviews*. 2006;58(1):15-28.
396. Linnankoski J, Mäkelä J, Palmgren J, Mauriala T, Vedin C, Ungell AL, et al. Paracellular porosity and pore size of the human intestinal epithelium in tissue and cell culture models. *Journal of pharmaceutical sciences*. 2010;99(4):2166-75.

397. Gonzalez-Mariscal L, Betanzos A, Nava P, Jaramillo B. Tight junction proteins. *Progress in biophysics and molecular biology*. 2003;81(1):1-44.
398. Fanning AS, Ma TY, Anderson JM. Isolation and functional characterization of the actin binding region in the tight junction protein ZO-1. *The FASEB Journal*. 2002;16(13):1835-7.
399. Lee SH. Intestinal permeability regulation by tight junction: implication on inflammatory bowel diseases. *Intestinal research*. 2015;13(1):11-8.
400. Suzuki T. Regulation of intestinal epithelial permeability by tight junctions. *Cellular and molecular life sciences*. 2013;70(4):631-59.
401. Furuse M, Hirase T, Itoh M, Nagafuchi A, Yonemura S, Tsukita S. Occludin: a novel integral membrane protein localizing at tight junctions. *The Journal of cell biology*. 1993;123(6):1777-88.
402. Furuse M, Itoh M, Hirase T, Nagafuchi A, Yonemura S, Tsukita S. Direct association of occludin with ZO-1 and its possible involvement in the localization of occludin at tight junctions. *The Journal of cell biology*. 1994;127(6):1617-26.
403. Al-Sadi R, Khatib K, Guo S, Ye D, Youssef M, Ma T. Occludin regulates macromolecule flux across the intestinal epithelial tight junction barrier. *American Journal of Physiology-Gastrointestinal and Liver Physiology*. 2011;300(6):G1054-G64.
404. Wong V, Gumbiner BM. A synthetic peptide corresponding to the extracellular domain of occludin perturbs the tight junction permeability barrier. *The Journal of cell biology*. 1997;136(2):399-409.
405. Furuse M, Fujita K, Hiiragi T, Fujimoto K, Tsukita S. Claudin-1 and-2: novel integral membrane proteins localizing at tight junctions with no sequence similarity to occludin. *The Journal of cell biology*. 1998;141(7):1539-50.
406. Van Itallie CM, Anderson JM. Claudins and epithelial paracellular transport. *Annu Rev Physiol*. 2006;68:403-29.
407. Tsukita S, Furuse M. Pores in the wall claudins constitute tight junction strands containing aqueous pores. *The Journal of cell biology*. 2000;149(1):13-6.
408. Tamura A, Hayashi H, Imasato M, Yamazaki Y, Hagiwara A, Wada M, et al. Loss of claudin-15, but not claudin-2, causes Na⁺ deficiency and glucose malabsorption in mouse small intestine. *Gastroenterology*. 2011;140(3):913-23.
409. Cunningham SA, Arrate MP, Rodriguez JM, Bjercke RJ, Vanderslice P, Morris AP, et al. A Novel Protein with Homology to the Junctional Adhesion Molecule CHARACTERIZATION OF LEUKOCYTE INTERACTIONS. *Journal of Biological Chemistry*. 2000;275(44):34750-6.
410. Chen X, Macara IG. Par-3 controls tight junction assembly through the Rac exchange factor Tiam1. *Nature cell biology*. 2005;7(3):262-9.
411. Coombe DR. Biological implications of glycosaminoglycan interactions with haemopoietic cytokines. *Immunology and cell biology*. 2008;86(7):598-607.
412. Thippawong J. Inhaled cytokines and cytokine antagonists. *Advanced drug delivery reviews*. 2006;58(9):1089-105.
413. Boyaka PN, McGhee JR. Cytokines as adjuvants for the induction of mucosal immunity. *Advanced drug delivery reviews*. 2001;51(1):71-9.
414. Farhadi A, Banan A, Fields J, Keshavarzian A. Intestinal barrier: an interface between health and disease. *Journal of gastroenterology and hepatology*. 2003;18(5):479-97.

415. Kagnoff MF. The intestinal epithelium is an integral component of a communications network. *The Journal of clinical investigation*. 2014;124(7):2841-3.
416. Onyiah JC, Colgan SP. Cytokine responses and epithelial function in the intestinal mucosa. *Cellular and Molecular Life Sciences*. 2016:1-10.
417. Haller D, Bode C, Hammes W, Pfeifer A, Schiffrin E, Blum S. Non-pathogenic bacteria elicit a differential cytokine response by intestinal epithelial cell/leucocyte co-cultures. *Gut*. 2000;47(1):79-87.
418. Vallee S, Laforest S, Fouchier F, Montero MP, Penel C, Champion S. Cytokine-induced upregulation of NF- κ B, IL-8, and ICAM-1 is dependent on colonic cell polarity: implication for PKC δ . *Experimental cell research*. 2004;297(1):165-85.
419. Grivennikov S, Karin E, Terzic J, Mucida D, Yu G-Y, Vallabhapurapu S, et al. IL-6 and Stat3 are required for survival of intestinal epithelial cells and development of colitis-associated cancer. *Cancer cell*. 2009;15(2):103-13.
420. Kuhn KA, Manieri NA, Liu T-C, Stappenbeck TS. IL-6 stimulates intestinal epithelial proliferation and repair after injury. *PloS one*. 2014;9(12):e114195.
421. Eckmann L, Kagnoff M, Fierer J. Epithelial cells secrete the chemokine interleukin-8 in response to bacterial entry. *Infection and immunity*. 1993;61(11):4569-74.
422. Reinecker H-C, Loh EY, Ringler DJ, Mehta A, Rombeau JL, MacDermott RP. Monocyte-chemoattractant protein 1 gene expression in intestinal epithelial cells and inflammatory bowel disease mucosa. *Gastroenterology*. 1995;108(1):40-50.
423. Stadnyk AW. Intestinal epithelial cells as a source of inflammatory cytokines and chemokines. *Canadian Journal of Gastroenterology and Hepatology*. 2002;16(4):241-6.
424. Sierro F, Dubois B, Coste A, Kaiserlian D, Kraehenbuhl J-P, Sirard J-C. Flagellin stimulation of intestinal epithelial cells triggers CCL20-mediated migration of dendritic cells. *Proceedings of the National Academy of Sciences*. 2001;98(24):13722-7.
425. Colgan SP, Hershberg RM, Furuta GT, Blumberg RS. Ligation of intestinal epithelial CD1d induces bioactive IL-10: critical role of the cytoplasmic tail in autocrine signaling. *Proceedings of the National Academy of Sciences*. 1999;96(24):13938-43.
426. Liang SC, Tan X-Y, Luxenberg DP, Karim R, Dunussi-Joannopoulos K, Collins M, et al. Interleukin (IL)-22 and IL-17 are coexpressed by Th17 cells and cooperatively enhance expression of antimicrobial peptides. *The Journal of experimental medicine*. 2006;203(10):2271-9.
427. Cella M, Fuchs A, Vermi W, Facchetti F, Otero K, Lennerz JK, et al. A human natural killer cell subset provides an innate source of IL-22 for mucosal immunity. *Nature*. 2009;457(7230):722-5.
428. Dinarello CA. Proinflammatory cytokines. *Chest Journal*. 2000;118(2):503-8.
429. Strid J, McLean WI, Irvine AD. Too Much, Too Little or Just Enough: A Goldilocks Effect for IL-13 and Skin Barrier Regulation? *Journal of Investigative Dermatology*. 2016;136(3):561-4.
430. SCHULZKE JD, Bojarski C, Zeissig S, Heller F, Gitter AH, Fromm M. Disrupted barrier function through epithelial cell apoptosis. *Annals of the New York Academy of Sciences*. 2006;1072(1):288-99.
431. Petersen AMW, Pedersen BK. The anti-inflammatory effect of exercise. *Journal of applied physiology*. 2005;98(4):1154-62.

432. Capaldo CT, Nusrat A. Cytokine regulation of tight junctions. *Biochimica et Biophysica Acta (BBA)-Biomembranes*. 2009;1788(4):864-71.
433. Holgate ST. Epithelium dysfunction in asthma. *Journal of Allergy and Clinical Immunology*. 2007;120(6):1233-44.
434. Swindle EJ, Collins JE, Davies DE. Breakdown in epithelial barrier function in patients with asthma: identification of novel therapeutic approaches. *Journal of Allergy and Clinical Immunology*. 2009;124(1):23-34.
435. McKay D, Baird A. Cytokine regulation of epithelial permeability and ion transport. *Gut*. 1999;44(2):283-9.
436. Luttmann W, Matthiesen T, Matthys H, Virchow Jr JC. Synergistic effects of interleukin-4 or interleukin-13 and tumor necrosis factor- α on eosinophil activation in vitro. *American journal of respiratory cell and molecular biology*. 1999;20(3):474-80.
437. Colgan SP, Resnick MB, Parkos CA, Delp-Archer C, McGuirk D, Bacarra AE, et al. IL-4 directly modulates function of a model human intestinal epithelium. *The Journal of immunology*. 1994;153(5):2122-9.
438. Holgate ST. Pathophysiology of asthma: what has our current understanding taught us about new therapeutic approaches? *Journal of Allergy and Clinical Immunology*. 2011;128(3):495-505.
439. Gauchat JF, Schlagenhaut E, Feng NP, Moser R, Yamage M, Jeannin P, et al. A novel 4-kb interleukin-13 receptor α mRNA expressed in human B, T, and endothelial cells encoding an alternate type-II interleukin-4/interleukin-13 receptor. *European journal of immunology*. 1997;27(4):971-8.
440. Miloux B, Laurent P, Bonnin O, Lupker J, Caput D, Vita N, et al. Cloning of the human IL-13R α 1 chain and reconstitution with the IL-4R α of a functional IL-4/IL-13 receptor complex. *FEBS letters*. 1997;401(2-3):163-6.
441. Rychter JW, Van Nassauw L, Brown J, Van Marck E, Knight PA, Miller HR, et al. Impairment of intestinal barrier and secretory function as well as egg excretion during intestinal schistosomiasis occur independently of mouse mast cell protease-1. *Parasite immunology*. 2010;32(4):221-31.
442. Moelants EA, Mortier A, Van Damme J, Proost P. Regulation of TNF- α with a focus on rheumatoid arthritis. *Immunology and cell biology*. 2013;91(6):393-401.
443. Walsh SV, Hopkins AM, Nusrat A. Modulation of tight junction structure and function by cytokines. *Advanced drug delivery reviews*. 2000;41(3):303-13.
444. Hart PH. Regulation of the inflammatory response in asthma by mast cell products. *Immunology and Cell Biology*. 2001;79(2):149-53.
445. Buttner C, Skupin A, Reimann T, Rieber EP, Unteregger G, Geyer P, et al. Local production of interleukin-4 during radiation-induced pneumonitis and pulmonary fibrosis in rats: macrophages as a prominent source of interleukin-4. *American journal of respiratory cell and molecular biology*. 1997;17(3):315-25.
446. Bui CT, Shollenberger LM, Paterson Y, Harn DA. *Schistosoma mansoni* soluble egg antigens enhance *Listeria monocytogenes* vector HIV-1 vaccine induction of cytotoxic T cells. *Clinical and Vaccine Immunology*. 2014;21(9):1232-9.
447. Amiri P, Locksley RM, Parslow TG, Sadick M, Rector E, Ritter D, et al. Tumor necrosis factor α restores granulomas and induces parasite egg-laying in schistosome-infected SCID mice. 1992.

448. Joseph AL, Boros DL. Tumor necrosis factor plays a role in *Schistosoma mansoni* egg-induced granulomatous inflammation. *The Journal of Immunology*. 1993;151(10):5461-71.
449. Merker HJ. Morphology of the basement membrane. *Microscopy research and technique*. 1994;28(2):95-124.
450. Basson MD, Turowski G, Emenaker NJ. Regulation of human (Caco-2) intestinal epithelial cell differentiation by extracellular matrix proteins. *Experimental cell research*. 1996;225(2):301-5.
451. Sanderson IR, Ezzell RM, Kedinger M, Erlanger M, Xu Z-X, Pringault E, et al. Human fetal enterocytes in vitro: modulation of the phenotype by extracellular matrix. *Proceedings of the National Academy of Sciences*. 1996;93(15):7717-22.
452. Falcone FH, Haas H, Gibbs BF. The human basophil: a new appreciation of its role in immune responses. *Blood*. 2000;96(13):4028-38.
453. Gould HJ, Sutton BJ, Beavil AJ, Beavil RL, McCloskey N, Coker HA, et al. The biology of IGE and the basis of allergic disease. *Annual review of immunology*. 2003;21(1):579-628.
454. Kinet J-P. The high-affinity IgE receptor (FcεRI): from physiology to pathology. *Annual review of immunology*. 1999;17(1):931-72.
455. Miller L, Blank U, Metzger H, Kinet J-P. Expression of high-affinity binding of human immunoglobulin E by transfected cells. *Science*. 1989;244(4902):334-7.
456. Falcone FH, Alcocer MJ, Okamoto-Uchida Y, Nakamura R. Use of Humanized Rat Basophilic Leukemia Reporter Cell Lines as a Diagnostic Tool for Detection of Allergen-Specific IgE in Allergic Patients: Time for a Reappraisal? *Current allergy and asthma reports*. 2015;15(11):1-9.
457. Wiegand TW, Williams PB, Dreskin SC, Jouvin M-H, Kinet J-P, Tasset D. High-affinity oligonucleotide ligands to human IgE inhibit binding to Fc epsilon receptor I. *The Journal of Immunology*. 1996;157(1):221-30.
458. Bernard H, Guillon B, Drumare M-F, Paty E, Dreskin SC, Wal J-M, et al. Allergenicity of peanut component Ara h 2: contribution of conformational versus linear hydroxyproline-containing epitopes. *Journal of Allergy and Clinical Immunology*. 2015;135(5):1267-74. e8.
459. Dibbern DA, Palmer GW, Williams PB, Bock SA, Dreskin SC. RBL cells expressing human FcεRI are a sensitive tool for exploring functional IgE-allergen interactions: studies with sera from peanut-sensitive patients. *Journal of immunological methods*. 2003;274(1):37-45.
460. Kaul S, Lüttkopf D, Kastner B, Vogel L, Höltz G, Vieths S, et al. Mediator release assays based on human or murine immunoglobulin E in allergen standardization. *Clinical & Experimental Allergy*. 2007;37(1):141-50.
461. Marchand F, Mecheri S, Guilloux L, Iannascoli B, Weyer A, Blank U. Human serum IgE-mediated mast cell degranulation shows poor correlation to allergen-specific IgE content. *Allergy*. 2003;58(10):1037-43.
462. Takagi K, Nakamura R, Teshima R, Sawada J-i. Application of Human Fc. EPSILON. RI. ALPHA.-Chain-Transfected RBL-2H3 Cells for Estimation of Active Serum IgE. *Biological and Pharmaceutical Bulletin*. 2003;26(2):252-5.
463. Gilfillan AM, Kado-Fong H, Wiggan GA, Hakimi J, Kent U, Kochan J. Conservation of signal transduction mechanisms via the human Fc epsilon RI alpha after

- transfection into a rat mast cell line, RBL 2H3. *The Journal of Immunology*. 1992;149(7):2445-51.
464. Taudou G, Varin-Blank N, Jouin H, Marchand F, Weyer A, Blank U. Expression of the alpha chain of human FcεRI in transfected rat basophilic leukemia cells: Functional activation after sensitization with human mite-specific IgE. *International archives of allergy and immunology*. 1993;100(4):344-50.
465. Wang X, Cato P, Lin H-C, Li T, Wan D, Alcocer MJ, et al. Optimisation and use of humanised RBL NF-AT-GFP and NF-AT-DsRed reporter cell lines suitable for high-throughput scale detection of allergic sensitisation in array format and identification of the ECM–Integrin interaction as critical factor. *Molecular biotechnology*. 2014;56(2):136-46.
466. Wan D, Wang X, Nakamura R, Alcocer MJ, Falcone FH. Use of humanized rat basophil leukemia (RBL) reporter systems for detection of allergen-specific IgE sensitization in human serum. *Basophils and Mast Cells: Methods and Protocols*. 2014:177-84.
467. Nakamura R, Uchida Y, Higuchi M, Tsuge I, Urisu A, Teshima R. A convenient and sensitive allergy test: IgE crosslinking-induced luciferase expression in cultured mast cells. *Allergy*. 2010;65(10):1266-73.
468. Kusel J. *Parasitism and the Platyhelminthes*. Elsevier; 1998.
469. Basch PF. *Schistosomes: Development, reproduction, and host relations*1991.
470. File S. Interaction of schistosome eggs with vascular endothelium. *The Journal of parasitology*. 1995:234-8.
471. Turner JD, Narang P, Coles MC, Mountford AP. Blood flukes exploit Peyer's Patch lymphoid tissue to facilitate transmission from the mammalian host. *PLoS Pathog*. 2012;8(12):e1003063.
472. Pearce EJ, Caspar P, Grzych J-M, Lewis FA, Sher A. Downregulation of Th1 cytokine production accompanies induction of Th2 responses by a parasitic helminth, *Schistosoma mansoni*. *The Journal of experimental medicine*. 1991;173(1):159-66.
473. Dalton JP, Robinson MW, Mulcahy G, O'Neill SM, Donnelly S. Immunomodulatory molecules of *Fasciola hepatica*: Candidates for both vaccine and immunotherapeutic development. *Veterinary parasitology*. 2013;195(3):272-85.
474. Gallagher I, Nair MG, Zang X, Brombacher F, Mohrs M, Allison JP, et al. Alternative activation is an innate response to injury that requires CD4+ T cells to be sustained during chronic infection. *The Journal of Immunology*. 2007;179(6):3926-36.
475. Anthony RM, Rutitzky LI, Urban JF, Stadecker MJ, Gause WC. Protective immune mechanisms in helminth infection. *Nature Reviews Immunology*. 2007;7(12):975-87.
476. Zaccone P, Cooke A. Vaccine against autoimmune disease: can helminths or their products provide a therapy? *Current opinion in immunology*. 2013;25(3):418-23.
477. Brunet LR, Finkelman FD, Cheever AW, Kopf MA, Pearce EJ. IL-4 protects against TNF-alpha-mediated cachexia and death during acute schistosomiasis. *The Journal of Immunology*. 1997;159(2):777-85.
478. Flohr C, Quinnell R, Britton J. Do helminth parasites protect against atopy and allergic disease? *Clinical & Experimental Allergy*. 2009;39(1):20-32.

479. Mathieson W, Wilson RA. A comparative proteomic study of the undeveloped and developed *Schistosoma mansoni* egg and its contents: the miracidium, hatch fluid and secretions. *International journal for parasitology*. 2010;40(5):617-28.
480. Hewitson JP, Grainger JR, Maizels RM. Helminth immunoregulation: the role of parasite secreted proteins in modulating host immunity. *Molecular and biochemical parasitology*. 2009;167(1):1-11.
481. Cornes J. Number, size, and distribution of Peyer's patches in the human small intestine: Part I The development of Peyer's patches. *Gut*. 1965;6(3):225.
482. Mohamed A, Al Karawi M, Yasawy MI. Schistosomal colonic disease. *Gut*. 1990;31(4):439-42.
483. Mostafa OM, Eid RA, Adly MA. Antischistosomal activity of ginger (*Zingiber officinale*) against *Schistosoma mansoni* harbored in C57 mice. *Parasitology research*. 2011;109(2):395-403.
484. Nakamura R, Ishiwatari A, Higuchi M, Uchida Y, Nakamura R, Kawakami H, et al. Evaluation of the luciferase assay-based in vitro elicitation test for serum IgE. *Allergology International*. 2012;61(3):431-7.
485. Weinstock J, Boros D. Organ-dependent differences in composition and function observed in hepatic and intestinal granulomas isolated from mice with *Schistosomiasis mansoni*. *The Journal of Immunology*. 1983;130(1):418-22.
486. Frangogiannis NG, Lindsey ML, Michael LH, Youker KA, Bressler RB, Mendoza LH, et al. Resident cardiac mast cells degranulate and release preformed TNF- α , initiating the cytokine cascade in experimental canine myocardial ischemia/reperfusion. *Circulation*. 1998;98(7):699-710.
487. Doenhoff M, Pearson S, Dunne D, Bickle Q, Lucas S, Bain J, et al. Immunological control of hepatotoxicity and parasite egg excretion in *Schistosoma mansoni* infections: stage specificity of the reactivity of immune serum in T-cell deprived mice. *Transactions of the Royal Society of Tropical Medicine and Hygiene*. 1981;75(1):41-53.
488. Gobert GN, Nawaratna SK, Harvie M, Ramm GA, McManus DP. An ex vivo model for studying hepatic schistosomiasis and the effect of released protein from dying eggs. *PLoS Negl Trop Dis*. 2015;9(5):e0003760.
489. Doenhoff M, Hassounah O, Murare H, Bain J, Lucas S. The schistosome egg granuloma: immunopathology in the cause of host protection or parasite survival? *Transactions of the Royal Society of Tropical Medicine and Hygiene*. 1986;80(4):503-14.
490. Karanja D, Colley DG, Nahlen BL, Ouma JH, Secor WE. Studies on schistosomiasis in western Kenya: I. Evidence for immune-facilitated excretion of schistosome eggs from patients with *Schistosoma mansoni* and human immunodeficiency virus coinfections. *The American journal of tropical medicine and hygiene*. 1997;56(5):515-21.
491. Pekary AE, Hershman JM, Berg L. Tumor Necrosis Factor, Ceramide, Transforming Growth Factor- β 1, and Aging Reduce Na⁺/I⁻ Symporter Messenger Ribonucleic Acid Levels in FRTL-5 Cells 1. *Endocrinology*. 1998;139(2):703-12.
492. Lewis M, Tartaglia LA, Lee A, Bennett GL, Rice GC, Wong G, et al. Cloning and expression of cDNAs for two distinct murine tumor necrosis factor receptors

- demonstrate one receptor is species specific. *Proceedings of the National Academy of Sciences*. 1991;88(7):2830-4.
493. Aggarwal BB, Samanta A, Feldmann M. TNF receptors. *Cytokine reference*. 2000;1620-32.
494. Schmitz H, Fromm M, Bentzel CJ, Scholz P, Detjen K, Mankertz J, et al. Tumor necrosis factor-alpha (TNFalpha) regulates the epithelial barrier in the human intestinal cell line HT-29/B6. *Journal of Cell Science*. 1999;112(1):137-46.
495. Oliveira KC, Carvalho ML, Venancio TM, Miyasato PA, Kawano T, DeMarco R, et al. Identification of the *Schistosoma mansoni* TNF-alpha receptor gene and the effect of human TNF-alpha on the parasite gene expression profile. *PLoS Negl Trop Dis*. 2009;3(12):e556.
496. Fitzsimmons CM, Schramm G, Jones FM, Chalmers IW, Hoffmann KF, Grevelding CG, et al. Molecular characterization of omega-1: a hepatotoxic ribonuclease from *Schistosoma mansoni* eggs. *Molecular and biochemical parasitology*. 2005;144(1):123-7.
497. Dunne D, Jones F, Doenhoff M. The purification, characterization, serological activity and hepatotoxic properties of two cationic glycoproteins (α 1 and ω 1) from *Schistosoma mansoni* eggs. *Parasitology*. 1991;103(02):225-36.
498. Huang X-J, Choi Y-K, Im H-S, Yarimaga O, Yoon E, Kim H-S. Aspartate aminotransferase (AST/GOT) and alanine aminotransferase (ALT/GPT) detection techniques. *Sensors*. 2006;6(7):756-82.
499. Karmen A, Wroblewski F, Ladue JS. Transaminase activity in human blood. *Journal of Clinical Investigation*. 1955;34(1):126.
500. Yang RZ, Park S, Reagan WJ, Goldstein R, Zhong S, Lawton M, et al. Alanine aminotransferase isoenzymes: molecular cloning and quantitative analysis of tissue expression in rats and serum elevation in liver toxicity. *Hepatology*. 2009;49(2):598-607.
501. Clark JM, Brancati FL, Diehl AM. The prevalence and etiology of elevated aminotransferase levels in the United States. *The American journal of gastroenterology*. 2003;98(5):960-7.
502. Pendino GM, Mariano A, Surace P, Caserta CA, Fiorillo MT, Amante A, et al. Prevalence and etiology of altered liver tests: A population-based survey in a Mediterranean town. *Hepatology*. 2005;41(5):1151-9.
503. Chen CH, Huang MH, Yang JC, Nien CK, Yang CC, Yeh YH, et al. Prevalence and etiology of elevated serum alanine aminotransferase level in an adult population in Taiwan. *Journal of gastroenterology and hepatology*. 2007;22(9):1482-9.
504. Liangpunsakul S, Chalasani N. Unexplained elevations in alanine aminotransferase in individuals with the metabolic syndrome: results from the third National Health and Nutrition Survey (NHANES III). *The American journal of the medical sciences*. 2005;329(3):111-6.
505. Pratt DS, Kaplan MM. Evaluation of abnormal liver-enzyme results in asymptomatic patients. *New England Journal of Medicine*. 2000;342(17):1266-71.
506. Poustchi H, George J, Esmaili S, Esna-Ashari F, Ardalan G, Sepanlou SG, et al. Gender differences in healthy ranges for serum alanine aminotransferase levels in adolescence. *PloS one*. 2011;6(6):e21178.

507. Dong MH, Bettencourt R, Brenner DA, Barrett–Connor E, Loomba R. Serum levels of alanine aminotransferase decrease with age in longitudinal analysis. *Clinical Gastroenterology and Hepatology*. 2012;10(3):285-90. e1.
508. Gimeno J, Eattock N, Van Deynze A, Blumwald E. Selection and validation of reference genes for gene expression analysis in switchgrass (*Panicum virgatum*) using quantitative real-time RT-PCR. *PloS one*. 2014;9(3):e91474.
509. Bustin SA. Absolute quantification of mRNA using real-time reverse transcription polymerase chain reaction assays. *Journal of molecular endocrinology*. 2000;25(2):169-93.
510. Pfaffl MW, Hageleit M. Validities of mRNA quantification using recombinant RNA and recombinant DNA external calibration curves in real-time RT-PCR. *Biotechnology Letters*. 2001;23(4):275-82.
511. Pfaffl MW. A new mathematical model for relative quantification in real-time RT–PCR. *Nucleic acids research*. 2001;29(9):e45-e.
512. Takahashi K, Asabe S, Wieland S, Garaigorta U, Gastaminza P, Isogawa M, et al. Plasmacytoid dendritic cells sense hepatitis C virus–infected cells, produce interferon, and inhibit infection. *Proceedings of the National Academy of Sciences*. 2010;107(16):7431-6.
513. Beatch MD, Hobman TC. Rubella virus capsid associates with host cell protein p32 and localizes to mitochondria. *Journal of virology*. 2000;74(12):5569-76.
514. Miller H, Huntley J, Newlands G, Mackellar A, Lammas D, Wakelin D. Granule proteinases define mast cell heterogeneity in the serosa and the gastrointestinal mucosa of the mouse. *Immunology*. 1988;65(4):559.
515. De Jonge F, Van Nassauw L, Van Meir F, Miller HR, Van Marck E, Timmermans JP. Temporal distribution of distinct mast cell phenotypes during intestinal schistosomiasis in mice. *Parasite immunology*. 2002;24(5):225-31.
516. Knight PA, Wright SH, Lawrence CE, Paterson YY, Miller HR. Delayed Expulsion of the Nematode *Trichinella spiralis* In Mice Lacking the Mucosal Mast Cell–Specific Granule Chymase, Mouse Mast Cell Protease-1. *Journal of Experimental Medicine*. 2000;192(12):1849-56.
517. McDermott JR, Bartram RE, Knight PA, Miller HR, Garrod DR, Grecis RK. Mast cells disrupt epithelial barrier function during enteric nematode infection. *Proceedings of the National Academy of Sciences*. 2003;100(13):7761-6.
518. Doenhoff M, Musallam R, Bain J, McGregor A. Studies on the host-parasite relationship in *Schistosoma mansoni*-infected mice: the immunological dependence of parasite egg excretion. *Immunology*. 1978;35(5):771.
519. Cheever AW, Poindexter RW, Wynn TA. Egg Laying Is Delayed but Worm Fecundity Is Normal in SCID Mice Infected with *Schistosoma japonicum* and *S. mansoni* with or without Recombinant Tumor Necrosis Factor Alpha Treatment. *Infection and immunity*. 1999;67(5):2201-8.
520. Elliott T, Muller A, Brockwell Y, Murphy N, Grillo V, Toet H, et al. Evidence for high genetic diversity of NAD1 and COX1 mitochondrial haplotypes among triclabendazole resistant and susceptible populations and field isolates of *Fasciola hepatica* (liver fluke) in Australia. *Veterinary parasitology*. 2014;200(1):90-6.

521. Moll L, Gaasenbeek CP, Vellema P, Borgsteede FH. Resistance of *Fasciola hepatica* against triclabendazole in cattle and sheep in The Netherlands. *Veterinary parasitology*. 2000;91(1):153-8.
522. Johnston M, MacDonald J, McKay D. Parasitic helminths: a pharmacopeia of anti-inflammatory molecules. *Parasitology*. 2009;136(02):125-47.
523. McManus D, Dalton J. Vaccines against the zoonotic trematodes *Schistosoma japonicum*, *Fasciola hepatica* and *Fasciola gigantica*. *Parasitology*. 2006;133(2):S43-S61.
524. Panja A, Goldberg S, Eckmann L, Krishen P, Mayer L. The regulation and functional consequence of proinflammatory cytokine binding on human intestinal epithelial cells. *The Journal of Immunology*. 1998;161(7):3675-84.
525. Taylor C, Dzus A, Colgan S. Autocrine regulation of intestinal epithelial permeability induced by hypoxia: Role for basolateral release of tumor necrosis factor- α (TNF- α). *Gastroenterology*. 1998;114:657-68.
526. Kominsky DJ, Campbell EL, Ehrentraut SF, Wilson KE, Kelly CJ, Glover LE, et al. IFN- γ -Mediated Induction of an Apical IL-10 Receptor on Polarized Intestinal Epithelia. *The Journal of Immunology*. 2014;192(3):1267-76.
527. Commins S, Steinke JW, Borish L. The extended IL-10 superfamily: IL-10, IL-19, IL-20, IL-22, IL-24, IL-26, IL-28, and IL-29. *Journal of Allergy and Clinical Immunology*. 2008;121(5):1108-11.
528. Rout N, Woods A. Enhanced innate CD161+ T cell responses in mucosal tissues of nonhuman primates. *The Journal of Immunology*. 2016;196(1 Supplement):208.18-18.
529. Quiding M, Nordström I, Kilander A, Andersson G, Hanson LA, Holmgren J, et al. Intestinal immune responses in humans. Oral cholera vaccination induces strong intestinal antibody responses and interferon-gamma production and evokes local immunological memory. *Journal of Clinical Investigation*. 1991;88(1):143.
530. Ziegler SF, Roan F, Bell BD, Stoklasek TA, Kitajima M, Han H. The biology of thymic stromal lymphopoietin (TSLP). *Advances in pharmacology (San Diego, Calif)*. 2013;66:129.
531. Rochman Y, Spolski R, Leonard WJ. New insights into the regulation of T cells by γ c family cytokines. *Nature Reviews Immunology*. 2009;9(7):480-90.
532. Lee H-C, Ziegler SF. Inducible expression of the proallergic cytokine thymic stromal lymphopoietin in airway epithelial cells is controlled by NF κ B. *Proceedings of the National Academy of Sciences*. 2007;104(3):914-9.
533. Zeuthen LH, Fink LN, Frokiaer H. Epithelial cells prime the immune response to an array of gut-derived commensals towards a tolerogenic phenotype through distinct actions of thymic stromal lymphopoietin and transforming growth factor- β . *Immunology*. 2008;123(2):197-208.
534. Taylor BC, Zaph C, Troy AE, Du Y, Guild KJ, Comeau MR, et al. TSLP regulates intestinal immunity and inflammation in mouse models of helminth infection and colitis. *The Journal of experimental medicine*. 2009;206(3):655-67.
535. He B, Xu W, Santini PA, Polydorides AD, Chiu A, Estrella J, et al. Intestinal bacteria trigger T cell-independent immunoglobulin A 2 class switching by inducing epithelial-cell secretion of the cytokine APRIL. *Immunity*. 2007;26(6):812-26.

536. Bossen C, Schneider P, editors. BAFF, APRIL and their receptors: structure, function and signaling. *Seminars in immunology*; 2006: Elsevier.
537. Gorelik L, Flavell RA. Transforming growth factor- β in T-cell biology. *Nature Reviews Immunology*. 2002;2(1):46-53.
538. Chen W, Wahl SM. TGF- β : receptors, signaling pathways and autoimmunity. *Signal Transduction Pathways in Autoimmunity*. 5: Karger Publishers; 2002. p. 62-91.
539. Deshmane SL, Kremlev S, Amini S, Sawaya BE. Monocyte chemoattractant protein-1 (MCP-1): an overview. *Journal of interferon & cytokine research*. 2009;29(6):313-26.
540. Reibman J, Hsu Y, Chen LC, Bleck B, Gordon T. Airway epithelial cells release MIP-3 α /CCL20 in response to cytokines and ambient particulate matter. *American journal of respiratory cell and molecular biology*. 2003;28(6):648-54.
541. Shang L, Fukata M, Thirunarayanan N, Martin AP, Arnaboldi P, Maussang D, et al. Toll-like receptor signaling in small intestinal epithelium promotes B-cell recruitment and IgA production in lamina propria. *Gastroenterology*. 2008;135(2):529-38. e1.
542. Lopez-Castejon G, Brough D. Understanding the mechanism of IL-1 β secretion. *Cytokine & growth factor reviews*. 2011;22(4):189-95.
543. Al-Sadi RM, Ma TY. IL-1 β causes an increase in intestinal epithelial tight junction permeability. *The Journal of Immunology*. 2007;178(7):4641-9.
544. Al-Sadi R, Ye D, Boivin M, Guo S, Hashimi M, Ereifej L, et al. Interleukin-6 modulation of intestinal epithelial tight junction permeability is mediated by JNK pathway activation of claudin-2 gene. *PloS one*. 2014;9(3):e85345.
545. Suzuki T, Yoshinaga N, Tanabe S. Interleukin-6 (IL-6) regulates claudin-2 expression and tight junction permeability in intestinal epithelium. *Journal of Biological Chemistry*. 2011;286(36):31263-71.
546. Pachathundikandi SK, Brandt S, Madassery J, Backert S. Correction: Induction of TLR-2 and TLR-5 Expression by *Helicobacter pylori* Switches cagPAI-Dependent Signalling Leading to the Secretion of IL-8 and TNF- α . *PloS one*. 2015;10(10).
547. Ohta K, Ishida Y, Fukui A, Mizuta K, Nishi H, Takechi M, et al. Toll-like receptor (TLR) expression and TLR-mediated interleukin-8 production by human submandibular gland epithelial cells. *Molecular medicine reports*. 2014;10(5):2377-82.
548. Li L-J, Gong C, Zhao M-H, Feng B-S. Role of interleukin-22 in inflammatory bowel disease. *World J Gastroenterol*. 2014;20(48):18177-88.
549. Dumoutier L, Louahed J, Renauld J-C. Cloning and characterization of IL-10-related T cell-derived inducible factor (IL-TIF), a novel cytokine structurally related to IL-10 and inducible by IL-9. *The Journal of Immunology*. 2000;164(4):1814-9.
550. Kotenko SV, Izotova LS, Mirochnitchenko OV, Esterova E, Dickensheets H, Donnelly RP, et al. Identification, cloning, and characterization of a novel soluble receptor that binds IL-22 and neutralizes its activity. *The Journal of Immunology*. 2001;166(12):7096-103.
551. Zheng Y, Valdez PA, Danilenko DM, Hu Y, Sa SM, Gong Q, et al. Interleukin-22 mediates early host defense against attaching and effacing bacterial pathogens. *Nature medicine*. 2008;14(3):282-9.

552. Petersen BC, Budelsky AL, Baptist AP, Schaller MA, Lukacs NW. Interleukin-25 induces type 2 cytokine production in a steroid-resistant interleukin-17RB+ myeloid population that exacerbates asthmatic pathology. *Nature medicine*. 2012;18(5):751-8.
553. Howitt MR, Lavoie S, Michaud M, Blum AM, Tran SV, Weinstock JV, et al. Tuft cells, taste-chemosensory cells, orchestrate parasite type 2 immunity in the gut. *Science*. 2016;351(6279):1329-33.

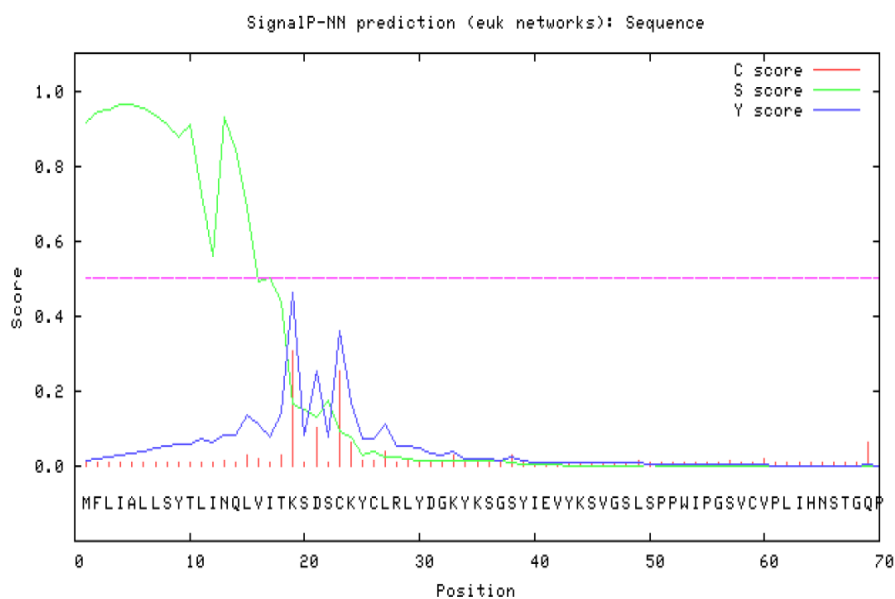
Appendix 1

Prediction of secretory signal sequence obtained from SignalP 3.0

A-D are five examples of protein predicted to exhibit secretory signal motif

- (A) **ShIPSE03** (NCBI Reference Sequence: XP_012802396.1), *Schistosoma haematobium*, expressed protein; protein; length= 404 nucleotides or 136 amino acids.

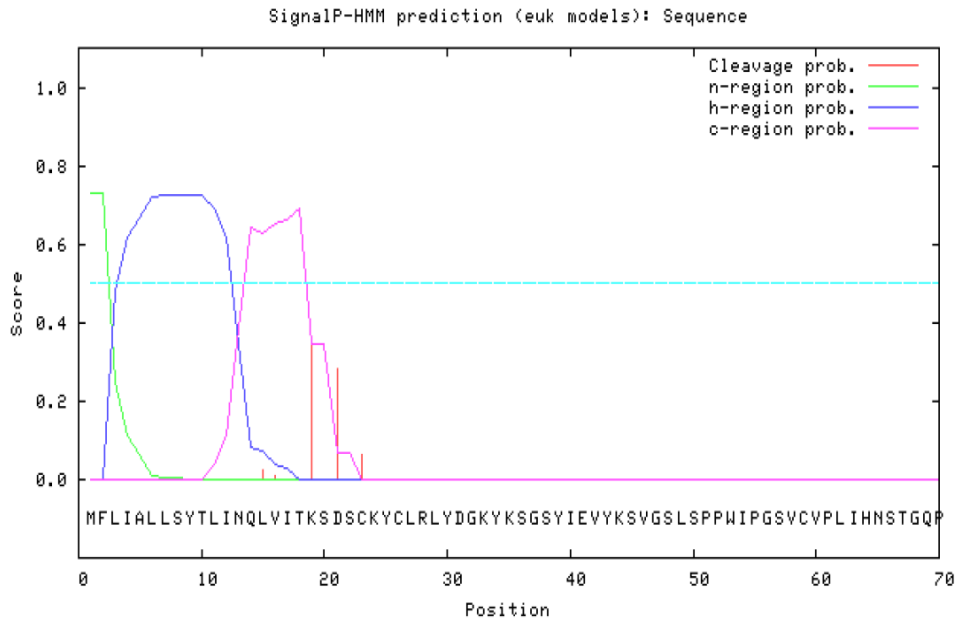
SignalP-NN result:



data

```
>Sequence          length = 70
# Measure  Position  Value  Cutoff  signal peptide?
max. C     19        0.305  0.32   NO
max. Y     19        0.461  0.33   YES
max. S      5         0.965  0.87   YES
mean S     1-18       0.805  0.48   YES
           D     1-18       0.633  0.43   YES
# Most likely cleavage site between pos. 18 and 19: VIT-KS
```

SignalP-HMM result:

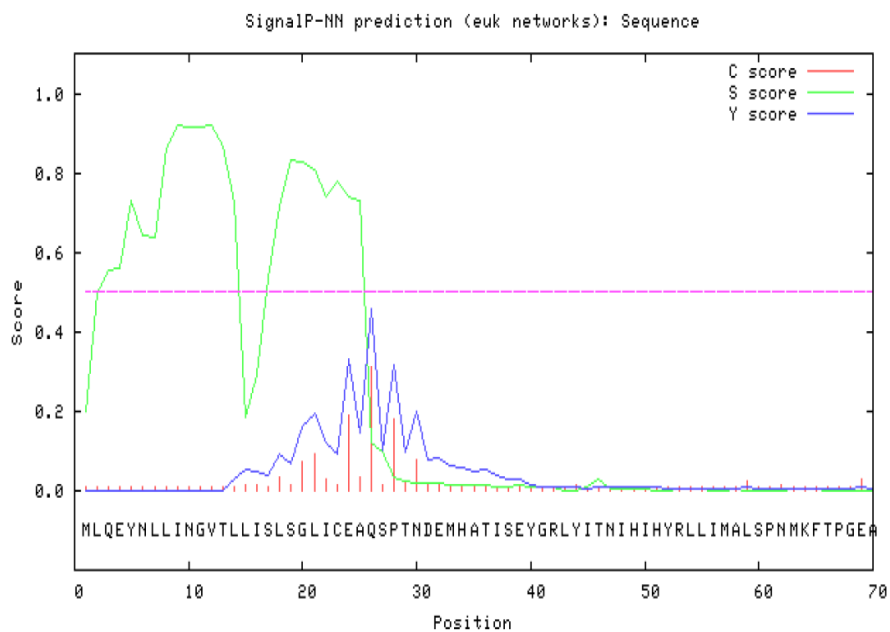


data

```
>Sequence
Prediction: Signal peptide
Signal peptide probability: 0.728
Signal anchor probability: 0.000
Max cleavage site probability: 0.345 between pos. 18 and 19
```

(B) **Smk5** (clone 4.1.2; GenBankTM accession number AY903301), *Schistosoma mansoni*, expressed protein; protein; length= 900 nucleotides or 300 amino acids.

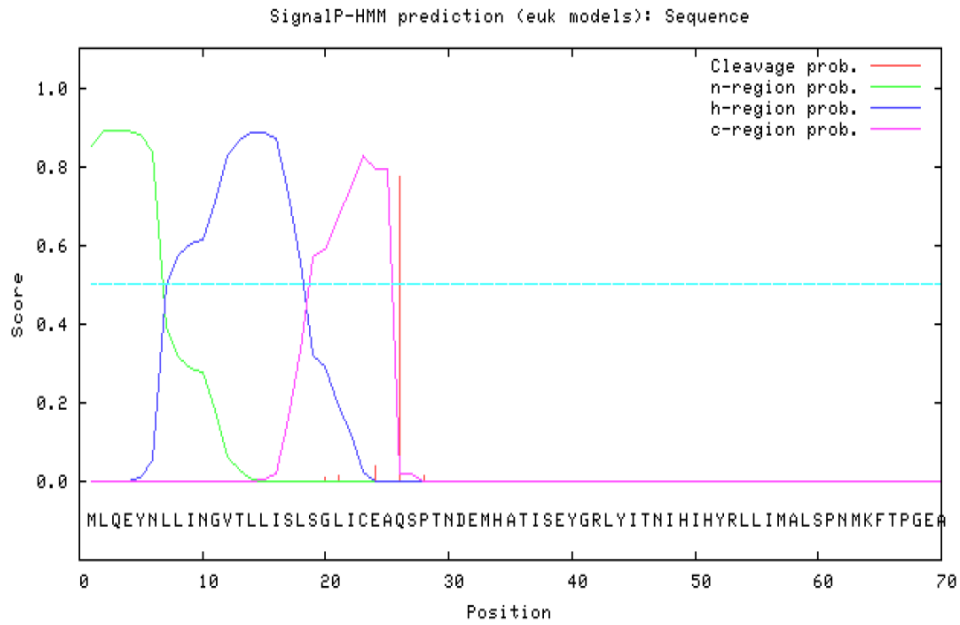
SignalP-NN result:



data

```
>Sequence          length = 70
# Measure  Position  Value  Cutoff  signal peptide?
max. C     26         0.313  0.32   NO
max. Y     26         0.455  0.33   YES
max. S     12         0.921  0.87   YES
mean S     1-25       0.685  0.48   YES
D          1-25       0.570  0.43   YES
# Most likely cleavage site between pos. 25 and 26: CEA-QS
```

SignalP-HMM result:



data

>Sequence

Prediction: Signal peptide

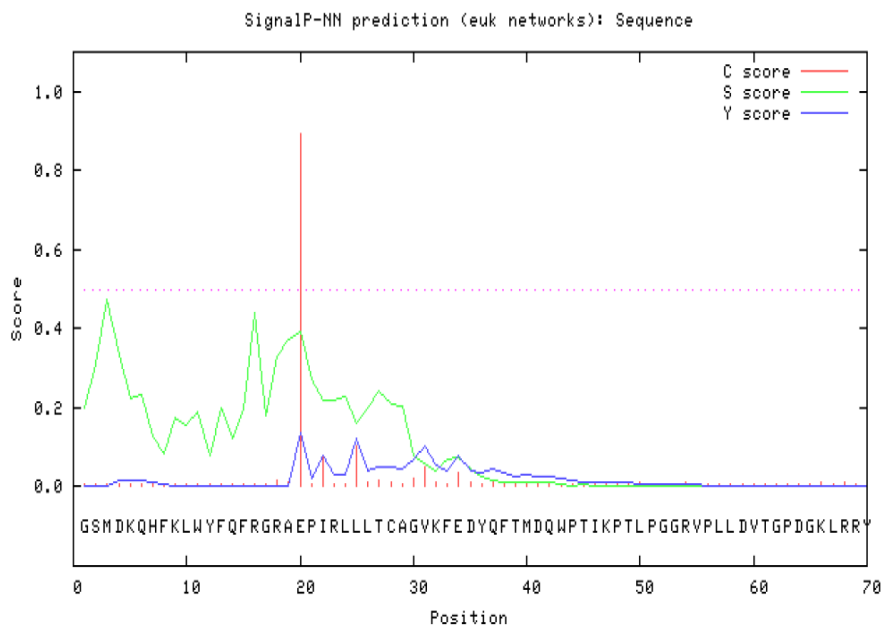
Signal peptide probability: 0.852

Signal anchor probability: 0.039

Max cleavage site probability: 0.773 between pos. 25 and 26

(C) **FhGST-si** (Wormbase database: BN1106_s1081B000242.mRNA-1), *Fasciola hepatica*, expressed protein; protein; length= 631 nucleotides or 211 amino acids.

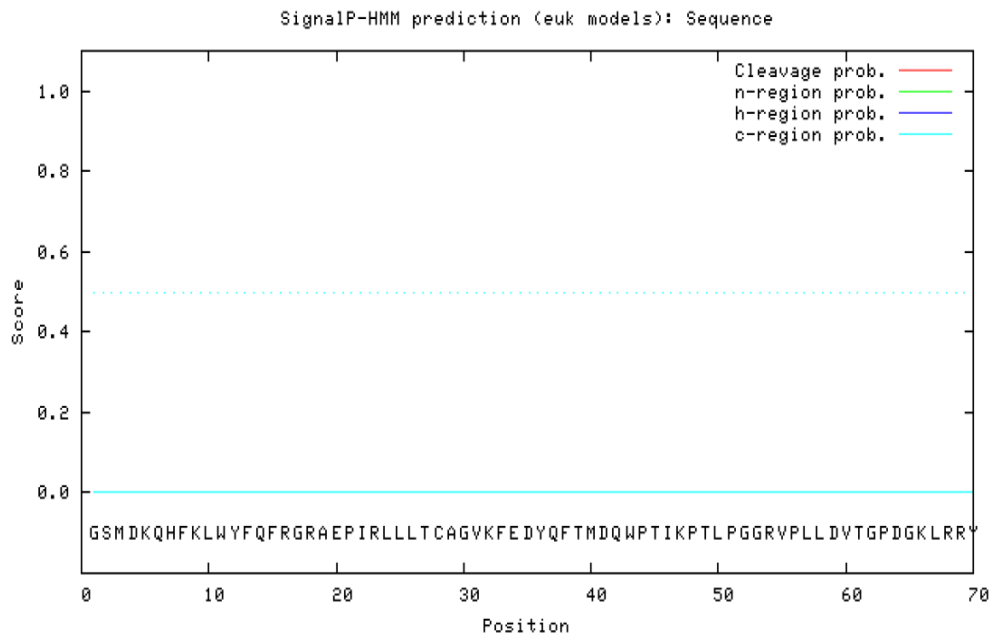
SignalP-NN result:



[data](#)

```
>Sequence          length = 70
# Measure  Position  Value  Cutoff  signal peptide?
max. C      20      0.894  0.32   YES
max. Y      20      0.135  0.33   NO
max. S       3      0.473  0.87   NO
mean S     1-19     0.233  0.48   NO
D           1-19     0.184  0.43   NO
```

SignalP-HMM result:

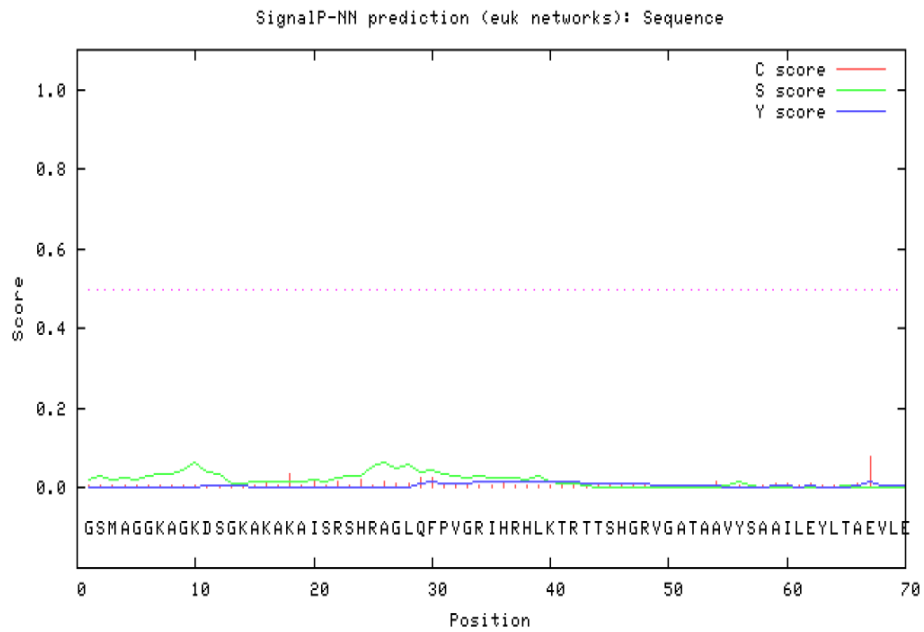


[data](#)

```
>Sequence
Prediction: Non-secretory protein
Signal peptide probability: 0.001
Signal anchor probability: 0.000
Max cleavage site probability: 0.000 between pos. 19 and 20
```

(D) **FhH2A** (Wormbase database: BN1106_s45B000421.mRNA-1), *Fasciola hepatica*, expressed protein; protein; length= 409 nucleotides or 138 amino acids.

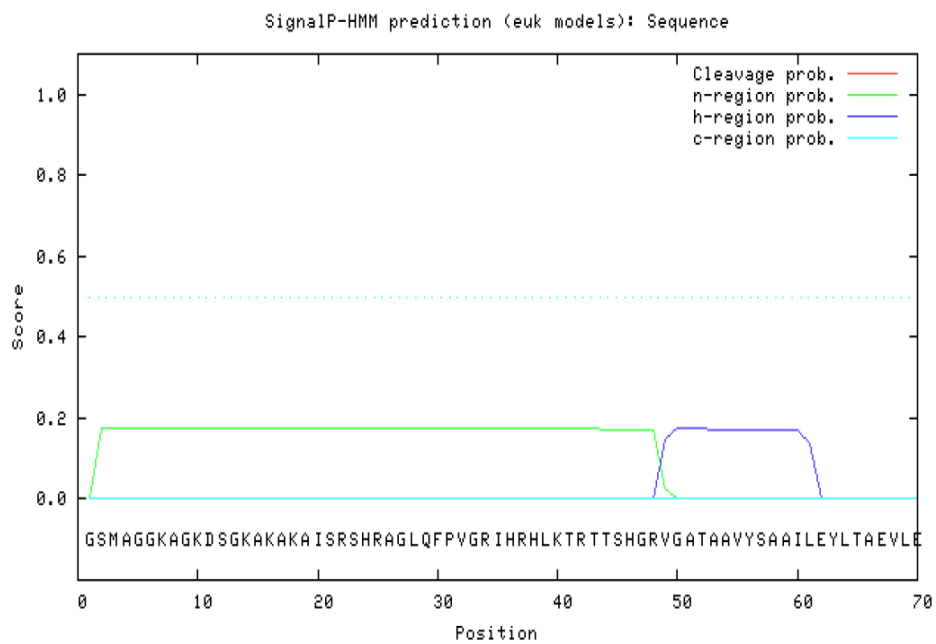
SignalP-NN result:



data

```
>Sequence          length = 70
# Measure  Position  Value  Cutoff  signal peptide?
max. C     67         0.080  0.32   NO
max. Y     36         0.017  0.33   NO
max. S     26         0.066  0.87   NO
mean S     1-35       0.032  0.48   NO
D         1-35       0.025  0.43   NO
```

SignalP-HMM result:



data

```
>Sequence
Prediction: Non-secretory protein
Signal peptide probability: 0.001
Signal anchor probability: 0.173
Max cleavage site probability: 0.001 between pos. 61 and 62
```

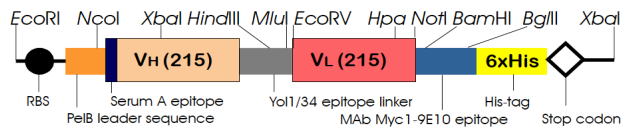
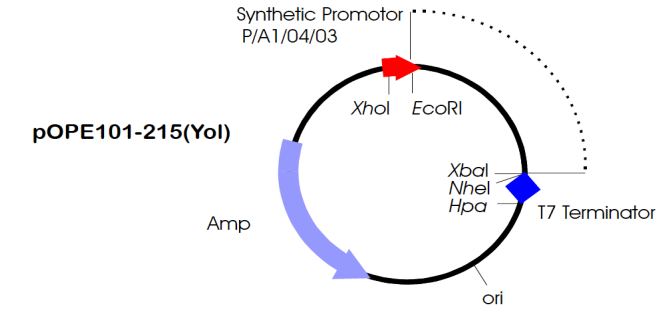
Appendix 2

pOPE101 Vector used for expression of infiltrins

Map of pOPE101 and the figures below summarizes the schematic diagram of the pOPE101_SmIPSE or Smk5 expression cassette.

More information about pCEP4 is available for downloading from our website

<https://www.progen.de/media/downloads/datasheets/PR3004.pdf>



VH insertion region of pOPE101

```

      NcoI                               HindIII                               MluI
ATG..54bp..GCATGGCGCAAGTTCAGTGCAG..339bp..TCGGCCCAAGCATTGAAGAAGTGAATTTTCAGAAGCACGCCT..
M... ..A M A Q V Q L Q... ..S A P K L E E G E F S E A R...
<-----> <-----> <----->
Signal Sequence          VH                      Y01-tag
  
```

VL insertion region of pOPE101

```

      MluI                               NotI                               BamHI
..GAAGAAGGTGAATTTTCAGAAGCACGGGTAGATATC..330bp..AAAGTGGGGCCGCTGGATCC
..E E G E F S E A R V D I... ..K R A A A G S...
<-----> <----->
Y01-tag          VL
  
```



Schematic diagram of the pOPE101_SmIPSE or Smk5

Pro – synthetic P/A1/04/03 lac promoter; lacO – lac operator; start codon (black circle); pelB – cleavable pelB leader sequence; SmIPSE or Smk5 gene fragment; c-Myc – c-Myc tag; 6x His – 6-histidine peptide tag; stop codon (red circle).

Appendix 3

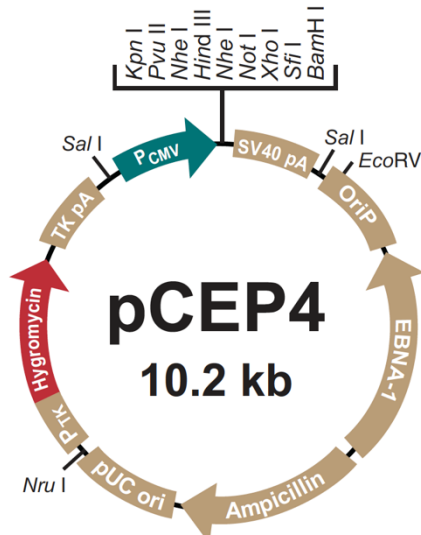
pCEP4 Vector used for expression of infiltrins

Map of pCEP4 and the figure below summarizes the features of the pCEP4 vector. More information

about

pCEP4 is available for downloading from our website

(https://tools.thermofisher.com/content/sfs/manuals/pcep4_man.pdf).



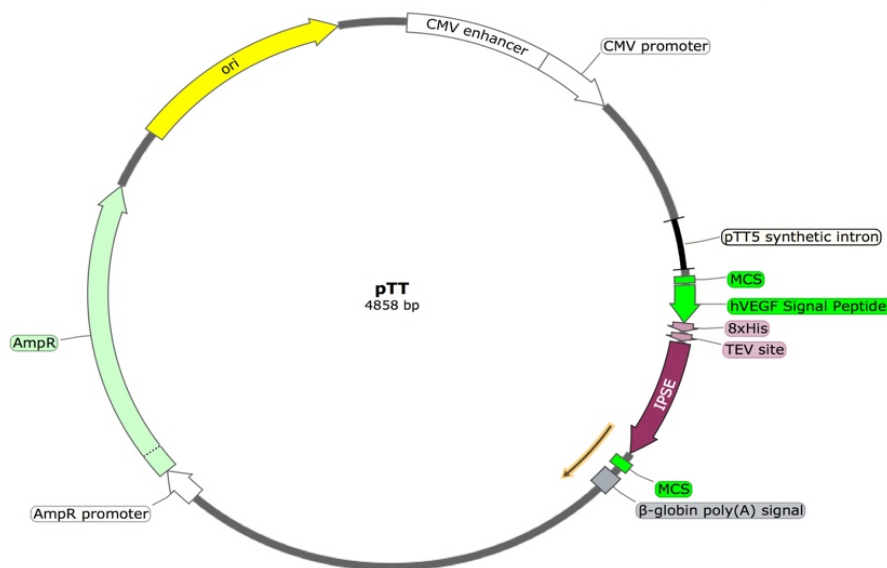
Start codon (black circle, SmIPSE or Smk5 gene fragment, 6x His –6-histidine peptide tag and stop codon (red circle). This sequence was cloned into the MCS of the destination expression vector.

Feature	Benefit
Human cytomegalovirus (CMV) immediate-early promoter/enhancer	Allows efficient, high-level expression of your recombinant protein
Multiple cloning site	Allows insertion of your gene and facilitates cloning
SV40 polyadenylation signal	Efficient transcription termination and polyadenylation of mRNA
EBV origin of replication (oriP) and nuclear antigen (EBNA-1)	High-copy episomal replication in primate and canine cell lines
pUC origin	High-copy number replication and growth in <i>E. coli</i>
Herpes Simplex Virus thymidine kinase (TK) promoter	Allows efficient, high-level expression of the hygromycin resistance gene
Hygromycin resistance gene	Selection of stable transfectants in mammalian cells
Herpes Simplex Virus thymidine kinase (TK) promoter polyadenylation signal	Efficient transcription termination and polyadenylation of mRNA

Appendix 4

pTT5 Vector used for expression of infiltrins

Map of pTT5 and the figure below summarizes the features of the pTT5 vector. More information about pTT5 is available at the Canadian National Research Council, Canada.

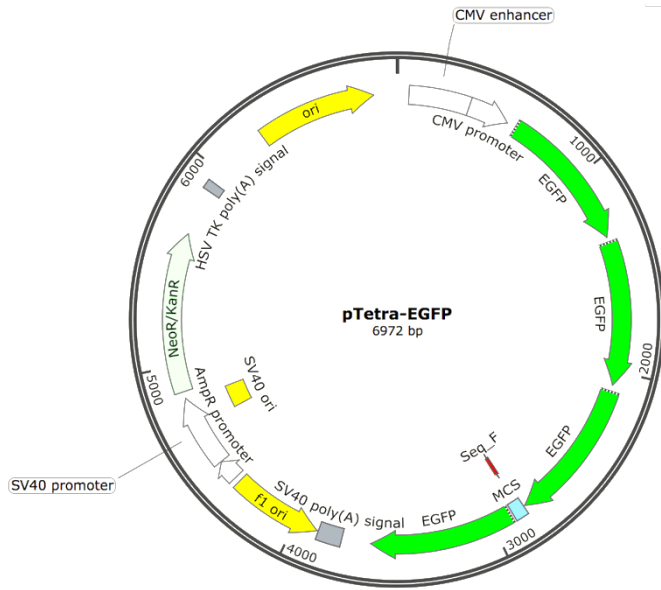


Schematic of pTT5 vector used for expression of infiltrins

The third vector is the pTT5 mammalian expression vector, which confers ampicillin for bacterial selection. This vector contains hVEGF Signal Peptide, 8 \times His-tag for purification at the *N*-terminus followed by the tobacco etch virus (TEV) cleavage site and then infiltrins. There is also β -globin polyadenylation site, Ori and an Epstein-Barr virus (EBV) origin of replication (OriP) replication fragment. The pTT system is licensed by the Canadian National Research Council, Canada.

Appendix 5 Tetra-EGFP vector

Map of Tetra-EGFP and the figure below summarizes the features of the Tetra-EGFP vector.



A multiple cloning site (MCS)

AAGTCCGGACTCAGATCTCGAGCTCAAGCTTCTGCAATTCTGCAGTCGACGGTACCGCGGGCCCGGGATCCATCGCCACC
ATG

BspEI BglIII SacI EcoRI SalI SacII XmaI
XhoI HindIII PstI KpnI ApaI BamHI

Schematic of Tetra-EGFP vector

The third vector is the Tetra-EGFP vector, which confers Neomycin-kanamycin for bacterial selection. This vector contains four EGFP copies and a multiple cloning site between the third and fourth EGFP into which the suspected NLS is inserted. There is also CMV promoter, origin of replication (OriP). This vector was created by Christian Beetz. In this thesis, the pTetra-EGFP vector were digested with the restriction enzyme *BglIII* (red).

Appendix 6

Role of cytokines in intestinal epithelial cells

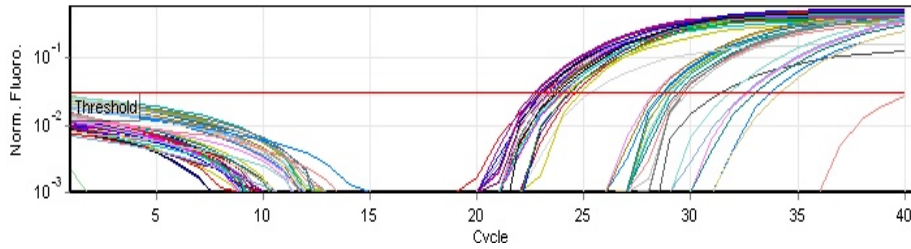
Cytokines	The role of cytokines
IFN-γ	Interferon (IFN- γ): The first regulatory cytokine discovered in intestinal epithelial cells (IEC). Able to regulate IL-6R and IL-1, encourages TNF- γ R II to express the IL-10 receptor alpha chain (524-527). The amount of IFN- γ production is significantly higher in the mucosa (528, 529) and this plays an important role in the regulation of solute/water transport in collaboration with IL-4 and IL-13 (416).
TSLP	Thymic stromal lymphopoietin (TSLP) , was discovered in thymic stromal cells and is a member of the IL-2 cytokine family (530). It is produced by IECs and plays an important role in the development of regulatory T cells (531). The expression of TSLP messenger RNA (mRNA) from airway epithelial cells interacts with proinflammatory cytokines, such as TNF- α and IL-1 β , which results in the release of Th2 cytokines from mast cells independently of T cells (532). DCs and epithelium-derived TSLP and TGF- β play a role in the down-regulated production of inflammatory cytokines (533). The absence of TSLP signalling in primary DCs increases proinflammatory cytokine production and TNF- γ ⁺ CD4 ⁺ T cells in mesenteric lymph nodes, as well as inadequate responses to helminth infection (534). TSLP-conditioned DCs are important in order to trigger IgA2 class switching through the induction of APRIL in effector B cells (535).
APRIL	A proliferation-inducing ligand (APRIL) is a member of the TNF ligand family and is recognised as a cell surface receptor transmembrane activator and Circulating cancer-associated macrophage-like cells (CAML) interactor TACI receptors. It is produced in IECs via TLR stimulation by commensal bacteria during the stimulation of DCs by epithelial TSLP (535, 536). APRIL-conditioned DCs are important to trigger IgA2 class switching through the induction of APRIL in effector B cells (535).
TGF-β	Transforming growth factor (TGF-β) is a cytokine secreted by IEC (417). TGF- β with TSLP plays a role in the down-regulated production of inflammatory cytokines (533). TGF- β , produced by IECs is trafficked to secondary lymphoid sites and plays an important role in the development of regulatory T cell mediated immune responses and in the induction of immune tolerance (531, 537, 538).
MCP-1	Monocyte chemoattractant protein (MCP-1) is a chemokine which regulates the migration and infiltration of macrophages (539). MCP-1, which is produced following the intracellular invasion of IECs, is up-regulated during inflammation, and is a potent chemoattractant for monocytes (422, 423).

Cytokines	The role of cytokines
CCL20	CC chemokine-ligand 20 (CCL20) is a small cytokine expressed by epithelial cells (540). CCL20 promotes the recruitment of B cells, DCs and T cells by IECs (424, 541).
IL-1β	Interleukin (IL-1β): IL-1 β is a pro-inflammatory response to injury and infection (542). The permeability of TJs in epithelia cells is raised through IL-1 β due to the down-regulation of occludin expression in the endothelium in an NF- κ B-dependent manner (543). IL-1 β is expressed by IEC (532) and IL-1 β receptors are expressed by the polarisation of IECs at basolateral surfaces on mucosal immune cells (418).
IL-6	Interleukin-6 was initially classified as a pro-inflammatory cytokine but it also stimulates the production of anti-inflammatory cytokines (431). The production of IL-6, which occurs in different cell types, such as intraepithelial lymphocytes and including epithelial cells, enhances the proliferation of epithelial barrier and protect it during injury (419, 420) Moreover, IL-6 stimulates a claudin-2 expression dependent increase in the permeability of TJs (544, 545).
IL-8	Interleukin-8 is a chemoattractant cytokine and an activator of polymorphonuclear leukocytes produced by IECs (421). IL-8 secretion can be mediated after flagellin-induced activation by Toll-like receptor 5 (TLR5) (546) and TLR9 expression. Production of IL-8 plays an important role in increasing TLR9 levels (547).
IL-10	Interleukin-10 is anti-inflammatory cytokine and has been observed in IECs (425). The activation of IFN- γ in epithelial cells leads to the expression of the IL-10 receptor (15) Microarray analysis has shown that the activation of IFN- γ stimulates high levels of expression of the IL-10 receptor alpha chain (526, 527). The IL-10 family and IL-22 enhance the proliferation of the epithelial barrier and protect it during injury (425, 527, 548).
IL-22	Interleukin-22 was discovered in 2000 and is an α -helical cytokine (549). According to microarray analysis, signalling by the IL-10 family and IL-22 enhances the proliferation of the epithelial barrier and protects it during injury (416, 527, 548). The production of IL-22 by the lymphoid lineage of helper T cells, the lymphoid lineage and natural killer cells act on epithelial cells (426, 427). IL-22 binds a heterodimer composed of IL-22R1 and IL-10R2 that is located on the basolateral epithelial cells surface (550, 551).
IL-25	Interleukin-25 is a cytokine associated with allergies and functions as part of the Th2 immune response on epithelial surfaces (552). The secretion of IL-25 in gut epithelial cells during parasitic infection is increased significantly (553).

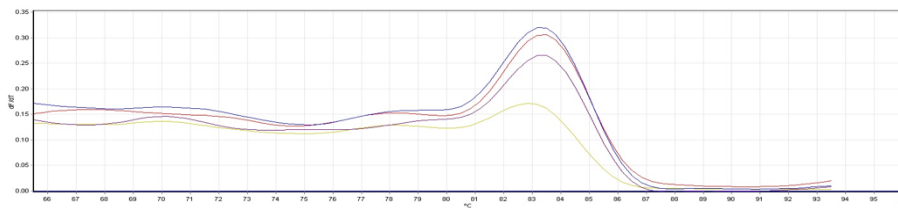
Appendix 7

Huh7 cells were incubated with 10 μ g wild type and mutant recombinant IPSE/ α -1 and without treatment (Control) at different time points (2 and 4 h). Melting curve analysis obtained for gene RPL and GPT (target genes).

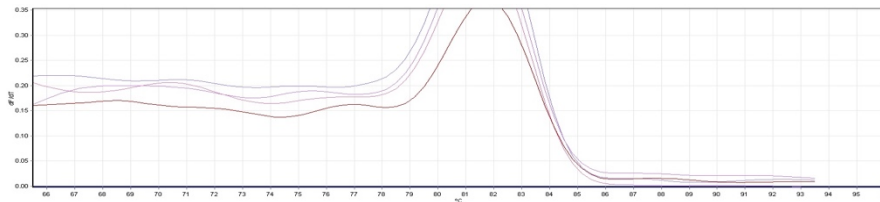
Melt Curve Graph for KAPA SYBR® FAST (all groups but the following graphs from 1 to 10 show each group in separately)



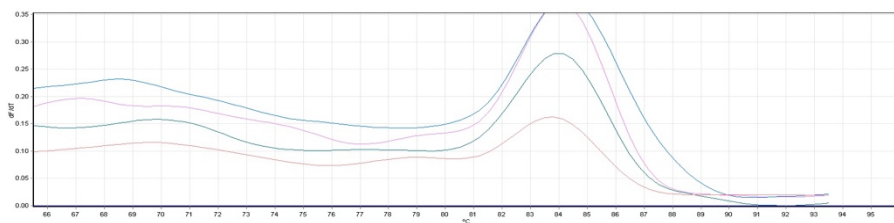
1. RPL after 2h (wild type)



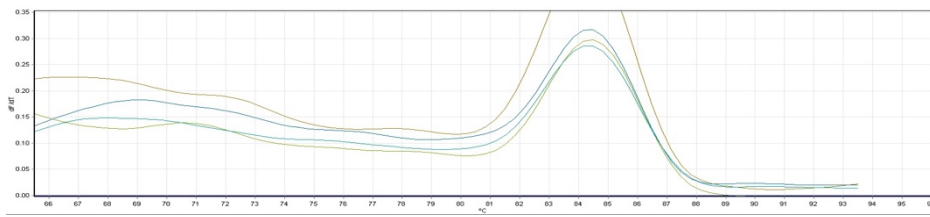
2. RPL after 4 h (wild type)



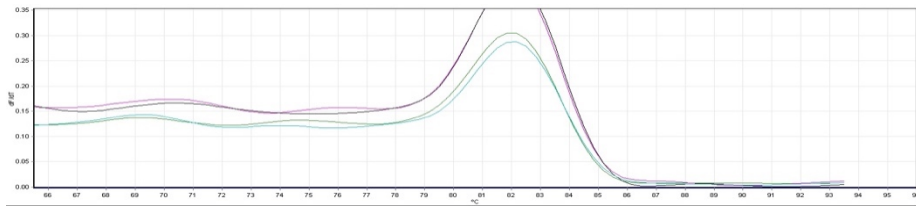
3. GPT after 2 h (wild type)



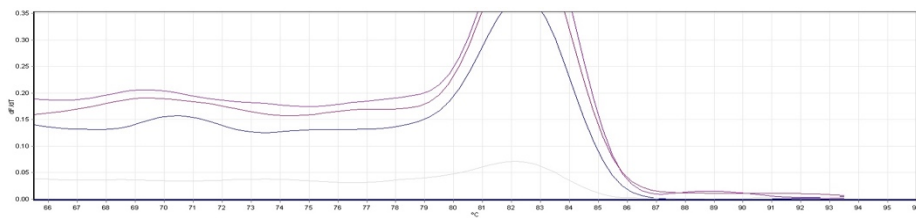
4. GPT after 4 h (wild type)



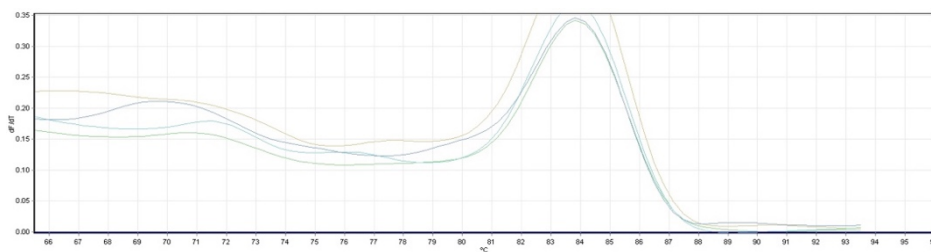
5. RPL after 2h (mutant)



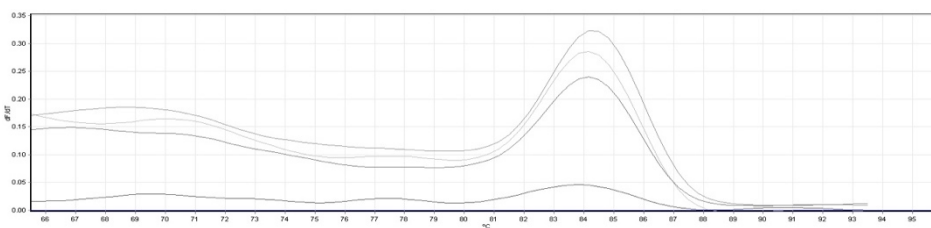
6. RPL after 4 h (mutant)



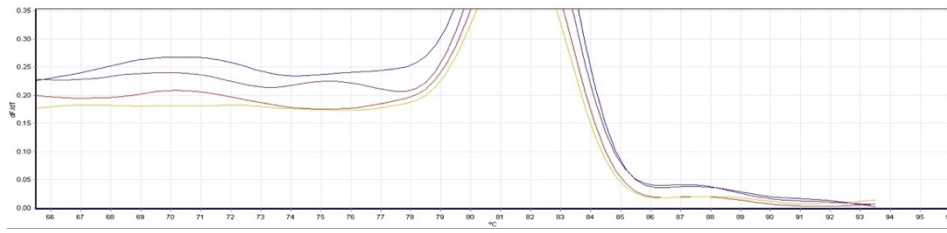
7. GPT after 2 h (mutant)



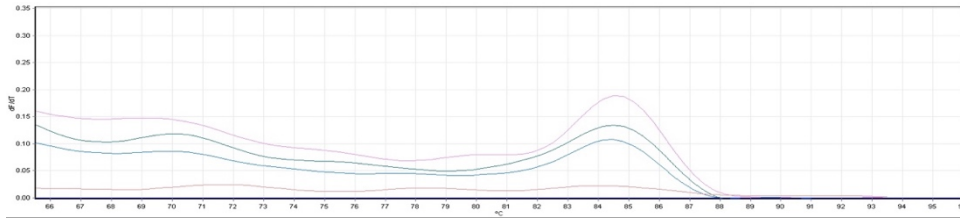
8. GPT after 4h (mutant)



9. RPL (control)



GPT (control)



Appendix 8

Changes GPT1 GPT2 in gene array DCs and HUVECs

	Primary Sequence	Sequence Description	Accession #	Log(Ratio)	Log(Error)	Ratio	Fold Change
Dendritic cells	GPT	Homo sapiens glutamic-pyruvate transaminase (alanine aminotransferase) (GPT), mRNA [NM_005309]	NM_005309	-0.03001	0.06155	0.93324	-1.07154
	GPT2	Homo sapiens glutamic pyruvate transaminase (alanine aminotransferase) 2 (GPT2), transcript variant 1, mRNA [NM_133443]	NM_133443	0.17826	0.10305	1.5075	1.5075
	GPT2	Homo sapiens glutamic pyruvate transaminase (alanine aminotransferase) 2 (GPT2), transcript variant 1, mRNA [NM_133443]	NM_133443	0.086	0.06836	1.21899	1.21899
HUVECs	GPT	Homo sapiens glutamic-pyruvate transaminase (alanine aminotransferase) (GPT), mRNA [NM_005309]	NM_005309	0.0597	0.06418	1.14736	1.14736
	GPT2	Homo sapiens glutamic pyruvate transaminase (alanine aminotransferase) 2 (GPT2), transcript variant 1, mRNA [NM_133443]	NM_133443	0.03444	0.06166	1.08254	1.08254
	GPT2	Homo sapiens glutamic pyruvate transaminase (alanine aminotransferase) 2 (GPT2), transcript variant 1, mRNA [NM_133443]	NM_133443	0.06459	0.06305	1.16035	1.16035

Appendix 9

```

1   M   D   K   Q   H   F   K   L   W   Y   F   Q   F   R   G   R   A
    ATG GAC AAA CAG CAT TTC AAG TTG TGG TAT TTT CAA TTC CGT GGG CGA GCA

18  E   P   I   R   L   L   L   T   C   A   G   V   K   F   E   D   Y
    GAA CCA ATT CGC CTT CTG CTC ACT TGC GCC GGT GTC AAA TTC GAG GAC TAT

35  Q   F   T   M   D   Q   W   P   T   I   K   P   T   L   P   G   G
    CAA TTC ACA ATG GAT CAG TGG CCT ACC ATC AAA CCC ACC CTA CCC GGC GGT

52  R   V   P   L   L   D   V   T   G   P   D   G   K   L   R   R   Y
    CGG GTT CCT CTC TTG GAT GTG ACC GGA CCA GAC GGG AAA CTT AGA CGT TAT

69  Q   E   S   M   A   I   R   L   L   A   R   Q   F   K   M   M   G
    CAA GAA TCG ATG GCC ATT GCT CGA TTG CTT GCC AGA CAA TTC AAA ATG GGT

86  E   T   D   E   E   Y   Y   L   I   E   R   I   I   G   E   C   E
    GAA ACA GAC GAA GAG TAT TAC TTG ATT GAA CGT ATC ATT GGT GAG TGT GAA

103 D   L   Y   R   E   V   Y   T   I   F   R   T   P   Q   G   E   K
    GAC CTT TAT CGG GAA GTG TAC ACC ATT TTC CGG ACA CCC CAA GGT GAG AAG

120 E   A   K   I   K   E   F   K   E   N   N   G   P   T   L   L   K
    GAA GCC AAA ATC AAG GAA TTC AAA GAG AAT AAC GGA CCG ACG TTG TTG AAA

137 L   V   S   E   S   L   E   S   S   G   G   K   H   V   A   G   N
    TTA GTT TCA GAA TCA TTG GAA TCC AGT GGT GGA AAA CAC GTG GCT GGG AAT

154 R   I   T   L   G   D   L   F   L   F   T   T   L   T   H   V   M
    CGG ATC ACT TTG GGC GAT TTG TTC TTG TTC ACC ACG TTG ACT CAT GTC ATG

171 E   T   V   P   G   F   L   E   Q   K   F   P   K   L   H   E   F
    GAG ACA GTG CCC GGA TTC CTC GAA CAG AAG TTC CCA AAA CTG CAT GAA TTT

188 H   K   S   L   P   T   S   C   S   R   L   S   E   Y   L   K   K
    CAC AAA TCT TTG CCT ACG AGT TGC AGC AGG CTA TCG GAA TAC CTG AAA AAA

205 R   A   K   T   P   F   *
    CGT GCA AAA ACT CCA TTC TAG

```

Figure 8.1: Full length FhGST-si from *F. hepatica*

Wormbase database: BN1106_s1081B000242.mRNA-1

The 633 nucleotides or 211 amino acids represent the full length of FhH2A. There are three cysteine residues (highlighted in red).

```

1   G   S   M   A   G   G   K   A   G   K   D   S   G   K   A   K   A
    GGA TCC ATG GCA GGC GGT AAA GCA GGT AAA GAT AGT GGT AAA GCA AAA GCC

18  K   A   I   S   R   S   H   R   A   G   L   Q   F   P   V   G   R
    AAA GCA ATT AGC CGT AGC CAT CGT GCA GGT CTG CAG TTT CCG GTT GGT CGT

35  I   H   R   H   L   K   T   R   T   T   S   H   G   R   V   G   A
    ATT CAT CGT CAT CTG AAA ACC CGT ACC ACC AGT CAT GGT CGT GTT GGT GCA

52  T   A   A   V   Y   S   A   A   I   L   E   Y   L   T   A   E   V
    ACC GCA GCA GTT TAT AGC GCA GCA ATT CTG GAA TAT CTG ACC GCA GAA GTT

69  L   E   L   A   G   N   A   S   K   D   L   K   V   K   R   I   T
    CTG GAA CTG GCA GGT AAT GCA AGC AAA GAT CTG AAA GTG AAA CGT ATT ACA

86  P   R   H   L   Q   L   A   I   R   G   D   E   E   L   D   T   L
    CCG CGT CAT CTG CAG CTG GCA ATT CGT GGT GAT GAA GAA CTG GAT ACC CTG

103 I   K   A   T   I   A   G   G   G   V   I   P   H   I   H   K   S
    ATT AAA GCA ACC ATT GCC GGT GGT GGT GTT ATT CCG CAT ATT CAT AAA AGC

120 L   I   G   K   K   V   P   P   A   K   P   L   G   M   *   L   E
    CTG ATC GGC AAA AAA GTT CCG CCT GCA AAA CCG CTG GGT ATG TAA CTC GAG

```

Figure 8.2: Full length FhH2A from *F. hepatica*

Wormbase database: BN1106_s45B000421.mRNA-1

The 408 nucleotides or 136 amino acids represent full length of FhH2A. There is one potential N-glycosylation site (highlighted in green).

```

1  M  F  L  I  A  L  L  S  Y  T  L  I  N  Q  L  V  I
   ATG TTT CTC ATT GCT TTA TTG TCA TAC ACA TTG ATA AAT CAA TTA GTC ATA

18 T  K  S  D  S  C  K  Y  C  L  R  L  Y  D  G  K  Y
   ACC AAA TCA GAT TCA TGC AAG TAT TGT CTA CGA TTG TAC GAT GGA AAG TAT

35 K  S  G  S  Y  I  E  V  Y  K  S  V  G  S  L  S  P
   AAG AGT GGT TCA TAT ATT GAA GTG TAC AAG AGC GTT GGC TCA CTC TCA CCA

52 P  W  I  P  G  S  V  C  V  P  L  I  H  N  S  T  G
   CCA TGG ATA CCT GGA TCT GTT TGT GTA CCT TTG ATA CAT AAT TCG ACG GGA

69 Q  P  P  Y  W  R  I  Y  E  D  V  N  Y  S  G  K  D
   CAG CCT CCA TAC TGG CGT ATA TAT GAA GAC GTC AAC TAC TCT GGT AAG GAC

86 T  A  V  G  H  G  A  C  I  D  D  F  M  K  S  G  L
   ACT GCT GTT GGA CAT GGT GCC TGC ATT GAT GAC TTC ATG AAA TCC GGA TTG

103 R  R  I  S  S  I  Q  K  C  V  Y  G  E  N  G  M  V
   AGA AGG ATT TCC TCC ATT CAG AAG TGT GTT TAT GGG GAA AAT GGA ATG GTT

120 Q  C  S  S  E  S  K  R  R  R  K  Y  C  R  Y
   CAA TGT ATC AGT GAA TCG AAA CGT CGT AGG AAA TAT TGT CGA TAC

```

Figure 8.3: Full length ShIPSE03 from *S. haematobium* eggs

NCBI Reference Sequence: XP_012802396.1

The 402 nucleotides or 134 amino acids represent the full length of ShIPSE03. There are seven cysteine residues (highlighted in red) and two potential N-glycosylation sites (highlighted in green).

```

1  M L Q E Y N L L I N G V T L L I S
   ATG TTG CAG GAA TAC AAC CTT CTA ATA AAC GGA GTC ACT TTA CTG ATT TCA

18  L S G L I C E A Q S P T N D E M H
   CTA AGT GGT CTC ATT TGC GAA GCT CAG TCT CCT ACA AAC GAT GAG ATG CAT

35  A T I S E Y G R L Y I T N I H I H
   GCC ACT ATA TCG GAA TAC GGG CGA CTT TAT ATA ACA AAT ATT CAC ATT CAC

52  Y R L L I M A L S P N M K F T P G
   TAT AGA CTT CTC ATT ATG GCG TTG AGT CCG AAT ATG AAG TTC ACA CCG GGA

69  E A D N I L H K S E E E H Q V K W
   GAA GCT GAT AAC ATT CCT CAC AAG TCG GAA GAA GAA CAC CAA GTG AAG TGG

86  A L N Y L N A A R S T W K L E N E
   GCA CTT AAT TAT CTC AAC GCT GCT AGA TCA ACT TGG AAA CTG GAA AAT GAA

103 D M F K K T M S S Y V G V N K T I
   GAC ATG TTC AAA AAA ACT ATG AGT TCC TAT GTG GGT GTG AAC AAA ACC ATT
      K
120 V P N F C M T M L Q Q S S A R N W
   GTA CCA AAC TTC TGT ATG ACT ATG TTG CAG CAA AGT AGT GCT AGA AAC TGG
      N
137 D T N I Q K D I T Y G C E V L K K
   GAT ACG AAT ATT CAA AAA GAC ATA ACA TAT GGT TGT GAA GTC CTG AAA AAA

154 Y S E L K W G A R K K L D L M T I
   TAT TCC GAG TTG AAA TGG GGA GCA AGA AAA AAA TTA GAT TTG ATG ACA ATT

171 R W L N G S D E N G Q S Q H I S D
   CGA TGG TTG AAC GGT TCG GAT GAA AAC GGT CAA TCA CAA CAC ATT TCA GAT

188 K G F N Y H S K K E Y L E C A Q S
   AAG GGA TTC AAT TAC CAT TCG AAA AAA GAA TAT CTC GAA TGT GGT CAG AGT

205 V M K I H R T K A E V D C R S T V
   GTG ATG AAG ATA CAC CGA ACT AAA GCC GAG GTT GAC TGT AGG TCA ACA GTA

222 G E F L K L Q Q V K D T P S S K T
   GGA GAA TTT TTG AAG CTA CAA CAA GTA AAA GAT ACC CCG AGC TCA AAA ACC

239 Q A I Q F D K I N E N F N K S L V
   CAA GCT ATA CAA TTT GAC AAA ATT AAC GGA AAT TTC AAC AAA TCA CTA GTC

256 E L K R R V E N L E I N R I N Y L
   GAG TTG AAG AGA AGA GTG GAA AAC CTC GAA ATC AAC AGG ATT AAT TAT TTA

273 K F M N P M E R V I S V I D A M E
   AAA TTT ATG AAT CCC ATG GGA AGG GTC ATC TCA GTT ATA GAT GCA ATG GAA
      I
290 E E V D H K Y G V Y M *
   GAA GAG GTG GAT CAC AAG TAT GGA GTC TAC ATG TAA

```

Figure 8.4: Full length Smk5 from *S. mansoni* eggs

clone 4.1.2; GenBank™ accession number AY903301

The 903 nucleotides or 301 amino acids represent the full length of Smk5. The 75 nucleotides at the 5' end are an N-terminal secretory signal (highlighted in grey). There are four cysteine residues (highlighted in red) and four potential N-glycosylation sites (highlighted in green)(226).